THÈSE

En vue de l'obtention du

DOCTORAT DE L'UNIVERSITÉ DE TOULOUSE

Délivré par :

Institut National Polytechnique de Toulouse (Toulouse INP)

Discipline ou spécialité :

Ecologie Fonctionnelle

Présentée et soutenue par :

M. MATHIEU LEROY

le vendredi 15 décembre 2023

Titre :

Etude des effets d'un multistress combinant un contaminant historique et un contaminant émergent dans les agrosystèmes : cas des éléments traces métalliques et des nanotubes de carbone

---

Ecole doctorale :

Sciences de l'Univers de l'Environnement et de l'Espace (SDU2E)

Unité de recherche :

Laboratoire Ecologie Fonctionnelle et Environnement (LEFE)

Directeur(s) de Thèse :

MME CAMILLE LARUE

M. EMMANUEL FLAHAUT

Rapporteurs :

M. JEROME ROSE, CNRS

MME CATHERINE SANTAELLA, CEA CADARACHE

Membre(s) du jury :

M. CHRISTIAN MOUGIN, INRA VERSAILLES GRIGNON, Président

M. EMMANUEL FLAHAUT, UNIVERSITE TOULOUSE 3, Membre

M. MATHIEU PEDROT, UNIVERSITE RENNES 1, Membre

MME CAMILLE LARUE, CNRS TOULOUSE, Membre

Table des matières

Chapitre 1 : Introduction générale 9
1. Nanomatériaux carbonés (NMC) 11
1.1. Définition 11
1.2. Origines, rejets dans l'environnement et devenir des NMC 13
2. Eléments traces métalliques (ETM) 15
2.1. Définition 15
2.2. Origines, rejets dans l'environnement et devenir des ETM 16
2.3. Notion de spéciation et de biodisponibilité 18
3. Interaction NMC et ETM: article de revue 19
3.1. Introduction 22
3.2. Interaction CNM - metal(loid)s 24
3.2.1. Mechanisms of interactions between CNM and metal(loid)s 24
3.2.2. Factors influencing the CNM - metal(loid) interactions in simplified media 26
3.2.3. Metal(loid) adsorption by CNM in complex media 34
3.3. Metal(loid)s, CNM and CNM-metal(loid) complex uptake and impacts on agrosystem organisms 38
3.3.1. Uptake and impacts of metal(loid)s and CNM as single contaminant 38
3.3.2. Impacts of the interaction between metal(loid)s and CNM 46
3.4. Conclusion – Knowledge gaps and Perspectives 51
3.5. Supporting information 69
4. Questionnements scientifiques de la thèse 87
Chapitre 2 : Matériels et méthodes 95
1. Caractérisation des nanomatériaux 95
1.1. BET 95
1.2. Spectroscopie Raman 96
1.3. Microscope électronique à transmission (MET) 98
2. Caractérisation des interactions NMC/ETM : expériences d'adsorption 99
2.1. Principe général des expériences d'adsorption 99
2.1.1. Isothermes d'adsorption 103
2.1.2. Cinétique d'adsorption 106
3. Détermination du transfert des NTC et ETM 107
3.1. Quantification du ^{13}C par py-IRMS (pyrolysis-Isotope Ratio Mass Spectrometry) 107
3.2. Analyse par faisceaux d'ions (^{13}C, ETM) 108
3.3. Quantification élémentaire par ICP-AES (Inductively Coupled Plasma - Atomic Emission Spectroscopy) 111

4. Evaluation des impacts écotoxicologiques 112
4.1. qPCR (quantitative Polymerase Chain Reaction) 113
Chapitre 3 : Caractérisation des interactions NMC et ETM en milieux simplifiés 119
1. Introduction 123
2. Material and methods 125
2.1 Materials 125
2.2. CNM characterization techniques 127
2.3. Adsorption experiments 128
2.4. Analytical measurements 130
2.5. Modelling and statistical analyses 130
3. Results and discussion 132
3.1 Influence of the pH 132
3.2. Isotherms 134
3.3. Kinetics 137
3.4. CNM type 139
3.5. OM 141
3.6. Soil solution 143
4. General conclusion 144
5. Supporting information 149
Competitive adsorption on carbon based nanomaterials of a mixture of cadmium, copper, lead and zinc and influence of environmental parameters 149
Chapitre 4 : Mise en évidence des impacts d'une contamination monospécifique en NTC sur un agrosystème 157
1. Introduction 164
2. Material and methods 166
2.1. CNT synthesis and characterization 166
2.2. Soil characterization and contamination 167
2.3. Microcosm set-up 167
2.4. Bacterial abundance, litter decomposition and functional genes 168
2.5. Plant morphology and metabolism 169
2.6. Gas measurements and analysis 169
2.7. Sample preparation and chemical analysis by ICP-AES 170
2.8. Statistical analyses 170
3. Results 172
3.1. Microbial responses to CNT exposure 172
3.2. Crop plant response to CNT exposure 173

3.3. Gas exchange....175
3.4. Multifunctionality....176
4. Discussion....177
4.1. Impacts of CNT on C cycle....177
4.2. Impacts of CNT on N cycle....178
4.3. Impacts of CNT on H_2O cycle....179
4.4. Impacts of CNT on agrosystem multifunctionality....180
5. Supporting information....187
Chapitre 5 : Caractérisation des impacts d'une co-contamination en NTC et ETM sur un agrosystème....192
1. Introduction....198
2. Material and methods....200
2.1. CNT synthesis and characterization....200
2.2. Soil characterization and contamination....201
2.3. Experimental set-up....201
2.4. Enzymatic activities, fungal abundance and litter decomposition....202
2.5. Plant morphology and metabolism....203
2.6. Gas exchange measurements and analysis....203
2.7. Sample preparation and chemical analysis by ICP-AES....204
2.8. Statistical analyses....204
3. Results....205
3.1. Mixture and aging impact on belowground processes....205
3.2. Impact on plant development, metabolism and elemental transfer....208
3.3. Gas exchange....213
4. Discussion....214
4.1. CNT exposure impacts....214
4.2. TME exposure impacts....216
4.3. Aging of contaminant impacts....217
4.4. Co-contaminants impacts....218
5. Supporting Information....224
Chapitre 6 : Caractérisation du transfert de NTC et ETM au sein d'un réseau trophique reconstitué226
1. Intoduction....230
2. Material and methods....232
2.1. CNT synthesis and characterization....232
2.2. Soil characterization and contamination....234
2.3. Experimental set-up....234

2.4. Sample preparation and chemical analysis by ICP-AES 236
2.5. Sample preparation and isotopic ^{13}C analysis by py-IRMS....236
2.6. Sample preparation and microbeam analysis....236
2.7. Statistical analyses and calculations....237
3. Results....238
3.1. Trophic transfer from soils to lettuce to snails....238
3.2. Soil to snail transfer experiment....242
4. Discussion....245
4.1. CNT isotopic labeling for detection in environmental matrices....245
4.2. Trophic transfer and toxicity along the soil-plant-snail system....246
4.3. Contaminant transfer to snails after soil exposure....248
4.4. Exposure pathway comparison....248
5. Conclusion....249
6. Supporting Information....254
Conclusion générale....255
Discussion générale....261
Annexe :....279

Tout d’abord, je tiens à adresser mes sincères remerciements à la Région Occitanie, à l’Université fédérale de Toulouse Midi-Pyrénées, et à l’école doctorale SDU2E pour avoir généreusement financé ma thèse de doctorat.

Mes salutations les plus distinguées vont aux rapporteurs et aux membres du jury qui, tels un équipage attentif, ont pris le temps d'examiner et de critiquer mon manuscrit. Je vous remercie également d’être venus à ma soutenance de thèse.

Durant ces 3 années de recherche, j'ai eu le privilège d'embarquer à bord d'un laboratoire de recherche, un vaisseau intrépide voguant au gré des vents de la connaissance. Chaque membre de cet équipage, tel un moussaillon indispensable, a contribué à cette aventure. Je tiens à exprimer ma gratitude envers tous les collègues des deux laboratoires avec lesquels j'ai collaboré, échangé, et partagé d'inspirants moments de convivialité.

Mes remerciements vont aux officiers dédiés à l'administratif, les secrétaires Régine et Annick, ainsi que toute l’équipe de gestion : Catherine, Anne, Rachida et Cyril, qui ont été les navigateurs experts maintenant le cap administratif du navire. Mes remerciements sincères s'étendent aux membres des différentes plateformes d’analyses avec lesquelles j'ai partagé le pont :

• Jess, Corinne, Didier et Fred du PAPC du LEFE

• Fred et David de l’ICP du LEFE

• Stéphanie de la plateforme AIFIRA de Gradignan

• Anne-Lise de la plateforme GISMO de Dijon

Mes partenaires du CIRIMAT ont été les compagnons fidèles sur le pont de recherche, notamment Brigitte et Anne-Marie, qui ont apporté leur précieuse aide sur les résultats d’adsorption. Un salut particulier à Morgan, un marin dévoué qui a synthétisé et caractérisé la quasi-exclusivité des matériaux utilisés. Mes remerciements s'étendent également à d'autres membres du CIRIMAT avec qui j'ai collaboré ponctuellement, notamment Vincent pour l’analyse de potentiel zêta et Marie-Claire pour les mesures de surface spécifique des nanomatériaux.

Mes camarades de l'équipage de recherche ECI du LEFE ont été des compagnons de voyage exceptionnels, et je tiens à les remercier chaleureusement. Une mention spéciale à Annie, l'une de mes mamans du laboratoire, pour les échanges passionnants autour du Jura et le réconfort offert dans les moments difficiles. La longue traversée à leurs côtés m’a permis de ne pas trop avoir le mal du pays. Merci à Olivier pour les analyses réalisées et les échanges fructueux. Melissa, pour toutes les extractions et analyses qPCR, et à Maialen pour la formation qPCR. Séverine, pour la bonne humeur et les TP terrains que nous avons partagés. Christophe, pour ses lumières en statistiques. Arnaud, pour la proposition à Camille lors du stage de M2 et son accompagnement. Merci à toute l'équipe qui m’a encadré en DRU, notamment Éric, Laury, Lauris et Franck. Je remercie chaleureusement Flo, une autre maman du labo. Merci d’avoir su trouver les mots justes aux moments de fortes angoisses pendant le Covid. Merci Bertrand et Swan pour les différentes sorties en bar que nous avons fait. Un très grand merci au capitaine de bord Jérôme, dit le pilier de l’ENSAT. Merci pour ta bonne humeur, tes blagues et jeux de mots qui n’ont jamais cessé de me faire sourire. Merci aussi pour toutes les discussions sur la recherche et sur la société en générale que j’ai pris beaucoup de plaisir à avoir avec toi. Un merci aux différents mousses qui ont ramé en éclaireur sous ma direction, mes stagiaires. Merci Mathilde, Eva, Laura, Maximilien et Florian. Merci pour votre investissement et l’aide précieuse que vous m’avez apportée.

Je remercie la p'tiote frégate de Besac pour leur accueil et leur aide. Merci Fred pour m'avoir transmis tes connaissances sur l'escargot et l'aide que tu m'as apportée lors de notre collaboration à Besançon. Merci Carole pour ta gentillesse et pour m'avoir mis le pied à l'étrier dans la recherche. Je remercie aussi les différents collaborateurs qui m'ont accompagné au cours de mes expériences, que cela soit pour un prêt de matériel ou pour une collaboration plus prononcée. Merci Vincent sur les aspects bactériens et de multifonctionnalités. Merci Joséphine pour le prêt de la table d'agitation orbitale que j'aurai empruntée pendant 2 ans. Benjamin Pey qui m'a encadré sur les aspects liés aux vers de terre. Qui aurait pu croire qu'un jour j'allais mettre la main dans du crottin de cheval pour nourrir des vers de terre !

Je remercie les moussaillons avec qui j'ai partagé ma cage au laboratoire. Merci Antoine pour ta gentillesse et ton dévouement pour la communauté doctorante du laboratoire. Merci Paul pour ton grain de folie et les sorties que nous avons faites au bikini. Je garde précieusement ton vinyle et même si je te l'ai déjà dit, je te le redis : chapeau l'artiste ! Merci Sara, la grande sœur du bureau. Merci pour ta spontanéité, ta gentillesse et pour toute la bouffe que tu as ramenée au bureau. J'espère que ta famille et toi-même se porteront bien. Merci aussi pour tous pétages de plombs que nous avons eu tous ensemble au bureau. Gros bisous les co-bureaux ! Merci aussi à mes co-bureaux d'adoption du bâtiment 4R1 du LEFE. Merci Marie et Camille pour tous les bons moments que j'ai passés avec vous. J'ai pris beaucoup de plaisir à venir dans votre bureau les grils !

Bien évidemment, je remercie mes commandants de bords qui ont tenu le cap et maîtrisé le gouvernail : mes deux directeurs de thèses. Sans vous, ce travail ne serait pas aussi abouti. Merci Emmanuel pour tes conseils et les réflexions que tu as apportées au cours de ce travail. Je suis parti en galère avec ces manips d'adsorption, mais j'y suis parvenu !

Un MERCI tout particulier à Camille, merci pour lequel je n'arrive pas à trouver de qualificatif tellement je me sens reconnaissant. Merci d'avoir su voir quelque chose que je n'avais jamais décelé chez moi. Merci de m'avoir poussé, de m'avoir relevé, de m'avoir soutenu sans relâche au cours de ces 4 dernières années. Je suis extrêmement heureux d'avoir collaboré avec toi toutes ces années, d'avoir appris à tes côtés et du rendu de notre travail. Je n'arrive pas avoir de sentiment de fierté car ce n'est pas mon tempérament, mais je sais que dans 10 ans, je me dirai : « bordel on a été un binôme du tonnerre ». J'ai pu découvrir quelqu'un d'une grande gentillesse, soucieuse de l'humeur des autres, engagée dans ce qu'elle entreprend, avec une volonté et une détermination sans faille. Mais surtout, j'ai découvert une personne avec qui on pouvait facilement discuter de tout, avec qui on envie rire et de partager des moments. Je n'oublierai jamais nos escapades à Copenhague (a star is born héhé), à Banyuls (surtout la bouffe) et aussi Gradignan (la bouffe aussi était bien là-bas) dans lesquelles on a partagé des moments bien ancrés dans la tradition française, mais toujours avec modération 😉. Je te remercie pour la confiance que tu m'as faite et pour toutes les choses que tu m'as transmises. Je te souhaite de vivre une vie professionnelle et personnelle riche de bonheur car tu le mérites ! Merci, Camille.

Un merci à mes potes qui ont su me faire décrocher de la thèse à des moments opportuns, qui m'ont épaulé dans les moments difficiles et avec qui nous avons bien ri durant ces dernières années.

Enfin, le dernier merci sera adressé aux gens qui me supportent depuis maintenant 27 ans. Des gens sans qui je ne serais rien. Des gens qui ont toujours été présents, dans les bons comme dans les mauvais moments. Des gens pour qui mon amour et mon admiration n'ont pas d'égal pour le moment. Ma famille ! Merci Mimi, Steve et Thom, mes frères et sœurs qui m'ont toujours soutenu, quoi que je fasse. Merci à la Bulle et au Stumpy, qui ont toujours souhaité que l'on ne manque de rien et qui ont réussi à nous offrir bien plus que l'on ne pouvait l'espérer. Merci, je vous aime.

Cette thèse est dédiée à la mémé Danielle, le Dédé et le pépé Alexandre dit le Roger

Chapitre 1 : Introduction générale

Depuis son apparition sur le globe terrestre, la curiosité de l'*Homo sapiens* l'a conduit à franchir d'innombrables obstacles afin de découvrir des terres qui restaient jusqu'ici inconnues. Au fil des siècles, cette curiosité s'est assouvie et d'autres désirs tels que la volonté d'agrandir les communautés existantes ont rendu l'espèce sédentaire principalement en raison de la découverte de l'agriculture. Dès lors, l'*Homo sapiens* n'aura de cesse de façonner les écosystèmes afin de satisfaire ses besoins, toujours plus accrus et il faudra attendre le XXème siècle pour que l'Homme s'interroge sur les impacts de la modification des écosystèmes par ses activités. Petit à petit, l'Homme moderne découvre que ses activités ont laissé des traces qui aujourd'hui sont à l'origine de nombreuses préoccupations environnementales et sanitaires pour les autorités publiques. En effet, un grand nombre de contaminants a été rejeté par le passé et d'autres contaminants émergents, issus des avancées techniques et technologiques, polluent à leur tour les écosystèmes. En parallèle, les pronostics démographiques mondiaux soulèvent des questions quant à la capacité à nourrir l'être humain. En effet, selon l'Organisation des Nations Unies (ONU), la population mondiale atteindrait 9,8 milliards de personnes à l'horizon 2050[1]. Dans ce contexte, le besoin de protéger la fertilité des écosystèmes modifiés par l'homme pour les utiliser à des fins de culture ou d'élevage intensif pour l'alimentation[2], que l'on nomme agrosystèmes, mais aussi leur santé afin de garantir suffisamment de nourriture saine pour nourrir convenablement nos sociétés se révèle être une priorité et un défi majeur.

Parmi les premières préoccupations sanitaires et écotoxicologiques, qui aujourd'hui encore subsistent, figurent les éléments traces métalliques (ETM), qui montrent à certains endroits et notamment dans les agrosystèmes une présence anormalement élevée en raison de l'épandage continu d'engrais organiques et inorganiques[3,4]. Au lendemain du cri d'alarme lancé par le club de Rome sur les risques liés à la pollution des sols agricoles par l'abus de fertilisants[5], la France décida de créer le ministère de l'Environnement afin de multiplier les actions de recherche autour de la capacité des sols à recevoir et

à épurer de manière durable les déchets qui y étaient épandus, en particulier des boues de stations d'épuration (STEP) urbaines plus ou moins chargées en ETM potentiellement toxiques[5].

A l'issue des innovations techniques et technologiques, d'autres contaminants émergents ont été découverts pour lesquels les préoccupations écotoxicologiques se sont immédiatement soulevées fort des exemples passés des contaminations historiques. Pour les agrosystèmes, les nanomatériaux carbonés (NMC) font partie des contaminants émergents qui suscitent des inquiétudes prononcées. Il s'agit d'une famille de matériaux dont la plupart ont une structure basée sur le graphène (graphène, oxyde de graphène et ses composés réduits, nanotubes de carbone), considérés comme un "matériau miracle du XXIe siècle" tant ses propriétés sont étonnantes[6], lui valant même le prix Nobel de physique en 2010[7]. En effet, les propriétés remarquables de ces nanomatériaux offrent des possibilités dans l'agriculture afin d'augmenter la production de biomasse[8] mais aussi dans la dépollution des eaux[9]. De plus, ces matériaux sont connus pour s'accumuler dans les boues de STEP, comme les ETM ; elles pourraient donc être vecteurs de pollution conjointe des NMC et ETM. Soucieux des questions concernant la toxicité et l'écotoxicité des NMC, une unité de travail de recherche (WP4) est formée dans le cadre du projet européen H2020 FET Graphene Flagship afin de caractériser la toxicité et l'écotoxicité du graphène et de ses dérivés afin de réagir adéquatement dans le futur[10].

Dès 1986, Dexler dans son ouvrage *Engines of Creation* évoque le possible revers de médaille que le monde pourrait connaître face à l'utilisation des nanomatériaux en raison de leur échelle et des incertitudes qu'ils soulèvent à l'époque. Il évoque l'idée que ces matériaux et les technologies qui en résultent pourrait devenir destructrices, pour la faune, la flore et même l'humanité, si elles ne sont pas entièrement maîtrisées[11]. L'échelle des nanomatériaux leur offre une réactivité de surface élevée[12], leur permettant de fortement interagir avec leur environnement, incluant d'autres contaminants. En particulier, des études ont montré que les NMC étaient capables d'adsorber à leur surface des ETM[13–17], ce qui soulève des questions quant aux transferts et aux impacts toxicologiques de ces deux

contaminants lorsqu'ils se retrouvent en mélange comme ce pourrait être le cas dans les agrosystèmes.

Aujourd'hui encore, l'évaluation des risques liés aux contaminants en mélange se réalise par additivité des effets des substances considérées individuellement. Or, les recherches de ces deux dernières décennies ont mis en évidence que les interactions entre contaminants pouvaient produire des effets toxicologiques plus ou moins prononcés que les effets obtenus en ajoutant ceux des contaminants pris individuellement[18].

En raison de (1) la pression qui subsiste sur les agrosystèmes afin de nourrir la population, (2) des innovations créées afin d'augmenter la capacité de production des agrosystèmes, (3) de la pression en terme de pollution par des contaminants qui peuvent facilement être introduits dans les agrosystèmes par les boues de STEP comme les NMC et ETM et (4) des interactions qui existent entre certains contaminants comme c'est le cas pour les NMC et les ETM, il convient de mener des recherches afin de comprendre quelle est la nature de ses interactions, par quoi sont-elles régies et de quelles manière elles modifient ou non le transfert et la toxicité des NMC et ETM pour les organismes des agrosystèmes.

1. Nanomatériaux carbonés (NMC)

1.1. Définition

Les NMC sont des nano-objets essentiellement composés de carbone, possédant au moins une dimension externe à l'échelle nanométrique et dont les autres dimensions externes peuvent être significativement plus grandes. Beaucoup de NMC ont une structure basée sur le graphène, une feuille d'atomes de carbone réunis dans un réseau hexagonal de carbone hybridé sp^2, d'un atome d'épaisseur[6,19–21] (Figure 1). La longueur de la liaison carbone-carbone est d'environ 0,142 nm.

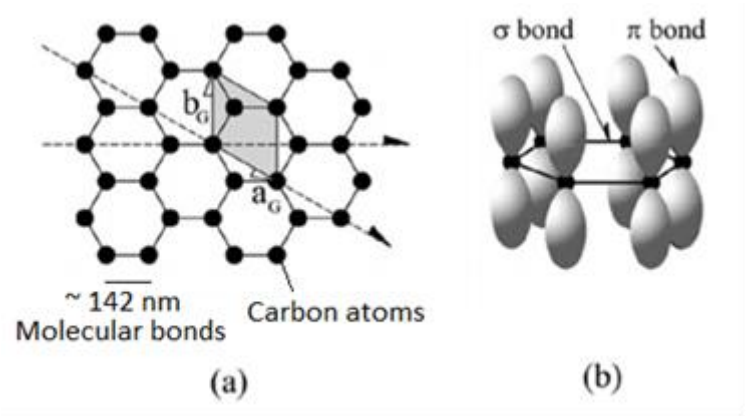

Figure 1: (a) Structure hexagonale du graphène. Les directions « zigzag » et « armchair » (chaise) sont montrées respectivement par les vecteurs a_G et b_G. La partie grisée représente l'unité permettant de définir la densité de surface du carbone. (b) Représentation schématique des liaisons σ dans le plan du feuillet de carbone et des orbitales π perpendiculaires à ce plan (Schéma modifié d'après celui de Hass et al.[22])

Au fil des années, l'intérêt des chercheurs pour le graphène n'a cessé de croître, conduisant à l'apparition progressive de matériaux dérivés utilisant le graphène comme précurseur[23]. Aujourd'hui, il est possible de distinguer le graphène monocouche du graphène multicouche, des NTC (Figure 2AB), des matériaux de graphène fonctionnalisés comme le graphène oxydé (GO) ou d'autres composites de graphène (Au, Ni, Cu, TiO_2, ZnO, etc.), du fullerène (Figure 2C), etc. Cependant, le terme graphène est parfois utilisé de manière générique pour décrire certains NMC basés sur sa structure et cela peut conduire à des interprétations trompeuses par les parties prenantes (chercheurs, industries, gouvernements, régulateurs, médias, etc.)[6].

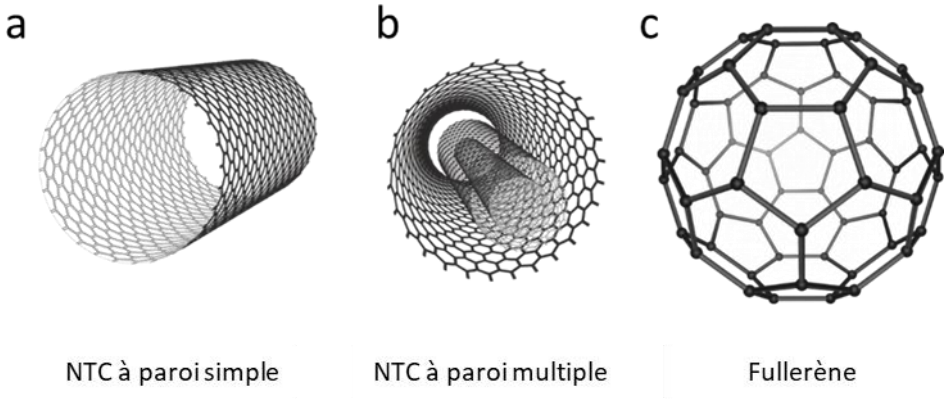

Figure 2 : Schéma représentant différents nanomatériaux possédant une structure à base d graphène à savoir un NTC à parois (a) simple et (b) multiples et (c) un fullerène C60.

1.2. Origines, rejets dans l'environnement et devenir des NMC

Les NMC peuvent exister naturellement dans la biosphère. Par exemple, l'érosion naturelle du graphite peut conduire à du graphène multicouche et l'oxydation du graphite dans l'air (combustion, foudre) peut également conduire à l'oxyde de graphite[24], qui est encore plus facile que le graphite à exfolier en oxyde de graphène. La formation de NTC a été décrite à de nombreuses reprises après combustion incomplète d'hydrocarbures[25] (bien que leur structure et leur morphologie soient relativement différentes de « l'idéal » représenté sur la Figure 2) ou encore la combustion du charbon[26]. Cependant, la plupart des NMC sont conçus (et donc synthétisés) pour des applications pratiques.

De nombreux produits de consommation courante contiennent des NMC tels que certains équipements sportifs et les produits aéronautiques, par exemple[27]. Ainsi, ils peuvent désormais être disséminés dans la biosphère via des sources de nature anthropique. Compte tenu de leurs propriétés exceptionnelles et de leurs applications potentielles dans différents secteurs d'activité, leurs concentrations dans les écosystèmes terrestres et aquatiques auront tendance à augmenter dans les années à venir[28].

Les NMC peuvent être rejetés dans l'environnement tout au long de leur cycle de vie. Cela comprend leur production, leur transformation (incorporation dans des produits manufacturés, fonctionnalisation, etc.), leur utilisation, leur recyclage ou leur destruction[29]. De plus, c'est cette dernière phase, à savoir la destruction des matériaux contenant les NMC par incinération, qui est une étape clé pour leur relargage potentiel. En particulier, les NMC peuvent se retrouver dans les cendres en cas d'incinération insuffisante, qui sont normalement transférées vers des installations de stockage de déchets dangereux[30]. De plus, le rejet d'eaux usées et le rejet accidentel de NMC lors de la manipulation peuvent entraîner leur retour dans les écosystèmes.

La distribution géographique des NMC pourrait dépendre de leurs applications[31] et par conséquent, l'usure (par abrasion, dégradation, etc.) des matériaux contenant des NMC devrait être à l'origine d'une grande partie de la libération incontrôlée de NMC dans l'environnement. Enfin, les voies

potentielles de pénétration des NMC dans l'environnement peuvent être liées à des sources ponctuelles (usine de production, zone d'enfouissement, effluents d'eaux usées) ou diffuses (dépôts atmosphériques, ruissellement des eaux pluviales, usure des produits contenant des NMC lors de leur utilisation) de contamination entraînant des expositions aiguës ou chroniques. Comme pour de nombreux autres contaminants particulaires, le vent et les dépôts atmosphériques, les précipitations, le ruissellement ou le lessivage peuvent affecter leur transport et leur distribution. Le comportement (transfert et interaction) des NMC au sein des écosystèmes repose sur : 1) leurs propriétés fondamentales et de leurs modifications qui peuvent évoluer lorsqu'ils se retrouvent dans l'environnement, 2) les propriétés physico-chimiques de l'environnement (texture, pH, matière organique (MO), etc.) et 3) les interactions avec les autres contaminants présents dans l'environnement (ETM, pesticides, etc.) [32].

L'écotoxicité des NMC n'est pas, comme pour la majorité des contaminants, dose dépendante. Au contraire, nombreuses sont les études qui ont observé une toxicité aux plus faibles concentrations testées en raison du comportement d'agglomération des NMC qui limite l'exposition[33,34]. Pour les organismes majeurs des agrosystèmes (micro-organismes, invertébrés et cultures), de nombreux NMC présentent des propriétés antimicrobiennnes[35], une toxicité faible pour les invertébrés en raison de leur capacité de dépuration et des effets contrastés sur les plantes allant d'une diminution à une augmentation des paramètres de croissance (système racinaire, production de biomasse, fleurs et fruits)[36,37]. L'un des marqueurs de toxicité les plus récurrents chez les organismes est une réponse inflammatoire produisant des espèces réactives à l'oxygène (ROS) suite aux contacts des NMC[38] et une réponse impliquant un stress oxydant[39]. L'écotoxicité des NMC sur les organismes des maillons trophiques supérieurs (oiseaux, reptiles, mammifères) est très peu étudiée puisque les NMC sont pour l'heure peu retrouvés dans l'environnement et que la quasi-totalité des recherches sur ce sujet se font en laboratoire, sur les organismes modèles autorisés.

Les écosystèmes terrestres sont l'un des puits importants pour les nanomatériaux après leur rejet dans l'environnement[40]. Les nanomatériaux, qui présentent une grande mobilité, peuvent pénétrer dans

diverses strates du sol et, à terme, via les systèmes d'eaux souterraines et les bassins versants, se retrouver dans des écosystèmes aquatiques reconnus comme le réceptacle ultime des NMC[41]. Ces transferts d'un écosystème à un autre présentent des risques car ils peuvent ensuite s'intégrer dans les réseaux trophiques de ces ecosystèmes[42–44]. Compte tenu du verrou actuel concernant la détection/quantification des NMC, aucune étude à ce jour n'a su quantifier les flux de NMC au sein des réseaux trophiques, des écosystèmes et des grands compartiments de la biosphère. Toutefois, à l'aide de modélisation, Keller et al (2013)[31] ont estimé que près de 63 à 91 % des nanoparticules manufacturées produites en 2010 finissaient dans les décharges, 8 à 28 % dans les sols, 0,4 à 7 % dans l'eau et 0,1 à 1,5 % dans l'atmosphère. Parmi ces particules, 83 à 98 % des NTC se retrouveraient dans les décharges, 2,2 à 14,8 % dans le sol, 0,1 à 1,4 % dans l'air et 0,01 à 0,6 % dans l'eau. Selon la modélisation de Sun et al.[45] la concentration de NTC dans les sols agricoles serait de 11 $\mu g.kg^{-1}$ de sol[45]. De plus, leur concentration dans les sols agricoles amendés avec des boues d'épuration devrait augmenter annuellement de 74 $ng.kg^{-1}$[46]. Il est à noter que ces estimations se font sur la base d'hypothèses limitées à une zone géographique précise à savoir ici le territoire Suisse et ne sont pas nécessairement représentatives pour toutes les zones géographiques.

2. Eléments traces métalliques (ETM)

2.1. Définition

Les ETM sont des éléments présents à l'état naturel dans un biotope à des concentrations inférieures à 100 ppm[2]. Ils ont été largement étudiés au cours des dernières décennies, notamment le cuivre (Cu), le zinc (Zn), le fer (Fe), le manganèse (Mn), le molybdène (Mo), le bore (B), le cobalt (Co), le nickel (Ni), le plomb (Pb), le cadmium (Cd), le chrome (Cr), l'arsenic (As) et le sélénium (Se). Cu, Zn, Fe, Mn, Mo et B sont essentiels à la croissance normale des plantes ; Cu, Zn, Fe, Mn, Mo, Co et Se sont essentiels à la croissance et à la santé des animaux et des êtres humains ; et Cu, Zn, Pb et Cd sont les éléments les plus préoccupants pour l'environnement qui ont souvent été signalés comme étant à l'origine de la contamination du sol, de l'eau et des réseaux trophiques[47]. Au-delà d'une certaine concentration

propre à chaque ETM, ce dernier peut avoir des effets délétères sur les organismes ainsi que des conséquences en termes de sécurité alimentaire.

2.2. Origines, rejets dans l'environnement et devenir des ETM

À l'origine, les ETM présents dans les sols résultent de processus naturels tels que la dégradation du matériau géologique d'origine (roche-mère), qui est le processus prédominant, et les émissions volcaniques issues des éruptions[48,4]. Ces processus établissent le fond géochimique naturel des éléments du sol. Cependant, ces substances présentent, à certains endroits, une concentration anormalement élevée par rapport aux fonds géochimiques locaux en raison des activités anthropiques. Les principales sources anthropiques d'ETM dans l'environnement terrestre, et dans les sols agricoles en particulier, sont les dépôts atmosphériques, l'épandage de fumier de bétail, l'irrigation avec des eaux usées ou polluées, les métallo-pesticides ou herbicides, les engrais à base de phosphate et les amendements à base de boues de STEP[4,49].

Devant le manque de données sur les teneurs naturelles en ETM dans les sols français, l'INRA a lancé en 1994 un programme de recherche intitulé "Apports d'une Stratification Pédologique pour l'Interprétation des Teneurs en Éléments Traces" afin d'acquérir des références sur les concentrations en éléments traces dans les sols[50]. Aujourd'hui encore, la contamination des sols par les ETM est l'une des préoccupations les plus pressantes dans le débat sur la sécurité sanitaire en Europe[51] et dans le monde[52]. En conséquence, les pouvoirs publics ont décidé de réglementer les concentrations d'ETM en fixant des seuils maximaux admissibles dans les sols agricoles et les engrais appliqués aux agrosystèmes (Tableau 1).

Tableau 1 : Concentrations limites des ETM dans les sols agricoles européens et dans les boues de STEP à usage agricole en Europe (Directive 86/278/EEC[53], ms = matière sèche).

ETM	Concentrations limites autorisées dans les sols (6 < pH < 7 en mg.kg^{-1} ms)	Concentrations limites autorisées dans les boues de STEP (mg.kg^{-1} ms)
Cd	1-3	20-40
Cu	50-140	1000-1750
Ni	30-75	300-400
Pb	50-300	750-1200
Zn	150-300	2500-4000
Hg	1-1.5	16-25

L'ingestion de légumes contaminés par des ETM provoque de graves problèmes de santé humaine, tels que des cancers gastro-intestinaux, la fragilisation des mécanismes immunologiques, des retards de développement mental et de la malnutrition[54–60]. De plus, les ETM peuvent s'accumuler dans les os ou les tissus adipeux humains par l'apport alimentaire, entraînant ainsi l'épuisement des nutriments essentiels et l'affaiblissement des défenses immunitaires. Certains ETM (Al, Cd, Mn et Pb) sont, en outre, suspectés de provoquer un retard de croissance intra-utérine[49,54,55,57].

Pour les organismes principaux des agrosystèmes (micro-organismes, invertébrés et cultures), l'excès d'ETM peut être délétère pour leur maintien et leurs fonctions écosystémiques (minéralisation et séquestration du carbone, par exemple)[48,4,61,62]. La plupart des ETM présents dans le sol peuvent s'accumuler dans les cultures ou être transférés vers d'autres milieux tels que les eaux souterraines ou les eaux de surface[63] et des écosystèmes connexes contaminés. De plus, avec l'accumulation d'ETM dans les organismes des agrosystèmes, tous les autres organismes dépendant de cet écosystème comme les eu-arthropodes, les amphibiens, les oiseaux et les micro-mammifères peuvent bioaccumuler les ETM[64]. Cependant, il semble que la bioaccumulation d'ETM dépende du métal et des taxons considérés[64].

2.3. Notion de spéciation et de biodisponibilité

Dans le contexte de l'évaluation du risque environnemental, les concepts de biodisponibilité et de spéciation chimique revêtent une importance capitale pour la compréhension et l'interprétation de la toxicité des contaminants[65]. D'un point de vue environnemental, la spéciation désigne la répartition des différentes espèces chimiques d'un élément au sein d'un système[66]. Cette approche englobe l'identification, la séparation et la détermination de toutes les formes physico-chimiques d'un élément dans un échantillon, qui, une fois combinées, constituent la concentration totale de cet élément[67]. La mobilité, la biodisponibilité et la toxicité des ETM dépendent de leurs formes chimiques spécifiques et de leur état de liaison (précipités avec des minéraux primaires ou secondaires, complexés par des ligands organiques, par exemple) contrôlés par les variations des conditions physico-chimiques du milieu (pH, température, force ionique, etc.)[68]. Des techniques ont été mises en place afin de différencier des fractions susceptibles d'être affectées par diverses conditions environnementales et qui renseignent sur la biodisponibilité des ETM[69]. Ainsi, Maiz et al.[70] ont développé une méthode d'extraction rapide en 3 étapes qui permet de différencier 2 fractions: fraction mobile facilement échangeable pour les organismes et fraction complexée ou adsorbée sur des carbonates difficile d'accès pour les organismes.

De la même façon, les NMC peuvent subir des transformations dans l'environnement comme par exemple des réductions en raison des conditions abiotiques et biotiques (notamment pour le GO)[41]. Cette réduction pourrait se produire à long terme dans les écosystèmes et être accélérée en présence de rayonnement UV[71,72], d'agents réducteurs inorganiques tels que les métaux ou certains composés soufrés ($NaHSO_3$, Na_2SO_3, $Na_2S_2O_3$, Na_2S, $SOCl_2$ et SO_2)[73], de réducteurs organiques tels que les polyphénols et les vitamines[74,75] ou d'autres composés organiques tels que les acides aminés (glycine)[76], les saccharides et polysaccharides (glucose, fructose et saccharose, cellulose naturelle)[77,78] et les protéines[79]. Récemment, certaines recherches ont révélé que des micro-organismes comme *Escherichia coli* et *Shewanella* pourraient réduire le GO[80–82]. En ce qui concerne l'oxydation des NMC dans l'environnement, celle-ci semble peu probable par le biote mais peut se produire par des facteurs

abiotiques tels que les UV et les ROS[83]. Enfin, le vieillissement des NMC dans l'environnement peut mener à des modifications de leur spéciation et biodisponibilité et ainsi modifier le impacts écotoxicologiques associés.

3. Interaction NMC et ETM: article de revue

Il est démontré dans cette article de revue de la littérature que l'adsorption des ETM sur les NMC dépend de paramètres du milieu comme le pH, la température et le rapport de concentrations NMC/ETM, des paramètres de l'expérience (par exemple le temps de contact), des propriétés et de la nature des NMC et des ETM utilisés. La plupart des études en écotoxicologie sur les effets conjoints d'une contamination NMC/ETM démontrent un changement dans le transfert des ETM dans les organismes représentatifs des agrosystèmes en raison de la présence de NMC. Aussi, la plupart des études ont montré des effets synergiques et/ou antagonistes sur la toxicité du cocktail NMC/ETM pour lesquels le modèle des effets additifs pour l'évaluation des risques n'est pas approprié dans de nombreux cas. Pour conclure, l'utilisation de marqueurs plus intégratifs devraient être envisagés pour évaluer correctement la santé des écosystèmes.

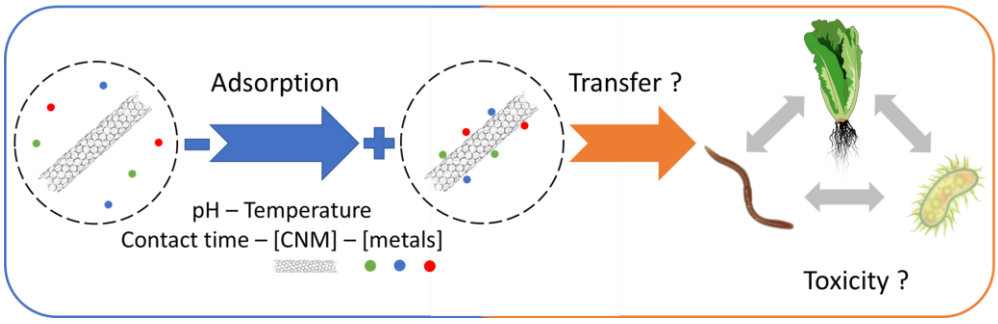

Carbon based nanomaterial interactions with metals and metalloids in terrestrial environment: a review

Mathieu Leroy[1,2], Emmanuel Flahaut[2*], Camille Larue[1*]

[1]Laboratoire écologie fonctionnelle et environnement, Université de Toulouse, CNRS, Toulouse, France, [2]CIRIMAT, Université de Toulouse, CNRS, INPT, UPS, UMR CNRS-UPS-INP N°5085, Université Toulouse 3 Paul Sabatier, Bât. CIRIMAT, 118, route de Narbonne, 31062 Toulouse cedex 9, France

*Corresponding authors: emmanuel.flahaut@univ-tlse3.fr; +00-33-(0)5-61-55-69-70; camille.larue@ensat.fr; +00-33-(0)5 34-32-37-55

Abstract: The use of carbon based nanomaterials (CNM) is diversifying and is being considered in so many sectors that their release into the environment is inevitable. Terrestrial ecosystems and particularly agrosystems are considered a major sink for CNM due to their accumulation in sewage sludge widely used for crop production. These ecosystems already accumulated other contaminants such as metals and metalloids which are more closely monitored to date. Although reviews about these contaminants considered individually have already been published, no review focused on their interactions and the impact of these interactions on their respective transfer and impacts on dwelling organisms (bacteria, earthworms and plants). Indeed, CNM and metal(loid)s can interact together as metal(loid)s are able to adsorb on the surface of CNM under the influence of diverse parameters such as pH, organic matter content or intrinsic CNM properties, among others. In ecotoxicity studies, interactive mechanisms (synergy and antagonism) were most of the time highlighted even though the underlying mechanisms are not yet fully understood. This work questions the current paradigm in use for risk assessment related to the additivity of the risks in presence of a cocktail of contaminants and *in fine* on the strategies to be applied in order to guarantee food safety.

Keywords: adsorption, carbon nanotube, cocktail effect, organism, metal(loid), toxicity, soil

Highlights:

- Metal(loid) adsorption on CNM depends on pH, contact time, temperature, CNM properties.
- Most studies demonstrate a change in metal transfer in organisms due to CNM presence.
- Most studies showed synergic and/or antagonist effect on the toxicity of the cocktail.
- Additive effect model for risk assessment is not appropriate in many cases.
- More integrative markers should be considered to properly evaluate ecosystem health.

3.1. Introduction

Scientific and industrial interest in carbon-based nanomaterials (CNM) continues to grow because of their remarkable properties and the applications they make possible[1]. A CNM is a nanomaterial essentially composed of carbon with any external dimension in the nanoscale or having internal structure or surface structure in the nanoscale (*i.e*. nanometric scale particles aggregated together)[1]. Among CNM, most have a structure based on graphene, a sheet of carbon atoms joined together in a hexagonal lattice, one atom thick, sp^2 bonded[2–4]. Over the years, the number of derived materials using graphene as a precursor grew up[5]. Examples include multilayer graphene, functionalized graphene materials such as graphene oxide (GO), carbon nanotubes (CNT), fullerene, and many metal-CNT composite

The potential applications of CNM are such that models already predict the evolution of their concentrations in natural ecosystems after release at the end of life of commercial goods in which they are included, or expected during their life cycle. For example, Sun al.[6] predicted that agricultural soils treated with sewage sludge are the main sink for CNT with an annual increase of 74 $ng.kg^{-16}$. Furthermore, the use of CNM as nanofertilizers[7], nanopesticides[8] and as decontamination agents[9] is also increasingly being considered.

Indeed, CNM are capable of adsorbing different compounds on their surface. Among these many compounds are metal(loid)s, which are elements present in natural conditions in biotope at concentrations below 100 $mg.kg^{-1}$ including copper (Cu), zinc (Zn), iron (Fe), manganese (Mn), molybdenum (Mo), boron (B), cobalt (Co), nickel (Ni), lead (Pb), cadmium (Cd), chromium (Cr), arsenic (As), and selenium (Se)[10]. Cu, Zn, Fe, Mn, Mo, and B are essential for plant growth, and Cu, Zn, Fe, Mn, Mo, Co and Se are essential to the growth and health of animals including human beings[11] while others are toxic (Ni, Pb, Cd, As). For example, it has been largely reported that CNT can adsorbed metal(loid)s in aqueous solution[12–17] and this ability raises questions about its influence on heavy metal transfer and subsequent impacts along food webs.

Agrosystems seems to be particularly suitable for the coexistence of both CNM and metal(loid)s (among others) due to cultural practices. Indeed, the continuous spreading of organic and inorganic fertilizers and the application of sludge from wastewater treatment plants have progressively led to the accumulation of both CNM and metal(loid)s in agrosystems[18–20].

Toxicological risk assessment of contaminants is usually carried out using additive models that do not take into account the interactions between contaminants and their underlying toxicological effects. For several years, metal(loid)s are submitted to a close monitoring in sludge and food to ensure safety for populations, but the emerging contaminants such as CNM are not yet regulated. Studies report that interactions (both synergy and/or antagonism) between contaminants can modify their transfer and toxicity to different organisms[21–30] (Figure 3).

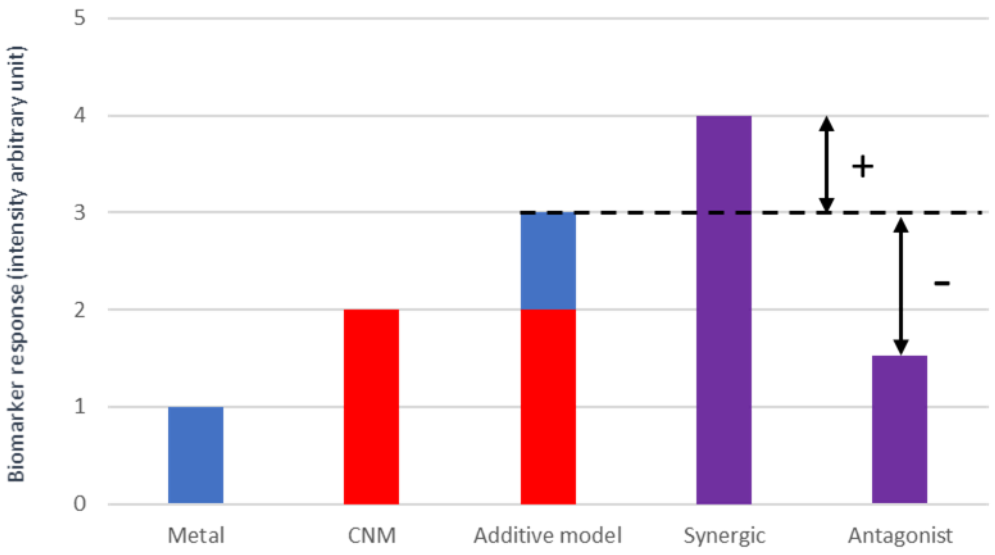

Figure 3 : Schematic differences on additive model compared to synergic and antagonist due to exposure to a cocktail of metal(loid) and CNM substances.

Tools have been developed to reveal possible interactions between stressors such as mixture of substances[31–33]. A meta-analysis by Vijver *et al.* aimed at predicting the response of organisms exposed to mixtures of metals (Cd, Cu and Zn) and showed that the frequency of occurrence of antagonism was 51%, and a synergistic response was detected in 28% of cases[31]. Thus, in nearly 80% of the cases,

interactive and non-additive patterns were demonstrated. This finding may lead to a profound questioning of the current risk assessment performed by the authorities.

The main goal of this work was to extensively review articles related to 1) CNM-metal(loid) interactions in aqueous medium to better understand implied mechanisms and the influencing parameters and 2) ecotoxicological studies related to simultaneous CNM-metal(loid) contamination and their consequences on the transfer and impacts on agrosystem organisms to reveal the extent of the interactive phenomenon.

3.2. Interaction CNM - metal(loid)s

3.2.1. Mechanisms of interactions between CNM and metal(loid)s

Several interaction mechanisms have been described between CNM and metal(loid)s and their predominance depends on the material considered. Interactions can be related to physical adsorption, chemical interaction, electrostatic attraction and sorption-precipitation[34–36].

For CNM with surface functional groups, the chemical interactions between CNM and metal cations is the most observed mechanism[16]. Metal cations are adsorbed onto the surface of CNM via oxygenated functional groups (*e.g.*, -COOH, -OH, or C=O) and then release a H^+ ion from the surface of the CNM (Figure 4, example for GO and CNT). The release of H^+ causes a decrease in the pH of the medium. The adsorption mechanism of divalent metal ions on CNM is illustrated according to the following equations (where CNM stands for carbon-based nanomaterials, and M for metal(loid)):

$$\mathrm{CNM-COOH + M^{2+} \rightarrow CNM-COOM^{+} + H^{+}}$$
$$\mathrm{CNM-OH + M^{2+} \rightarrow CNM-OM^{+} + H^{+}}$$
$$\mathrm{CNM-2COOH + M^{2+} \rightarrow CNM-COOMOOC + 2H^{+}}$$

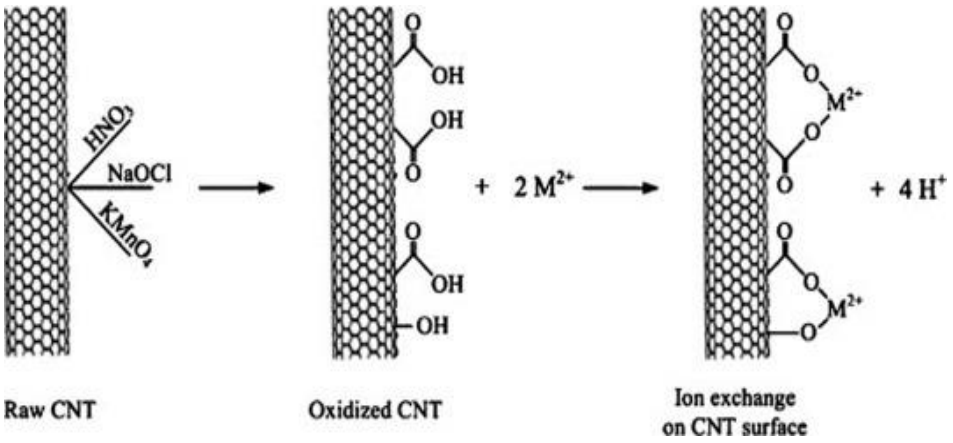

Figure 4 : Structure of carbon nanotubes (CNT) and their interactions with *metal cations* (=M^{2+}) (Figure adapted from Rao et al. (2007)[37])

Metal ion adsorption can also result from the combined effects of electrostatic attraction and sorption-precipitation processes[38,39]. Liang *et al.*[39] observed that Cd^{2+} ions were adsorbed on the surface of modified Al_2O_3-CNT *via* physical interactions as electrostatic interactions and van der Waals interactions occurred between Cd^{2+} ions and carbon atoms in the CNT[39]. On another study, following an increase in the pH value of the medium, Zn^{2+} ions were adsorbed more on the surface of the CNT due to the prevalence of carboxylate functions on their surface. The authors attributed this observation to the electrostatic interactions between the surface and divalent Zn^{2+} ions[40].

In addition, CNM have also been explored for the removal of anionic pollutants, such as phosphates (PO_4^{3-}), perchlorates (ClO_4^-) and fluorides (F^-), from aqueous solutions[41–43]. In contrast to the immobilization of cationic metal species, the mechanism of anion adsorption was previously attributed to electronic interactions with π electrons of the carbon sp^2 network[43]. This anion -π association is based on the interaction between the negatively charged anion with an electron-deficient aromatic ring on a graphene layer[43].

Finally, new adsorbents have also been prepared by modifying CNM with organic molecules that have a natural ability to complex metal ions. For instance, intrinsic functional groups on GO present a large variety and thus the specificity of interaction with given species of interest may be limited. To

counteract this, the number of adsorption sites may be increased by grafting compounds such as ethylenediaminetetraacetic acid (EDTA)[44] and chitosan[45].

3.2.2. Factors influencing the CNM - metal(loid) interactions in simplified media

3.2.2.1. CNM intrinsic properties

Due to the predominance of the adsorption mechanism by chemical interaction, it is obvious that the oxidation state of CNM influences the sorption of metal(loid)s on their surface. The greater the oxidation of the CNM, the more it provides oxygenated functional groups capable of interacting with the surrounding metal ions, regardless of CNM shape and size[9,46,47]. Similarly, following the same idea, the degree of reduction of the CNM acts on their adsorption capacity. The maximum adsorption capacity of rGO (12.6% of O) was much lower than that of GO (51.6% of O) due to the decrease in available oxygenated functional groups[48]. If the oxidation state can be tuned upon synthesis, it is very unlikely that it evolves in the natural environment (with the exception of fullerenes). Their reduction may however be easier to occur in environmental conditions. There are many examples of partial reduction of GO by natural molecules extracted from plant leaves[49]. However, enzymatic transformations of CNM are unfortunately often investigated using only pure enzymes and under laboratory conditions and they are consequently not very representative of enzymatic transformations in the natural environment[50]

The specific surface area (SSA, $m^2.g^{-1}$) strongly influences the adsorption of metals. In the case of graphene, most interaction sites with pollutants are present at the top and bottom faces[51,52], even if sites located at the edge may also play some role. While all the surface of monolayer graphene is available for the adsorption, multilayer graphene and CNT have internal layers respectively little or not accessible by adsorbates[51]. Similarly, it has been observed that single walled CNT are good adsorbents, which can be attributed to their high SSA. Practically, the measured SSA of graphene-based CNM is

generally very disappointing (often below a few tens of $m^2.g^{-1}$) when compared to the expected theoretical values (> 2600 $m^2.g^{-1}$ for graphene)[53] due to their significant agglomeration.

3.2.2.2. Environmental parameters

The relative concentrations of CNM and metal ions in the medium is an important parameter controlling adsorption phenomenon. To better understand these interactions, some theoretical model isotherms were developed, the most common being the Langmuir and the Freundlich models[54] according to the following equations:

$$Langmuir: \ q_e = k_L q_m C_e / \ (1 + \ k_L \ C_e)$$

$$Feundlich: \ q_e = \ k_F C_e^{1/n}$$

where q_e and q_m ($mg.g^{-1}$) represent equilibrium and maximum adsorption capacities, respectively; C_e ($mg.L^{-1}$) is the equilibrium aqueous concentration; k_L ($L.mg^{-1}$) the equilibrium constant and k_F and n the Freundlich constant.

These two models differ in particular by the fact that Langmuir model is considering the adsorption of a monolayer of atoms on a homogeneous surface and is empirical while Freundlich considers the adsorption of a multilayer of atoms on a heterogeneous surface and is a theoretical model.

Adsorption kinetics are generally described by diffusion models such as the pseudo-first-order and pseudo-second-order following the equations[54]:

$$Pseudo\ first\ order: \log(q_e - \ q_t) = \log q_e - \ k_1 t / 2.303$$

$$Pseudo\ second\ order: \ q_t = k_2 q_e^2 t / (t k_2 q_e + 1)$$

where q_t and q_e are the adsorption capacities ($mg.g^{-1}$) at time t and equilibrium, k_1 (min^{-1}) and k_2 (min^{-1}) are the rate constants of the pseudo-first-order, pseudo-second-order, respectively.

Results extracted from these models show that the main environmental factors affecting the adsorption of metal ions on the surface of CNM include the initial metal(loid) ion and CNM concentrations, pH, contact time, temperature, ionic strength and competition with other molecules. Table S1 summarizes the data found in the literature regarding CNM interactions with different metal(loid)s.

Regarding the intrinsic properties of the CNM and the properties of the experimental medium, which both influence the adsorption of metal(loid)s, a criticism can be raised related to the lack of reported experimental details in the literature. Indeed, out of the 102 CNM tested, the SSA was reported for only 48 of them. Furthermore, as the Freundlich and Langmuir models are thermodynamic processes, it is unfortunate that the study temperature was provided only in 56 cases out of 102. This lack of reporting makes the intercomparability of the studies impossible and thus weakens the conclusions and slows down the scientific progress, especially for the safer-by-design and nanoecotoxicity fields.

The average adsorption values from the Langmuir model for CNT, oxidized CNT and graphene oxide have been extracted from related articles for different metal(loid)s (Cd, Cr, Cu, Hg, Ni, Pb and Zn; Table 2).

Table 2: Mean of maximum adsorption (qm = mg.g^{-1}) of metal(loid)s (Cd, Cr, Cu, Hg, Ni, Pb and Zn) on the surface of carbon nanotubes (CNT), oxidized carbon nanotubes (CNT-oxidized) and graphene oxide (GO) in monoelemental conditions extracted from the reported studies in Table S1 described with Langmuir model. Data were selected on restricted pH range (4 < pH < 8) in which adsorption is favored (n_{tot}=117).

	Cd (n=20)	Cr (n=13)	Cu (n=17)	Hg (n=19)	Ni (n=9)	Pb (n=20)	Zn (n=19)
qm_{CNT}	12.4 (± 9.9)	3.1 (n=1)	22.9 (± 2.6)	24.4 (± 38.9)	11.1 (± 3.8)	30.9 (± 2.6)	35.6 (± 9.4)
$qm_{CNT\text{-}oxidized}$	35.9 (± 28.2)	21.3 (± 11.7)	37.4 (± 27.3)	27.3 (n = 1)	49.2 (n = 1)	75.7 (± 31.3)	24.4 (± 28.8)
qm_{GO}	306.9 (± 315.7)	-	183.3 (± 156.6)	-	84.4 (± 19.7)	1280.7 (± 516.5)	345.0 (n=1)

The adsorption of each metal(loid) appears to be always higher for GO than for CNT and oxidized CNT. Similarly, the oxidation of CNT promotes the adsorption of metal(loid)s since the average adsorption of metal(loid)s on the surface of oxidized CNT is higher for each metal (except Zn, probably related to the high variability for Zn adsorption onto oxidized CNT) than on the surface of raw CNT. On the basis of the data in Table 2, the sequence of adsorption affinities in mono-elemental conditions can be drawn up:

- for CNT: Zn≥Pb>Hg≥Cu>Cd≥Ni>Cr

- for CNT oxidized: Pb>Ni>Cu≥Cd>Hg≥Cr≥Zn.

It is also important to note that these adsorption experiments were carried out in mono-elemental conditions (one adsorbent + one ionic species) thus not considering potential ionic repulsions possibly induced if several ionic species would be present in the solution.

3.2.2.3. pH

The pH is a parameter that greatly influences the interactions between CNM and metal cations because it determines not only metal speciation but also surface charge of CNM and complexation behavior of functional groups[55,56]. Most of the studies in Table S1 evidenced that the adsorption capacity of CNM was affected by variations in the pH of the solution[34,37,57,58]. Adsorption of the metal(loid) is partly related to the point of zero charge (pH_{PZC}) of a given CNM; when pH > pH_{PZC}, cation adsorption is higher due to the electrostatic interactions between the cations and the negative surface charge of CNM. On the other hand, the adsorption of cations is lower when pH ≤ pH_{PZC} due to the neutralization of the surface charge of CNM, or even the presence of repulsive positive charges. A change in pH also affects competing complexing reactions and metal ion species[36]. Generally, the state of the divalent metal ions in solution depends on the pH. The most common species would be present in the form of M^{2+}, $M(OH)^{+}$, $M(OH)_2$ et $M(OH)_3^{-}$ depending on the pH of the medium due to hydrolysis[16,34,36]. It is

important to note that precipitation of metal cations may occur when the pH increases, which also affects the removal of metal ions[59].

3.2.2.4. CNM concentration

Increasing the concentration of CNM up to a certain point, increases the overall surface available for reactions and thus increases the sorption of metal(loid)s. For instance, adsorption of Ni^{2+}, Cd^{2+}, Cu^{2+} and Pb^{2+} increased with increasing CNT concentration in different experiments[35,37,38,60]. Similar results were also observed for GO[61]. However, beyond a threshold mass (specific to the CNM studied), the adsorption capacity reaches saturation and then decreases[15,61,62]. For a exposition of 50 $mg.L^{-1}$ of oxidized SWCNT, Moradi et al.[15] observed a maximum adsorption capacity up to 55, 68 and 90 $mg.g^{-1}$ for Cd, Cu and Pb respectively, while this adsorption decreased at 45, 58 and 82 $mg.g^{-1}$ with a exposition to 100 $mg.L^{-1}$. Indeed, beyond the threshold, an increase in the concentration of adsorbent could reduce the available sites because the effective surface area is likely to decrease due to homo-agglomeration, entanglement and/or folding of the CNM (depending on its morphology)[15,63]. In addition, metal ions can induce CNM agglomeration due to their interactions with carboxylic groups[64].

3.2.2.5. Ionic strength

Increasing the ionic strength of the solution can be achieved by increasing the concentration of an ion or in multi-elemental conditions by having several types of metal ions in the medium. However, this last experimental set-up even though more relevant in environmental context has been much less studied. The adsorption capacities of ions by CNM decreased with increasing ionic strength for two reasons : (i) the formation of double-layer electrical complexes between cations and CNM and (ii) the influence of the ionic strength on the activity coefficients of ions, which limit their transfer to the CNM surfaces[38]. In multi-elemental conditions, the increase in number of ions present in the media

decreases the part of metal ions adsorbed onto CNM. Affinity sequences of metal ions for adsorption sites could be deduced from these multi-elemental adsorption experiments (Table 3). For instance, Salam *et al.*[65] showed that ion binding affinity followed the order of Cu(II) > Zn(II) > Pb(II) > Cd(II) for MWCNT (initial metal concentrations = 1 $mg.L^{-1}$, pH = 7, contact time = 2h). For GO, Sitko *et al.*[66] observed another ranking of affinity: Pb(II)> Cu(II) > Cd(II) > Zn(II) (initial concentration = 1 $mg.L^{-1}$, GO = 0.1 $g.L^{-1}$, pH = 5, contact time = 2h). Metal precipitation related to the pH of the solution could explain differences observed on affinity sequences[67]. Furthermore, the addition of metals in the medium could increase the co-precipitation[68] and could modified the fitting of experimental adsorption measured with Langmuir and/or Freundlich modelling. To date, very little studies dealing with competitive adsorptions are available and more work needs to be carried out to understand the underlying mechanisms responsible for the establishment of these adsorption affinity sequences.

Table 3: Maximum adsorption capacity of different CNM established by adsorption models for various metal(loid)s in multi-elemental conditions extracted from the cited articles (SSA = specific area ($m^2.g^{-1}$), qm = maximum modelled adsorption ($mg.g^{-1}$), R^2 = correlation coefficient, C = metal concentration range ($mg.L^{-1}$), A = Adsorbent dosage ($mg.L^{-1}$), T = temperature (°C), Ct = Contact time (hours), RPM = agitation (Rotation Per Minutes))

M^{n+}	**Adsorbent**	**SSA**	**Isotherm model**		**C**	**A**	**Seq affinity**	**Parameters**				**References**
			Langmuir					**T**	**Ct**	**pH**	**RPM**	
			qm	R2								
Cd(II), Cu(II), Pb(II), Zn(II)	MWCNT	61.5			1	2500 to 15 000	Cu>Zn>Pb>Cd		2	7	400	Salam *et al.*[65]
Cu(II), Pb(II), phenol	N_2H_4–SH–Fe_3O_4/o-MWCNT		Pb: 40, Zn: 21, Phenol: 56	Pb: 0.91, Zn: 0.96, Phenol: 0.9	20 to 60	200	Pb>Cu	25	12	6		Jiang *et al.*[69]
Pb(II), Cu(II), Ni(II)	carbonaceous nanofibers	150.3	Pb: 470.3, Cu: 98.5, Ni: 64.6		0.1 to 0.6 $mmol.L^{-1}$ (Pb: 20.7 to 124.3 ; Cu: 6.5 to 39.3 ; Ni: 5.9 to 35 $mg.L^{-1}$)	200	Pb>Cu>Ni	25		5.5		Ding *et al.*[70]
Cd(II), Hg(II), As(II)	GO		Cd: 66.8, Hg: 55.4, As: 23.7			333.3	Cd>Hg>As					Alimohammady *et al.*[71]
Cd(II), Hg(II), As(II)	GO-3-aminopyrazole		Cd: 85.3, Hg: 74.6, As: 38.3		20	333.3	Cd>Hg>As		2	8	250	
Cd(II), Cu(II), Pb(II), Zn(II)	GO				5 µmol.g^{-1} of GO	100	Pb>Cu>Cd>Zn					Sitko *et al.*[66]

Cd(II), Cu(II), Ni(II)	GO membrane				0.1 to 1 mmol.L^{-1} (Cd: 11 to 112 ; Cu: 6 to 64 ; Ni: 6 to 59 mg.L^{-1})	200	Cu>Cd>Ni	30	12	5.5	150	Tan *et al.*[72]
Cd(II), Cu(II), Pb(II)	O-MWCNT		Cd: 3.3, Cu: 17.0, Pb: 34.0	Cd: 0.21, Cu: 0.97, Pb: 0.97	5 to 30	1000	Pb>Cu>Cd			5		Li *et al.*[38]
Ni(II), Zn(II)	SWCNT	700	Ni: 28.4, Zn: 29.5	Ni: 0.98, Zn : 0.98	10 to 80	500	Ni=Zn		12		180	Lu *et al.*[73]
Ni(II) and Zn(II)	MWCNT	459	Ni: 18.6, Zn: 19.4	Ni: 0.98, Zn: 0.98	10 to 80	500	Ni=Zn		12		180	

3.2.2.6. Contact time

As the contact time increases, the percentage of metal removal increases until an equilibrium is established[16,36]. The equilibrium depends on all the experimental parameters of the medium, including the initial concentration of metal ions. However, the two most important parameters on the adsorption kinetics of metals is the number of adsorption sites available for a given metal concentration and contact time[16,36].

3.2.2.7. Temperature

The most common observation is that sorption capacity increases with rising temperature[16,36]. For example, the sorption of Pb^{2+}, Cu^{2+} and Zn^{2+} on CNT is an endothermic process and increases with increasing temperature[14,74]. Similar results were observed for the same metals for GO[66]. Authors explained that the increase in temperature could lead to an increase in the rate of diffusion of ions through the outer boundary layer and into the pores of CNM due to a temperature-induced decrease in the viscosity of the solution[36,66].

3.2.3. Metal(loid) adsorption by CNM in complex media

Due to the increasing use of CNM, their potential in the agricultural and environmental fields and their interactions with metal(loid)s in simplified environments (aqueous solution), it is important to investigate how interactions investigated in simplified medium can be transposed in more complex environments. Various studies have thus recently been carried out (i) to characterize interactions of CNM with compounds that are widely found in ecosystems, such as organic matter (OM) and sedimentary matrices and (ii) to investigate the role of some key parameters.

3.2.3.1. Organic Matter

Humic substances generally represent a predominant part of the natural OM distributed in soils, sediments and water[75]. It has been reported that 3 to 28% of the OM dissolved in wastewater treatment plant effluents are humic substances[76]. They are hydrophobic organic acids mainly derived from soil humus and plants. These humic substances are often encountered in agrosystems especially due to the use of wastewater treatment plant effluents for fertilizing agricultural soils. Humic acid (HA) and fulvic acid (FA) are the two most important components of humic substances. It is expected that HA/FA will have a significant influence on the sorption of metal ions by CNM because the hydrophobic parts as well as the aromatic monomers of HA/FA have a strong affinity for CNM via hydrophobic and π - π interactions. At the same time, the hydrophilic fractions of HA/FA contain various functional groups (carboxyl, phenol, hydroxyl, amine and quinine) which can bind to metal(loid)s[77]. For instance, Lin *et al.*[77] observed that HA bound to the surface of MWCNT significantly favoured Pb(II) sorption (pH = 5.0) (Figure 3A). Similar results were also observed for the sorption of Cd(II) (pH = 6.0) on HA-coated MWCNT[78]. Additionally, OM can also increase the stability of CNM in suspension as the OM polymeric chains adsorbed to their surface tend to avoid each other in solution so as not to constrain the conformational space available to each of them inducing repulsive forces and thus decreasing the chances of homo-agglomeration[79,80] (and in turn increasing the potential available sites for metal(loid) adsorption) (Figure 3B and 3C). These interactions also depend on both pH and OM composition. Indeed, Sheng *et al.* reported an increase in the adsorption of Cu(II) on MWCNT due to dissolved HA/FA at pH < 7.5 (up to 90%), while a decrease was found at pH > 7.5 (to 80%)[81]. In parallel, Sun *et al.*[82] found that there was a higher binding affinity between Cu(II) and FA compared to HA, due to more oxygenated functional groups present in FA that could also complex with Cu(II) (pH = 6). Thus, it seems that there are different OM-metal(loid)- CNM interaction processes.

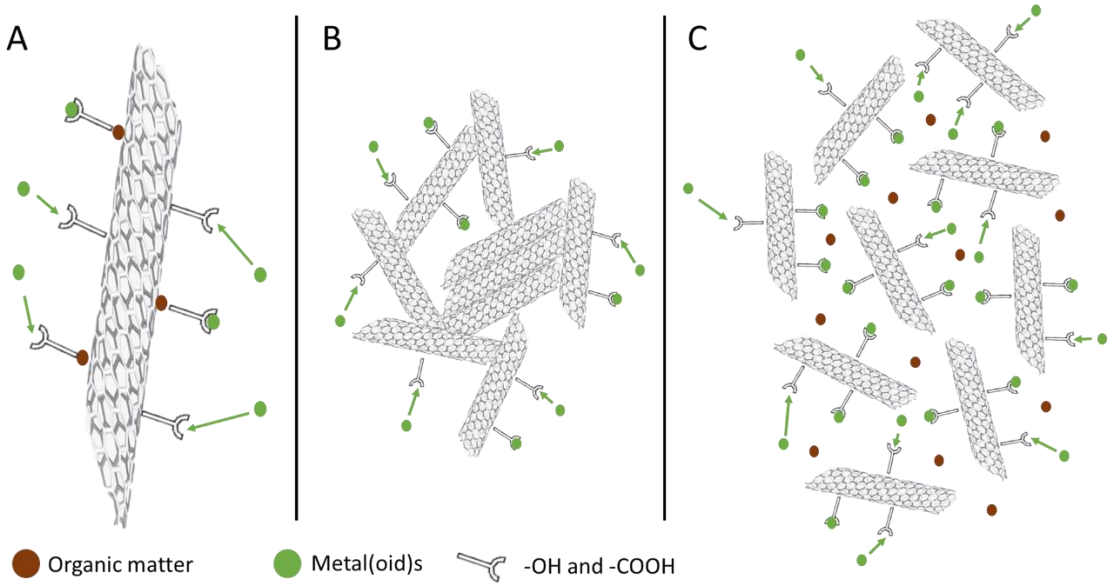

Figure 5 : Effects of organic matter (A) bound on CNT which increase metal(loid) adsorption onto CNT and (B-C) on the dispersion of CNT in media (B: without OM, C: with OM)

3.2.3.2.2. Soil

First of all, it should be reminded that due to the complexity of both soil and sediment, very few studies have been conducted to understand (i) what are the properties of these matrices that influence the mobility and/or agglomeration of CNM and (ii) the related mechanisms.

However, as in simplified conditions, CNM influence the fate of metal(loid)s in soil. For instance, a study revealed that Pb and Cu immobilization in soil increased with increasing MWCNT concentration correlated with the increased adsorption sites on the surface of CNT available for Pb and Cu ion adsorption[83].

These interactions between CNM and metal(loid)s in soil vary according to CNM intrinsic properties such as their morphology (diameter, length) and their surface chemistry (surface charge and functionalization)[84–86]. While it can be expected that the smaller the CNM, the higher their mobility in soils, it remains difficult to support this assumption from available data in the literature.

In addition, properties such as soil texture, structure, porosity, permeability, or type of clay contribute to the actual flow of CNM through the soil[84]. It appears that MWCNT[87,88] and GO[89] generally tend to have higher retention (low transport) in clay than in sandy soils. For example, the retention profile indicated that retention was higher in soil with smaller size sand particles (240 µm) than soil with higher size sand particles (607 µm)[90]. Lu *et al.* showed that the type of clay influenced CNM transport because the addition of 5% of kaolinite inhibited more graphene transport in soil column than montmorillonite and illite which presented the same particle size (Kaolinite: 28.0 µm, montmorillonite: 20.0 µm and illite: 23.9 µm) due to greater amounts of positively charged edge sites. Furthermore, the ionic strength of the soil solution is also a key parameter to consider. Indeed, Qi *et al.* demonstrated that the addition of 0.5 mM of Ca^{2+} significantly inhibited GO transport in clay soil in contrast to sandy soil by complexing with the surface oxygen of GO and soil components leading to enhance GO agglomeration and link GO with soil grains[91].

Several studies using Toxicity Characteristic Leaching Procedures (TCLP) determined the leachability of metal(loid)s in CNT-amended soils. For instance, Yang *et al.* [92] observed that the bioaccessible Sb content in a loamy soil was significantly reduced (20.7%) with the addition of 0.9 wt.% MWCNT compared to control (without CNT addition). In sandy soil, Vithanage *et al.* [93] did not observe any significant difference in extractable Sb at the tested MWCNT concentrations (0.5, 1 and 2.5 wt.%). The immobilisation and, consequently, the bioavailability of Sb differed between the two studies, which could be related to different texture and other related parameters (cation exchange capacity, structure, water holding capacity).

As in simplified medium, the interaction of CNM and metal(loid)s is metal dependent. Indeed, a study using 0.2, 1 and 5 wt.% GO in a historically polluted soil showed that the availability of Pb and Cu followed a dose-dependent relationship so that at the highest concentration of GO, their availabilities relative to the controls were found to be reduced by 2.5% and 5.6% respectively. This decrease was much smaller for Zn and Cd (*ca.* 1%) and As availability was increased by 191%[94]. Regarding the kinetics,

it seems that reaching the equilibrium takes much longer in more complex environments than in simplified medium. For example, Song *et al.*[95] observed that in soil solution the adsorption of Cd^{2+} on MWCNT reached 65% after 7 days and up to 87% and 88% after 30 and 60 days, respectively. To compare with aqueous media, the time to reach equilibrium does not exceed 12 hours (Table S1).

Overall, more studies involving solid matrices under environmentally relevant conditions need to be carried out as the risk of CNM release into the environment is increasing. It is important to understand all the physico-chemical characteristics of soils affecting the interactions among contaminants in order to better predict their transfer and toxicity in the environment and along trophic chains.

3.3. Metal(loid)s, CNM and CNM-metal(loid) complex uptake and impacts on agrosystem organisms

3.3.1. Uptake and impacts of metal(loid)s and CNM as single contaminant

The toxicological impacts of metal(loid)s and CNM and their potential consequences on agrosystems have been widely studied. Thus, the scientific corpus available is abundant and compiled in several scientific articles for microorganisms[96–101], invertebrates[96,102–106] and crop plants[19,96,101,102,107–110] which are the major organisms of agrosystems due to their functions and interactions. This corpus is regularly updated according to the technical advances, offering a step further on the scientific knowledge in these fields of research especially for metal(loid)s due to older knowledge.

Microorganisms are essential for many agrosystem services like mineralization, C, N and P biogeochemical cycles and because of their interactions with plants like mycorrhizal association[111]. Microorganisms are capable of accumulating metal(loid)s, this accumulation is generally governed by the sorptivity of the cell envelope and the ability to absorb metal(loid)s into the cytosol[112]. The metal membrane transporters are not highly selective and thus metal(loid)s can be taken up through this pathway[112,113] leading to alterations in the microorganisms at different scales. Metal(loid) toxicity could occur through displacement of essential metals from their original binding sites or through ligand

interactions and conformational structure alterations with oxidative phosphorylation and osmotic balance[114]. Damage to the DNA structure, the cell membrane and the activity of some enzymes was also reported[97,98,115–117]. Thus, metal(loid)s can affect the microbial population by decreasing their growth/proliferation, and altering their morphology and biochemical activities[100,118]. Due to these alterations, the functions performed by microorganisms such as the decomposition of organic matter[97,98], C sequestration or N fixation could be negatively impacted[98,99,119]. According to a study that compiled the lowest metal(loid) amount added that resulted in a decrease in the rate of basal respiration (LOAED), the mean LOAED for Hg, C, Cu, Pb, Ni, Cd, Zn was 257, 411, 500, 506, 576, 594 and 697 $mg.kg^{-1}$, respectively (Table S2)[98].

In parallel, for CNM, transmission electron microscopy observations have evidenced that they may interact strongly with bacterial cell membranes. These interactions may disrupt the integrity of the membrane structure by oxidative stress and/or physical damage, allowing CNM to be internalized in bacteria[120–122]. In addition, a majority of studies has observed a decrease in soil microbial activity following exposure to CNM[122–127]. CNM would present an antimicrobial potential since a whole set of studies reported a loss of viability following exposure[123,124,128–130]. Changes in microbial community structure have also been reported[123,126,131,132] . Finally, microbial functions such as mineralization, N and CO_2 fixation could be decreased[133]. The effect of CNM on microbial activity[122] and biomass appeared at 85 $mg.L^{-1}$ and 1-5 $mg.g^{-1}$, respectively[124,126,127].

Oligochaetes are considered as soil engineers because of their involvement in physical and chemical processes such as litter mixing, soil porosity, active soil water transport, OM mineralization and nutrient mobilization and cycles[134–136]. These organisms present two pathways of contamination: the oral pathway by ingestion of soil and the tegumentary pathway by contact with soil. After absorption, metal(loid)s can accumulate in the posterior alimentary canal[137]. Metal(loid)s may decrease the growth of earthworms through delayed biomass gain[138–141] and act on energy reserves by decreasing the production of lipid reserves[142,143] and modifying the gut microbiota[144]. In addition, morphological and

behavioural changes have been demonstrated following exposure to metal(loid)s[145]. It was observed that metal(loid)s can interfere with earthworm reproduction by reducing the number of juveniles produced[138,139,146] induced by a reduction of number of sperm produced[147], the production of cocoons[138,141,146,148–150] and the success of cocoon hatching[139,151,152]. Median lethal concentrations (LC_{50}) of metal(loid) after a 17 day exposure were on average 97, 663, 756, 791, 836, 1415, 7542 $mg.kg^{-1}$ for As, Cu, Ni, Cd, Zn, Cr(III) and Pb, respectively[103].

For CNM exposure, it has been demonstrated that earthworms are able to eliminate orally ingested CNM by depuration thus limiting the toxicity of these contaminants[153–155]. As a result, many studies have not observed any apparent effects on earthworms following CNM exposure[154,156,157]. However, few works reported DNA damages[158,159] and a decreased cocoon production[160] (up to -60% and -78% at 495 and 1000 mg $DWCNT.kg^{-1}$ food). According to Scott-Fordsmand *et al.*[160] and Hu *et al.*[158], the median effective concentration (EC_{50}) for earthworms exposed to DWCNT and MWCNT would be >500 and 1480.3 $mg.kg^{-1}$ for growth and mortality, respectively.

Plants can take up metal(loid)s from the soil through their roots, transport them through the xylem and accumulate them in the different tissues of all organs (roots, stem, leaves, grains and fruits) by symplastic and apoplastic pathways[161]. Generally, the roots tend to accumulate metal(loid)s such as Al, Cd, Cr, Cu, Hg, Ni, P and Zn, vegetative parts have a lower accumulation level and the reproductive parts tend to exclude them[162,161]. During their transport in the plant, metal(loid)s are largely bound to the cell walls, which explains why most of the metal(loid)s are bound in the roots (about 75-90%) and a smaller fraction in the shoots[161]. However, some particularities exist and accumulation is a function of the stage of development of the plant and the metal(loid) considered[161]. The stress imposed by meta(loid)l accumulation can induce reactive oxygen species (ROS), promote DNA damage, impair functional membrane integrity, nutrient homeostasis and disrupt protein and enzyme function and activity[163–165]. These toxic effects lead to a slowing down of cellular parameters, *i.e.* a reduction of photosynthetic activity, lipid production[107,166], plant growth parameters, and consequently of the

yield[107,166–172]. The phytotoxicity of the metal(loid)s under their ionic form follows the trend (from most to least toxic): Pb≈Hg > Cu > Cd≈As > Co≈Ni > Zn > Mn, with median toxic concentrations of : 0.06, 0.09, 0.13, 0.56, 0.67, 1.00, 1.12, 1.63 and 2.53 $mg.L^{-1}$ (hydroponic exposure)[173].

Although the entry mechanisms of CNM are not well known, it is established that they can interact with plants at the root system level. Once absorbed, they can share the vascular system with water and nutrients and can be transported by transpiration in the upper part of the plants[96]. Several studies have observed CNM accumulations in all parts of the plant[110,174,175]. CNM can act on plants starting from the seed germination process with a trend to activate and increase the seed germination rate[176–179]. The scientific corpus of research on the effects of CNM reports contrasting effects on plant growth and physiological status. It reports an increase, a decrease or even a neutral effect on growth parameters (root system, biomass production, flowers and fruits)[110,174]. In case of toxicity, it was associated with generation of ROS, antioxidant activity, necrotic lesions of cells and leaf tissues as well as root and leaf morphological changes, decreased chlorophyll, and programmed cell death[180–183]. The inherent properties of CNM (functionalization, length, diameter) and experimental designs (exposure medium, duration, plant species) could be a reason for the observed variability in CNM toxicity. The mean “lowest observed effect level” (LOEC) for plants exposed to CNT was 389 $mg.L^{-1}$ according to Jackson *et al.* [120].

Regardless to LOAED, NOEC, LOEC and EC_{50}, it seems that metal(loid) concentrations needed to induce toxicity were much lower than those required for CNM.

Table 4: Effects of simultaneous CNM-metal(loid) exposure on transfer and associated toxicity for three representative agrosystem organisms (bacteria, earthworms and plants). The light blue lines represent studies with hydroponic exposure and the dark blue lines represent studies with soil exposure (SOD = superoxide dismutase, POD = peroxidase, MDA = malondialdehyde, CAT = catalase, GR = glutathione reductase, GP = glutathione peroxidase, Chlo = chlorophyll, n.p = data not provided).

Type and CNM concentration	CNM size	Type and metal(loid) concentration	Organisms	Exposure medium	Exposure duration	Transfer effects	Interactive toxicological effects	References
GO (0, 1 and 10 mg.kg^{-1})	n.p	Cd (0 and 1 mg.L^{-1})	Plant: *Oryza sativa*	Culture solution	30 days	Increase of Cd transfer: +15% and +32% of Cd in roots and shoots with addition of 10 mg.L^{-1} GO compared to control (without GO with Cd)	No interactive effects on germination and dry biomass of roots and shoots	Li *et al.*[23]
GO (0.1, 1, 10 mg.L^{-1})	n.p	As (0 and 10 mg.L^{-1})	Plant: *Triticum aestivum*	Water	n.p	Compared with the 19.9% rate of As uptake recorded without GO exposure, the uptake rate of As increased to 24.6% and 32.1%, then decreased to 16.1% in the presence of GO concentrations of 0.1, 1 and 10 mg.L^{-1}, respectively	Synergic effects in the presence of both contaminants: reduction of root number and fresh biomass, reduction of root length, increase of antioxidant enzymes activity (SOD and POD), decrease of photosynthetic pigments (chlo a/b)	Hu *et al.*[24]
GO (0, 1, 2.5, 5, 10, 20, and 40 mg L^{-1})	n.p	Cd (0, 1, and 5 mg.L^{-1})	Plant: *Triticum aestivum*	Water	7 days	Increase of Cd transfer in roots and leaves at every GO and Cd concentrations tested.	Synergic effects: decrease in dry mass of roots and shoots, decrease in chlorophyll concentration and rubisco, increase in H_2O_2 and O_2 concentration in roots and leaves, increase in antioxidant enzymes activity (MDA, POD and SOD)	Gao *et al.*[25]

GO (0, 30, 60 mg.L^{-1})	n.p	Cd (0 and 2 mg.L^{-1})	Plant: *Lactuca sativa*	Culture solution. Addition of GO on foliar way.	28 days	n.p	Antagnist effects: increase in dry mass, photosynthetic parameters (quantum yield, chlorophyll a and total chlorophyll content and electron transfer rate), decrease in O_2 concentration in leaves and roots, activity of antioxidant enzymes (SOD, CAT, GR, GP) and glutathione concentration	Gao *et al.*[184]
GO (0, 30, 60 mg.L^{-1})	n.p	Cd (0 and 2 mg.L^{-1})	Plant: *Lactuca sativa*	Culture solution. Addition of GO on foliar way.	28 days	Decrease of Cd transfer: - 19 and -9% of Cd in roots with the addition of 30 and 60 mg.L^{-1} of GO respectively, - 33% of Cd in leaves with 30 mg.L^{-1} of GO	Antagnist effect on the number and diameter of roots and the concentration of vitamin C	Gao *et al.*[26]
GO (1.0, 2.5, 5.0, 10, 20, and 40 mg.L^{-1})	n.p	Cd solution (1.0 and 5.0 mg.L^{-1})	Plant : wheat seedlings	Culture solution	n.p	n.p	Decrease in roots growth and microtubule protein. Increase on cytochrome P450	Gao et al.[185]
MWCNT (0, 100, 500, 1000 mg.kg^{-1})	Length: 3–12 µm, diameter : 12–15 nm, SSA : 245,28 $m^2.g^{-1}$	Cd and As (Cd: 1.41 mg kg^{-1}, As: 54.80 mg.kg^{-1})	Plant : *Solanum nigrum L.*	Natural soil	60 days	No effect on Cd transfer with the addition of MWCNT. Decrease on As in stem (-25%) at 100 mg.kg-1, in leaf (-31%) at 1000 mg.kg^{-1}	Increase in antioxidant enzymes activities (MDA, PRO and APX)	Chen et al.[186]

FNCB (10 $mg.L^{-1}$)	Diameter : 47.35 ± 1.67 nm, SSA: 635.96 $m^2.g^{-1}$	Cd (20 and 60 $mg.L^{-1}$)	Worms (*Eisenia fetida*) cells (coelomocytes)	Culture plate	12H	Decrease on Cd transfer (-31%) in supernatants at 60 $mg.L^{-1}$ of FNCB. Increase on Cd transfer (+37%) in free Cd conetent inside cells	No effect on viability of coelomocytes	Xu et al.[187]
GO (1000 and 2000 $mg.kg^{-1}$)	n.p	Cd (0.1 $mg.kg^{-1}$)	Bacteria	Soil	3-15-60 days	n.p	No Interactive effect but the addition of GO changes in the composition and diversity of the bacterial community	Xiong *et al.*[188]
MWCNT (0, 10, 50, 100 $mg.kg^{-1}$)	Length = 5–30 µm, diameter < 8 nm	Cd (0, 2.0 and 10 $mg.kg^{-1}$)	Earthworms: *Eisenia fetida*	Soil	14 days	Decrease in Cd concentration: at 2 $mg.L^{-1}$ of Cd -24%, -18%, and -12% with addition of 10, 50 and 100 $mg.kg^{-1}$ of MWCNT. Decrease more pronounced at 10 $mg.L^{-1}$ of Cd (-42%, -34%, -26% of Cd with addition of 10, 50 and 100 $mg.kg^{-1}$ of MWCNT).	There appear to be an interaction: decreased percentage of inhibition of worm growth, detoxifying enzymes, and metabolites for the lowest the MWCNT concentration.	Yang *et al.*[32]
GO spheres (5 $mg.L^{-1}$)	n.p	Cu (0 and 240 $mg.L^{-1}$)	Plant: *Triticum aestivum*	Soil	14 days	Reduction of transfer: decrease of Cu concentration in roots and stems by 60% and 67% and it was similar in leaves (increase only in 2%) with addition of GO compared to the control (without GO with Cu)	No interactive effects growth parameters (biomass, root, stem and leaf lengths). cellular: photosynthesis, transpiration and stomatal conductance	Zhao *et al.*[21]
GO (1000 and 3000 $mg.kg^{-1}$)	n.p	Cd (0 and 10 $mg.kg^{-1}$)	Plant: *Oryza sativa*	Soil	40 days	Increase in Cd with 3000 $mg.kg^{-1}$ addition of 12.5% in total rice biomass compared to control (no GO with Cd)	No interactive effects on the growth parameters studied (fresh biomass and size)	He *et al.*[22]
MWNCT (0, 100, 500, 1000 and 5000 $mg.kg^{-1}$)	n.p	Cd (22.4 $mg.kg^{-1}$)	Plant: *Boehmeria nivea*	Natural soil	60 days	Increase in Cd concentration: in leaves by +15%, +12% and +9% at 100, 500 and 1000 $mg.kg^{-1}$, in stems by +33% and +28% at 100 and 500 $mg.kg^{-1}$. Decreased Cd transfer: in stems by -10% at 5000 $mg.kg^{-1}$, in roots by -22%, -21%, -29% and -30% at 100, 500, 1000, 5000 $mg.kg^{-1}$	Interactive effects: increase in leaf dry mass with the addition of 1000 $mg.kg^{-1}$ of MWCNT, stem dry mass at 500 $mg.kg^{-1}$ of MWCNT and root dry mass at 500 and 1000 $mg.kg^{-1}$ of MWCNT, increase in H_2O_2, MDA concentration and SOD activity from the addition of 100 mg. kg^{-1} of MWCNT and decrease of POD activity from 100 $mg.kg^{-1}$ of MWCNT	Gong *et al.*[27]

MWCNT (0, 100, 500, 1000 mg.kg^{-1})	Length: 3–12 µm, diameter : 12–15 nm, SSA : 245,28 m^2.g^{-1}	Cd and As (Cd: 1.41 mg kg−1, As: 54.80 mg.kg^{-1})	Plant : Solanum nigrum L.	Natural soil	60 days	No effect on Cd transfer with the addition of MWCNT. Decrease on As in stem (-25%) at 100 mg.kg-1, in leaf (-31%) at 1000 mg.kg^{-1}	Increase in antioxidant enzymes activities (MDA, PRO and APX)	Chen et al.[186]
MWCNT (0, 0.1 and 10 mg.kg^{-1})	Lenght = 1 to 20 µm, average diameter of 16.8 ± 6. 7 nm	Two types of soil with two contaminatio n level on 3 metals: 1 = Cd : 13, Pb : 524 and Zn : 689 mg.kg^{-}1) and 2 = Cd : 28, Pb : 1471 and Zn 1825 mg.kg^{-1})	Plant: *Lactuca sativa,* earthworms*:* *Eisenia fetida* and native soil bacteria	Natural soil	42 days	In lower contaminated soil: no effects on metals transfer for earthworms. Increase in Cd (+37%) and Zn (+21%) transfer with 10 mg.kg^{-1} of MWCNT for lettuces. In higher contaminated soil: increase in Pb (+34%) and Zn (+25%) transfer with 10 mg.kg^{-1} of MWCNT for earthworms. Decrease in Cd (-29%) and Zn (-30%) transfer with 0.1 mg.kg^{-1} of MWCNT for lettuces.	Interactive effects on higher contaminated soil: biomass reduction for lettuces exposed to 0.1 mg.kg^{-1} of MWCNT. Increase in flavonoid concentration with 10 mg.kg^{-1} of MWCNT.	Leroy *et al.*[30]

396

3.3.2. Impacts of the interaction between metal(loid)s and CNM

After an extensive literature survey on the topic, only articles focusing on CNT, graphene and GO together with a proper statistical analysis were kept for this review. Considering studies evaluating both the transfer and the toxicity of metal(loid)s and CNM (Table 4) (11 studies), 18% focused on bacteria, 18% on earthworms and 82% on plants. Among these studies, about 64% reported interactive toxicological effects due to the simultaneous presence of CNM and metal(loid)s. Within these interactive effects, when all control conditions were set-up (without metal(loid) and without CNM contamination, metal(loid) alone, CNM alone), we could distinguish antagonist (18%) and synergic (18%) effects (Figure 3).

3.3.2.1. Bacteria

For bacteria, very few studies have been conducted. Furthermore, in the available articles the experimental design did not permit to highlight the existence of interactive effects since the impact of CNM alone or metal(loid)s alone were not tested (not the purpose of the study). However, a study using soil contaminated with Cd (0.1 $mg.kg^{-1}$) and GO (1000 and 2000 $mg.kg^{-1}$) evidenced a decrease in soil microbial diversity after addition of GO, indicating that the microbial communities in the Cd-contaminated group without GO were more diverse than those in the treated groups (Cd x GO)[188]. In addition, authors observed some changes in bacterial communities after addition of GO with an increase in several bacterial abundances (*Acidobacteria* and *Actinobacteria*) compared to single Cd contamination and a decrease in phyla such as *WD272* and *TM6* revealing phylum-specific sensitivities[188]. Interestingly, the abundance of *Rhodospirillales* and *Nitrospirae* which are symbiotic N_2-fixing bacteria was reduced at 3 days and then restored at 15 and 60 days evoking some resilience in the ecosystem.

These few studies alone do not allow generalization to be made and highlight the need to initiate more studies on microorganisms with simultaneous CNM and metal(loid) exposure. Indeed, due to

adsorption of metal(loid)s on CNM and to CNM strong interactions with bacterial cell membranes, CNM could be a vector to increase metal(loid) transfer to microorganisms and associated toxicity or depending on their interactions with soil particle they could also mitigate the metal(loid) toxicity (*i.e.* the complex CNM-metal(loid) could adsorb to soil particles making metal less bioavailable to bacteria cells and thus less toxic).

3.3.2.2. Earthworms

Studies focused on earthworms report contrasting results of the addition of CNM on metal(loid) transfer and toxicity. Yang *et al.* observed a decrease of Cd transfer (antagonist effect) ranging from -43% to -31% with the addition of 10 $mg.kg^{-1}$ and 100 $mg.kg^{-1}$ of MWCNT, respectively after 14 days of exposure in the model *Eisenia fetida* (Cd: 10$mg.kg^{-1}$)[32]. The decrease in Cd transfer was thus inversely proportional to the dose of MWCNT. Additionally, the change in transfer was also metal dose-dependent: at 10 $mg.kg^{-1}$ MWCNT, a -43% decrease was noticed at 10 $mg.kg^{-1}$ of Cd but decreased to -28% at 2 $mg.kg^{-1}$ of Cd. In agreement with transfer results, the addition of MWCNT decreased earthworm growth inhibition caused by Cd, detoxifying enzymes and metabolites[32]. At the highest Cd concentration (10 $mg.kg^{-1}$), a growth inhibition rate of 27% was registered in comparison with earthworms exposed to control conditions (no Cd, no MWCNT), this rate was decreased to 8% and 22% at 10 and 100 $mg.kg^{-1}$ of MWCNT, respectively.

In contrast, Leroy *et al.* rather observed synergic effects of metals and CNT when earthworms were exposed to two contaminated soils (Zn, Pb and Cd) and demonstrated either no impact of the addition of MWCNT on metal uptake in one soil or an increase up to +34% and +25% of Pb and Zn in the second soil (with no impact on Cd transfer) after 6 weeks[30]. Furthermore, when an increased uptake was detected it was CNT dose dependent. Even though earthworms are able to eliminate orally ingested CNM by depuration, it appears that CNM ingestion could lead to metal release in earthworm tissues,

maybe due to changing physico-chemical conditions in the gut (especially pH) leading to desorption. Despite transfer increase, no toxicological effects were found.

The difference between these articles could partly be explained by different soil texture. Indeed, the first one which induced Pb and Zn transfer increase upon CNT addition had a lower OM content than the other soil. Authors reminded that a low OM is less favorable for earthworm feeding an burrowing activities[189] and thus metal transfer[30,190].

3.3.2.3. Plants

Among studies on the transfer and toxicological impacts of simultaneous contamination with CNM and metal(loid)s on plants (9 studies reviewed), 89% present results on the transfer of metal(loid)s from the exposure medium to the plants and 100% on toxicity. In the transfer studies, 91% of the studies showed CNM - metal(loid) interactions with either an increase[24,23,25,21,22,27,30,191,192] and/or a decrease[21,24,26,27,29,30] of metal(loid) transfer differing from the additive risk model.

Furthermore in the studies evidencing a synergic effect with an increased uptake of metal(loid)s, some authors demonstrated a dose dependent effect of the addition of CNM on the transfer of metal(loid)s both in hydroponics and in soil[21–29]. For example, Gao *et al.* found that the addition of GO to a Cd contaminated medium (1 $mg.L^{-1}$ Cd) led to a dose-dependent increase in Cd concentration in both roots and leaves: the addition of 5 $mg.L^{-1}$ of GO increased by 12% the Cd concentration in leaves while an addition of 40 $mg.L^{-1}$ led to a 50% increase[25]. Hypotheses such as facilitating metal entry into root cells due to interactions between CNM and root cells and/or uptake of CNM with surface adsorbed metals may explain the increased transfer observed in these examples. Additionally, it seems that at high concentrations, CNM may have a different impact than at lower concentrations in the medium[24,30]. Indeed, wheat plants exposed to As(III) took up 20% of this As while the uptake rate of As increased to 25% and 32% in presence of GO concentrations of 0.1 and 1 $mg.L^{-1}$, then decreased to 16% at 10 $mg.L^{-1}$ [24]. Likewise, Leroy *et al.* also observed contrasted results depending on CNM

concentrations and explained these results by CNM dispersion in the medium (soil): at low concentrations (0.1 mg.kg^{-1}), CNT may be better dispersed in the soil than at higher concentration (10 mg.kg^{-1})[193,194] offering thus, a higher exchange surface and higher adsorption. This hypothesis is supported also by the study of Zhang *et al.* in which the authors observed that the agglomeration of CNT decreased the adsorption of some organic compounds[193]. Several hypotheses can be suggested for this increased uptake: CNM with adsorbed metal(loid)s can act as vectors by damaging root cell walls and facilitate metal(loid)s entry in crops tissues or this complex might accumulate in the rhizosphere and lead to an enhanced metal release with the pH modification at the vicinity of the root surface.

When an increased transfer of metals due to the presence of CNM in the medium was detected, it was mostly accompanied by an increased toxicity. Indeed, among the studies that investigated the toxicological impacts of simultaneous contamination, 75% of them found interactive effects highlighting an increase in oxidative stress[24,25,27–29,184], decrease in different plant components[24–26,29,184,195] (chlorophyll, protein, sugar) and in plant biomass[24–29,184,195,196] (Table 4). For instance, synergistic effects were evidenced on rubisco concentration : indeed a decrease by 53% was detected in the presence of both Cd (5 mg.L^{-1}) and GO (40 mg.L^{-1}) while Cd alone reduced it by 14.5% and GO alone by 18.5%; additive model would have suggested a decrease by 33% ((-14.5%) + (-18.5%)) = -33%) much lower than the 53% observed here[25]. This observation was similar for other parameters (root and shoot biomass, chlorophyll, O_2 and H_2O_2 concentrations) and more pronounced with higher Cd and GO contamination. Similarly, Hu *et al.* demonstrated that the addition of GO (10 mg.L^{-1}) decreased plant development and photosynthetic pigments concentrations together with an increase in antioxidant enzymes activities (SOD and POD) in *Triticum aestivum L.* exposed to As solution (10 mg.L^{-1})[24]; for instance after exposure to the co-contamination SOD increased by 426%, while it increased by

56% after exposure to As alone and decreased by 4% after exposure to GO alone (additive model would suggest a 52% increase).

However, some studies also highlighted antagonist interactions between metal(loid)s and CNM with a decrease in the transfer of metal(loid)s from soil to plants and finally lower or no toxicity symptoms[26–29,184]. These effects can also be organ dependent. Indeed, Zhao *et al.* showed that GO-chitosan spheres significantly decreased Cu bioaccumulation in roots (-60%) and stems (-67%) of wheat compare to single metal contamination, but not in leaves (almost similar with an increase of Cu bioaccumulation around +2%)[21]. Despite changes in Cu transfer with the addition of GO, the co-exposure did not impact growth parameters studied (root, stem and leaf length) but decreased the photosynthetic rate and stomatal conductance up to -58% and -34%, respectively. Likewise, Gong *et al.* found similar pattern with a decrease in Cd bioaccumulation in roots up to -22% upon MWCNT addition (100 $mg.kg^{-1}$) and an increase in Cd accumulation in stem and leaves up to +15% and +33%, respectively[27]. These differences on metal bioaccumulation according to plant organ could reflect a plant defence strategy. It is known that plants have defence mechanisms against metal(loid) exposure like accumulating metal(loid)s in specific compartments of the plant such as cell walls and leaves to reduce their toxicity[197].

There are some disparities on transfer and toxicity of CNM-metal(loid) simultaneous exposure. The adsorption mechanism alone does not seem to explain such disparities and the concentration in CNM, which directly affects their dispersion and aggregation in the medium, could be a possible explanation.

Although the studies carried out in liquid media (water, culture solution, soil solution, etc.) are a first approach privileged at the beginning of new researches on new substances, they do not allow to apprehend the complex relations between solid matrix and contaminants since some studies show their importance to determine the fate of contaminants in organisms[30]. Indeed, the type of soil could explain differences observed on interactive effects on transfer and toxicity due to the strong influence

of soil physico-chemical parameters (clay, OM, pH *etc.*). Whatever the types of interactive effects, these largely dominate in the studies compared to additive effects used in risk assessment.

3.4. Conclusion – Knowledge gaps and Perspectives

In 2012, the European Commission stated that they are “committed to ensuring that the risks associated with chemical mixtures are properly considered and assessed”. In parallel, in 2019, the European Environmental Agency warned again about the "cocktail effect" of chemical pollutants, especially those found in European waters, whose cocktail effects are assumed or proven[198]. However up to date lots of progress remain to be done on that matter.

Indeed, after reviewing extensively the literature, we can conclude that strong interactions exist between CNM and metal(loid)s which have been demonstrated in simplified medium (solution) and whose impacts are visible in the environment by modifying the behaviour of contaminants in cocktail and their impact on organisms. These interactions include physical adsorption, chemical interaction, electrostatic attraction and sorption-precipitation. In the environment, the vast majority of studies concluded that these interactions modify the fate (uptake and toxicity) of these contaminants in cocktail in comparison with an additive model. The nature of the impact (synergic or antagonist) is influenced by many parameters : 1) CNM nature which influences metal(loid) adsorption capabilities, 2) CNM concentration which influences their behaviour, in particular their agglomeration, 3) CNM morphology and SSA as well as adsorption abilities and CNM transfer through biological barriers, 4) metal(loid) nature and number of different metallic species because of their specific affinity and potential competition and repulsion for adsorption sites onto CNM, 5) exposure medium which influences CNM and metal(loid) behaviour, 6) soil characteristics (clay content, OM and pH) which influence metal(loid) adsorption onto CNM as well as organism behaviour and 7) type of organisms (crops, earthworms or bacteria) and environmental relevance of exposure conditions (exposure pathways, organism lifestyle, organism interactions, etc.). So, in conclusion, the additive model used

so far for risk assessment of chemical substances in mixture is not relevant; instead a multiplicative model which integrates synergy and antagonism would seem more suitable with correction factors for the different influencing parameters highlighted in this review to encompass processes which remain unclear so far and leading to seemingly contradictory results in the literature.

Knowledge gaps

The knowledge gaps we identified through this literature survey are listed below:

(1) More information on CNM characteristics are needed in the articles to further understand contrasted results observed on transfer and toxicity.

(2) The use of element speciation models (such as Minteq or ChemEQL among others) in solution and their comparison with experimental data and their fitting with Langmuir or Freundlich equations would be interesting to identify if these models could give relevant predictions, especially in multi-metallic conditions.

(3) More studies need to be conducted on agrosystem organisms to have more information on the toxicological effects resulting from exposure to a mixture of contaminants. For instance, only 3 metal(loid)s (Cu = 1, As = 1 and Cd = 8, studies and one study with Cd, Pb and Zn simultaneously) were tested in interactions with CNM, which represents a small proportion of the existing metals.

(4) Another important point is the difficulty to properly analuse the results in many studies due to incomplete experimental designs that do not permit to highlight possible interactions. On several occasions, the studies did not investigate the effects of CNM alone or metal(loid)s alone (missing control conditions). Thus, recurrent increases and decreases of the studied biomarkers of toxicity were attributed to the addition of CNM in the presence of metal(loid)s, but these interpretations are only partial in the absence of tests with single contaminant.

(5) The statistics are sometimes performed only by modality of metal(loid) contamination, not allowing to establish possible interactions between CNM and metal(loid)s (ANOVA 1-way *vs* ANOVA 2-ways).

(6) More studies on ecosystem functions (mineralization and recycling) and biogeochemical cycles (C, N and P) are needed to have a more integrative view of these contaminant impacts on agrosystems. So far, these markers have only been studied after exposure to a single contaminant even though they are very good indicators of an ecosystem health.

(7) Studies are also needed to identify a potential bioaccumulation along food webs. Studies in micro-mesocosms with trophic chains seem to be a relevant experimental set-up to answer this question[199]. Due to CNM-metal(loid) interactions, the exposure duration in micro-mesocosms needs to be adapted to organism cycles, especially to know if CNM-metal(loid) exposure is putting at risk crop productions and human health.

(8) Technical development is also mandatory as the mechanisms explaining transfer and toxicity results are still not well understood, in particular because data about CNM actual concentrations in the organisms are rarely available.

Perspectives

Using combined toxicity interaction indices could be a practice to generalize to gain a deeper understanding of these interactions among contaminants. For example, Yang *et al.*[32] demonstrated synergic and antagonist effects using indices such as the Biomarker Response Index (BRI) coupled with the Concentration Addition Index (CAI) and the Effect Addition Index (EAI), which together quantify the joint effects of mixtures for a range of effect levels. BRI is an index based on the level of alteration of the response of the biomarkers tested in the treatments with contamination(s) compared to the control (without contamination). The level of biomarker impairment is classified into four distinct levels, each corresponding to a score: mild = 4, moderate = 3, major = 2 and severe = 1[200]. The score

for each biomarker is multiplied by the corresponding weighting to form an integrated index that is used to assess the overall effect of contaminants in a system submitted to multiple stress[201]. This allows the integration of complex biomarker responses into a single predefined class. It is thus possible to establish a dose-response relationship between contamination levels and biomarker responses[202]. This index has been used in the risk assessment of chemicals under the Water Framework Directive in Wales[200]. The BRI coupled with the CAI and EAI allow to determine respectively additive (=0), synergic (>0) or antagonist (<0) effects[203]. The CAI and EAI are derived from the commonly used concentration addition (CA) and independent action (IA) models that assess the toxicity of substances in non-interactive mixtures.

Another factor which is usually not considered is contamination aging. Indeed, the impact of metal(loid)s is influenced by their origin and aging[204–207]. The toxicological effects of metal(loid)s spiked in soil in laboratory experiments (in salt form) differ with soils with an aged contamination under the influence of natural processes[204–207]. For example, oxidation and precipitation of some metal(loid)s can affect their bioavailability and consequently their toxicity[208]. This parameter should be more considered in future experiments.

Although micro and nanoplastics have different properties than CNM, they are principally made of carbon and also display adsorption capacities leading to similar effects on transfer and toxicity (Table S3). Plastic concentration in agricultural soils could be much higher that the predicted CNM concentrations related to sludge application or mulching practices in particular. Special attention should thus be paid to the potential transfer and toxicological impacts of these micro and nanoplastics in co-exposure situations with other contaminants such as metal(loid)s.

Finally, agrosystems interact closely with other organisms such as insects, small mammals and birds on which they depend for part or all of their life cycles. Considering how these organisms rely on agrosystems, they may be an entry point for the contamination to spread up to other ecosystems.

Acknowledgement

The authors would like to acknowledge the Région Occitanie, Toulouse Federal University, and EC2CO program CARBOSTRESS (CNRS-INSU) for their funding support.

Bibliography (review):

(1) *ISO/TS 80004-3:2020(fr), Nanotechnologies — Vocabulaire — Partie 3: Nano-objets carbonés*. https://www.iso.org/obp/ui/#iso:std:iso:ts:80004:-3:ed-2:v1:fr (accessed 2021-05-09).

(2) Singh, V.; Joung, D.; Zhai, L.; Das, S.; Khondaker, S. I.; Seal, S. Graphene Based Materials: Past, Present and Future. *Progress in Materials Science* **2011**, *56* (8), 1178–1271. https://doi.org/10.1016/j.pmatsci.2011.03.003.

(3) Bianco, A.; Cheng, H.-M.; Enoki, T.; Gogotsi, Y.; Hurt, R. H.; Koratkar, N.; Kyotani, T.; Monthioux, M.; Park, C. R.; Tascon, J. M. D.; Zhang, J. All in the Graphene Family – A Recommended Nomenclature for Two-Dimensional Carbon Materials. *Carbon* **2013**, *65*, 1–6. https://doi.org/10.1016/j.carbon.2013.08.038.

(4) Wick, P.; Louw-Gaume, A. E.; Kucki, M.; Krug, H. F.; Kostarelos, K.; Fadeel, B.; Dawson, K. A.; Salvati, A.; Vázquez, E.; Ballerini, L.; Tretiach, M.; Benfenati, F.; Flahaut, E.; Gauthier, L.; Prato, M.; Bianco, A. Classification Framework for Graphene-Based Materials. *Angewandte Chemie International Edition* **2014**, *53* (n° 30), 7714–7718. https://doi.org/10.1002/anie.201403335.

(5) Huang, X.; Yin, Z.; Wu, S.; Qi, X.; He, Q.; Zhang, Q.; Yan, Q.; Boey, F.; Zhang, H. Graphene-Based Materials: Synthesis, Characterization, Properties, and Applications. *Small* **2011**, *7* (14), 1876–1902. https://doi.org/10.1002/smll.201002009.

(6) Gottschalk, F.; Sun, T.; Nowack, B. Environmental Concentrations of Engineered Nanomaterials: Review of Modeling and Analytical Studies. *Environmental Pollution* **2013**, *181*, 287–300. https://doi.org/10.1016/j.envpol.2013.06.003.

(7) Butt, B. Z.; Naseer, I. Nanofertilizers. In *Nanoagronomy*; Javad, S., Ed.; Springer International Publishing: Cham, 2020; pp 125–152. https://doi.org/10.1007/978-3-030-41275-3_8.

(8) Paramo, L. A.; Feregrino-Pérez, A. A.; Guevara, R.; Mendoza, S.; Esquivel, K. Nanoparticles in Agroindustry: Applications, Toxicity, Challenges, and Trends. *Nanomaterials* **2020**, *10* (9), 1654. https://doi.org/10.3390/nano10091654.

(9) Perreault, F.; Faria, A. F. de; Elimelech, M. Environmental Applications of Graphene-Based Nanomaterials. *Chem. Soc. Rev.* **2015**, *44* (16), 5861–5896. https://doi.org/10.1039/C5CS00021A.

(10) Ramade, F. *Dictionnaire Encyclopédique Des Sciences De La Nature Et De La Biodiversité*, Dunod.; Paris, 2008.

(11) Marschner, H. *Marschner's Mineral Nutrition of Higher Plants*; Academic Press, 2011.

(12) Addo Ntim, S.; Mitra, S. Adsorption of Arsenic on Multiwall Carbon Nanotube–Zirconia Nanohybrid for Potential Drinking Water Purification. *Journal of Colloid and Interface Science* **2012**, *375* (1), 154–159. https://doi.org/10.1016/j.jcis.2012.01.063.

(13) Tofighy, M. A.; Mohammadi, T. Adsorption of Divalent Heavy Metal Ions from Water Using Carbon Nanotube Sheets. *Journal of Hazardous Materials* **2011**, *185* (1), 140–147. https://doi.org/10.1016/j.jhazmat.2010.09.008.

(14) Moradi, O. The Removal of Ions by Functionalized Carbon Nanotube: Equilibrium, Isotherms and Thermodynamic Studies. *Chemical and Biochemical Engineering Quarterly* **2011**, *25* (2), 229–240.

(15) Moradi, O.; Zare, K. Adsorption of Pb(II), Cd(II) and Cu(II) Ions in Aqueous Solution on SWCNT and SWCNT –COOH Surfaces: Kinetics Studies. *Fullerenes, Nanotubes and Carbon Nanostructures* **2011**, *19* (7), 628–652. https://doi.org/10.1080/1536383X.2010.504955.

(16) Peng, W.; Li, H.; Liu, Y.; Song, S. A Review on Heavy Metal Ions Adsorption from Water by Graphene Oxide and Its Composites. *Journal of Molecular Liquids* **2017**, *230*, 496–504. https://doi.org/10.1016/j.molliq.2017.01.064.

(17) Gao, X.; Hassan, I.; Peng, Y.; Huo, S.; Ling, L. Behaviors and Influencing Factors of the Heavy Metals Adsorption onto Microplastics: A Review. *Journal of Cleaner Production* **2021**, *319*, 128777. https://doi.org/10.1016/j.jclepro.2021.128777.

(18) Nicholson, F. A.; Smith, S. R.; Alloway, B. J.; Carlton-Smith, C.; Chambers, B. J. An Inventory of Heavy Metals Inputs to Agricultural Soils in England and Wales. *Science of The Total Environment* **2003**, *311* (1), 205–219. https://doi.org/10.1016/S0048-9697(03)00139-6.
(19) Nagajyoti, P. C.; Lee, K. D.; Sreekanth, T. V. M. Heavy Metals, Occurrence and Toxicity for Plants: A Review. *Environmental Chemistry Letters* **2010**, *8* (3), 199–216. https://doi.org/10.1007/s10311-010-0297-8.
(20) *Toxic Metals in Soil-Plant Systems*; Ross, S., Ed.; Wiley: Chichester, West Sussex, England ; New York, 1994.
(21) Zhao, L.; Guan, X.; Yu, B.; Ding, N.; Liu, X.; Ma, Q.; Yang, S.; Yilihamu, A.; Yang, S.-T. Carboxylated Graphene Oxide-Chitosan Spheres Immobilize Cu2+ in Soil and Reduce Its Bioaccumulation in Wheat Plants. *Environment International* **2019**, *133*, 105208. https://doi.org/10.1016/j.envint.2019.105208.
(22) He, Y.; Qian, L.; Zhou, K.; Hu, R.; Huang, M.; Wang, M.; Zhao, G.; Liu, Y.; Xu, Z.; Zhu, H. Graphene Oxide Promoted Cadmium Uptake by Rice in Soil. *ACS Sustainable Chem. Eng.* **2019**, *7* (12), 10283–10292. https://doi.org/10.1021/acssuschemeng.8b06823.
(23) Li, J.; Wu, F.; Fang, Q.; Wu, Z.; Duan, Q.; Li, X.; Ye, W. The Mutual Effects of Graphene Oxide Nanosheets and Cadmium on the Growth, Cadmium Uptake and Accumulation in Rice. *Plant Physiology and Biochemistry* **2020**, *147*, 289–294. https://doi.org/10.1016/j.plaphy.2019.12.034.
(24) Hu, X.; Kang, J.; Lu, K.; Zhou, R.; Mu, L.; Zhou, Q. Graphene Oxide Amplifies the Phytotoxicity of Arsenic in Wheat. *Scientific Reports* **2014**, *4* (1), 6122. https://doi.org/10.1038/srep06122.
(25) Gao, M.; Yang, Y.; Song, Z. Effects of Graphene Oxide on Cadmium Uptake and Photosynthesis Performance in Wheat Seedlings. *Ecotoxicology and Environmental Safety* **2019**, *173*, 165–173. https://doi.org/10.1016/j.ecoenv.2019.01.093.
(26) Gao, M.; Xu, Y.; Chang, X.; Dong, Y.; Song, Z. Effects of Foliar Application of Graphene Oxide on Cadmium Uptake by Lettuce. *Journal of Hazardous Materials* **2020**, *398*, 122859. https://doi.org/10.1016/j.jhazmat.2020.122859.
(27) Gong, X.; Huang, D.; Liu, Y.; Zeng, G.; Wang, R.; Xu, P.; Zhang, C.; Cheng, M.; Xue, W.; Chen, S. Roles of Multiwall Carbon Nanotubes in Phytoremediation: Cadmium Uptake and Oxidative Burst in Boehmeria Nivea (L.) Gaudich. *Environ. Sci.: Nano* **2019**, *6* (3), 851–862. https://doi.org/10.1039/C8EN00723C.
(28) Lian, J.; Wu, J.; Zeb, A.; Zheng, S.; Ma, T.; Peng, F.; Tang, J.; Liu, W. Do Polystyrene Nanoplastics Affect the Toxicity of Cadmium to Wheat (Triticum Aestivum L.)? *Environmental Pollution* **2020**, *263*, 114498. https://doi.org/10.1016/j.envpol.2020.114498.
(29) Dong, Y.; Gao, M.; Song, Z.; Qiu, W. Microplastic Particles Increase Arsenic Toxicity to Rice Seedlings. *Environmental Pollution* **2020**, *259*, 113892. https://doi.org/10.1016/j.envpol.2019.113892.
(30) Leroy, M.; Pey, B.; Jassey, V. E. J.; Liné, C.; Elger, A.; Probst, A.; Flahaut, E.; Silvestre, J.; Larue, C. Interactive Effects of Metals and Carbon Nanotubes in a Microcosm Agrosystem. *Journal of Hazardous Materials* **2022**, *431*, 128613. https://doi.org/10.1016/j.jhazmat.2022.128613.
(31) Vijver, M. G.; Elliott, E. G.; Peijnenburg, W. J. G. M.; de Snoo, G. R. Response Predictions for Organisms Water-Exposed to Metal Mixtures: A Meta-Analysis. *Environmental Toxicology and Chemistry* **2011**, *30* (6), 1482–1487. https://doi.org/10.1002/etc.499.
(32) Yang, X.; Gong, J.; Zhang, X.; Huang, Y.; Zhang, W.; Yang, J.; Lin, J.; Chai, Y.; Liu, J. Evaluation of the Combined Toxicity of Multi-Walled Carbon Nanotubes and Cadmium on Earthworms in Soil Using Multi-Level Biomarkers. *Ecotoxicology and Environmental Safety* **2021**, *221*, 112441. https://doi.org/10.1016/j.ecoenv.2021.112441.
(33) Rodea-Palomares, I.; González-Pleiter, M.; Martín-Betancor, K.; Rosal, R.; Fernández-Piñas, F. Additivity and Interactions in Ecotoxicity of Pollutant Mixtures: Some Patterns, Conclusions, and Open Questions. *Toxics* **2015**, *3* (4), 342–369. https://doi.org/10.3390/toxics3040342.

(34) Ren, X.; Chen, C.; Nagatsu, M.; Wang, X. Carbon Nanotubes as Adsorbents in Environmental Pollution Management: A Review. *Chemical Engineering Journal* **2011**, *170* (2), 395–410. https://doi.org/10.1016/j.cej.2010.08.045.

(35) Gupta, V. K.; Moradi, O.; Tyagi, I.; Agarwal, S.; Sadegh, H.; Shahryari-Ghoshekandi, R.; Makhlouf, A. S. H.; Goodarzi, M.; Garshasbi, A. Study on the Removal of Heavy Metal Ions from Industry Waste by Carbon Nanotubes: Effect of the Surface Modification: A Review. *Critical Reviews in Environmental Science and Technology* **2016**, *46* (2), 93–118. https://doi.org/10.1080/10643389.2015.1061874.

(36) Ihsanullah; Abbas, A.; Al-Amer, A. M.; Laoui, T.; Al-Marri, M. J.; Nasser, M. S.; Khraisheh, M.; Atieh, M. A. Heavy Metal Removal from Aqueous Solution by Advanced Carbon Nanotubes: Critical Review of Adsorption Applications. *Separation and Purification Technology* **2016**, *157*, 141–161. https://doi.org/10.1016/j.seppur.2015.11.039.

(37) Rao, G. P.; Lu, C.; Su, F. Sorption of Divalent Metal Ions from Aqueous Solution by Carbon Nanotubes: A Review. *Separation and Purification Technology* **2007**, *58* (1), 224–231. https://doi.org/10.1016/j.seppur.2006.12.006.

(38) Li, Y.-H.; Ding, J.; Luan, Z.; Di, Z.; Zhu, Y.; Xu, C.; Wu, D.; Wei, B. Competitive Adsorption of Pb2+, Cu2+ and Cd2+ Ions from Aqueous Solutions by Multiwalled Carbon Nanotubes. *Carbon* **2003**, *41* (14), 2787–2792. https://doi.org/10.1016/S0008-6223(03)00392-0.

(39) Liang, J.; Liu, J.; Yuan, X.-Z.; Dong, H.; Zeng, G.; Wu, H.; Hou, W.; Liu, J.; Hua, S.; Zhang, S.; Zhigang, Y.; He, X.; He, Y. Facile Synthesis of Alumina-Decorated Multi-Walled Carbon Nanotubes for Simultaneous Adsorption of Cadmium Ion and Trichloroethylene. *Chemical Engineering Journal* **2015**, *273*. https://doi.org/10.1016/j.cej.2015.03.069.

(40) Lu, C.; Chiu, H. Adsorption of Zinc(II) from Water with Purified Carbon Nanotubes. *Chemical Engineering Science* **2006**, *61* (4), 1138–1145. https://doi.org/10.1016/j.ces.2005.08.007.

(41) Vasudevan, S.; Lakshmi, J. The Adsorption of Phosphate by Graphene from Aqueous Solution. *RSC Adv.* **2012**, *2* (12), 5234–5242. https://doi.org/10.1039/C2RA20270K.

(42) Zhang, S.; Shao, Y.; Liu, J.; Aksay, I. A.; Lin, Y. Graphene–Polypyrrole Nanocomposite as a Highly Efficient and Low Cost Electrically Switched Ion Exchanger for Removing ClO4– from Wastewater. *ACS Appl. Mater. Interfaces* **2011**, *3* (9), 3633–3637. https://doi.org/10.1021/am200839m.

(43) Shi, G.; Ding, Y.; Fang, H. Unexpectedly Strong Anion–π Interactions on the Graphene Flakes. *Journal of Computational Chemistry* **2012**, *33* (14), 1328–1337. https://doi.org/10.1002/jcc.22964.

(44) Madadrang, C. J.; Kim, H. Y.; Gao, G.; Wang, N.; Zhu, J.; Feng, H.; Gorring, M.; Kasner, M. L.; Hou, S. Adsorption Behavior of EDTA-Graphene Oxide for Pb (II) Removal. *ACS Appl. Mater. Interfaces* **2012**, *4* (3), 1186–1193. https://doi.org/10.1021/am201645g.

(45) Liu, L.; Li, C.; Bao, C.; Jia, Q.; Xiao, P.; Liu, X.; Zhang, Q. Preparation and Characterization of Chitosan/Graphene Oxide Composites for the Adsorption of Au(III) and Pd(II). *Talanta* **2012**, *93*, 350–357. https://doi.org/10.1016/j.talanta.2012.02.051.

(46) Shim, J.-W.; Park, S.-J.; Ryu, S.-K. Effect of Modification with HNO3 and NaOH on Metal Adsorption by Pitch-Based Activated Carbon Fibers. *Carbon* **2001**, *39* (11), 1635–1642. https://doi.org/10.1016/S0008-6223(00)00290-6.

(47) Bian, Y.; Bian, Z.-Y.; Zhang, J.-X.; Ding, A.-Z.; Liu, S.-L.; Wang, H. Effect of the Oxygen-Containing Functional Group of Graphene Oxide on the Aqueous Cadmium Ions Removal. *Applied Surface Science* **2015**, *329*, 269–275. https://doi.org/10.1016/j.apsusc.2014.12.090.

(48) Li, Z.; Chen, F.; Yuan, L.; Liu, Y.; Zhao, Y.; Chai, Z.; Shi, W. Uranium(VI) Adsorption on Graphene Oxide Nanosheets from Aqueous Solutions. *Chemical Engineering Journal* **2012**, *210*, 539–546. https://doi.org/10.1016/j.cej.2012.09.030.

(49) Khan, J.; Jaafar, M. Reduction Efficiencies of Natural Substances for Reduced Graphene Oxide Synthesis. *J Mater Sci* **2021**, *56* (33), 18477–18492. https://doi.org/10.1007/s10853-021-06492-y.

(50) Sigmund, G.; Jiang, C.; Hofmann, T.; Chen, W. Environmental Transformation of Natural and Engineered Carbon Nanoparticles and Implications for the Fate of Organic Contaminants. *Environmental Science: Nano* **2018**, *5* (11), 2500–2518. https://doi.org/10.1039/C8EN00676H.
(51) Sitko, R.; Zawisza, B.; Malicka, E. Graphene as a New Sorbent in Analytical Chemistry. *TrAC Trends in Analytical Chemistry* **2013**, *51*, 33–43. https://doi.org/10.1016/j.trac.2013.05.011.
(52) Zhao, J.; Wang, Z.; White, J. C.; Xing, B. Graphene in the Aquatic Environment: Adsorption, Dispersion, Toxicity and Transformation. *Environ. Sci. Technol.* **2014**, *48* (17), 9995–10009. https://doi.org/10.1021/es5022679.
(53) Peigney, A.; Laurent, C.; Flahaut, E.; Bacsa, R.; Rousset, A. Specific Surface Area of Carbon Nanotubes and Bundles of Carbon Nanotubes. *Carbon* **2001**, *39*, 507–514. https://doi.org/10.1016/S0008-6223(00)00155-X.
(54) Xu, J.; Cao, Z.; Zhang, Y.; Yuan, Z.; Lou, Z.; Xu, X.; Wang, X. A Review of Functionalized Carbon Nanotubes and Graphene for Heavy Metal Adsorption from Water: Preparation, Application, and Mechanism. *Chemosphere* **2018**, *195*, 351–364. https://doi.org/10.1016/j.chemosphere.2017.12.061.
(55) Suzuki, S. *Physical and Chemical Properties of Carbon Nanotubes*; BoD – Books on Demand, 2013.
(56) Zhu, Y.; Murali, S.; Cai, W.; Li, X.; Suk, J. W.; Potts, J. R.; Ruoff, R. S. Graphene and Graphene Oxide: Synthesis, Properties, and Applications. *Advanced Materials* **2010**, *22* (35), 3906–3924. https://doi.org/10.1002/adma.201001068.
(57) Marques, P. A. S. S.; Rosa, M. F.; Pinheiro, H. M. PH Effects on the Removal of Cu2+, Cd2+ and Pb2+ from Aqueous Solution by Waste Brewery Biomass. *Bioprocess Engineering* **2000**, *23* (2), 135–141. https://doi.org/10.1007/PL00009118.
(58) Fu, F.; Wang, Q. Removal of Heavy Metal Ions from Wastewaters: A Review. *Journal of Environmental Management* **2011**, *92* (3), 407–418. https://doi.org/10.1016/j.jenvman.2010.11.011.
(59) Yu, J.-G.; Zhao, X.-H.; Yu, L.-Y.; Jiao, F.-P.; Jiang, J.-H.; Chen, X.-Q. Removal, Recovery and Enrichment of Metals from Aqueous Solutions Using Carbon Nanotubes. *J Radioanal Nucl Chem* **2014**, *299* (3), 1155–1163. https://doi.org/10.1007/s10967-013-2818-y.
(60) Ihsanullah; Al-Khaldi, F. A.; Abusharkh, B.; Khaled, M.; Atieh, M. A.; Nasser, M. S.; laoui, T.; Saleh, T. A.; Agarwal, S.; Tyagi, I.; Gupta, V. K. Adsorptive Removal of Cadmium(II) Ions from Liquid Phase Using Acid Modified Carbon-Based Adsorbents. *Journal of Molecular Liquids* **2015**, *204*, 255–263. https://doi.org/10.1016/j.molliq.2015.01.033.
(61) Cui, L.; Wang, Y.; Gao, L.; Hu, L.; Yan, L.; Wei, Q.; Du, B. EDTA Functionalized Magnetic Graphene Oxide for Removal of Pb(II), Hg(II) and Cu(II) in Water Treatment: Adsorption Mechanism and Separation Property. *Chemical Engineering Journal* **2015**, *281*, 1–10. https://doi.org/10.1016/j.cej.2015.06.043.
(62) Wang, H.; Yuan, X.; Wu, Y.; Huang, H.; Zeng, G.; Liu, Y.; Wang, X.; Lin, N.; Qi, Y. Adsorption Characteristics and Behaviors of Graphene Oxide for Zn(II) Removal from Aqueous Solution. *Applied Surface Science* **2013**, *279*, 432–440. https://doi.org/10.1016/j.apsusc.2013.04.133.
(63) Sen, T. K.; Sarzali, M. V. Removal of Cadmium Metal Ion (Cd2+) from Its Aqueous Solution by Aluminium Oxide (Al2O3): A Kinetic and Equilibrium Study. *Chemical Engineering Journal* **2008**, *142* (3), 256–262. https://doi.org/10.1016/j.cej.2007.12.001.
(64) Yang, S.-T.; Chang, Y.; Wang, H.; Liu, G.; Chen, S.; Wang, Y.; Liu, Y.; Cao, A. Folding/Aggregation of Graphene Oxide and Its Application in Cu2+ Removal. *J Colloid Interface Sci* **2010**, *351* (1), 122–127. https://doi.org/10.1016/j.jcis.2010.07.042.
(65) Salam, M. A.; Al-Zhrani, G.; Kosa, S. A. Simultaneous Removal of Copper(II), Lead(II), Zinc(II) and Cadmium(II) from Aqueous Solutions by Multi-Walled Carbon Nanotubes. *Comptes Rendus Chimie* **2012**, *15* (5), 398–408. https://doi.org/10.1016/j.crci.2012.01.013.
(66) Sitko, R.; Turek, E.; Zawisza, B.; Malicka, E.; Talik, E.; Heimann, J.; Gagor, A.; Feist, B.; Wrzalik, R. Adsorption of Divalent Metal Ions from Aqueous Solutions Using Graphene Oxide. *Dalton Trans.* **2013**, *42* (16), 5682–5689. https://doi.org/10.1039/C3DT33097D.

(67) Lewis, A. Precipitation of Heavy Metals. In *Sustainable Heavy Metal Remediation: Volume 1: Principles and Processes*; Rene, E. R., Sahinkaya, E., Lewis, A., Lens, P. N. L., Eds.; Environmental Chemistry for a Sustainable World; Springer International Publishing: Cham, 2017; pp 101–120. https://doi.org/10.1007/978-3-319-58622-9_4.
(68) Patnaik, P. *Dean's Analytical Chemistry Handbook*, 2nd edition.; McGraw Hill: New York, 2004.
(69) Jiang, L.; Yu, H.; Zhou, X.; Hou, X.; Zou, Z.; Li, S.; Li, C.; Yao, X. Preparation, Characterization, and Adsorption Properties of Magnetic Multi-Walled Carbon Nanotubes for Simultaneous Removal of Lead(II) and Zinc(II) from Aqueous Solutions. *Desalination and Water Treatment* **2016**, *57* (39), 18446–18462. https://doi.org/10.1080/19443994.2015.1090924.
(70) Ding, C.; Cheng, W.; Wang, X.; Wu, Z.-Y.; Sun, Y.; Chen, C.; Wang, X.; Yu, S.-H. Competitive Sorption of Pb(II), Cu(II) and Ni(II) on Carbonaceous Nanofibers: A Spectroscopic and Modeling Approach. *Journal of Hazardous Materials* **2016**, *313*, 253–261. https://doi.org/10.1016/j.jhazmat.2016.04.002.
(71) Alimohammady, M.; Jahangiri, M.; Kiani, F.; Tahermansouri, H. Highly Efficient Simultaneous Adsorption of Cd(II), Hg(II) and As(III) Ions from Aqueous Solutions by Modification of Graphene Oxide with 3-Aminopyrazole: Central Composite Design Optimization. *New J. Chem.* **2017**, *41* (17), 8905–8919. https://doi.org/10.1039/C7NJ01450C.
(72) Tan, P.; Hu, Y.; Bi, Q. Competitive Adsorption of Cu2+, Cd2+ and Ni2+ from an Aqueous Solution on Graphene Oxide Membranes. *Colloids and Surfaces A: Physicochemical and Engineering Aspects* **2016**, *509*, 56–64. https://doi.org/10.1016/j.colsurfa.2016.08.081.
(73) Lu, C.; Liu, C.; Su, F. Sorption Kinetics, Thermodynamics and Competition of Ni2+ from Aqueous Solutions onto Surface Oxidized Carbon Nanotubes. *Desalination* **2009**, *249* (1), 18–23. https://doi.org/10.1016/j.desal.2009.06.009.
(74) Lu, C.; Chiu, H.; Liu, C. Removal of Zinc(II) from Aqueous Solution by Purified Carbon Nanotubes: Kinetics and Equilibrium Studies. *Ind. Eng. Chem. Res.* **2006**, *45* (8), 2850–2855. https://doi.org/10.1021/ie051206h.
(75) Morales, J.; Manso, J. A.; Cid, A.; Mejuto, J. C. Degradation of Carbofuran and Carbofuran-Derivatives in Presence of Humic Substances under Basic Conditions. *Chemosphere* **2012**, *89* (11), 1267–1271. https://doi.org/10.1016/j.chemosphere.2012.05.018.
(76) Imai, A.; Fukushima, T.; Matsushige, K.; Kim, Y.-H.; Choi, K. Characterization of Dissolved Organic Matter in Effluents from Wastewater Treatment Plants. *Water Research* **2002**, *36* (4), 859–870. https://doi.org/10.1016/S0043-1354(01)00283-4.
(77) Lin, D.; Tian, X.; Li, T.; Zhang, Z.; He, X.; Xing, B. Surface-Bound Humic Acid Increased Pb2+ Sorption on Carbon Nanotubes. *Environmental Pollution* **2012**, *167*, 138–147. https://doi.org/10.1016/j.envpol.2012.03.044.
(78) Tian, X.; Li, T.; Yang, K.; Xu, Y.; Lu, H.; Lin, D. Effect of Humic Acids on Physicochemical Property and Cd(II) Sorption of Multiwalled Carbon Nanotubes. *Chemosphere* **2012**, *89* (11), 1316–1322. https://doi.org/10.1016/j.chemosphere.2012.05.082.
(79) Bandyopadhyaya, R.; Nativ-Roth, E.; Regev, O.; Yerushalmi-Rozen, R. Stabilization of Individual Carbon Nanotubes in Aqueous Solutions. *Nano Lett.* **2002**, *2* (1), 25–28. https://doi.org/10.1021/nl010065f.
(80) Hyung, H.; Fortner, J. D.; Hughes, J. B.; Kim, J.-H. Natural Organic Matter Stabilizes Carbon Nanotubes in the Aqueous Phase. *Environ. Sci. Technol.* **2007**, *41* (1), 179–184. https://doi.org/10.1021/es061817g.
(81) Sheng, G.; Li, J.; Shao, D.; Hu, J.; Chen, C.; Chen, Y.; Wang, X. Adsorption of Copper(II) on Multiwalled Carbon Nanotubes in the Absence and Presence of Humic or Fulvic Acids. *Journal of Hazardous Materials* **2010**, *178* (1–3), 333–340. https://doi.org/10.1016/j.jhazmat.2010.01.084.
(82) Sun, W.-L.; Xia, J.; Li, S.; Sun, F. Effect of Natural Organic Matter (NOM) on Cu(II) Adsorption by Multi-Walled Carbon Nanotubes: Relationship with NOM Properties. *Chemical Engineering Journal* **2012**, *200–202*, 627–636. https://doi.org/10.1016/j.cej.2012.06.118.

(83) Rizwan, M. S.; Imtiaz, M.; Huang, G.; Chhajro, M. A.; Liu, Y.; Fu, Q.; Zhu, J.; Ashraf, M.; Zafar, M.; Bashir, S.; Hu, H. Immobilization of Pb and Cu in Polluted Soil by Superphosphate, Multi-Walled Carbon Nanotube, Rice Straw and Its Derived Biochar. *Environ Sci Pollut Res* **2016**, *23* (15), 15532–15543. https://doi.org/10.1007/s11356-016-6695-0.

(84) Jaisi, D. P.; Elimelech, M. Single-Walled Carbon Nanotubes Exhibit Limited Transport in Soil Columns. *Environ. Sci. Technol.* **2009**, *43* (24), 9161–9166. https://doi.org/10.1021/es901927y.

(85) Kasel, D.; Bradford, S. A.; Šimůnek, J.; Pütz, T.; Vereecken, H.; Klumpp, E. Limited Transport of Functionalized Multi-Walled Carbon Nanotubes in Two Natural Soils. *Environmental Pollution* **2013**, *180*, 152–158. https://doi.org/10.1016/j.envpol.2013.05.031.

(86) Lu, Y.; Yang, K.; Lin, D. Transport of Surfactant-Facilitated Multiwalled Carbon Nanotube Suspensions in Columns Packed with Sized Soil Particles. *Environmental Pollution* **2014**, *192*, 36–43. https://doi.org/10.1016/j.envpol.2014.05.008.

(87) Zhang, W.; Zhang, F.; Han, Z.; Lü, X.; Lin, D.; Werner, D. Effect of Clay Minerals on Transport of Surfactants Dispersed Multi-walled Carbon Nanotubes in Porous Media. *Acta Geologica Sinica - English Edition* **2017**, *1* (91), 135–144. https://doi.org/10.1111/1755-6724.13067.

(88) Han, B.; Liu, W.; Zhao, X.; Cai, Z.; Zhao, D. Transport of Multi-Walled Carbon Nanotubes Stabilized by Carboxymethyl Cellulose and Starch in Saturated Porous Media: Influences of Electrolyte, Clay and Humic Acid. *Science of The Total Environment* **2017**, *599–600*, 188–197. https://doi.org/10.1016/j.scitotenv.2017.04.222.

(89) Lu, T.; Xia, T.; Qi, Y.; Zhang, C.; Chen, W. Effects of Clay Minerals on Transport of Graphene Oxide in Saturated Porous Media. *Environ Toxicol Chem* **2017**, *36* (3), 655–660. https://doi.org/10.1002/etc.3605.

(90) Kasel, D.; Bradford, S. A.; Šimůnek, J.; Heggen, M.; Vereecken, H.; Klumpp, E. Transport and Retention of Multi-Walled Carbon Nanotubes in Saturated Porous Media: Effects of Input Concentration and Grain Size. *Water Research* **2013**, *47* (2), 933–944. https://doi.org/10.1016/j.watres.2012.11.019.

(91) Qi, Z.; Zhang, L.; Chen, W. Transport of Graphene Oxide Nanoparticles in Saturated Sandy Soil. *Environ. Sci.: Processes Impacts* **2014**, *16* (10), 2268–2277. https://doi.org/10.1039/C4EM00063C.

(92) Vithanage, M.; Herath, I.; Almaroai, Y. A.; Rajapaksha, A. U.; Huang, L.; Sung, J.-K.; Lee, S. S.; Ok, Y. S. Effects of Carbon Nanotube and Biochar on Bioavailability of Pb, Cu and Sb in Multi-Metal Contaminated Soil. *Environ Geochem Health* **2017**, *39* (6), 1409–1420. https://doi.org/10.1007/s10653-017-9941-6.

(93) Yang, Z.; Xu, Z.; Geng, L.; Shu, W.; Zhu, T. Effect of Multi-Walled Carbon Nanotubes on Extractability of Sb and Cd in Contaminated Soil. *Ecotoxicology and Environmental Safety* **2020**, *205*, 111316. https://doi.org/10.1016/j.ecoenv.2020.111316.

(94) Baragaño, D.; Forján, R.; Welte, L.; Gallego, J. L. R. Nanoremediation of As and Metals Polluted Soils by Means of Graphene Oxide Nanoparticles. *Scientific Reports* **2020**, *10* (1), 1896. https://doi.org/10.1038/s41598-020-58852-4.

(95) Song, B.; Zeng, G.; Gong, J.; Zhang, P.; Deng, J.; Deng, C.; Yan, J.; Xu, P.; Lai, C.; Zhang, C.; Cheng, M. Effect of Multi-Walled Carbon Nanotubes on Phytotoxicity of Sediments Contaminated by Phenanthrene and Cadmium. *Chemosphere* **2017**, *172*, 449–458. https://doi.org/10.1016/j.chemosphere.2017.01.032.

(96) Liné, C.; Larue, C.; Flahaut, E. Carbon Nanotubes: Impacts and Behaviour in the Terrestrial Ecosystem - A Review. *Carbon* **2017**, *123*, 767–785. https://doi.org/10.1016/j.carbon.2017.07.089.

(97) Baath, E. Effects of Heavy Metals in Soil on Microbial Processes and Populations (a Review). *Water, Air, and Soil Pollution* **1989**, *47* (3–4), 335–379. https://doi.org/10.1007/BF00279331.

(98) Giller, K. E.; Witter, E.; Mcgrath, S. P. Toxicity of Heavy Metals to Microorganisms and Microbial Processes in Agricultural Soils: A Review. *Soil Biology and Biochemistry* **1998**, *30* (10), 1389–1414. https://doi.org/10.1016/S0038-0717(97)00270-8.

(99) Giller, K. E.; Witter, E.; McGrath, S. P. Heavy Metals and Soil Microbes. *Soil Biology and Biochemistry* **2009**, *41* (10), 2031–2037. https://doi.org/10.1016/j.soilbio.2009.04.026.
(100) Abdu, N.; Abdullahi, A. A.; Abdulkadir, A. Heavy Metals and Soil Microbes. *Environ Chem Lett* **2017**, *15* (1), 65–84. https://doi.org/10.1007/s10311-016-0587-x.
(101) Jastrzębska, A. M.; Kurtycz, P.; Olszyna, A. R. Recent Advances in Graphene Family Materials Toxicity Investigations. *J Nanopart Res* **2012**, *14* (12), 1320. https://doi.org/10.1007/s11051-012-1320-8.
(102) Gall, J. E.; Boyd, R. S.; Rajakaruna, N. Transfer of Heavy Metals through Terrestrial Food Webs: A Review. *Environ Monit Assess* **2015**, *187* (4), 201. https://doi.org/10.1007/s10661-015-4436-3.
(103) Sivakumar, S. Effects of Metals on Earthworm Life Cycles: A Review. *Environmental monitoring and assessment* **2015**, *187*, 4742. https://doi.org/10.1007/s10661-015-4742-9.
(104) Tyler, G.; Påhlsson, A.-. M. B.; Bengtsson, G.; Bååth, E.; Tranvik, L. Heavy-Metal Ecology of Terrestrial Plants, Microorganisms and Invertebrates. *Water Air Soil Pollut* **1989**, *47* (3), 189–215. https://doi.org/10.1007/BF00279327.
(105) Nahmani, J.; Hodson, M. E.; Black, S. A Review of Studies Performed to Assess Metal Uptake by Earthworms. *Environmental Pollution* **2007**, *145* (2), 402–424. https://doi.org/10.1016/j.envpol.2006.04.009.
(106) Sizmur, T.; Hodson, M. E. Do Earthworms Impact Metal Mobility and Availability in Soil? – A Review. *Environmental Pollution* **2009**, *157* (7), 1981–1989. https://doi.org/10.1016/j.envpol.2009.02.029.
(107) Shahid, M.; Khalid, S.; Abbas, G.; Shahid, N.; Nadeem, M.; Sabir, M.; Aslam, M.; Dumat, C. Heavy Metal Stress and Crop Productivity; 2015; pp 1–25.
(108) Kumar, S.; Trivedi, P. K. Chapter 25 - Heavy Metal Stress Signaling in Plants. In *Plant Metal Interaction*; Ahmad, P., Ed.; Elsevier, 2016; pp 585–603. https://doi.org/10.1016/B978-0-12-803158-2.00025-4.
(109) Vardhan, K. H.; Kumar, P. S.; Panda, R. C. A Review on Heavy Metal Pollution, Toxicity and Remedial Measures: Current Trends and Future Perspectives. *Journal of Molecular Liquids* **2019**, *290*, 111197. https://doi.org/10.1016/j.molliq.2019.111197.
(110) Wang, Q.; Li, C.; Wang, Y.; Que, X. Phytotoxicity of Graphene Family Nanomaterials and Its Mechanisms: A Review. *Front. Chem.* **2019**, *7*. https://doi.org/10.3389/fchem.2019.00292.
(111) Rovira, A. D. Interactions Between Plant Roots and Soil Microorganisms. *Annual Review of Microbiology* **1965**, *19* (1), 241–266. https://doi.org/10.1146/annurev.mi.19.100165.001325.
(112) Haferburg, G.; Kothe, E. Microbes and Metals: Interactions in the Environment. *Journal of Basic Microbiology* **2007**, *47* (6), 453–467. https://doi.org/10.1002/jobm.200700275.
(113) Gadd, G. M. 2010. Metals, Minerals and Microbes: Geomicrobiology and Bioremediation. *Microbiology 156* (3), 609–643. https://doi.org/10.1099/mic.0.037143-0.
(114) Bruins, M. R.; Kapil, S.; Oehme, F. W. Microbial Resistance to Metals in the Environment. *Ecotoxicology and Environmental Safety* **2000**, *45* (3), 198–207. https://doi.org/10.1006/eesa.1999.1860.
(115) I.v.n, R.; M, M.; N, B. TOLERANCE OF HEAVY BY GRAM POSITIVE SOIL BACTERIA. **2009**, *2* (4), 1185–1189.
(116) Gadd, G. M. Heavy Metal Accumulation by Bacteria and Other Microorganisms. *Experientia* **1990**, *46* (8), 834–840. https://doi.org/10.1007/BF01935534.
(117) Chander, K.; Brookes, P. C.; Harding, S. A. Microbial Biomass Dynamics Following Addition of Metal-Enriched Sewage Sludges to a Sandy Loam. *Soil Biology and Biochemistry* **1995**, *27* (11), 1409–1421. https://doi.org/10.1016/0038-0717(95)00074-O.
(118) Roane, T. M.; Pepper, I. L. Microbial Responses to Environmentally Toxic Cadmium. *Microbial Ecology* **1999**, *38* (4), 358–364.
(119) Giller, K. E.; McGrath, S. P.; Hirsch, P. R. Absence of Nitrogen Fixation in Clover Grown on Soil Subject to Long-Term Contamination with Heavy Metals Is Due to Survival of Only Ineffective

Rhizobium. *Soil Biology and Biochemistry* **1989**, *21* (6), 841–848. https://doi.org/10.1016/0038-0717(89)90179-X.

(120) Jackson, P.; Jacobsen, N. R.; Baun, A.; Birkedal, R.; Kühnel, D.; Jensen, K. A.; Vogel, U.; Wallin, H. Bioaccumulation and Ecotoxicity of Carbon Nanotubes. *Chem Cent J* **2013**, *7*, 154. https://doi.org/10.1186/1752-153X-7-154.

(121) Zheng, X.; Su, Y.; Chen, Y.; Wan, R.; Li, M.; Wei, Y.; Huang, H. Carboxyl-Modified Single-Walled Carbon Nanotubes Negatively Affect Bacterial Growth and Denitrification Activity. *Sci Rep* **2014**, *4*. https://doi.org/10.1038/srep05653.

(122) Hu, W.; Peng, C.; Luo, W.; Lv, M.; Li, X.; Li, D.; Huang, Q.; Fan, C. Graphene-Based Antibacterial Paper. *ACS Nano* **2010**, *4* (7), 4317–4323. https://doi.org/10.1021/nn101097v.

(123) Jin, L.; Son, Y.; DeForest, J. L.; Kang, Y. J.; Kim, W.; Chung, H. Single-Walled Carbon Nanotubes Alter Soil Microbial Community Composition. *Sci. Total Environ.* **2014**, *466–467*, 533–538. https://doi.org/10.1016/j.scitotenv.2013.07.035.

(124) Chung, H.; Son, Y.; Yoon, T. K.; Kim, S.; Kim, W. The Effect of Multi-Walled Carbon Nanotubes on Soil Microbial Activity. *Ecotoxicology and Environmental Safety* **2011**, *74* (4), 569–575. https://doi.org/10.1016/j.ecoenv.2011.01.004.

(125) Jin, L.; Son, Y.; Yoon, T. K.; Kang, Y. J.; Kim, W.; Chung, H. High Concentrations of Single-Walled Carbon Nanotubes Lower Soil Enzyme Activity and Microbial Biomass. *Ecotoxicology and Environmental Safety* **2013**, *88*, 9–15. https://doi.org/10.1016/j.ecoenv.2012.10.031.

(126) Ge, Y.; Priester, J. H.; Mortimer, M.; Chang, C. H.; Ji, Z.; Schimel, J. P.; Holden, P. A. Long-Term Effects of Multiwalled Carbon Nanotubes and Graphene on Microbial Communities in Dry Soil. *Environ. Sci. Technol.* **2016**, *50* (7), 3965–3974. https://doi.org/10.1021/acs.est.5b05620.

(127) Chung, H.; Kim, M. J.; Ko, K.; Kim, J. H.; Kwon, H.; Hong, I.; Park, N.; Lee, S.-W.; Kim, W. Effects of Graphene Oxides on Soil Enzyme Activity and Microbial Biomass. *Science of The Total Environment* **2015**, *514*, 307–313. https://doi.org/10.1016/j.scitotenv.2015.01.077.

(128) Liu, S.; Zeng, T. H.; Hofmann, M.; Burcombe, E.; Wei, J.; Jiang, R.; Kong, J.; Chen, Y. Antibacterial Activity of Graphite, Graphite Oxide, Graphene Oxide, and Reduced Graphene Oxide: Membrane and Oxidative Stress. *ACS Nano* **2011**, *5* (9), 6971–6980. https://doi.org/10.1021/nn202451x.

(129) Giraud, L.; Tourrette, A.; Flahaut, E. Carbon Nanomaterials-Based Polymer-Matrix Nanocomposites for Antimicrobial Applications: A Review. *Carbon* **2021**. https://doi.org/10.1016/j.carbon.2021.06.002.

(130) Akhavan, O.; Ghaderi, E. Toxicity of Graphene and Graphene Oxide Nanowalls Against Bacteria. *ACS Nano* **2010**, *4* (10), 5731–5736. https://doi.org/10.1021/nn101390x.

(131) Kerfahi, D.; Tripathi, B. M.; Singh, D.; Kim, H.; Lee, S.; Lee, J.; Adams, J. M. Effects of Functionalized and Raw Multi-Walled Carbon Nanotubes on Soil Bacterial Community Composition. *PLOS ONE* **2015**, *10* (3), e0123042. https://doi.org/10.1371/journal.pone.0123042.

(132) Evariste, L.; Braylé, P.; Mouchet, F.; Silvestre, J.; Gauthier, L.; Flahaut, E.; Pinelli, E.; Barret, M. Graphene-Based Nanomaterials Modulate Internal Biofilm Interactions and Microbial Diversity. *Front. Microbiol.* **2021**, *12*. https://doi.org/10.3389/fmicb.2021.623853.

(133) Wu, F.; You, Y.; Werner, D.; Jiao, S.; Hu, J.; Zhang, X.; Wan, Y.; Liu, J.; Wang, B.; Wang, X. Carbon Nanomaterials Affect Carbon Cycle-Related Functions of the Soil Microbial Community and the Coupling of Nutrient Cycles. *Journal of Hazardous Materials* **2020**, *390*, 122144. https://doi.org/10.1016/j.jhazmat.2020.122144.

(134) Lavelle, P.; Spain, A. *Soil Ecology*; Springer Science & Business Media, 2001.

(135) Kristensen, E.; Penha-Lopes, G.; Delefosse, M.; Valdemarsen, T.; Quintana, C. O.; Banta, G. T. What Is Bioturbation? The Need for a Precise Definition for Fauna in Aquatic Sciences. *Marine Ecology Progress Series* **2012**, *446*, 285–302. https://doi.org/10.3354/meps09506.

(136) Medina-Sauza, R. M.; Álvarez-Jiménez, M.; Delhal, A.; Reverchon, F.; Blouin, M.; Guerrero-Analco, J. A.; Cerdán, C. R.; Guevara, R.; Villain, L.; Barois, I. Earthworms Building Up Soil Microbiota, a Review. *Front. Environ. Sci.* **2019**, *7*. https://doi.org/10.3389/fenvs.2019.00081.

(137) Morgan, J. E.; Morgan, A. J. The Distribution of Cadmium, Copper, Lead, Zinc and Calcium in the Tissues of the Earthworm Lumbricus Rubellus Sampled from One Uncontaminated and Four Polluted Soils. *Oecologia* **1990**, *84* (4), 559–566.
(138) Spurgeon, D. J.; Hopkin, S. P.; Jones, D. T. Effects of Cadmium, Copper, Lead and Zinc on Growth, Reproduction and Survival of the Earthworm Eisenia Fetida (Savigny): Assessing the Environmental Impact of Point-Source Metal Contamination in Terrestrial Ecosystems. *Environmental Pollution* **1994**, *84* (2), 123–130. https://doi.org/10.1016/0269-7491(94)90094-9.
(139) van Gestel, C. A. M.; Dirven-van Breemen, E. M.; Baerselman, R. Accumulation and Elimination of Cadmium, Chromium and Zinc and Effects on Growth and Reproduction in Eisenia Andrei (Oligochaeta, Annelida). *Science of The Total Environment* **1993**, *134*, 585–597. https://doi.org/10.1016/S0048-9697(05)80061-0.
(140) Neuhauser, E. F.; Loehr, R. C.; Milligan, D. L.; Malecki, M. R. Toxicity of Metals to the Earthworm Eisenia Fetida. *Biol Fert Soils* **1985**, *1* (3), 149–152. https://doi.org/10.1007/BF00301782.
(141) Ma, W. Sublethal Toxic Effects of Copper on Growth, Reproduction and Litter Breakdown Activity in the Earthworm Lumbricus Rubellus, with Observations on the Influence of Temperature and Soil PH. *Environmental Pollution Series A, Ecological and Biological* **1984**, *33* (3), 207–219. https://doi.org/10.1016/0143-1471(84)90011-4.
(142) Li, M.; Liu, Z.; Xu, Y.; Cui, Y.; Li, D.; Kong, Z. Comparative Effects of Cd and Pb on Biochemical Response and DNA Damage in the Earthworm Eisenia Fetida (Annelida, Oligochaeta). *Chemosphere* **2009**, *74* (5), 621–625. https://doi.org/10.1016/j.chemosphere.2008.10.048.
(143) Beaumelle, L.; Vile, D.; Lamy, I.; Vandenbulcke, F.; Gimbert, F.; Hedde, M. A Structural Equation Model of Soil Metal Bioavailability to Earthworms: Confronting Causal Theory and Observations Using a Laboratory Exposure to Field-Contaminated Soils. *Science of The Total Environment* **2016**, *569–570*, 961–972. https://doi.org/10.1016/j.scitotenv.2016.06.023.
(144) Wang, H.-T.; Ding, J.; Chi, Q.-Q.; Li, G.; Pu, Q.; Xiao, Z.-F.; Xue, X.-M. The Effect of Biochar on Soil-Plant-Earthworm-Bacteria System in Metal(Loid) Contaminated Soil. *Environmental Pollution* **2020**, *263*, 114610. https://doi.org/10.1016/j.envpol.2020.114610.
(145) GOPAL, V.; CLEMENT, T.; NAGARAJAN, K. Potential of Megascolex Pumilio in Biomonitoring Environmental Pollution. *Indian J. Environ. Health* **1988**, *28* (3), 194–199.
(146) Abbasi, S. A.; Soni, R. Stress-induced Enhancement of Reproduction in Earthworm Octochaetus Pattoni Exposed to Chromium (vi) and Mercury (Ii)— Implications in Environmental Management. *International Journal of Environmental Studies* **1983**, *22* (1), 43–47. https://doi.org/10.1080/00207238308710100.
(147) Cikutovic, M. A.; Fitzpatrick, L. C.; Venables, B. J.; Goven, A. J. Sperm Count in Earthworms (Lumbricus Terrestris) as a Biomarker for Environmental Toxicology: Effects of Cadmium and Chlordane. *Environmental Pollution* **1993**, *81* (2), 123–125. https://doi.org/10.1016/0269-7491(93)90076-Z.
(148) Spurgeon, D. J.; Hopkin, S. P. Comparisons of Metal Accumulation and Excretion Kinetics in Earthworms (Eisenia Fetida) Exposed to Contaminated Field and Laboratory Soils. *Applied Soil Ecology* **1999**, *11* (2), 227–243. https://doi.org/10.1016/S0929-1393(98)00150-4.
(149) Lock, K.; Janssen, C. R. Toxicity of Arsenate to the Compostworm Eisenia Fetida, the Potworm Enchytraeus Albidus and the Springtail Folsomia Candida. *Bull. Environ. Contam. Toxicol.* **2002**, *68* (5), 760–765. https://doi.org/10.1007/s001280320.
(150) Lock, K.; Janssen, C. R. Ecotoxicity of Nickel to Eisenia Fetida, Enchytraeus Albidus and Folsomia Candida. *Chemosphere* **2002**, *46* (2), 197–200. https://doi.org/10.1016/S0045-6535(01)00112-6.
(151) Bengtsson, G.; Gunnarsson, T.; Rundgren, S. Effects of Metal Pollution on the Earthwormdendrobaena Rubida (Sav.) in Acidified Soils. *Water Air Soil Pollut* **1986**, *28* (3), 361–383. https://doi.org/10.1007/BF00583501.
(152) van Gestel, C. A. M.; van Dis, W. A.; van Breemen, E. M.; Sparenburg, P. M. Development of a Standardized Reproduction Toxicity Test with the Earthworm Species Eisenia Fetida Andrei

Using Copper, Pentachlorophenol, and 2,4-Dichloroaniline. *Ecotoxicology and Environmental Safety* **1989**, *18* (3), 305–312. https://doi.org/10.1016/0147-6513(89)90024-9.

(153) Petersen, E. J.; Pinto, R. A.; Zhang, L.; Huang, Q.; Landrum, P. F.; Weber, W. J. Effects of Polyethyleneimine-Mediated Functionalization of Multi-Walled Carbon Nanotubes on Earthworm Bioaccumulation and Sorption by Soils. *Environ. Sci. Technol.* **2011**, *45* (8), 3718–3724. https://doi.org/10.1021/es103004r.

(154) Li, S.; Irin, F.; Atore, F. O.; Green, M. J.; Cañas-Carrell, J. E. Determination of Multi-Walled Carbon Nanotube Bioaccumulation in Earthworms Measured by a Microwave-Based Detection Technique. *Science of The Total Environment* **2013**, *445–446*, 9–13. https://doi.org/10.1016/j.scitotenv.2012.12.037.

(155) Eom, H.-J.; Roca, C. P.; Roh, J.-Y.; Chatterjee, N.; Jeong, J.-S.; Shim, I.; Kim, H.-M.; Kim, P.-J.; Choi, K.; Giralt, F.; Choi, J. A Systems Toxicology Approach on the Mechanism of Uptake and Toxicity of MWCNT in Caenorhabditis Elegans. *Chemico-Biological Interactions* **2015**, *239*, 153–163. https://doi.org/10.1016/j.cbi.2015.06.031.

(156) Petersen, E. J.; Pinto, R. A.; Landrum, P. F.; Weber, Jr., Walter J. Influence of Carbon Nanotubes on Pyrene Bioaccumulation from Contaminated Soils by Earthworms. *Environ. Sci. Technol.* **2009**, *43* (11), 4181–4187. https://doi.org/10.1021/es803023a.

(157) Calisi, A.; Grimaldi, A.; Leomanni, A.; Lionetto, M. G.; Dondero, F.; Schettino, T. Multibiomarker Response in the Earthworm Eisenia Fetida as Tool for Assessing Multi-Walled Carbon Nanotube Ecotoxicity. *Ecotoxicology* **2016**, *25* (4), 677–687. https://doi.org/10.1007/s10646-016-1626-x.

(158) Hu, C. W.; Zhang, L. J.; Wang, W. L.; Cui, Y. B.; Li, M. Evaluation of the Combined Toxicity of Multi-Walled Carbon Nanotubes and Sodium Pentachlorophenate on the Earthworm Eisenia Fetida Using Avoidance Bioassay and Comet Assay. *Soil Biology and Biochemistry* **2014**, *70*, 123–130. https://doi.org/10.1016/j.soilbio.2013.12.018.

(159) Zhao, S.; Wang, Y.; Duo, L. Biochemical Toxicity, Lysosomal Membrane Stability and DNA Damage Induced by Graphene Oxide in Earthworms. *Environmental Pollution* **2021**, *269*, 116225. https://doi.org/10.1016/j.envpol.2020.116225.

(160) Scott-Fordsmand, J. J.; Krogh, P. H.; Schaefer, M.; Johansen, A. The Toxicity Testing of Double-Walled Nanotubes-Contaminated Food to Eisenia Veneta Earthworms. *Ecotoxicology and Environmental Safety* **2008**, *71* (3), 616–619. https://doi.org/10.1016/j.ecoenv.2008.04.011.

(161) Tremel-Schaub, A.; Feix, I. *Contamination des sols: Transferts des sols vers les plantes*; EDP Sciences: Les Ulis France; Angers, 2005.

(162) Comité Européen de Normalisation (CEN). Standards for the Safety of Users, the Environment and Plants 1995 CEN/TC 223/WG2 N.136 Version 2. 1995.

(163) Assche, F. V.; Clijsters, H. Effects of Metals on Enzyme Activity in Plants. *Plant, Cell & Environment* **1990**, *13* (3), 195–206. https://doi.org/10.1111/j.1365-3040.1990.tb01304.x.

(164) Jadia, C. D.; Fulekar, M. H. Phytoremediation of Heavy Metals: Recent Techniques. *African Journal of Biotechnology* **2009**, *8* (6).

(165) Tamás, M. J.; Sharma, S. K.; Ibstedt, S.; Jacobson, T.; Christen, P. Heavy Metals and Metalloids As a Cause for Protein Misfolding and Aggregation. *Biomolecules* **2014**, *4* (1), 252–267. https://doi.org/10.3390/biom4010252.

(166) Marin, A. R.; Pezeshki, S. R.; Masschelen, P. H.; Choi, H. S. Effect of Dimethylarsenic Acid (DMAA) on Growth, Tissue Arsenic, and Photosynthesis of Rice Plants. *Journal of Plant Nutrition* **1993**, *16* (5), 865–880. https://doi.org/10.1080/01904169309364580.

(167) Panda, S. K.; Patra, H. K. Nitrate and Ammonium Ions Effect on the Chromium Toxicity in Developing Wheat Seedlings. *Proceedings of the National Academy of Sciences India. Section B, Biological Sciences* **2000**, *70* (1), 75–80.

(168) Abedin, Md. J.; Cotter-Howells, J.; Meharg, A. A. Arsenic Uptake and Accumulation in Rice (Oryza Sativa L.) Irrigated with Contaminated Water. *Plant and Soil* **2002**, *240* (2), 311–319. https://doi.org/10.1023/A:1015792723288.

(169) Sheldon, A. R.; Menzies, N. W. The Effect of Copper Toxicity on the Growth and Root Morphology of Rhodes Grass (Chloris Gayana Knuth.) in Resin Buffered Solution Culture. *Plant Soil* **2005**, *278* (1), 341–349. https://doi.org/10.1007/s11104-005-8815-3.
(170) Du, X.; Zhu, Y.-G.; Liu, W.-J.; Zhao, X.-S. Uptake of Mercury (Hg) by Seedlings of Rice (Oryza Sativa L.) Grown in Solution Culture and Interactions with Arsenate Uptake. *Environmental and Experimental Botany* **2005**, *54* (1), 1–7. https://doi.org/10.1016/j.envexpbot.2004.05.001.
(171) Wang, M.; Zou, J.; Duan, X.; Jiang, W.; Liu, D. Cadmium Accumulation and Its Effects on Metal Uptake in Maize (Zea Mays L.). *Bioresource Technology* **2007**, *98* (1), 82–88. https://doi.org/10.1016/j.biortech.2005.11.028.
(172) Chibuike, G. U.; Obiora, S. C. *Heavy Metal Polluted Soils: Effect on Plants and Bioremediation Methods*. Applied and Environmental Soil Science. https://doi.org/10.1155/2014/752708.
(173) Kopittke, P. M.; Blamey, F. P. C.; Asher, C. J.; Menzies, N. W. Trace Metal Phytotoxicity in Solution Culture: A Review. *Journal of Experimental Botany* **2010**, *61* (4), 945–954. https://doi.org/10.1093/jxb/erp385.
(174) Liné, C.; Larue, C.; Flahaut, E. Carbon Nanotubes: Impacts and Behaviour in the Terrestrial Ecosystem - A Review. *Carbon* **2017**, *123*, 767–785. https://doi.org/10.1016/j.carbon.2017.07.089.
(175) Larue, C.; Pinault, M.; Czarny, B.; Georgin, D.; Jaillard, D.; Bendiab, N.; Mayne-L'Hermite, M.; Taran, F.; Dive, V.; Carrière, M. Quantitative Evaluation of Multi-Walled Carbon Nanotube Uptake in Wheat and Rapeseed. *Journal of Hazardous Materials* **2012**, *227–228*, 155–163. https://doi.org/10.1016/j.jhazmat.2012.05.033.
(176) Oleszczuk, P.; Jośko, I.; Xing, B. The Toxicity to Plants of the Sewage Sludges Containing Multiwalled Carbon Nanotubes. *Journal of Hazardous Materials* **2011**, *186* (1), 436–442. https://doi.org/10.1016/j.jhazmat.2010.11.028.
(177) Ratnikova, T. A.; Podila, R.; Rao, A. M.; Taylor, A. G. *Tomato Seed Coat Permeability to Selected Carbon Nanomaterials and Enhancement of Germination and Seedling Growth*. The Scientific World Journal. https://doi.org/10.1155/2015/419215.
(178) Lahiani, M. H.; Chen, J.; Irin, F.; Puretzky, A. A.; Green, M. J.; Khodakovskaya, M. V. Interaction of Carbon Nanohorns with Plants: Uptake and Biological Effects. *Carbon* **2015**, *81*, 607–619. https://doi.org/10.1016/j.carbon.2014.09.095.
(179) Lahiani, M. H.; Dervishi, E.; Ivanov, I.; Chen, J.; Khodakovskaya, M. Comparative Study of Plant Responses to Carbon-Based Nanomaterials with Different Morphologies. *Nanotechnology* **2016**, *27* (26), 265102. https://doi.org/10.1088/0957-4484/27/26/265102.
(180) Lin, C.; Fugetsu, B.; Su, Y.; Watari, F. Studies on Toxicity of Multi-Walled Carbon Nanotubes on Arabidopsis T87 Suspension Cells. *Journal of Hazardous Materials* **2009**, *170* (2), 578–583. https://doi.org/10.1016/j.jhazmat.2009.05.025.
(181) Shen, C.-X.; Zhang, Q.-F.; Li, J.; Bi, F.-C.; Yao, N. Induction of Programmed Cell Death in Arabidopsis and Rice by Single-Wall Carbon Nanotubes. *American Journal of Botany* **2010**, *97* (10), 1602–1609. https://doi.org/10.3732/ajb.1000073.
(182) Mondal, A.; Basu, R.; Das, S.; Nandy, P. Beneficial Role of Carbon Nanotubes on Mustard Plant Growth: An Agricultural Prospect. *J Nanopart Res* **2011**, *13* (10), 4519. https://doi.org/10.1007/s11051-011-0406-z.
(183) Begum, P.; Fugetsu, B. Phytotoxicity of Multi-Walled Carbon Nanotubes on Red Spinach (Amaranthus Tricolor L) and the Role of Ascorbic Acid as an Antioxidant. *Journal of Hazardous Materials* **2012**, *243*, 212–222. https://doi.org/10.1016/j.jhazmat.2012.10.025.
(184) Gao, M.; Chang, X.; Yang, Y.; Song, Z. Foliar Graphene Oxide Treatment Increases Photosynthetic Capacity and Reduces Oxidative Stress in Cadmium-Stressed Lettuce. *Plant Physiology and Biochemistry* **2020**, *154*, 287–294. https://doi.org/10.1016/j.plaphy.2020.06.021.
(185) Gao, M.; YujuanYang; Song, Z. Toxicity of Cadmium to Wheat Seedling Roots in the Presence of Graphene Oxide. *Chemosphere* **2019**, *233*, 9–16. https://doi.org/10.1016/j.chemosphere.2019.05.127.

(186) Chen, X.; Wang, J.; Hayat, K.; Zhang, D.; Zhou, P. Small Structures with Big Impact: Multi-Walled Carbon Nanotubes Enhanced Remediation Efficiency in Hyperaccumulator Solanum Nigrum L. under Cadmium and Arsenic Stress. *Chemosphere* **2021**, *276*, 130130. https://doi.org/10.1016/j.chemosphere.2021.130130.

(187) Xu, K.; Liu, Y.-X.; Wang, X.-F.; Li, S.-W.; Cheng, J.-M. Combined Toxicity of Functionalized Nano-Carbon Black and Cadmium on Eisenia Fetida Coelomocytes: The Role of Adsorption. *Journal of Hazardous Materials* **2020**, *398*, 122815. https://doi.org/10.1016/j.jhazmat.2020.122815.

(188) Xiong, T.; Yuan, X.; Wang, H.; Leng, L.; Li, H.; Wu, Z.; Jiang, L.; Xu, R.; Zeng, G. Implication of Graphene Oxide in Cd-Contaminated Soil: A Case Study of Bacterial Communities. *Journal of Environmental Management* **2018**, *205*, 99–106. https://doi.org/10.1016/j.jenvman.2017.09.067.

(189) Capowiez, Y.; Gilbert, F.; Vallat, A.; Poggiale, J.-C.; Bonzom, J.-M. Depth Distribution of Soil Organic Matter and Burrowing Activity of Earthworms—Mesocosm Study Using X-Ray Tomography and Luminophores. *Biol Fertil Soils* **2021**, *57* (3), 337–346. https://doi.org/10.1007/s00374-020-01536-y.

(190) Wen, B.; Hu, X.; Liu, Y.; Wang, W.; Feng, M.; Shan, X. The Role of Earthworms (Eisenia Fetida) in Influencing Bioavailability of Heavy Metals in Soils. *Biol Fertil Soils* **2004**, *40* (3), 181–187. https://doi.org/10.1007/s00374-004-0761-3.

(191) Manjate, E.; Ramos, S.; Almeida, C. M. R. Potential Interferences of Microplastics in the Phytoremediation of Cd and Cu by the Salt Marsh Plant Phragmites Australis. *Journal of Environmental Chemical Engineering* **2020**, *8* (2), 103658. https://doi.org/10.1016/j.jece.2020.103658.

(192) Li, M.; Liu, Y.; Xu, G.; Wang, Y.; Yu, Y. Impacts of Polyethylene Microplastics on Bioavailability and Toxicity of Metals in Soil. *Science of The Total Environment* **2021**, *760*, 144037. https://doi.org/10.1016/j.scitotenv.2020.144037.

(193) Zhang, S.; Shao, T.; Bekaroglu, S. S. K.; Karanfil, T. The Impacts of Aggregation and Surface Chemistry of Carbon Nanotubes on the Adsorption of Synthetic Organic Compounds. *Environmental Science & Technology* **2009**, *43* (15), 5719–5725. https://doi.org/10.1021/es900453e.

(194) Petosa, A. R.; Jaisi, D. P.; Quevedo, I. R.; Elimelech, M.; Tufenkji, N. Aggregation and Deposition of Engineered Nanomaterials in Aquatic Environments: Role of Physicochemical Interactions. *Environmental Science & Technology* **2010**, *44* (17), 6532–6549. https://doi.org/10.1021/es100598h.

(195) Dong, Y.; Gao, M.; Qiu, W.; Song, Z. Uptake of Microplastics by Carrots in Presence of As (III): Combined Toxic Effects. *Journal of Hazardous Materials* **2021**, *411*, 125055. https://doi.org/10.1016/j.jhazmat.2021.125055.

(196) Wang, F.; Zhang, X.; Zhang, S.; Zhang, S.; Adams, C. A.; Sun, Y. Effects of Co-Contamination of Microplastics and Cd on Plant Growth and Cd Accumulation. *Toxics* **2020**, *8* (2), 36. https://doi.org/10.3390/toxics8020036.

(197) Singh, S.; Zacharias, M.; Kalpana, S.; Mishra, S. Heavy Metals Accumulation and Distribution Pattern in Different Vegetable Crops. *JECE* **2012**, *4* (4), 75–81. https://doi.org/10.5897/JECE11.076.

(198) Whalley, C.; Mohaupt, V. *Chemicals in European Waters — European Environment Agency*; Publication 18; European Environment Agency, 2019; p 80. https://www.eea.europa.eu/publications/chemicals-in-european-waters (accessed 2022-05-10).

(199) Evariste, L.; Mottier, A.; Lagier, L.; Cadarsi, S.; Barret, M.; Sarrieu, C.; Soula, B.; Mouchet, F.; Flahaut, E.; Pinelli, E.; Gauthier, L. Assessment of Graphene Oxide Ecotoxicity at Several Trophic Levels Using Aquatic Microcosms. *Carbon* **2020**, *156*, 261–271. https://doi.org/10.1016/j.carbon.2019.09.051.

(200) Hagger, J. A.; Jones, M. B.; Lowe, D.; Leonard, D. R. P.; Owen, R.; Galloway, T. S. Application of Biomarkers for Improving Risk Assessments of Chemicals under the Water Framework Directive:

A Case Study. *Marine Pollution Bulletin* **2008**, *56* (6), 1111–1118. https://doi.org/10.1016/j.marpolbul.2008.03.040.

(201) Broeg, K.; Westernhagen, H. v.; Zander, S.; Körting, W.; Koehler, A. The "Bioeffect Assessment Index" (BAI): A Concept for the Quantification of Effects of Marine Pollution by an Integrated Biomarker Approach. *Marine Pollution Bulletin* **2005**, *50* (5), 495–503. https://doi.org/10.1016/j.marpolbul.2005.02.042.

(202) Li, X.; Wang, M.; Chen, W.; Jiang, R. Evaluation of Combined Toxicity of Siduron and Cadmium on Earthworm (Eisenia Fetida) Using Biomarker Response Index. *Science of The Total Environment* **2019**, *646*, 893–901. https://doi.org/10.1016/j.scitotenv.2018.07.380.

(203) Zhang, J.; Liu, S.-S.; Zhang, J.; Qin, L.-T.; Deng, H.-P. Two Novel Indices for Quantitatively Characterizing the Toxicity Interaction between Ionic Liquid and Carbamate Pesticides. *Journal of Hazardous Materials* **2012**, *239–240*, 102–109. https://doi.org/10.1016/j.jhazmat.2012.07.063.

(204) Lock, K.; Janssen, C. R. Influence of Aging on Metal Availability in Soils. In *Reviews of Environmental Contamination and Toxicology*; Ware, G. W., Ed.; Reviews of Environmental Contamination and Toxicology; Springer: New York, NY, 2003; pp 1–21. https://doi.org/10.1007/0-387-21728-2_1.

(205) Ma, Y.; Lombi, E.; Oliver, I. W.; Nolan, A. L.; McLaughlin, M. J. Long-Term Aging of Copper Added to Soils. *Environ. Sci. Technol.* **2006**, *40* (20), 6310–6317. https://doi.org/10.1021/es060306r.

(206) Schreck, E.; Foucault, Y.; Geret, F.; Pradère, P.; Dumat, C. Influence of Soil Ageing on Bioavailability and Ecotoxicity of Lead Carried by Process Waste Metallic Ultrafine Particles. *Chemosphere* **2011**, *85*, 1555–1562. https://doi.org/10.1016/j.chemosphere.2011.07.059.

(207) McBride, M. B.; Cai, M. Copper and Zinc Aging in Soils for a Decade: Changes in Metal Extractability and Phytotoxicity. *Environ. Chem.* **2015**, *13* (1), 160–167. https://doi.org/10.1071/EN15057.

(208) Martínez, C. E.; McBride, M. B. Cd, Cu, Pb, and Zn Coprecipitates in Fe Oxide Formed at Different PH: Aging Effects on Metal Solubility and Extractability by Citrate. *Environmental Toxicology and Chemistry* **2001**, *20* (1), 122–126. https://doi.org/10.1002/etc.5620200112.

3.5. Supporting information

Carbon based nanomaterial interactions with metals and metalloids in terrestrial environment: a review

Mathieu Leroy[1,2], Emmanuel Flahaut[2*], Camille Larue[1*]

[1]Laboratoire écologie fonctionnelle et environnement, Université de Toulouse, CNRS, Toulouse, France, [2]CIRIMAT, Université de Toulouse, CNRS, INPT, UPS, UMR CNRS-UPS-INP N°5085, Université Toulouse 3 Paul Sabatier, Bât. CIRIMAT, 118, route de Narbonne, 31062 Toulouse cedex 9, France

*Corresponding author: emmanuel.flahaut@univ-tlse3.fr; camille.larue@ensat.fr

Table S1: Maximum adsorption capacity of different CNM established by adsorption models for various metal(loid)s in mono-elemental conditions extracted from the cited articles (grey lines represent data used to build Table 1, SSA = specific area ($m^2.g^{-1}$), n= Freundlich constant, R^2 = correlation coefficient, qm = maximum modelled adsorption ($mg.g^{-1}$), C = meta(loid)l concentration range ($mg.L^{-1}$), A = Adsorbent dosage ($mg.L^{-1}$), T = temperature (°C), Ct = Contact time (hours), RPM = agitation (Rotation Per Minute), R = Room temperature, GO = Graphene Oxide, CNT = Carbon Nanotubes, MWCNT = Multi-Walled Carbon Nanotubes)

M^{n+}	Adsorbent	SSA	Thermodynamics				C	A	Parameters				References
			Freudlich		Langmuir				T	Ct	pH	RPM	
			n	R^2	qm	R^2							
As(III)	MWCNT–ZrO_2	152	1.02	0.99	0.2	1	0.1	1000-10000		6	6	175	Addo Ntim *et al.*[1]
	Fe-MWCNT		3.24	0.99	4	0.99	0.1	100-200			8		Tawabini et al .[2]
	ethylenediamine-MWNCT-Fe^{2+}	198.5	0.43	0.99	18.05	0.96	0 to 4	100	25	1.67	4		Veličković *et al.*[3]
			0.45	0.99	20.66	0.95			35				
			0.48	0.99	23.47	0.95			45				
	ethylenediamine-MWNCT-Fe^{3+}	240.9	0.43	0.99	10.56	0.96			25				
			0.46	0.99	12.29	0.95			35				
			0.47	0.99	13.74	0.96			45				
	Fe-MWCNT		1.18	0.99	1.72	0.99	0.1	1000 to 10000		12	4	175	Addo Ntim *et al.*[4]
As(V)	Fe-MWCNT		1.94	0.99	189	0.99	0.1	1000 to 10000		12	4	175	Addo Ntim *et al.*[4]
Cd(II)	O-CNT	170	3.66	0.9	4.35	0.99	?	150 mg		2	7		Ihsanullah *et al.*[5]
	O-Carbon nanofibers	35.1	3.70	0.77	0.93	0.96	?						
	HNO_3-modified CNT				10.86	0.99	2 to 15	500	R	4	5		Li *et al.*[6]
	O-MWCNT	78.49	0.6	0.97	22.39	0.99	0.1 to 5	100	25	0.75	8		Vuković *et al.*[7]
			0.59	0.96	22.97	0.99			35				
			0.57	0.96	24.15	0.99			45				
	ethylenediamine-functionalized-MWCNT	101.24	0.6	0.97	21.67	0.99			25				
			0.56	0.96	23.28	0.99			35				

			0.53	0.97	25.7	0.99			45				
	MWCNT	187.58	0.52	0.97	1.26	0.99			25				
			0.54	0.96	2.2	0.99			35				
			0.54	0.96	3.19	0.99			45				
	Oxidized CNT		0.41	0.95	92.59	0.91	100 to 1200	2000	25			100	Tofighy *et al.*[8]
	SWCNT-COOH	400	10.01	0.99	50.23	0.99	10 to 50	50	10	4	5		Moradi *et al.*[9]
			10.59	0.99	52.35	0.99			20				
			11.03	0.99	55.34	0.99			30				
			11.09	0.99	58.89	0.99			40				
	SWCNT		9.76	0.99	16.13	0.99			10				
			11.07	0.99	18.87	0.99			20				
			13.34	0.99	21.23	0.99			30				
			17.05	0.99	24.06	0.99			40				
	GO		3.4	0.95	530	0.99	0 to 80	200	25	2	5		Sitko *et al.*[10]
	GO		4.25	0.94	83.8	0.99	5 to 100	200	30		5.7	200	Tan *et al.*[11]
Co(II)	Oxidized CNT		0.42	0.99	85.74	0.95	100 to 1200	2000	25			100	Tofighy *et al.*[8]
	CNT soaked in HNO_3	40–600	1.05	0.99			1 to 20	50		4	9		Stafiej *et al.*[12]
	CNT refluxed in HNO_3		1	0.98									
	GO		2.43	0.99	21.28	0.96	2 to 25	1000	25		5.5		Lingamdinne *et al.*[13]
Cr(III)	O-MWCNT		2.48	0.95	0.38	0.91	?	5-400 mg			7	150	Atieh *et al.*[14]
Cr(VI)	Oxidized MWCNT	197	14.53	0.97	2.6	0.99	10	750	20	165	2.88		Hu *et al.*[15]
			11.74	0.99	2.87	0.99		1250					
			11.82	0.95	3.04	0.99		1250					
	CNT	156	2.01	0.79	3.11	0.97							Ihsanullah *et al.*[16]
	Oxidized CNT	170	5.99	0.28	1.31	0.92							

	acid-refluxed CNT	250.55			26.11	0.99	2 to 14	1000			4.5		Di *et al.*[17]
					26.47	0.98					5.5		
					26.67	0.99					6.5		
					26.88	0.97					7.5		
					23.81	0.99					8.5		
					16.11	0.99					9.5		
	aligned Ceria CNT		4.01	0.97	26.81	0.93	2-35	1000	25	24	3.0		Di *et al.*[18]
			4	0.97	28.49	0.96	2-35				5.0		
			4.16	0.95	31.55	0.99	2-35				7.0		
			2.8	0.97	26.04	0.99	2-35				9.0		
			1.75	0.95	23.26	0.99	2-35				11.0		
	O-MWCNT	87.4	1.55	0.99	85.83	0.96	20-500	750		0.67	2.5 to 4.0		Kumar *et al.*[19]
Cu(II)	HNO_3-modified CNT				28.49	0.98	5 to 30	500	R	4	5		Li *et al.*[6]
	CNT	153	3.87	0.97	26.41	0.99	5 to 40	500	25	2	5		Li *et al.*[20]
	CNT-calcium alginate	28	1.84	0.95	84.88	0.99							
	MWCNT	169.7	0.96	0.94			10 to 100	500	25	6			Ge *et al.*[21]
	Sulfonate-MWCNT	28.7	1.39	0.98									
	Oxidized CNT		0.52	0.99	64.93	0.89	100 to 1200	2000	25			100	Tofighy *et al.*[8]
	SWCNT-COOH	400	6.33	0.99	65.12	0.99	10 to 50	50	10	4	5		Moradi *et al.*[9]
			7.97	0.99	68.96	0.99			20				
			8.99	0.99	72.33	0.99			30				
			10	0.99	77	0.99			40				
	SWCNT		9.32	0.99	19.89	0.99			10				
			9.86	0.99	21	0.99			20				
			10.31	0.99	22.87	0.99			30				
			10.79	0.99	24.29	0.99			40				
	CNT soaked in HNO_3	40–600	1.01	0.99			1 to 20	50		4	9		Stafiej *et al.*[12]

	CNT refluxed in HNO_3		0.99	0.99									
	As-produced CNT	82.2	1.32	0.9	6.39	0.89	0 to 120	500	7	24	6	125	Wu *et al.*[22]
			1.6	0.86	7.87	0.91			17				
			1.74	0.86	8.25	0.84			27				
			2.06	0.8	9.34	0.8			37				
			2.29	0.61	10.17	0.64			47				
	HNO_3-modified CNT	64.3	1.45	0.86	12.46	0.9			7				
			2.4	0.94	13.1	0.92			17				
			2.33	0.99	13.87	0.96			27				
			3.24	0.7	15.11	0.97			37				
			2.84	0.7	16.04	0.94			47				
	NaOCl-modified CNT	94.9	2.89	0.87	44.64	0.99			7				
			3.61	0.94	45.87	0.99			17				
			5.33	0.99	47.39	0.97			27				
			5.54	0.95	49.02	0.95			37				
			7.71	0.87	51.81	0.93			47				
	As-grown CNT		0.59	0.93	16.55	0.97	6 to 30	50		2	5.2		Li *et al.*[23]
	Oxidized CNT		1.23	0.89	28.49	0.98							
	GO		3	0.97	294	0.99	0 to 80	200	25	2	5		Sitko *et al.*[10]
	GO		3.58	0.96	72.6	0.99	5 to 100	200	30		5.7	200	Tan *et al.*[11]
	GO				46.6	0.99	0 to 40	500		12	5		Yang *et al.*[24]
Hg(II)	MWCNT		1.17	0.99	13.16	0.99	0 to 5.8	40 mg			8		Tawabini *et al.*[25]
	MWCNT		4.54	0.99	78.12	0.99	15 to 145	50	17	24	6.7		Shadbad *et al.*[26]
			35.4	0.99	87.72	0.99			27				
			36.5	0.99	93.45	0.99			37				
	MWNCT	233	0.61	0.93	0.41	0.99	0.02	20-500		24			Chen *et al.*[27]
			0.91	0.89	32.4	0.88	4						

	OH-MWCNT		1.28	0.97	0.43	0.99	0.02						
			0.9	0.89	120.1	0.95	4						
	COOH-MWCNT		0.54	0.91	0.51	0.99	0.02						
			1.18	0.85	127.6	0.99	4						
	MWCNT		0.13	0.78	3.83	0.98	1–10	250	25		7		El-Sheikh *et al.*[28]
			0.12	0.7	1.32	0.97							
			0.32	0.84	3.75	0.94							
			0.98	0.93	2.06	0.99							
			0.06	0.87	0.7	0.93							
			0.29	0.7	0.7	0.93							
	3-Mercaptopropyltriethoxysilane (MPTS) grafted MWCNT-Fe_3O_4	97.163	2.27	0.98	65.52	0.99	5 to 90	1000			6.5	100	Zhang *et al.*[29]
	SWCNT-SH		1.95	0.95	131.58	0.97	10 to 80	250	25	1	5.0		Bandaru *et al.*[30]
	SWCNT		1.83	0.98	40.16	0.97							
	MWCNT	85.1	2.5	0.99	5.48	0.97	10 to 120	1000		4	6		Gupta *et al.*[30]
	MWCNT-Ox	152.5	3.04	0.98	27.32	0.97							
	MWCNT-Iodide	153	2.07	0.93	123.45	0.99							
	MWCNT-Suflur	155.3	1.83	0.94	151.51	0.99							
Ni(II)	MWCNT	102	1.67	0.95	17.86	0.97	10 to 30	800	25				Mobasherpour et al .[31]
	MWCNT iron-ox	56.78	2.48	0.96	9.18	0.98	0 to 14	750	25	24	6.4		Chen *et al.*[32]
	MWCNT-ox	145	1.72	0.98	49.26	0.97	10 to 200	200			6		Kandah *et al.*[33]
	MWCNT-arsenic	134	1.51	0.98	18.08	0.97							
	MWCNT	197	1.09	0.92	8.77	0.99	0 to 14	750	18		6.55	300	Chen *et al.*[34]
			1.04	0.96	9.43	0.99			30				
			1.04	0.96	9.52	0.99			40				
			1.11	0.9	9.8	0.99			60				

	GO		3.25	0.97	100	0.92	10 to 25	1000	25	0.83	6		Najafi *et al.*[35]
	GO-glycine		2.34	0.99	90.9	0.88							
	GO		1.94	0.95	62.3	0.99	5 to 100	200	30		5.7	200	Tan *et al.*[11]
Pb(II)	Acidified MWCNT		1.8	0.99	1.66	0.99	2 to 14	500	R	6	3		Li *et al.*[36]
			1.91	0.99	17.44	0.99	2 to 14	500	R	6	5		
			1.09	0.99	49.95		2 to 14	500	R	6	7		
	Acidified MWCNT	122-153	4.53	0.99			10 to 80	500	7		5		Li *et al.*[37]
			4.48	0.97			10 to 80	500	25		5		
			4.34	0.98			10 to 80	500	48		5		
	HNO_3-modified CNT				97.08	0.99	10 to 60	500	R	4	5		Li *et al.*[6]
	Acidified MWCNT	237.33	0.19	0.86	49.71	0.99	10 to 60	500	10	6	5	210	Wang *et al.*[38]
			0.2	0.88	51.81	0.99	10 to 60	500	50	6	5	210	
	MnO_2/CNT	275	3.96	0.87	82.6	0.99	10 to 60	500	25	2	5	210	Wang *et al.*[39]
	MWCNT-Fe_3O_4	97.163	2.2	0.95	65.4	0.99	5 to 90	1000	25		6.5	100	Zhang *et al.*[29]
	3-Mercaptopropyltriethoxysilane (MPTS) grafted MWCNT-Fe_3O_4												

	TiO_2/MWCNT composites		1.42	0.97	137	0.99		2000	20	2.5	6		Zhao *et al.*[40]
	MWCNT		2.11	0.93	33	0.99		2000	20	2.5	6		
	Oxidized CNT		0.41	0.98	117.65	0.93	100 to 1200	2000	25		7	100	Tofighy *et al.*[8]
	SWCNT-COOH	400	3.89	0.99	90.23	0.99	10 to 50	50	10	4	5		Moradi *et al.*[9]
			4.11	0.99	92.59	0.99			20				
			4.32	0.99	94.69	0.99			30				
			4.522	0.99	96.02	0.99			40				
	SWCNT		9.21	0.99	27.11	0.99			10				
			9.9	0.99	29.85	0.99			20				
			10.11	0.99	31.23	0.99			30				
			13	0.99	33.54	0.99			40				
	CNT soaked in HNO_3	40–600	0.94	0.99			1 to 20	50		4	9		Stafiej *et al.*[12]
	CNT refluxed in HNO_3		0.94	0.99									
	GO		5.33	0.91	842	0.98		100	20		6		Zhao *et al.*[41]
			5.86	0.98	1150	0.98			40				
			4.72	0.96	1850	0.99			60				
	GO		4.5	0.97	1119	0.98	0 to 150		25	2	5		Sitko *et al.*[10]
Zn(II)	Oxidized CNT		0.5	0.94	74.63	0.88	100 to 1200	2000	25			100	Tofighy *et al.*[8]
	MWCNT				10.46	0.97	0.01 to 0.20	1000	23		6.5 - 6.8		Cho *et al.*[42]
	O-MWCNT				15.69	0.99	0.01 to 0.20	1000	23		6.5 - 6.8		
					15.69	0.99	0.01 to 0.20	1000	23		6.5 - 6.8		

					15.04	0.97	0.01 to 0.20	1000	23		6.5 - 6.8		
	SWCNT	423	0.29	0.94	43.66	0.99	10 to 80	500	25	12	7	180	Lu *et al.*[43]
	MWCNT	297	0.24	0.94	32.68	0.99							
	SWCNT	423	3.3	0.98	37.03	0.99	10 to 80	500	5	12	7	180	Lu *et al.*[24]
			3.47	0.98	40.65	0.99			15				
			3.46	0.98	41.84	0.99			25				
			3.28	0.97	45.45	0.99			35				
			3.31	0.97	46.94	0.99			45				
	MWCNT	297	3.53	0.98	30.3	0.98			5				
			4.13	0.98	31.74	0.99			15				
			4.03	0.98	33.33	0.98			25				
			4.57	0.97	33.78	0.98			35				
			4.65	0.98	34.36	0.98			45				
	MWCNT-ox	256			27.2	0.99	10 to 80	500		12		180	Lu *et al.*[44]
	MWCNT-ox	250	0.23	0.99	1.05	0.99	1.1	300 to 900					Mubarak *et al.*[45]
	GO		3.1	0.96	345	0.99	0 to 80	200	25	2	5		Sitko *et al.*[10]

Table S2. Mean of lowest metal(loid) amount added that resulted in a decrease in the rate of basal respiration of soil bacteria (LOAED) or the highest amount of metal added that did not produce an effect (HNOED) for Cd, Cr, Cu, Hg, Ni, Pb and Zn according to McGrath et al.[46] (unit : µg.g^{-1}).

	LOAED	**HNOED**
Cd	593.8	169.7
Cr	411.5	127.3
Cu	499.9	1315.9
Hg	257.5	60.0
Ni	576.5	1837.6
Pb	506.2	3956.7
Zn	696.9	252.7

Co-exposure of metal(loid)s with micro and nanoplastics

Table S3. Effects of simultaneous microplastics and nanoplastics (MNP)/metal(loid) exposure on transfer and associated toxicity for three representative agrosystem organisms (bacteria, earthworms and plants). The light blue lines represent studies with hydroponic exposure and the dark blue lines represent studies with soil exposure (PS = polystyrene, PTFE = polytetrafluoroethylene, SOD = superoxide dismutase, POD = peroxidase, MDA = malondialdehyde, CAT = catalase, GR = glutathione reductase, GP = glutathione peroxidase, Chlo = chlorophyll, n.p = data not provided)

Type and MNP concentration	**MNP size**	**Type and metal(loid) concentration**	**Organisms**	**Exposure medium**	**Exposure duration**	**Transfer effects**	**Interactive toxicological effects**	**References**
Polystyrene nanoplastics (10 mg.L^{-1})	87 nm	Cd (2,25 mg.L^{-1})	Plant: *Triticum aestivum*	Culture solution	21 days	No effects in Cd transfer	Antagonist effect on dry biomass with the addition of nanoplastic, synergic effect on SOD activity in roots but antagonist in leaves with the addition of nanoplastics	Lian *et al.*[47]
Microplastics (40, 100, and 200 mg.L^{-1})	n.p	As (0, 1.6, 3.2, or 4.0 mg.L^{-1})	Plant: *Oryza sativa*	Culture solution	7 days	Reduction of transfer: decrease of As concentration in roots and leaves with the addition of PS	Antagnist effects on the studied parameters: biomass, O_2 and H_2O_2 concentrations, photosynthetic parameters (chlo a/b and total, Fv/Fm) and SOD and CAT activity.	Dong *et al.*[48]
Microplastics	0.1-1 and 5 µm	As (1, 2 and 4 mg.L^{-1})	Plant: *Daucus carota*	Hydroponic	7days	n.p	Synergic effects: decreased on total biomass and carrot quality (soluble protein, soluble sugar, α-/β-carotene and pectin methyl esterase)	Dong *et al.*[49]

Polyethylene microspheres (1500 mg.L^{-1})	850−1000 µm	Cd and Cu (10 mg.L^{-1})	Plant : *Phragmites australis*	Soil solution	7 days	Increase in Cd transfer to roots, rhizomes and leaves in the presence of microplastics. Increase in Cu transfer to roots, rhizomes in the presence of microplastics.	n.p	Manjate *et al.*[50]
Micro and nanoplastics (2000 mg.kg−1 and 200 mg.kg^{-1})	n.p	As	Bacteria	Natural soil	74 days	n.p	No effect on bacterial communities	Zhu *et al.*[51]
Polyethylene microplastics (100, 500 and 1000 mg.kg^{-1})	30 µm and 100 µm	Cu and Ni (Cu = 100 mg.kg^{-1} and Ni = 40 mg.kg^{-1})	Earthworms : *Eisenia fetida*	Soil	7, 14 and 21 days	Increased on Cu and Ni transfer at 7, 14 and 21 days whatever the diameter and the concentration of microplastics.	Synergetic effects with Cu/Ni with the addition of 500 mg.kg^{-1} of microplastics (size: 100 µm): increase in malondialdehyde concentration, antioxidant enzyme activity (SOD, CAT, POD)	Li *et al.*[52]
HDPE Microplastics (0, 100, 1000, and 10 000 mg.kg^{-1})	100-154 µm	Cd (0 and 5 mg.kg^{-1})	Plant : *Zea mays*	Natural soil	30 days	n.p	Synergic effects on roots (root mass reduction) with addition of 10 000 mg.kg^{-1} plastics, on shoots (shoot mass reduction) with addition of 100, 1000 and 10 000 mg.kg^{-1} of HDPE, on total mass (total mass reduction) with At 10 000 mg.kg^{-1} HDPE	Wang *et al.*[53]

On bacteria:

After 74 days, Zhu *et al.* did not observe major impacts of the single contaminant exposure (NPs at 200 mg.kg^{-1} and As at 40 mg.kg^{-1}) nor of their combination on the bacterial community compared to control (without NPs and As)[51].

On earthworms:

Another parameter that could explain discrepancies among studies is the physico-chemical characteristics of the MNPs added to the medium. Indeed, according to Li *et al.*[52] the smaller MNP sizes impact more metal(loid) transfer, certainly due to their larger SSA and therefore their greater adsorption capacity. Indeed, in Li *et al.* [52] the addition of MNP (up to 1 g.kg^{-1}) in the medium increased the concentration of metals in earthworm tissues: Cu transfer increase was higher with the addition of 0.05% smaller MPs (30 µm) than larger MPs (100 µm)[52] but equivalent for Ni transfer. This synergic impact on metal transfer was concomitant with interactive toxicological effects with increased oxidative stress: after 14 days, MDA (malondialdehyde) content increased by 64% with Cu/MPs compared to Cu single contamination[52].

On plants:

Wang *et al.* observed a synergic reduction of shoot (-26%) of maize crops induced by addition of MPs (100 mg.kg^{-1}) and Cd (5 mg.kg^{-1}) compared to single metallic exposure after 30 days in soil (Cd alone: -12% / MPs alone: - 8% / additive effects: -20%)[53].

MNP co-exposure with metal(loid)s also modifies elemental transfer: a decrease in As transfer was found in rice seedlings grown with MP addition in hydroponics (40, 100, and 200 mg.L^{-1}) compared to single As contamination[48] which significantly reduced its toxicity: plants exposed to 40 mg.L^{-1} MPs and 4 mg.L^{-1} As had a +7% increase in biomass and a +10% increase in total chlorophyll content compared

to plants exposed to As alone. At the same time, O_2 content in leaves was reduced by -30% and TBARS content by -32%, indicating that the plants underwent less ROS production and thus less cellular damage[48].

Finally, only one study did not evidence interactions between the contaminants and concluded that MNPs did not alter the transfer of metals from soil to plants in the case of wheat exposed to Cd and NPs (polystyrene, 87 nm) in hydroponics[47]. Interestingly, despite the fact that NPs had no influence on Cd transfer, researchers found antagonist and synergic effects on SOD activity in leaves and roots, respectively with simultaneous contamination (Cd: 2.25 $mg.L^{-1}$, NPs: 10 $mg.L^{-1}$) in comparison to single contamination and control conditions. Considering the substantial decrease in Fe, Mn, and Cu concentrations implicated in the biosynthesis of Fe-SOD, Mn-SOD and Cu/Zn-SOD, the reduction of these elements might explain the results[47].

Bibliography (Supporting Information review):

(1) Addo Ntim, S.; Mitra, S. Adsorption of Arsenic on Multiwall Carbon Nanotube–Zirconia Nanohybrid for Potential Drinking Water Purification. *Journal of Colloid and Interface Science* **2012**, *375* (1), 154–159. https://doi.org/10.1016/j.jcis.2012.01.063.

(2) Tawabini, B. S.; Al-Khaldi, S. F.; Khaled, M. M.; Atieh, M. A. Removal of Arsenic from Water by Iron Oxide Nanoparticles Impregnated on Carbon Nanotubes. *Journal of Environmental Science and Health, Part A* **2011**, *46* (3), 215–223. https://doi.org/10.1080/10934529.2011.535389.

(3) Veličković, Z.; Vuković, G. D.; Marinković, A. D.; Moldovan, M.-S.; Perić-Grujić, A. A.; Uskoković, P. S.; Ristić, M. Đ. Adsorption of Arsenate on Iron(III) Oxide Coated Ethylenediamine Functionalized Multiwall Carbon Nanotubes. *Chemical Engineering Journal* **2012**, *181–182*, 174–181. https://doi.org/10.1016/j.cej.2011.11.052.

(4) Addo Ntim, S.; Mitra, S. Removal of Trace Arsenic To Meet Drinking Water Standards Using Iron Oxide Coated Multiwall Carbon Nanotubes. *J. Chem. Eng. Data* **2011**, *56* (5), 2077–2083. https://doi.org/10.1021/je1010664.

(5) Ihsanullah; Al-Khaldi, F. A.; Abusharkh, B.; Khaled, M.; Atieh, M. A.; Nasser, M. S.; laoui, T.; Saleh, T. A.; Agarwal, S.; Tyagi, I.; Gupta, V. K. Adsorptive Removal of Cadmium(II) Ions from Liquid Phase Using Acid Modified Carbon-Based Adsorbents. *Journal of Molecular Liquids* **2015**, *204*, 255–263. https://doi.org/10.1016/j.molliq.2015.01.033.

(6) Li, Y.-H.; Ding, J.; Luan, Z.; Di, Z.; Zhu, Y.; Xu, C.; Wu, D.; Wei, B. Competitive Adsorption of Pb2+, Cu2+ and Cd2+ Ions from Aqueous Solutions by Multiwalled Carbon Nanotubes. *Carbon* **2003**, *41* (14), 2787–2792. https://doi.org/10.1016/S0008-6223(03)00392-0.

(7) Vuković, G. D.; Marinković, A. D.; Čolić, M.; Ristić, M. Đ.; Aleksić, R.; Perić-Grujić, A. A.; Uskoković, P. S. Removal of Cadmium from Aqueous Solutions by Oxidized and Ethylenediamine-Functionalized Multi-Walled Carbon Nanotubes. *Chemical Engineering Journal* **2010**, *157* (1), 238–248. https://doi.org/10.1016/j.cej.2009.11.026.

(8) Tofighy, M. A.; Mohammadi, T. Adsorption of Divalent Heavy Metal Ions from Water Using Carbon Nanotube Sheets. *Journal of Hazardous Materials* **2011**, *185* (1), 140–147. https://doi.org/10.1016/j.jhazmat.2010.09.008.

(9) Moradi, O. The Removal of Ions by Functionalized Carbon Nanotube: Equilibrium, Isotherms and Thermodynamic Studies. *Chemical and Biochemical Engineering Quarterly* **2011**, *25* (2), 229–240.

(10) Sitko, R.; Turek, E.; Zawisza, B.; Malicka, E.; Talik, E.; Heimann, J.; Gagor, A.; Feist, B.; Wrzalik, R. Adsorption of Divalent Metal Ions from Aqueous Solutions Using Graphene Oxide. *Dalton Trans.* **2013**, *42* (16), 5682–5689. https://doi.org/10.1039/C3DT33097D.

(11) Tan, P.; Sun, J.; Hu, Y.; Fang, Z.; Bi, Q.; Chen, Y.; Cheng, J. Adsorption of Cu2+, Cd2+ and Ni2+ from Aqueous Single Metal Solutions on Graphene Oxide Membranes. *Journal of Hazardous Materials* **2015**, *297*, 251–260. https://doi.org/10.1016/j.jhazmat.2015.04.068.

(12) Stafiej, A.; Pyrzynska, K. Adsorption of Heavy Metal Ions with Carbon Nanotubes. *Separation and Purification Technology* **2007**, *58* (1), 49–52. https://doi.org/10.1016/j.seppur.2007.07.008.

(13) Lingamdinne, L. P.; Koduru, J. R.; Roh, H.; Choi, Y.-L.; Chang, Y.-Y.; Yang, J.-K. Adsorption Removal of Co(II) from Waste-Water Using Graphene Oxide. *Hydrometallurgy* **2016**, *165*, 90–96. https://doi.org/10.1016/j.hydromet.2015.10.021.

(14) Atieh, M. A.; Bakather, O. Y.; Tawabini, B. S.; Bukhari, A. A.; Khaled, M.; Alharthi, M.; Fettouhi, M.; Abuilaiwi, F. A. *Removal of Chromium (III) from Water by Using Modified and Nonmodified Carbon Nanotubes*. Journal of Nanomaterials. https://doi.org/10.1155/2010/232378.

(15) Hu, J.; Chen, C.; Zhu, X.; Wang, X. Removal of Chromium from Aqueous Solution by Using Oxidized Multiwalled Carbon Nanotubes. *Journal of Hazardous Materials* **2009**, *162* (2), 1542–1550. https://doi.org/10.1016/j.jhazmat.2008.06.058.

(16) Ihsanullah; Al-Khaldi, F. A.; Abu-Sharkh, B.; Abulkibash, A. M.; Qureshi, M. I.; Laoui, T.; Atieh, M. A. Effect of Acid Modification on Adsorption of Hexavalent Chromium (Cr(VI)) from Aqueous Solution by Activated Carbon and Carbon Nanotubes. *Desalination and Water Treatment* **2016**, *57* (16), 7232–7244. https://doi.org/10.1080/19443994.2015.1021847.

(17) Di, Z.-C.; Li, Y.-H.; Luan, Z.-K.; Liang, J. Adsorption of Chromium(VI) Ions from Water by Carbon Nanotubes. *Adsorption Science & Technology* **2004**, *22* (6), 467–474. https://doi.org/10.1260/0263617042879537.
(18) Di, Z.-C.; Ding, J.; Peng, X.-J.; Li, Y.-H.; Luan, Z.-K.; Liang, J. Chromium Adsorption by Aligned Carbon Nanotubes Supported Ceria Nanoparticles. *Chemosphere* **2006**, *62* (5), 861–865. https://doi.org/10.1016/j.chemosphere.2004.06.044.
(19) Kumar, A. S. K.; Jiang, S.-J.; Tseng, W.-L. Effective Adsorption of Chromium(VI)/Cr(III) from Aqueous Solution Using Ionic Liquid Functionalized Multiwalled Carbon Nanotubes as a Super Sorbent. *J. Mater. Chem. A* **2015**, *3* (13), 7044–7057. https://doi.org/10.1039/C4TA06948J.
(20) Ge, Y.; Li, Z.; Xiao, D.; Xiong, P.; Ye, N. Sulfonated Multi-Walled Carbon Nanotubes for the Removal of Copper (II) from Aqueous Solutions. *Journal of Industrial and Engineering Chemistry* **2014**, *20* (4), 1765–1771. https://doi.org/10.1016/j.jiec.2013.08.030.
(21) Ren, X.; Li, J.; Tan, X.; Wang, X. Comparative Study of Graphene Oxide, Activated Carbon and Carbon Nanotubes as Adsorbents for Copper Decontamination. *Dalton Transactions* **2013**, *42* (15), 5266–5274. https://doi.org/10.1039/C3DT32969K.
(22) Tang, W.-W.; Zeng, G.-M.; Gong, J.-L.; Liu, Y.; Wang, X.-Y.; Liu, Y.-Y.; Liu, Z.-F.; Chen, L.; Zhang, X.-R.; Tu, D.-Z. Simultaneous Adsorption of Atrazine and Cu (II) from Wastewater by Magnetic Multi-Walled Carbon Nanotube. *Chemical Engineering Journal* **2012**, *211–212*, 470–478. https://doi.org/10.1016/j.cej.2012.09.102.
(23) Vellaichamy, S.; Palanivelu, K. Preconcentration and Separation of Copper, Nickel and Zinc in Aqueous Samples by Flame Atomic Absorption Spectrometry after Column Solid-Phase Extraction onto MWCNT Impregnated with D2EHPA-TOPO Mixture. *Journal of Hazardous Materials* **2011**, *185* (2), 1131–1139. https://doi.org/10.1016/j.jhazmat.2010.10.023.
(24) Lu, C.; Chiu, H.; Liu, C. Removal of Zinc(II) from Aqueous Solution by Purified Carbon Nanotubes: Kinetics and Equilibrium Studies. *Ind. Eng. Chem. Res.* **2006**, *45* (8), 2850–2855. https://doi.org/10.1021/ie051206h.
(25) Tawabini, B.; Al-Khaldi, S.; Atieh, M.; Khaled, M. Removal of Mercury from Water by Multi-Walled Carbon Nanotubes. *Water Science and Technology* **2010**, *61* (3), 591–598. https://doi.org/10.2166/wst.2010.897.
(26) Shadbad, M. J.; Mohebbi, A.; Soltani, A. Mercury(II) Removal from Aqueous Solutions by Adsorption on Multi-Walled Carbon Nanotubes. *Korean J. Chem. Eng.* **2011**, *28* (4), 1029–1034. https://doi.org/10.1007/s11814-010-0463-5.
(27) Chen, P. H.; Hsu, C.-F.; Tsai, D. D.-W.; Lu, Y.-M.; Huang, W.-J. Adsorption of Mercury from Water by Modified Multi-Walled Carbon Nanotubes: Adsorption Behaviour and Interference Resistance by Coexisting Anions. *Environmental Technology* **2014**, *35* (15), 1935–1944. https://doi.org/10.1080/09593330.2014.886627.
(28) El-Sheikh, A. H.; Al-Degs, Y. S.; Al-As'ad, R. M.; Sweileh, J. A. Effect of Oxidation and Geometrical Dimensions of Carbon Nanotubes on Hg(II) Sorption and Preconcentration from Real Waters. *Desalination* **2011**, *270* (1), 214–220. https://doi.org/10.1016/j.desal.2010.11.048.
(29) Zhang, C.; Sui, J.; Li, J.; Tang, Y.; Cai, W. Efficient Removal of Heavy Metal Ions by Thiol-Functionalized Superparamagnetic Carbon Nanotubes. *Chemical Engineering Journal* **2012**, *210*, 45–52. https://doi.org/10.1016/j.cej.2012.08.062.
(30) Gupta, A.; Vidyarthi, S. R.; Sankararamakrishnan, N. Enhanced Sorption of Mercury from Compact Fluorescent Bulbs and Contaminated Water Streams Using Functionalized Multiwalled Carbon Nanotubes. *Journal of Hazardous Materials* **2014**, *274*, 132–144. https://doi.org/10.1016/j.jhazmat.2014.03.020.
(31) Mobasherpour, I.; Salahi, E.; Ebrahimi, M. Removal of Divalent Nickel Cations from Aqueous Solution by Multi-Walled Carbon Nano Tubes: Equilibrium and Kinetic Processes. *Res Chem Intermed* **2012**, *38* (9), 2205–2222. https://doi.org/10.1007/s11164-012-0537-6.
(32) Chen, C.; Hu, J.; Shao, D.; Li, J.; Wang, X. Adsorption Behavior of Multiwall Carbon Nanotube/Iron Oxide Magnetic Composites for Ni(II) and Sr(II). *Journal of Hazardous Materials* **2009**, *164* (2), 923–928. https://doi.org/10.1016/j.jhazmat.2008.08.089.

(33) Kandah, M. I.; Meunier, J.-L. Removal of Nickel Ions from Water by Multi-Walled Carbon Nanotubes. *Journal of Hazardous Materials* **2007**, *146* (1), 283–288. https://doi.org/10.1016/j.jhazmat.2006.12.019.
(34) Chen, C.; Wang, X. Adsorption of Ni(II) from Aqueous Solution Using Oxidized Multiwall Carbon Nanotubes. *Ind. Eng. Chem. Res.* **2006**, *45* (26), 9144–9149. https://doi.org/10.1021/ie060791z.
(35) Najafi, F.; Moradi, O.; Rajabi, M.; Asif, M.; Tyagi, I.; Agarwal, S.; Gupta, V. K. Thermodynamics of the Adsorption of Nickel Ions from Aqueous Phase Using Graphene Oxide and Glycine Functionalized Graphene Oxide. *Journal of Molecular Liquids* **2015**, *208*, 106–113. https://doi.org/10.1016/j.molliq.2015.04.033.
(36) Li, Y.-H.; Wang, S.; Wei, J.; Zhang, X.; Xu, C.; Luan, Z.; Wu, D.; Wei, B. Lead Adsorption on Carbon Nanotubes. *Chemical Physics Letters* **2002**, *357* (3), 263–266. https://doi.org/10.1016/S0009-2614(02)00502-X.
(37) Li, Y.-H.; Di, Z.; Ding, J.; Wu, D.; Luan, Z.; Zhu, Y. Adsorption Thermodynamic, Kinetic and Desorption Studies of Pb2+ on Carbon Nanotubes. *Water Research* **2005**, *39* (4), 605–609. https://doi.org/10.1016/j.watres.2004.11.004.
(38) Wang, H. J.; Zhou, A. L.; Peng, F.; Yu, H.; Chen, L. F. Adsorption Characteristic of Acidified Carbon Nanotubes for Heavy Metal Pb(II) in Aqueous Solution. *Materials Science and Engineering: A* **2007**, *466* (1), 201–206. https://doi.org/10.1016/j.msea.2007.02.097.
(39) Wang, S.-G.; Gong, W.-X.; Liu, X.-W.; Yao, Y.-W.; Gao, B.-Y.; Yue, Q.-Y. Removal of Lead(II) from Aqueous Solution by Adsorption onto Manganese Oxide-Coated Carbon Nanotubes. *Separation and Purification Technology* **2007**, *58* (1), 17–23. https://doi.org/10.1016/j.seppur.2007.07.006.
(40) Zhao, X.; Jia, Q.; Song, N.; Zhou, W.; Li, Y. Adsorption of Pb(II) from an Aqueous Solution by Titanium Dioxide/Carbon Nanotube Nanocomposites: Kinetics, Thermodynamics, and Isotherms. *J. Chem. Eng. Data* **2010**, *55* (10), 4428–4433. https://doi.org/10.1021/je100586r.
(41) Zhao, G.; Ren, X.; Gao, X.; Tan, X.; Li, J.; Chen, C.; Huang, Y.; Wang, X. Removal of Pb(II) Ions from Aqueous Solutions on Few-Layered Graphene Oxide Nanosheets. *Dalton Trans.* **2011**, *40* (41), 10945–10952. https://doi.org/10.1039/C1DT11005E.
(42) Cho, H.-H.; Wepasnick, K.; Smith, B. A.; Bangash, F. K.; Fairbrother, D. H.; Ball, W. P. Sorption of Aqueous Zn[II] and Cd[II] by Multiwall Carbon Nanotubes: The Relative Roles of Oxygen-Containing Functional Groups and Graphenic Carbon. *Langmuir* **2010**, *26* (2), 967–981. https://doi.org/10.1021/la902440u.
(43) Lu, C.; Chiu, H. Adsorption of Zinc(II) from Water with Purified Carbon Nanotubes. *Chemical Engineering Science* **2006**, *61* (4), 1138–1145. https://doi.org/10.1016/j.ces.2005.08.007.
(44) Lu, C.; Chiu, H. Chemical Modification of Multiwalled Carbon Nanotubes for Sorption of Zn2+ from Aqueous Solution. *Chemical Engineering Journal* **2008**, *139* (3), 462–468. https://doi.org/10.1016/j.cej.2007.08.013.
(45) Mubarak, N. M.; Alicia, R. F.; Abdullah, E. C.; Sahu, J. N.; Haslija, A. B. A.; Tan, J. Statistical Optimization and Kinetic Studies on Removal of Zn2+ Using Functionalized Carbon Nanotubes and Magnetic Biochar. *Journal of Environmental Chemical Engineering* **2013**, *1* (3), 486–495. https://doi.org/10.1016/j.jece.2013.06.011.
(46) Giller, K. E.; Witter, E.; Mcgrath, S. P. Toxicity of Heavy Metals to Microorganisms and Microbial Processes in Agricultural Soils: A Review. *Soil Biology and Biochemistry* **1998**, *30* (10), 1389–1414. https://doi.org/10.1016/S0038-0717(97)00270-8.
(47) Lian, J.; Wu, J.; Zeb, A.; Zheng, S.; Ma, T.; Peng, F.; Tang, J.; Liu, W. Do Polystyrene Nanoplastics Affect the Toxicity of Cadmium to Wheat (Triticum Aestivum L.)? *Environmental Pollution* **2020**, *263*, 114498. https://doi.org/10.1016/j.envpol.2020.114498.
(48) Dong, Y.; Gao, M.; Song, Z.; Qiu, W. Microplastic Particles Increase Arsenic Toxicity to Rice Seedlings. *Environmental Pollution* **2020**, *259*, 113892. https://doi.org/10.1016/j.envpol.2019.113892.
(49) Dong, Y.; Gao, M.; Qiu, W.; Song, Z. Uptake of Microplastics by Carrots in Presence of As (III): Combined Toxic Effects. *Journal of Hazardous Materials* **2021**, *411*, 125055. https://doi.org/10.1016/j.jhazmat.2021.125055.

(50) Manjate, E.; Ramos, S.; Almeida, C. M. R. Potential Interferences of Microplastics in the Phytoremediation of Cd and Cu by the Salt Marsh Plant Phragmites Australis. *Journal of Environmental Chemical Engineering* **2020**, *8* (2), 103658. https://doi.org/10.1016/j.jece.2020.103658.
(51) Zhu, D.; Li, G.; Wang, H.-T.; Duan, G.-L. Effects of Nano- or Microplastic Exposure Combined with Arsenic on Soil Bacterial, Fungal, and Protistan Communities. *Chemosphere* **2021**, *281*, 130998. https://doi.org/10.1016/j.chemosphere.2021.130998.
(52) Li, M.; Liu, Y.; Xu, G.; Wang, Y.; Yu, Y. Impacts of Polyethylene Microplastics on Bioavailability and Toxicity of Metals in Soil. *Science of The Total Environment* **2021**, *760*, 144037. https://doi.org/10.1016/j.scitotenv.2020.144037.
(53) Wang, F.; Zhang, X.; Zhang, S.; Zhang, S.; Adams, C. A.; Sun, Y. Effects of Co-Contamination of Microplastics and Cd on Plant Growth and Cd Accumulation. *Toxics* **2020**, *8* (2), 36. https://doi.org/10.3390/toxics8020036.

4. Questionnements scientifiques de la thèse

A ce jour, des questions sont soulevées quant à l'actuelle évaluation des risques de contaminants en mélange, qui ne prennent pas en compte des interactions qui peuvent survenir entre les contaminants du mélange. Or, les contaminants émergents tels que les NMC montrent de fortes capacités d'interactions avec des contaminants historiques tels que les ETM, provoquant parfois une augmentation ou une diminution du transfert des ETM en raison de l'ajout des NMC dans le milieu et des effets synergiques ou antagonistes sur la toxicité du mélange NMC/ETM, remettant en cause l'évaluation des risques actuelle. Dans la conduite des expériences du projet doctoral, les NTC sont les NMC qui ont été le plus étudiés car ce sont les rares NMC pour lesquels des modélisations de leur concentration dans l'environnement existent. Aussi, les avancées dans le domaine de recherche de l'écologie ont permis de mettre au point des écomarqueurs afin de caractériser la santé des écosystèmes et qui restent très peu utilisés en écotoxicologie. La combinaison de ce type marqueurs avec ceux à l'échelle individuelle doivent être amplifiée. Le présent projet doctoral a été amorcé par mon stage de fin d'étude (Master 2) réalisé et financé dans le cadre de l'axe transverse DECOREM du laboratoire d'écologie fonctionnelle et environnement, qui a mené à la rédaction d'un article scientifique mais aussi à la rédaction du projet NANOMETAGRO financé par la région Occitanie et l'université de Toulouse ainsi qu'à la rédaction du projet EC2CO CARBOSTRESS ayant financé le fonctionnement du projet doctoral.

Le présent travail a été menée dans le but de répondre aux questions de recherches suivantes :

1) Quels sont paramètres physico-chimiques qui régissent les interactions entre NMC et ETM dans un contexte qui fait intervenir des conditions représentatives de l'environnement ?

Plusieurs études se sont déjà intéressées aux interactions entre NMC et ETM dans des systèmes mono-métalliques. Or, les ETM se retrouvent en nombre important et de manière simultanée dans les agrosystèmes et peu d'études faisant intervenir des systèmes multi-métalliques ont été menées. De plus, la plupart de ces études ont une approche mécanistique ne prenant donc pas en compte les

spécificités des conditions environnementales et leur influence sur les phénomènes d'interactions, de sorte que l'accent sur les interactions NMC/ETM dans un contexte environnementalement pertinent se retrouve sous-etudié. Ainsi, la mise en œuvre d'étude de ce genre dans un contexte représentatif des conditions environnementales permettrait de mieux comprendre les effets des NMC sur le transfert des ETM depuis le sol jusqu'aux organismes représentatifs des agrosystèmes.

Afin de répondre à la question, des expériences visant à déterminer le comportement d'adsorption des ETM en surface des NMC par modulation à la fois des propriétés intrinsèques des NMC et des paramètres physico-chimiques du milieu (pH, rapport de concentration NMC/ETM, concentration de MO et influence des composés du sol contenu dans la solution de sol) ont été menées et font l'objet du chapitre n°3 (basé sur un article à soumettre à ACS Nano).

2) Quels sont les impacts des NTC seuls sur les cycles biogéochimiques du carbone, de l'azote et de l'aeau dans un agrosystème ?

La toxicité des NTC sur les organismes commence à être bien documentée mais leurs impacts sur les cycles biogéochimiques d'éléments majeurs restent peu étudiés et mal compris contrairement aux ETM dont le corpus scientifique est large sur ces questions de recherche. Ainsi, avant de passer aux études s'intéressant aux impacts des interactions de ces deux contaminants sur les agrosystèmes, il paraissait judicieux de mettre en place une expérience visant à déterminer l'impacts des NTC seuls sur les cycles biogéochimiques du carbone, de l'azote et de l'eau à l'aide d'une approche multifonctionnelle. Ce travail est présenté en chapitre n°4 (basé sur un article soumis à Environmental Pollution)

3) Quels sont les effets d'une contamination simultanée en NTC et ETM sur un agrosystème ?

Plusieurs études ont démontré que des contaminants comme les NTC et les ETM interagissaient et pouvaient provoquer une modification de transfert des ETM en raison de la présence de NMC ainsi que des effets toxicologiques différents en mélange que s'ils étaient appliqués individuellement. En ce sens, les travaux antérieurs (stage de Master 2) s'intéressant aux effets de l'ajout de NTC sur le

transfert et la toxicité d'ETM provenant d'un sol historiquement contaminé sur des bactéries, des végétaux (salade) et des vers de terre ont été intégrés dans ce chapitre. Additionnellement, une étude a été menée afin de connaître les effets d'un cocktail NTC et ETM sur les organismes représentatifs des agrosystèmes (bactéries et végétaux – maïs) avec un focus sur le vieillissement des contaminants et en utilisant un sol aux caractéristiques physico-chimiques contrastées. Ces deux articles (un publié dans Journal of Hazardous Materials et un pour soumission dans Environmental Science and Technology) constituent le chapitre n°5.

4) Y-a-t il un transfert trophique des NTC ? La présence de NTC dans le milieu modifie-t-elle le transfert et la toxicité des ETM ?

L'internalisation des NTC a été démontrée à de rares occasions chez plusieurs organismes représentatifs des agrosystèmes. Toutefois, les verrous techniques concernant la quantification du transfert de NTC subsistent toujours. De plus, plusieurs indices révèlent une modification du transfert des ETM en raison de l'ajout de NTC ; or, les mécanismes sous-jacents de la modification du transfert sont aussi peu connus. Ainsi, une expérience visant à recréer un réseau trophique en laboratoire a été réalisée (sol – plante- escargot) afin d'y répondre et constitue le 6ème et dernier chapitre. Ce travail est basé sur une synthèse originale de NTC avec un précurseur 100% ^{13}C et des techniques de détection de pointe telles que l'analyse nucléaire par réactions (NRA) sur microsonde nucléaire et de spéctroscopie de masse à rapport isotopque par pyrolise (py-IRMS).

Bibliographie (chapitre 1):

(1) *World Population Prospects: The 2017 Revision | Multimedia Library - United Nations Department of Economic and Social Affairs*. https://www.un.org/development/desa/publications/world-population-prospects-the-2017-revision.html (accessed 2019-01-23).

(2) Ramade, F. *Dictionnaire Encyclopédique Des Sciences De La Nature Et De La Biodiversité*, Dunod.; Paris, 2008.

(3) Nicholson, F. A.; Smith, S. R.; Alloway, B. J.; Carlton-Smith, C.; Chambers, B. J. An Inventory of Heavy Metals Inputs to Agricultural Soils in England and Wales. *Science of The Total Environment* **2003**, *311* (1), 205–219. https://doi.org/10.1016/S0048-9697(03)00139-6.

(4) Nagajyoti, P. C.; Lee, K. D.; Sreekanth, T. V. M. Heavy Metals, Occurrence and Toxicity for Plants: A Review. *Environ Chem Lett* **2010**, *8* (3), 199–216. https://doi.org/10.1007/s10311-010-0297-8.

(5) Schvartz, C.; Cambier, P. *Contaminations métalliques des agrosystèmes et écosystèmes péri-industriels*; QUAE: Versailles, 2009.

(6) Wick, P.; Louw-Gaume, A. E.; Kucki, M.; Krug, H. F.; Kostarelos, K.; Fadeel, B.; Dawson, K. A.; Salvati, A.; Vázquez, E.; Ballerini, L.; Tretiach, M.; Benfenati, F.; Flahaut, E.; Gauthier, L.; Prato, M.; Bianco, A. Classification Framework for Graphene-Based Materials. *Angewandte Chemie International Edition* **2014**, *53* (n° 30), 7714–7718. https://doi.org/10.1002/anie.201403335.

(7) *The Nobel Prize in Physics 2010*. NobelPrize.org. https://www.nobelprize.org/prizes/physics/2010/geim/facts/ (accessed 2019-10-30).

(8) Abd-Elsalam, K. A. 1 - Carbon Nanomaterials: 30 Years of Research in Agroecosystems. In *Carbon Nanomaterials for Agri-Food and Environmental Applications*; Abd-Elsalam, K. A., Ed.; Micro and Nano Technologies; Elsevier, 2020; pp 1–18. https://doi.org/10.1016/B978-0-12-819786-8.00001-3.

(9) Thines, R. K.; Mubarak, N. M.; Nizamuddin, S.; Sahu, J. N.; Abdullah, E. C.; Ganesan, P. Application Potential of Carbon Nanomaterials in Water and Wastewater Treatment: A Review. *Journal of the Taiwan Institute of Chemical Engineers* **2017**, *72*, 116–133. https://doi.org/10.1016/j.jtice.2017.01.018.

(10) *Work Package 4: Health and Environment*. Graphene Flagship. https://graphene-flagship.eu/research/work-packages/work-package-4-health-and-environment/ (accessed 2023-08-24).

(11) Drexler, E. *Engines of Creation: The Coming Era of Nanotechnology*, Reprint.; Anchor: New York, 1987.

(12) Larue, C. Impact de nanoparticules de TiO2 et de nanotubes de carbone sur les végétaux. phdthesis, AgroParisTech, 2011. https://pastel.archives-ouvertes.fr/pastel-00765312 (accessed 2021-03-04).

(13) Li, Y.-H.; Wang, S.; Wei, J.; Zhang, X.; Xu, C.; Luan, Z.; Wu, D.; Wei, B. Lead Adsorption on Carbon Nanotubes. *Chemical Physics Letters* **2002**, *357* (3), 263–266. https://doi.org/10.1016/S0009-2614(02)00502-X.

(14) Li, Y.-H.; Ding, J.; Luan, Z.; Di, Z.; Zhu, Y.; Xu, C.; Wu, D.; Wei, B. Competitive Adsorption of Pb2+, Cu2+ and Cd2+ Ions from Aqueous Solutions by Multiwalled Carbon Nanotubes. *Carbon* **2003**, *41* (14), 2787–2792. https://doi.org/10.1016/S0008-6223(03)00392-0.

(15) Li, Y.-H.; Wang, S.; Luan, Z.; Ding, J.; Xu, C.; Wu, D. Adsorption of Cadmium(II) from Aqueous Solution by Surface Oxidized Carbon Nanotubes. *Carbon* **2003**, *41* (5), 1057–1062. https://doi.org/10.1016/S0008-6223(02)00440-2.

(16) Lu, C.; Chiu, H. Adsorption of Zinc(II) from Water with Purified Carbon Nanotubes. *Chemical Engineering Science* **2006**, *61* (4), 1138–1145. https://doi.org/10.1016/j.ces.2005.08.007.

(17) Salam, M. A.; Al-Zhrani, G.; Kosa, S. A. Simultaneous Removal of Copper(II), Lead(II), Zinc(II) and Cadmium(II) from Aqueous Solutions by Multi-Walled Carbon Nanotubes. *Comptes Rendus Chimie* **2012**, *15* (5), 398–408. https://doi.org/10.1016/j.crci.2012.01.013.

(18) Rodea-Palomares, I.; González-Pleiter, M.; Martín-Betancor, K.; Rosal, R.; Fernández-Piñas, F. Additivity and Interactions in Ecotoxicity of Pollutant Mixtures: Some Patterns, Conclusions, and Open Questions. *Toxics* **2015**, *3* (4), 342–369. https://doi.org/10.3390/toxics3040342.
(19) Singh, V.; Joung, D.; Zhai, L.; Das, S.; Khondaker, S. I.; Seal, S. Graphene Based Materials: Past, Present and Future. *Progress in Materials Science* **2011**, *56* (8), 1178–1271. https://doi.org/10.1016/j.pmatsci.2011.03.003.
(20) Bianco, A.; Cheng, H.-M.; Enoki, T.; Gogotsi, Y.; Hurt, R. H.; Koratkar, N.; Kyotani, T.; Monthioux, M.; Park, C. R.; Tascon, J. M. D.; Zhang, J. All in the Graphene Family – A Recommended Nomenclature for Two-Dimensional Carbon Materials. *Carbon* **2013**, *65*, 1–6. https://doi.org/10.1016/j.carbon.2013.08.038.
(21) Zhen, Z.; Zhu, H. 1 - Structure and Properties of Graphene. In *Graphene*; Zhu, H., Xu, Z., Xie, D., Fang, Y., Eds.; Academic Press, 2018; pp 1–12. https://doi.org/10.1016/B978-0-12-812651-6.00001-X.
(22) Hass, J.; Heer, W. A. de; Conrad, E. H. The Growth and Morphology of Epitaxial Multilayer Graphene. *J. Phys.: Condens. Matter* **2008**, *20* (32), 323202. https://doi.org/10.1088/0953-8984/20/32/323202.
(23) Huang, X.; Yin, Z.; Wu, S.; Qi, X.; He, Q.; Zhang, Q.; Yan, Q.; Boey, F.; Zhang, H. Graphene-Based Materials: Synthesis, Characterization, Properties, and Applications. *Small* **2011**, *7* (14), 1876–1902. https://doi.org/10.1002/smll.201002009.
(24) Contescu, C. I.; Azad, S.; Miller, D.; Lance, M. J.; Baker, F. S.; Burchell, T. D. Practical Aspects for Characterizing Air Oxidation of Graphite. *Journal of Nuclear Materials* **2008**, *381* (1), 15–24. https://doi.org/10.1016/j.jnucmat.2008.07.020.
(25) Kolosnjaj-Tabi, J.; Just, J.; Hartman, K. B.; Laoudi, Y.; Boudjemaa, S.; Alloyeau, D.; Szwarc, H.; Wilson, L. J.; Moussa, F. Anthropogenic Carbon Nanotubes Found in the Airways of Parisian Children. *EBioMedicine* **2015**, *2* (11), 1697–1704. https://doi.org/10.1016/j.ebiom.2015.10.012.
(26) Gredilla, A.; Fdez-Ortiz de Vallejuelo, S.; Rodriguez-Iruretagoiena, A.; Gomez, L.; Oliveira, M. L. S.; Arana, G.; de Diego, A.; Madariaga, J. M.; Silva, L. F. O. Evidence of Mercury Sequestration by Carbon Nanotubes and Nanominerals Present in Agricultural Soils from a Coal Fired Power Plant Exhaust. *Journal of Hazardous Materials* **2019**, *378*, 120747. https://doi.org/10.1016/j.jhazmat.2019.120747.
(27) *Search Database - The Nanodatabase*. https://nanodb.dk/en/search-database/ (accessed 2023-07-06).
(28) Gottschalk, F.; Sonderer, T.; Scholz, R. W.; Nowack, B. Modeled Environmental Concentrations of Engineered Nanomaterials (TiO2, ZnO, Ag, CNT, Fullerenes) for Different Regions. *Environ. Sci. Technol.* **2009**, *43* (24), 9216–9222. https://doi.org/10.1021/es9015553.
(29) Piccinno, F.; Gottschalk, F.; Seeger, S.; Nowack, B. Industrial Production Quantities and Uses of Ten Engineered Nanomaterials in Europe and the World. *J Nanopart Res* **2012**, *14* (9), 1109. https://doi.org/10.1007/s11051-012-1109-9.
(30) Koelmans. Comparison of Manufactured and Black Carbon Nanoparticle Concentrations in Aquatic Sediments. *Environmental Pollution* **2009**, *157*, 1110–1116.
(31) Keller, A. A.; McFerran, S.; Lazareva, A.; Suh, S. Global Life Cycle Releases of Engineered Nanomaterials. *J Nanopart Res* **2013**, *15* (6), 1692. https://doi.org/10.1007/s11051-013-1692-4.
(32) Oliveira, M. L. S.; Ward, C. R.; Izquierdo, M.; Sampaio, C. H.; de Brum, I. A. S.; Kautzmann, R. M.; Sabedot, S.; Querol, X.; Silva, L. F. O. Chemical Composition and Minerals in Pyrite Ash of an Abandoned Sulphuric Acid Production Plant. *Sci. Total Environ.* **2012**, *430*, 34–47. https://doi.org/10.1016/j.scitotenv.2012.04.046.
(33) Hussain, S. M.; Braydich-Stolle, L. K.; Schrand, A. M.; Murdock, R. C.; Yu, K. O.; Mattie, D. M.; Schlager, J. J.; Terrones, M. Toxicity Evaluation for Safe Use of Nanomaterials: Recent Achievements and Technical Challenges. *Advanced Materials* **2009**, *21* (16), 1549–1559. https://doi.org/10.1002/adma.200801395.
(34) Buzea, C.; Pacheco, I. I.; Robbie, K. Nanomaterials and Nanoparticles: Sources and Toxicity. *Biointerphases* **2007**, *2* (4), MR17–MR71. https://doi.org/10.1116/1.2815690.

(35) Giraud, L.; Tourrette, A.; Flahaut, E. Carbon Nanomaterials-Based Polymer-Matrix Nanocomposites for Antimicrobial Applications: A Review. *Carbon* **2021**. https://doi.org/10.1016/j.carbon.2021.06.002.
(36) Wang, Q.; Li, C.; Wang, Y.; Que, X. Phytotoxicity of Graphene Family Nanomaterials and Its Mechanisms: A Review. *Front. Chem.* **2019**, *7*. https://doi.org/10.3389/fchem.2019.00292.
(37) Liné, C.; Larue, C.; Flahaut, E. Carbon Nanotubes: Impacts and Behaviour in the Terrestrial Ecosystem - A Review. *Carbon* **2017**, *123*, 767–785. https://doi.org/10.1016/j.carbon.2017.07.089.
(38) Meunier, E.; Coste, A.; Olagnier, D.; Authier, H.; Lefèvre, L.; Dardenne, C.; Bernad, J.; Béraud, M.; Flahaut, E.; Pipy, B. Double-Walled Carbon Nanotubes Trigger IL-1β Release in Human Monocytes through Nlrp3 Inflammasome Activation. *Nanomedicine: Nanotechnology, Biology and Medicine* **2012**, *8* (6), 987–995. https://doi.org/10.1016/j.nano.2011.11.004.
(39) Lam, C.; James, J. T.; McCluskey, R.; Arepalli, S.; Hunter, R. L. A Review of Carbon Nanotube Toxicity and Assessment of Potential Occupational and Environmental Health Risks. *Critical Reviews in Toxicology* **2006**, *36* (3), 189–217. https://doi.org/10.1080/10408440600570233.
(40) Nowack, B.; Bucheli, T. D. Occurrence, Behavior and Effects of Nanoparticles in the Environment. *Environmental Pollution* **2007**, *150* (1), 5–22. https://doi.org/10.1016/j.envpol.2007.06.006.
(41) Zhao, J.; Wang, Z.; White, J. C.; Xing, B. Graphene in the Aquatic Environment: Adsorption, Dispersion, Toxicity and Transformation. *Environ. Sci. Technol.* **2014**, *48* (17), 9995–10009. https://doi.org/10.1021/es5022679.
(42) Jaisi, D. P.; Saleh, N. B.; Blake, R. E.; Elimelech, M. Transport of Single-Walled Carbon Nanotubes in Porous Media: Filtration Mechanisms and Reversibility. *Environ. Sci. Technol.* **2008**, *42* (22), 8317–8323. https://doi.org/10.1021/es801641v.
(43) Hennebert, P.; Avellan, A.; Yan, J.; Aguerre-Chariol, O. Experimental Evidence of Colloids and Nanoparticles Presence from 25 Waste Leachates. *Waste Management* **2013**, *33* (9), 1870–1881. https://doi.org/10.1016/j.wasman.2013.04.014.
(44) Saito, T.; Suzuki, Y.; Mizuno, T. Size and Elemental Analyses of Nano Colloids in Deep Granitic Groundwater: Implications for Transport of Trace Elements. *Colloids and Surfaces A: Physicochemical and Engineering Aspects* **2013**, *435*, 48–55. https://doi.org/10.1016/j.colsurfa.2012.11.031.
(45) Sun, T. Y.; Bornhöft, N. A.; Hungerbühler, K.; Nowack, B. Dynamic Probabilistic Modeling of Environmental Emissions of Engineered Nanomaterials. *Environ. Sci. Technol.* **2016**, *50* (9), 4701–4711. https://doi.org/10.1021/acs.est.5b05828.
(46) Gottschalk, F.; Sonderer, T.; Scholz, R. W.; Nowack, B. Modeled Environmental Concentrations of Engineered Nanomaterials (TiO(2), ZnO, Ag, CNT, Fullerenes) for Different Regions. *Environ. Sci. Technol.* **2009**, *43* (24), 9216–9222. https://doi.org/10.1021/es9015553.
(47) *Effect of Heavy Metal Pollution on Plants: Metals in the Environment*; Lepp, N. W., Ed.; Pollution Monitoring Series; Springer Netherlands, 1981. https://doi.org/10.1007/978-94-009-8099-0.
(48) He, Z. L.; Yang, X. E.; Stoffella, P. J. Trace Elements in Agroecosystems and Impacts on the Environment. *Journal of Trace Elements in Medicine and Biology* **2005**, *19* (2), 125–140. https://doi.org/10.1016/j.jtemb.2005.02.010.
(49) Rai, P. K.; Lee, S. S.; Zhang, M.; Tsang, Y. F.; Kim, K.-H. Heavy Metals in Food Crops: Health Risks, Fate, Mechanisms, and Management. *Environment International* **2019**, *125*, 365–385. https://doi.org/10.1016/j.envint.2019.01.067.
(50) Baize, D. Teneurs Totales En « métaux Lourds » Dans Les Sols Français : Résultats Généraux Du Programme ASPITET. *Courrier de l'Environnement de l'Inra* **2000**, *39*.
(51) SEC_2006_620.Pdf. https://ec.europa.eu/environment/archives/soil/pdf/SEC_2006_620.pdf (accessed 2020-11-27).
(52) Kong, X. China Must Protect High-Quality Arable Land. *Nature* **2014**, *506* (7486), 7. https://doi.org/10.1038/506007a.
(53) *EUR-Lex - 01986L0278-20180704 - FR - EUR-Lex*. https://eur-lex.europa.eu/legal-content/FR/TXT/?uri=CELEX%3A01986L0278-20180704 (accessed 2020-11-27).

(54) Iyengar, G. V.; Nair, P. P. Global Outlook on Nutrition and the Environment: Meeting the Challenges of the next Millennium. *Science of The Total Environment* **2000**, *249* (1), 331–346. https://doi.org/10.1016/S0048-9697(99)00529-X.
(55) Türkdoğan, M. K.; Kilicel, F.; Kara, K.; Tuncer, I.; Uygan, I. Heavy Metals in Soil, Vegetables and Fruits in the Endemic Upper Gastrointestinal Cancer Region of Turkey. *Environmental Toxicology and Pharmacology* **2003**, *13* (3), 175–179. https://doi.org/10.1016/S1382-6689(02)00156-4.
(56) Carrizales, L.; Razo, I.; Téllez-Hernández, J. I.; Torres-Nerio, R.; Torres, A.; Batres, L. E.; Cubillas, A.-C.; Díaz-Barriga, F. Exposure to Arsenic and Lead of Children Living near a Copper-Smelter in San Luis Potosi, Mexico: Importance of Soil Contamination for Exposure of Children. *Environmental Research* **2006**, *101* (1), 1–10. https://doi.org/10.1016/j.envres.2005.07.010.
(57) Khan, S.; Aijun, L.; Zhang, S.; Hu, Q.; Zhu, Y.-G. Accumulation of Polycyclic Aromatic Hydrocarbons and Heavy Metals in Lettuce Grown in the Soils Contaminated with Long-Term Wastewater Irrigation. *Journal of Hazardous Materials* **2008**, *152* (2), 506–515. https://doi.org/10.1016/j.jhazmat.2007.07.014.
(58) Hu, J.; Wu, F.; Wu, S.; Cao, Z.; Lin, X.; Wong, M. H. Bioaccessibility, Dietary Exposure and Human Risk Assessment of Heavy Metals from Market Vegetables in Hong Kong Revealed with an in Vitro Gastrointestinal Model. *Chemosphere* **2013**, *91* (4), 455–461. https://doi.org/10.1016/j.chemosphere.2012.11.066.
(59) Gress, J.; de Oliveira, L. M.; da Silva, E. B.; Lessl, J. M.; Wilson, P. C.; Townsend, T.; Ma, L. Q. Cleaning-Induced Arsenic Mobilization and Chromium Oxidation from CCA-Wood Deck: Potential Risk to Children. *Environment International* **2015**, *82*, 35–40. https://doi.org/10.1016/j.envint.2015.04.012.
(60) Dickin Sarah K.; Schuster-Wallace Corinne J.; Qadir Manzoor; Pizzacalla Katherine. A Review of Health Risks and Pathways for Exposure to Wastewater Use in Agriculture. *Environmental Health Perspectives* **2016**, *124* (7), 900–909. https://doi.org/10.1289/ehp.1509995.
(61) Baath, E. Effects of Heavy Metals in Soil on Microbial Processes and Populations (a Review). *Water, Air, and Soil Pollution* **1989**, *47* (3–4), 335–379. https://doi.org/10.1007/BF00279331.
(62) Gall, J. E.; Boyd, R. S.; Rajakaruna, N. Transfer of Heavy Metals through Terrestrial Food Webs: A Review. *Environ Monit Assess* **2015**, *187* (4), 201. https://doi.org/10.1007/s10661-015-4436-3.
(63) Purves, D. *Trace-Element Contamination of the Environment*; Elsevier, 2012.
(64) Soliman, M.; El-Shazly, M.; Abd-El-Samie, E.; Fayed, H. Variations in Heavy Metal Concentrations among Trophic Levels of the Food Webs in Two Agroecosystems. *African Zoology* **2019**, *54* (1), 21–30. https://doi.org/10.1080/15627020.2019.1583080.
(65) Reeder, R. J.; Schoonen, M. A. A.; Lanzirotti, A. Metal Speciation and Its Role in Bioaccessibility and Bioavailability. *Reviews in Mineralogy and Geochemistry* **2006**, *64* (1), 59–113. https://doi.org/10.2138/rmg.2006.64.3.
(66) Bernhard, M.; Brinckman, F. E.; Sadler, P. J. Importance of Chemical Speciation in Environmental Processes. **1986**.
(67) Florence, T. M. The Speciation of Trace Elements in Waters. *Talanta* **1982**, *29* (5), 345–364. https://doi.org/10.1016/0039-9140(82)80169-0.
(68) Gleyzes, C.; Tellier, S.; Astruc, M. Fractionation Studies of Trace Elements in Contaminated Soils and Sediments: A Review of Sequential Extraction Procedures. *TrAC Trends in Analytical Chemistry* **2002**, *21* (6), 451–467. https://doi.org/10.1016/S0165-9936(02)00603-9.
(69) Tessier, A.; Campbell, P. G. C.; Bisson, M. Sequential Extraction Procedure for the Speciation of Particulate Trace Metals. *Anal. Chem.* **1979**, *51* (7), 844–851. https://doi.org/10.1021/ac50043a017.
(70) I, M.; I, A.; R, G.; E, M. Evaluation of Heavy Metal Availability in Polluted Soils by Two Sequential Extraction Procedures Using Factor Analysis. *Environ Pollut* **2000**, *110* (1), 3–9. https://doi.org/10.1016/s0269-7491(99)00287-0.
(71) Williams, G.; Seger, B.; Kamat, P. V. TiO2-Graphene Nanocomposites. UV-Assisted Photocatalytic Reduction of Graphene Oxide. *ACS Nano* **2008**, *2* (7), 1487–1491. https://doi.org/10.1021/nn800251f.

(72) Guardia, L.; Villar-Rodil, S.; Paredes, J. I.; Rozada, R.; Martínez-Alonso, A.; Tascón, J. M. D. UV Light Exposure of Aqueous Graphene Oxide Suspensions to Promote Their Direct Reduction, Formation of Graphene–Metal Nanoparticle Hybrids and Dye Degradation. *Carbon* **2012**, *3* (50), 1014–1024. https://doi.org/10.1016/j.carbon.2011.10.005.
(73) Chen, W.; Yan, L.; Bangal, P. R. Chemical Reduction of Graphene Oxide to Graphene by Sulfur-Containing Compounds. *J. Phys. Chem. C* **2010**, *114* (47), 19885–19890. https://doi.org/10.1021/jp107131v.
(74) Wang, Y.; Shi, Z.; Yin, J. Facile Synthesis of Soluble Graphene via a Green Reduction of Graphene Oxide in Tea Solution and Its Biocomposites. *ACS Appl. Mater. Interfaces* **2011**, *3* (4), 1127–1133. https://doi.org/10.1021/am1012613.
(75) Gao, J.; Liu, F.; Liu, Y.; Ma, N.; Wang, Z.; Zhang, X. Environment-Friendly Method To Produce Graphene That Employs Vitamin C and Amino Acid. *Chem. Mater.* **2010**, *22* (7), 2213–2218. https://doi.org/10.1021/cm902635j.
(76) Bose, S.; Kuila, T.; Mishra, A. K.; Kim, N. H.; Lee, J. H. Dual Role of Glycine as a Chemical Functionalizer and a Reducing Agent in the Preparation of Graphene: An Environmentally Friendly Method. *J. Mater. Chem.* **2012**, *22* (19), 9696–9703. https://doi.org/10.1039/C2JM00011C.
(77) Zhu, C.; Guo, S.; Fang, Y.; Dong, S. Reducing Sugar: New Functional Molecules for the Green Synthesis of Graphene Nanosheets. *ACS Nano* **2010**, *4* (4), 2429–2437. https://doi.org/10.1021/nn1002387.
(78) Peng, H.; Meng, L.; Niu, L.; Lu, Q. Simultaneous Reduction and Surface Functionalization of Graphene Oxide by Natural Cellulose with the Assistance of the Ionic Liquid. *J. Phys. Chem. C* **2012**, *116* (30), 16294–16299. https://doi.org/10.1021/jp3043889.
(79) Liu, J.; Fu, S.; Yuan, B.; Li, Y.; Deng, Z. Toward a Universal "Adhesive Nanosheet" for the Assembly of Multiple Nanoparticles Based on a Protein-Induced Reduction/Decoration of Graphene Oxide. *J. Am. Chem. Soc.* **2010**, *132* (21), 7279–7281. https://doi.org/10.1021/ja100938r.
(80) Salas, E. C.; Sun, Z.; Lüttge, A.; Tour, J. M. Reduction of Graphene Oxide via Bacterial Respiration. *ACS Nano* **2010**, *4* (8), 4852–4856. https://doi.org/10.1021/nn101081t.
(81) Wang, Y.; Li, Z.; Wang, J.; Li, J.; Lin, Y. Graphene and Graphene Oxide: Biofunctionalization and Applications in Biotechnology. *Trends in Biotechnology* **2011**, *29* (5), 205–212. https://doi.org/10.1016/j.tibtech.2011.01.008.
(82) Akhavan, O.; Ghaderi, E. Escherichia Coli Bacteria Reduce Graphene Oxide to Bactericidal Graphene in a Self-Limiting Manner. **2012**.
(83) Zhao, X.; Liu, H.; Yan, Z.; Song, C. Aging of Carbon Nanotubes Increases Their Adsorption towards Tetracycline. *Water* **2022**, *14* (17), 2731. https://doi.org/10.3390/w14172731.

Chapitre 2 : Matériels et méthodes

Dans la partie suivante, le principe de fonctionnement des analyses ainsi que la préparation des échantillons correspondants sont décrits seulement pour les analyses dont les détails manquent dans les chapitres d'articles scientifiques. Cette option permet d'éviter les redondances et la lecture conjointe de la partie matériels et méthodes suivante et celle de chaque article scientifique offre un une vision large sur les matériels et les méthodes qui ont été employés au cours de ces travaux de thèse.

La quasi-totalité des NMC utilisés dans cette étude ont été synthétisés au CIRIMAT, et la plupart était oxydé car c'est en général sous cette forme qu'ils sont utilisés dans les biens de consommation courante. En effet, l'oxydation est couramment utilisée au niveau industriel pour deux raisons : (1) éliminer la majorité des résidus catalytiques issus de la synthèse (purification) et/ou (2) diminuer le caractère hydrophobe intrinsèque des NTC et ainsi faciliter leur dispersion dans des liquides ou des matrices au sens large. Le Cd, Cu, Pb et Zn sont les quatre ETM qui ont été majoritairement utilisés en raison de leur toxicité au-delà d'une certaine concentration et de leur étroite surveillance par les autorités pour garantir la sécurité sanitaire des cultures des agrosystèmes.

1. Caractérisation des nanomatériaux

Les principales caractéristiques physico-chimiques des NTC sont la surface spécifique (mesurée par BET), la quantité de défauts de structure (mesurée par spectroscopie Raman), les dimensions et éventuels impuretés (visibles par MET) et leur charge de surface (mesurée par DLS). Les trois premières techniques seront détaillées ici.

1.1. BET

La surface spécifique (SSA) représente la totalité de la surface d'un objet, englobant les aspérités des particules, telles que les pores (accessibles par le gaz sonde utilisé), rapportée à la masse. Elle est exprimée en mètres carrés par gramme ($m^2.g^{-1}$) et a été déterminée à l'aide de la méthode de

Brunauer, Emmet et Teller (BET)[1]. Cette méthode se base sur la quantité d'azote (N_2) adsorbée sur l'échantillon en supposant la formation d'une monocouche atomique, mesurée lors d'une désorption soudaine. Connaissant la surface occupée par une molécule individuelle de N_2, la mesure de la quantité de gaz désorbé permet de calculer la surface réelle (disponible pour le gaz) des grains de poudre. Avant l'analyse, les échantillons de poudre de NTC ont été soumis à un dégazage à 100°C sous atmosphère d'azote pendant 2 heures afin d'éliminer tout contaminant de la surface (comme l'eau adsorbée, par exemple). Par la suite, les échantillons ont été refroidis à 77 K (température de l'azote liquide) pour permettre l'adsorption d'une monocouche de molécules de N_2. Après le refroidissement, les échantillons ont été ramenés à température ambiante, et le pic de désorption du N_2 a été enregistré. La désorption du N_2 a été mesurée en utilisant l'appareil Micrometrics Flow Sorb II 2300. Une calibration a été réalisée en injectant une quantité connue de N_2 dans les mêmes conditions que pour la mesure de l'échantillon. L'incertitude de la mesure est évaluée à 3%. Cette analyse a été réalisé par Marie-Claire BARTHELEMY au CIRIMAT (Toulouse, France).

1.2. Spectroscopie Raman

La spectroscopie Raman est une technique d'analyse qui permet d'étudier les vibrations moléculaires d'un échantillon en utilisant la diffusion inélastique de la lumière. Le phénomène de diffusion Raman tire son nom du physicien indien C.V. Raman, qui a découvert cette interaction lumineuse avec la matière en 1928[2] et a été honoré par le prix Nobel de physique en 1930 . Le principe fondamental de la spectroscopie Raman repose sur l'interaction entre la lumière incidente et les molécules de l'échantillon. Lorsque de la lumière, généralement un laser, est dirigée vers l'échantillon, une partie de cette lumière est diffusée de manière élastique, c'est-à-dire qu'elle conserve son énergie et sa longueur d'onde d'origine. Cependant, une petite fraction de la lumière est diffusée de manière inélastique. Lors de cette diffusion inélastique, la lumière transfère de l'énergie aux molécules de l'échantillon, provoquant des vibrations moléculaires. Les vibrations moléculaires résultent de changements dans la distribution des charges électriques à l'intérieur des molécules. Ces vibrations sont spécifiques à chaque type de liaison chimique et à chaque molécule, ce qui permet à la

spectroscopie Raman de fournir des informations précises sur la composition chimique de l'échantillon. Le processus de détection de la diffusion Raman se fait en mesurant la différence de fréquence entre la lumière incidente et la lumière diffusée inélastiquement (appelée décalage Raman)[3]. Le décalage Raman est exprimé en nombre d'onde (cm^{-1}) et correspond à la fréquence de vibration moléculaire spécifique. La spectroscopie Raman nécessite un spectromètre Raman, composé principalement d'un laser, d'un système de focalisation pour concentrer la lumière sur l'échantillon, d'un dispositif de dispersion pour séparer la lumière diffusée et d'un détecteur pour enregistrer le spectre Raman (Figure 6). Lorsque la lumière laser est focalisée sur l'échantillon, les molécules vibrent et diffusent la lumière Raman. Cette lumière est ensuite dispersée par le dispositif de dispersion, qui sépare les différentes fréquences de vibration. Le détecteur enregistre ensuite le spectre Raman, qui montre l'intensité de la lumière diffusée en fonction du décalage Raman.

Les NTC ont un spectre Raman typique (Figure 6)[4]:

- la bande D est identifiable entre 1320 et 1340 cm^{-1} et se montre proportionnelle à la quantité de défauts structuraux présents dans la structure de carbone supposé être principalement de type sp^2. La présence de cette bande D peut, de manière simplifiée, être assimilée à la quantité de carbone sp^3 inséré dans le réseau de carbone sp^2. C'est l'unique bande Raman mesurable dans le diamant pur (carbone uniquement sp^3).

- la bande G se situe entre 1575 et 1590 cm^{-1} et permet d'obtenir des informations sur le réseau hexagonal du carbone sp^2. Cette bande G se révèle spécifique au graphite, au graphène et aux NTC (par rapport au carbone organique). On retrouve cette même bande à la même position en spectroscopie infrarouge pour la vibration C=C du carbone sp^2.

- la bande G’ ou bande 2D est repérable entre 2620 et 2640 cm^{-1} et correspond à la deuxième harmonique de la bande D. Contrairement à la bande D dont l'intensité est influencée par la quantité de défauts présents dans la structure du matériau, la bande G’ est beaucoup moins sensible à ce facteur[4].

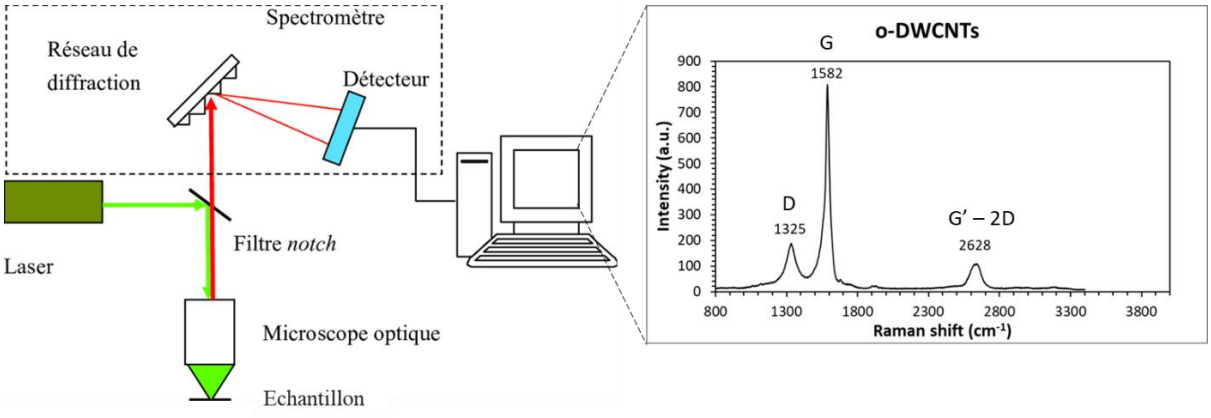

Figure 6 : Schéma d'un microscope RAMAN[5] et spectre associé pour des nanotubes de carbone bi-parois oxydés (o-DWCNT)

Les analyses Raman ont été réalisées à l'aide d'un microscope confocal Labram HR800 Horiba Jobin Yvon. Préalablement à l'analyse, les NTC sont dispersés dans de l'éthanol. Une goutte de suspension est placée sur une lame, séchée à l'air libre pendant quelques minutes avec l'aide d'une lampe rouge pour accélérer le séchage. Ensuite, l'échantillon est exposé à un laser de 633 nm à 8 MW sous microscope et observé avec l'objectif x100 offrant une résolution latérale et axiale de 0.833 µm et de 2.4 µm, respectivement. Après acquisition du spectre, la ligne de base est corrigée à l'aide du logiciel LabSpec et l'intensité des bandes D et G est mesurée afin de calculer le rapport d'intensité I_D/I_G utilisé comme indicateur de la proportion de défauts de structure dans les NTC.

Les caractérisations Raman ont été réalisées par Morgan LEGNANI au CIRIMAT (Toulouse, France).

1.3. Microscope électronique à transmission (MET)

Le MET est un instrument de microscopie qui permet d'observer les structures et les détails des échantillons à une échelle extrêmement fine, bien au-delà des limites des microscopes optiques traditionnels[6]. Il a été utilisé afin de caractériser le diamètre et le nombre de parois des NTC utilisés. Le MET utilise un faisceau d'électrons hautement énergétiques et focalisé. Ce faisceau est dirigé vers l'échantillon placé dans la colonne du microscope. Lorsque le faisceau d'électrons interagit avec l'échantillon, plusieurs processus se produisent. Certains électrons sont dispersés de manière élastique, c'est-à-dire qu'ils conservent leur énergie et leur direction d'origine. D'autres électrons subissent une diffusion inélastique, perdant de l'énergie lors de la collision avec les atomes de

l'échantillon. Le MET utilise un système de lentilles magnétiques pour focaliser le faisceau d'électrons avant son interaction avec l'échantillon. L'image est formée par transmission d'un faisceau d'électrons qui permet d'observer et d'obtenir des informations sur la composition chimique (analyseur EDX) de l'échantillon. L'image formée est projetée sur un écran fluorescent ou enregistrée numériquement (caméra) (Figure 7). Les variations d'intensité dans l'image correspondent aux différentes densités et épaisseurs des matériaux présents dans l'échantillon[6].

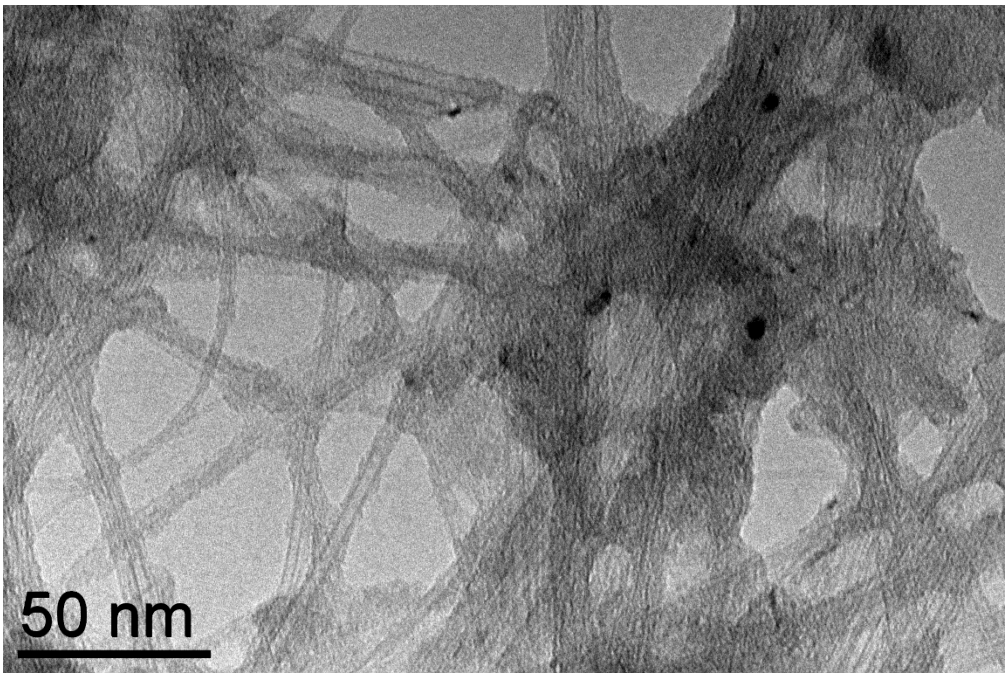

Figure 7: Image de NTC oxydés observé au MET

Les caractérisations MET ont été réalisées par Morgan LEGNANI au CIRIMAT (Toulouse, France).

2. Caractérisation des interactions NMC/ETM : expériences d'adsorption

2.1. Principe général des expériences d'adsorption

Les expériences d'adsorption ont été menées afin de déterminer quantitativement les ETM qui ont été adsorbés en surface des NTC et ce en fonction de la variation de certains paramètres environnementaux ou caractéristiques physico-chimiques des nanomatériaux utilisés. Selon l'expérience menée, les paramètres de l'expérience sont ajustés un à un de manière à tester leur influence sur l'adsorption des ETM en surface des NTC. Les expériences ont été réalisées afin de tester

l'influence du pH (5-8), du rapport de concentrations NTC/ETM ([ETM] = 0,2 à 8 mM, [NTC] = 10 $mg.L^{-1}$), de la durée de contact (10 à 360 min), de la nature des nanomatériaux [(GO, NTC oxydés et non oxydés, double et multi parois (o-DWCNT, o-MWCNT et DWCNT, MWNTC), NTC commerciaux (NC3100[7], Nanocyl SA.) possédant 8 parois (que l'on appelle 8NTC)], de la concentration en MO ([MO] = 10 et 20 $mg.L^{-1}$) et des composés contenus dans des solutions issues de deux sols aux caractéristiques physico-chimiques différentes (sol limono-sableux et un sol argileux nommés 2.1 et 6S et fournit par LUFA-Speyer).

Pour ce faire, l'ensemble des expériences suivent la procédure suivante (Figure 8) :

1. Elaboration d'une suspension fille à 1 $g.L^{-1}$ à partir d'une suspension mère de NTC à 3 $g.L^{-1}$ (CIRIMAT) et d'eau MilliQ (ultrapure) dans un tube Falcon (V = 50 ml)
2. Remise en suspension des NTC à l'aide d'un bain à ultrasons (PROLABO) pendant 15 min afin d'homogénéiser la suspension fille
3. Réalisation d'une solution mère multi-spécifique en ETM à l'aide de nitrate des éléments choisis : $Cd(NO_3)_2 \cdot 4H_2O$, $Cu(NO_3)_2 \cdot 2.5H_2O$, $Pb(NO_3)_2$ and $Zn(NO_3)_2 \cdot 6H_2O$ (pureté à 98%, Sigma-Aldrich, USA) et d'eau MilliQ. Les volumes de solutions ainsi que les concentrations de Cd, Cu, Pb et Zn sont ajustés selon le nombre d'échantillons et les concentrations sélectionnées pour l'expérience
4. Agitation de la solution mère à l'aide d'un agitateur magnétique à 200 RPM durant 15 min à 50°C afin d'homogénéiser la solution
5. Ajustement (ou non) du pH de la solution mère à l'aide d'une solution de NaOH à 10 M. La solution de NaOH est réalisée à l'aide de pastille de NaOH (Sigma Aldrich) et d'eau MilliQ.
6. A l'aide d'une éprouvette graduée, introduction de 50 mL de solution mère dans chaque erlenmeyer (V = 100 mL) puis ajout de 0,5 mL de suspension de NTC à 1 $g.L^{-1}$ à l'aide d'une pipette. La concentration finale de NTC dans les erlenmeyers était de 10 $mg.L^{-1}$. Pour chaque

condition expérimentale, les échantillons sont répliqués 5 fois. Les contrôles se font sans ajout de NTC.

7. Agitation des erlenmeyers sur une plaque d'agitation (STUART) selon la durée définie pour l'expérience à 200 RPM et à température ambiante

8. A l'issue de l'agitation, le contenu des erlenmeyers est transféré dans des tubes Falcon (V = 50 mL).

9. L'ensemble des échantillons est placé dans une centrifugeuse (Eppendorf) et centrifugé à 4000 RPM pendant 5 min à 20°C.

10. Chaque échantillon est ensuite filtré à l'aide d'une seringue (BD Plastipak) et d'un filtre en polypropylène de 25 mm de diamètre et de porosité de 0,45 µm (VWR). Le filtrat est placé dans des tubes ICP en verre (V = 10 mL, Fisherscientific)

11. Dilution des échantillons en prélevant 100 µL d'un échantillon dilué dans 10 mL d'une solution d'acide nitrique (Sigma Aldrich) à 3%

12. Les échantillons sont réservés en chambre froide jusqu'à analyse par ICP-AES.

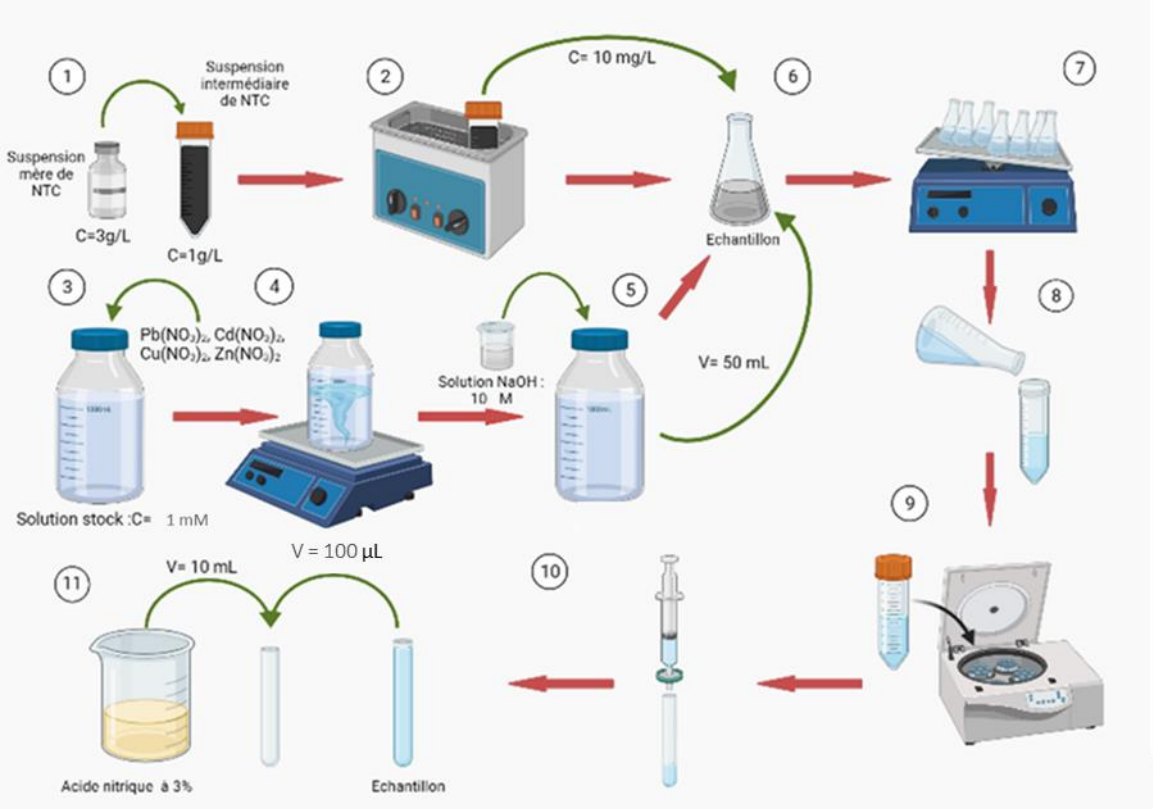

Figure 8: Représentation schématique de la procédure de préparation des échantillons pour les expériences d'adsorption

Les expériences sur le rapport de concentrations NTC/ETM et la durée de contact permettent de caractériser respectivement le comportement d'adsorption des ETM en surface des NTC à l'aide des modèles d'isotherme d'adsorption de Langmuir et de cinétique de pseudo-second ordre.

Afin de déterminer les quantités d'ETM adsorbés en surface des NTC, les données sont transformées de la manière suivante (exemple avec le Cd) :

Adsorption de Cd pour le réplicat n°1 = moyenne de la concentration de Cd des 5 réplicats sans NTC – concentration de Cd pour le réplicat n°1 avec NTC. Cette démarche est réalisée pour les 5 réplicats et la moyenne de ces 5 réplicats donne la quantité de métal adsorbé (en mM), qui est ramenée à 1 g de NTC ($mM.g^{-1}$).

2.1.1. Isothermes d'adsorption

2.1.1.1. Principe général

Dans le contexte d'une suspension aqueuse, les équilibres solide/liquide sont analysés en utilisant une approche scientifique basée sur la détermination de l'isotherme d'adsorption. L'isotherme d'adsorption est une représentation graphique qui illustre la variation de la quantité q_e ($mM.g^{-1}$) d'adsorbat adsorbée sur un solide à l'état d'équilibre, en fonction de la concentration à l'équilibre C_e (mM) du composé adsorbable, le tout à une température spécifique. La courbe $q_e = f(C_e)$ constitue donc l'isotherme d'adsorption. La quantité de molécules d'adsorbat qui se fixe à l'équilibre est généralement exprimée soit en nombre de moles d'adsorbat par unité de masse de solide, soit en masse d'adsorbat par unité de masse de solide.

Les isothermes d'adsorption en milieu aqueux sont déterminées par des méthodes expérimentales impliquant la mise en contact d'un adsorbat, tels que les ETM étudiés (Cd, Cu, Pb et Zn), en solution aqueuse avec un adsorbant, tels que les NTC. Au cours de ces expériences, la concentration initiale d'adsorbat diminue avec la durée d'incubation, ce qui permet d'obtenir plusieurs couples (C_e, q_e) une fois l'état d'équilibre atteint. Ces données expérimentales peuvent ensuite être soumises à des modèles mathématiques, lesquels ont pour objectif de représenter de manière optimale les isothermes d'adsorption observées sur une plage étendue de concentrations. Ces modèles étant thermodynamiques, la température n'a pas été modifiée au cours de nos expériences et correspondait à la température ambiante (18.3 ± 0.9 °C). En combinant les résultats expérimentaux avec les modèles mathématiques appropriés, il est possible d'obtenir une meilleure compréhension des interactions entre l'adsorbat et l'adsorbant en solution aqueuse, ce qui permet de mieux appréhender les phénomènes d'adsorption dans ce contexte spécifique.

Parmi les modèles d'isothermes d'adsorption, on peut notamment citer le modèle de Langmuir qui est couramment utilisé pour la détermination de la capacité maximum d'adsorption des matériaux et la constante d'adsorption K_{ads} qui caractérise les interactions adsorbant-adsorbat[8–12]. D'autres modèles

d'isothermes tels que celui de Freundlich, Redlich–Peterson, Sips, Toth, Temkin et Dubinin-Radushkevich permettent aussi de caractériser les interactions adsorbant-adsorbat, chacun possédant sa spécificité[13]. La modélisation de Langmuir a été choisi car il permet de décrire la formation d'une monocouche d'adsorbat sur une surface, qui est le cas dans les interactions NTC et ETM.

2.1.1.2. Isotherme de Langmuir

L'équation de Langmuir est valable pour une adsorption en monocouche sur une surface avec un nombre fini de sites identiques. Elle s'exprime par l'équation (1) ou par sa forme linéaire (2) :

$$(1)\ q_e = k_L q_m C_e / (1 + k_L C_e)$$

$$(2)\ 1/q_e = \frac{1}{q_{max}} + \left(\frac{1}{q_{max} \times K_L}\right) \times \frac{1}{C_e}$$

avec :

- q_m (mM.g^{-1}) : quantité d'adsorbat par unité de masse de l'adsorbant en vue de former une monocouche complète sur la surface,

- q_{max} (mM.g^{-1}) : quantité maximum d'adsorbat par unité de masse de l'adsorbant en vue de former une monocouche complète sur la surface,

- K_L (L.mM^{-1}) : la constante d'équilibre d'adsorption de Langmuir liée à l'affinité des sites de surface pour l'adsorbat et à l'énergie d'adsorption qui est égale au rapport des constantes de vitesses d'adsorption et de désorption. K_L caractérise l'étendue de l'interaction entre l'adsorbat et la surface. Plus la valeur de K_L est grande, plus l'interaction entre l'adsorbat et l'adsorbant est forte.

Les caractéristiques fondamentales de l'isotherme de Langmuir sont représentées par une grandeur sans dimension connue sous le nom de facteur de séparation ou paramètre d'équilibre, noté R_L. Cette grandeur a été définie par Weber *et al.*[14] et reprise par Ozcan *et al.*[15] (3) :

$$(3)\ R_L = \frac{1}{(1 + K_L \times C_0)}$$

avec C_0 la concentration initiale de l'adsorbat (ETM).

La valeur de R_L définit le type de l'adsorption (Tableau 5) :

Tableau 5: Correspondance du type de l'adsorption en fonction de la valeur de facteur de séparation R_L

Valeur de R_L	Type de l'adsorption
$R_L > 1$	Défavorable
$R_L = 1$	Linéaire
$0 < R_L < 1$	Favorable
$R_L = 0$	Irréversible

Ce modèle peut être caractérisé par 1 type d'isotherme pour le cas du modèle de Langmuir correspondant au type I (Figure 9) qui dans le cadre de la chimisorption, l'adsorption est caractérisée par une approche asymptotique d'une quantité limite indiquant que tous les sites de la surface sont occupés[16] (Figure 9).

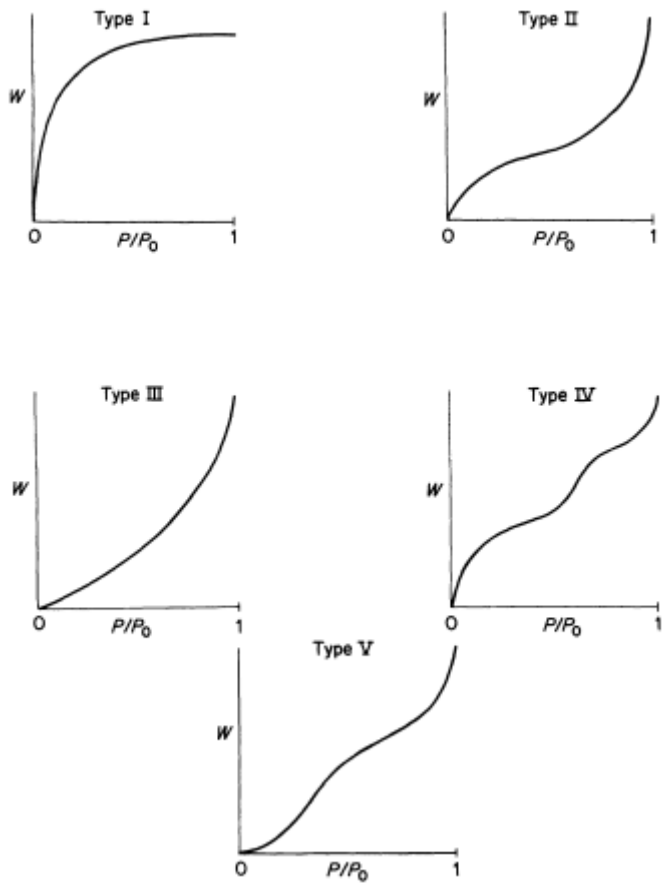

Figure 9: Classification des cinq types d'isothermes selon Brunauer et al.[17] (W : quantité adsorbée, P : pression d'équilibre de l'adsorbat, P_o : pression de vapeur saturée d'équilibre de l'adsorbat, P/P_o : pression relative. La condensation se produit à P/P_o[16]).

2.1.2. Cinétique d'adsorption

La cinétique d'adsorption joue un rôle clé dans la détermination du temps requis pour atteindre l'équilibre entre l'adsorbat (le soluté ou ETM) et l'adsorbant. Elle fournit également des indications sur le mécanisme d'adsorption et le mode de transfert entre les deux phases liquide et solide. Pour décrire cette cinétique et spécifier la nature des interactions à l'interface solide-liquide, plusieurs modèles cinétiques ont été développés. Parmi eux, le modèle de pseudo-second ordre, développé pour la première fois par Ho et McKay en 1999[18], est l'un des modèles les plus couramment utilisés pour décrire la cinétique d'adsorption d'adsorbat sur des adsorbants,. Ce modèle cinétique offre une caractérisation de l'adsorption en considérant une adsorption rapide du soluté sur les sites présentant une énergie élevée, tandis qu'une adsorption relativement lente se produit sur les sites de faible

énergie. La forme générale de l'équation cinétique de pseudo-second ordre peut être exprimée comme suivant l'équation (4):

$$(4)\ q_t = k_2 q_e^2 t/(tk_2 q_e + 1)$$

où :

- k_2 est la constante de vitesse de pseudo-second ordre ($g.mM.min^{-1}$),

- q_t est la quantité d'adsorbat adsorbée à l'instant t ($mM.g^{-1}$),

- q_e est la quantité d'adsorbat adsorbée à l'équilibre ($mM.g^{-1}$).

3. Détermination du transfert des NTC et ETM

3.1. Quantification du ^{13}C par py-IRMS (pyrolysis-Isotope Ratio Mass Spectrometry)

L'IRMS est basée sur la mesure précise des rapports isotopiques d'éléments spécifiques, tels que le carbone, l'hydrogène, l'azote, l'oxygène, le soufre. Ces éléments existent sous différentes formes isotopiques, ayant des masses différentes en raison du nombre différent de neutrons dans leur noyau. L'IRMS permet de mesurer la proportion de chaque isotope dans un échantillon par rapport à un isotope de référence[19,20]. Cette technique est utilisée dans notre cas pour mesurer les rapports des isotopes non radiogéniques (non issus de réactions de désintégrations nucléaires) $^{13}C/^{12}C$. Les NTC utilisés pour l'expérience de transfert trophique étant enrichis à 100% de ^{13}C, le rapport isotopique $^{13}C/^{12}C$ permet alors de renseigner sur la quantité de NTC accumulée par l'organisme considéré. Ces NTC ont été enrichis à hauteur de 100% afin de d'améliorer la sensibilité de la technique puisque selon F.Bourdiol[21], l'enrichissement doit être très largement supérieur à 20% afin d'espérer leur détection dans des matrices biologiques[21].

Afin de mettre en œuvre l'IRMS, l'échantillon (masse minimale = 500 µg) doit être préparé pour l'analyse c'est-à-dire préalablement séché et broyé. Ensuite, l'échantillon est pyrolysé de manière à le convertir en gaz simple (par exemple le CO_2, N_2, H_2, SO_2). Ces gaz sont ensuite analysés par un

spectromètre de masse où ils subissent une ionisation, c'est-à-dire qu'ils perdent des électrons pour former des ions. Ce processus se fait généralement en utilisant un faisceau d'électrons, un laser ou une source d'ions. Les ions ainsi formés sont ensuite accélérés dans un champ électrique afin de leur donner une énergie cinétique suffisante. Les ions accélérés entrent dans un analyseur de masse. Dans le cas des isotopes légers, les ions de rapport masse sur charge (m/z) plus élevé seront moins déviés que les ions de m/z plus faible par le champ magnétique, permettant ainsi leur séparation. Les ions séparés atteignent un détecteur, où ils sont dénombrés. Les rapports isotopiques de l'échantillon sont déterminés en comparant l'intensité des ions mesurés aux intensités d'un standard de référence ayant des rapports isotopiques connus. Les rapports isotopiques de l'échantillon sont calculés et exprimés en termes de δ (delta) en pour mille (‰) par rapport au standard de référence[19,20]. L'ensemble des analyses IRMS a été réalisé à la plateforme GISMO de l'UMR 6282 Biogéosciences par Anne-Lise SANTONI à l'aide d'un FlashSmar tEA couplé à un Delta 5 advantage Fisher (Dijon, France).

3.2. Analyse par faisceaux d'ions (^{13}C, ETM)

L'analyse par faisceau d'ions repose sur la détection des radiations émises après l'interaction d'un faisceau d'ions avec les atomes de l'échantillon à analyser. Ce faisceau est généré par un accélérateur de particules, puis accéléré par une différence de potentiel (plusieurs millions d'électronvolts). Les ions se déplacent ensuite dans une ligne composée de déflecteurs pour guider la trajectoire, des fentes d'objets pour définir la taille du faisceau et contrôler sa position, une cage de Faraday pour mesurer l'intensité du faisceau, différentes lentilles pour focaliser le faisceau en un point de quelques micromètres, et enfin des plaques électrostatiques pour contrôler le balayage de l'échantillon. La chambre d'analyse, maintenue sous vide (10^{-6} mbar), comprend plusieurs détecteurs permettant d'acquérir différents signaux. Plusieurs techniques analytiques peuvent être réalisées en utilisant la microsonde nucléaire, notamment l'émission de rayons X induite par des micro-particules (PIXE), la spectroscopie de rétrodiffusion Rutherford (RBS) ou l'analyse nucléaire par réactions (NRA) qui seront décrites ci-après. Ces différentes techniques ont été mise en œuvre en mode imagerie grâce à l'utilisation d'un micro-faisceau.

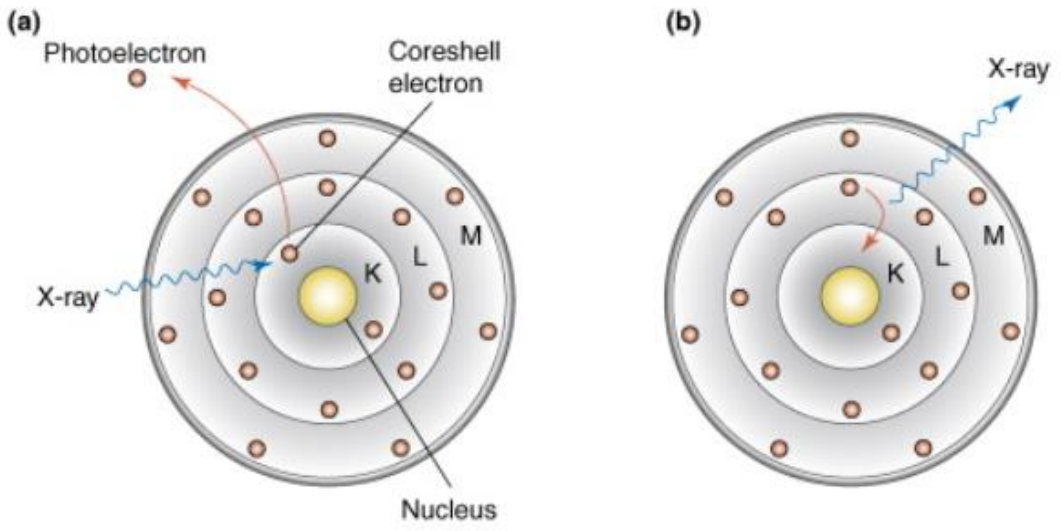

Figure 10: Modèle d'atome de Bohr illustrant le principe de la fluorescence X. L'excitation des rayons X conduit à l'éjection d'un électron de l'atome. La lacune générée est comblée par un électron de couche supérieure, un processus qui se traduit par l'émission d'un photon dont l'énergie est égale à la différence des énergies de liaison des deux couches impliquées dans la transition (d'après Fahrni 2007[22])

L'analyse µPIXE est une méthode non destructive permettant la cartographie élémentaire des échantillons. L'excitation des rayons X, comme illustrée par le modèle schématique de l'atome de Bohr (Figure 10), entraîne l'éjection d'un électron de la couche interne de l'atome. La lacune ainsi créée est ensuite comblée par un électron d'une couche supérieure, entraînant l'émission d'un photon dont l'énergie est caractéristique de chaque élément. Ces photons sont recueillis par un détecteur qui transforme ce signal en un spectre. Dans le spectre, la plupart du temps, chaque pic correspond à un élément, mais certaines superpositions peuvent compliquer l'identification. La déconvolution des pics du spectre sur chaque pixel analysé permet d'obtenir des cartographies élémentaires. Sur chaque pixel, le nombre de coups pour chaque élément considéré est disponible, permettant de créer une image avec une intensité de couleur proportionnelle au nombre de coups. La technique µPIXE présente plusieurs avantages par rapport à d'autres méthodes de fluorescence des rayons X. En particulier, grâce à l'énergie élevée de la source incidente (de l'ordre du MeV), la profondeur analysée varie de 0,1 à 150 µm selon le type d'échantillon. Toutefois, les éléments légers (C, H, O, N, etc.) échappent à la détection par le détecteur PIXE.

La µRBS est une technique d'analyse utilisée pour étudier la composition des matériaux en mesurant la diffusion élastique des particules à haute énergie (généralement des ions) par les noyaux des atomes constituant l'échantillon. Lorsque ces particules interagissent avec les noyaux des atomes du matériau cible, elles subissent une déviation dans leur trajectoire et certaines d'entre elles subissent une rétrodiffusion, c'est-à-dire qu'elles sont renvoyées dans la direction opposée à leur direction initiale. La quantité d'énergie perdue par les particules pendant leur interaction avec les noyaux est également mesurée. La mesure de la rétrodiffusion des particules permet d'obtenir des informations sur la composition élémentaire et la structure atomique du matériau cible. En effet, les noyaux des différents éléments présents dans l'échantillon ont des masses différentes, ce qui entraîne des angles de rétrodiffusion caractéristiques pour chaque élément[23]. En analysant ces angles, on peut déterminer les éléments présents dans l'échantillon et leur concentration en profondeur. La RBS est particulièrement utile pour l'analyse de matériaux minces et de couches superficielles, car elle offre une excellente résolution en profondeur, permettant de caractériser les différentes couches composant un matériau multicouches[23]. Cette technique complète la µPIXE puisqu'elle permet d'obtenir des renseignements concernant les atomes légers (C, H, O et N) non déterminés en µPIXE.

L'analyse µNRA est basée sur l'étude des rayons gamma électromagnétiques ou des particules émises lors des interactions nucléaires entre un faisceau d'ions à haute énergie et le noyau de la cible étudiée. Cette technique permet la détection et le dosage des éléments légers (de l'hélium au fluor) et de leurs isotopes, quelle que soit la nature de la matrice. Ainsi, cette technique a été utilisée afin de renseigner sur le transfert trophique de NTC dopés au C^{13} utilisés dans l'expérience en chapitre n°6 La profondeur d'analyse est comprise entre 50 Å et 150 µm, en fonction de la matrice et des conditions du faisceau[23].

Les analyses ont été conduites au Centre d'Études Nucléaires de Bordeaux-Gradignan (CENBG) sur la microsonde AIFIRA (Applications Interdisciplinaires des Faisceaux d'Ions en Région Aquitaine) avec le soutien technique de Stéphanie SORIEUL.

Les résultats sont toujours en cours de traitement au moment de la rédaction de ce manuscrit de thèse.

3.3. Quantification élémentaire par ICP-AES (Inductively Coupled Plasma - Atomic Emission Spectroscopy)

L'ICP-AES est une technique d'analyse chimique utilisée pour déterminer la concentration des éléments présents dans un échantillon liquide.

L'échantillon d'analyse doit être préalablement broyé à l'aide d'un broyeur à bille (FastPrep-24™, MpBio) puis digéré. Après une prédigestion durant une nuit avec l'ajout de 3 ml de HNO_3, un mélange de HNO_3 et de $HClO_4$ (3:1 v/v) et 1 ml de H_2O_2 ont été ajoutés pour les sols. Il en a été de même pour les cultures, mais sans ajout de mélange acide (HNO_3 et $HClO_4$). Ensuite, les échantillons ont été placés dans un four à micro-ondes (MARS) pour effectuer la digestion à un niveau de pression et de température (190°C) adapté au type d'échantillon. Pour les sols, les échantillons ont été filtrés (0,45 µm) avant dilution. Ensuite, l'échantillon liquide est dilué et acidifié (3-5% d'HNO_3) avantanalyse par ICP-AES. L'échantillon est ensuite introduit dans le système d'ICP-AES (Figure 11). Le gaz argon est introduit dans la chambre de plasma et est ionisé à l'aide d'un bobinage inductif. Cela crée un plasma à haute température (entre 6000 et 10000 °C) composé d'ions, d'électrons et d'atomes neutres hautement énergétiques. Les atomes des éléments présents dans l'échantillon sont excités à des niveaux d'énergie supérieurs en absorbant l'énergie du plasma. Lorsque les atomes excités reviennent à leurs niveaux d'énergie inférieurs, ils émettent de l'énergie sous forme de lumière. Chaque élément émet une lumière caractéristique à des longueurs d'onde spécifiques. La lumière émise par le plasma est dispersée en utilisant un spectromètre, qui sépare la lumière en différentes longueurs d'onde. La lumière émise est ensuite détectée par un détecteur, qui mesure l'intensité de chaque longueur d'onde. Les intensités des signaux lumineux à des longueurs d'onde spécifiques sont utilisées pour déterminer les concentrations des éléments présents dans l'échantillon en les comparant à des étalons calibrés. L'ICP-AES est une technique d'analyse sensible, rapide et précise, ce qui en fait un outil essentiel dans de nombreux domaines tels que l'analyse environnementale, l'analyse des matériaux, la géochimie, l'analyse des métaux dans l'industrie, la recherche médicale et bien d'autres applications[24]. L'ensemble des analyses ICP-AES a été réalisé à la plateforme FBil du laboratoire

d'écologie fonctionnelle et environnement par David BAQUE et Frédéric CANDAUDAP (ARCOS FHX22, AMETEK Spectral, Toulouse, France).

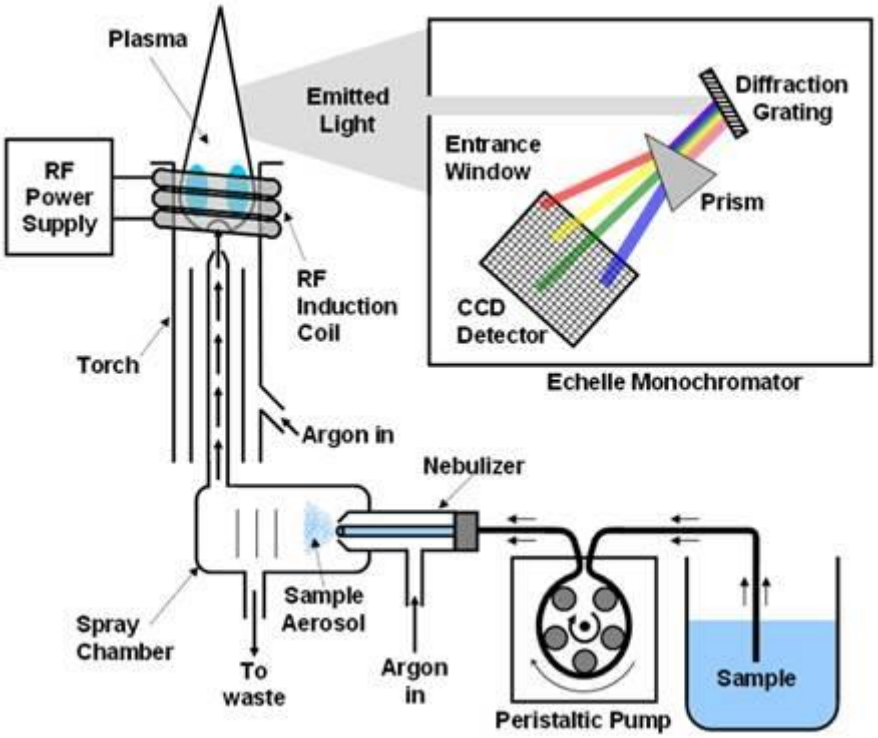

Figure 11: Schéma d'une machine d'ICP-AES[25]

4. Evaluation des impacts écotoxicologiques

Au cours de ce projet doctoral, beaucoup de marqueurs ont été utilisés afin de rendre compte de la toxicité des contaminants utilisés sur les organismes représentatifs des agrosystèmes. Spécifiquement, les études ont porté sur :

- les micro-organismes vivant dans le sol tels que les bactéries et champignons. Ces organismes réalisent tous deux une fonction essentielle pour tous les écosystèmes à savoir la décomposition de la matière organique qui a été suivie à l'aide d'un sachet de thé (à l'instar du tea bag index). De plus, les bactéries du sol ont été quantifiées par cytométrie en flux des quantités d'ADN des taxons bactériens reliés aux cycles biogéochimiques du C et N ont été analysées par qPCR et les activités enzymatiques reliées aux cycles biogéochimiques du C, N et P par spectrophotométrie. Enfin, les champignons du sol

ont été suivis avec la quantification de la molécule d'ergostérol présente chez ces organismes par chromatographie liquide à haute performance selon le protocole de Gesner[26]. La quantification de l'ergostérol a été réalisé par Didier Lambrigot Toulouse, France).

- les plantes d'intérêt agronomique (laitue et maïs). Au niveau métabolique, les quantifications de la chlorophylle (a et b), des tanins, des composés phénoliques et des flavonoïdes ont été réalisées par spectrophotométrie. A l'échelle macroscopique, la masse fraîche, la masse sèche, la surface foliaire, la transpiration foliaire (LI-1600, LICOR), l'efficacité photosynthétique avec le rendement quantique des photosystèmes (DivingPAM) ont été suivis.

- les organismes ingénieurs du sol comme les vers de terre. La croissance à travers le gain ou la perte de biomasse et le stade de développement des vers ont été suivis.

- les consommateurs primaires des agrosystèmes comme les escargots, avec notamment un suivi de biomasse

- l'ensemble de l'agrosystème recrée à petite échelle (microcosme) par le suivi de l'émission des gaz tels que le CO_2, CH_4 et H_2O. Aussi, afin de rendre compte de la santé de l'ensemble de l'agrosystème, des fonctions ont été sélectionnées et insérées dans un éco-marqueur à savoir un indice de multifonctionnalité.

Les protocoles utilisés pour ces différents marqueurs de toxicité sont développés dans les articles scientifiques des chapitres suivants. Toutefois, un focus particulier sera porté dans la section 2.4.1. sur la détermination des quantités d'ADN des taxons bactériens reliés aux cycles biogéochimiques du C et N par qPCR puisque le principe de cette technique n'est pas détaillé ailleurs et que la bonne compréhension des résultats peut s'avérer difficile sans le détail du fonctionnement de cette technique.

4.1. qPCR (quantitative Polymerase Chain Reaction)

La qPCR est une méthode d'amplification de l'ADN en temps réel qui permet de quantifier la quantité d'ADN spécifique dans un échantillon. La qPCR menée au cours des expériences est basée sur le

principe de la PCR classique mais avec l'ajout d'un colorant fluorescent appelé SYBR Green. Le SYBR Green est un colorant qui se lie spécifiquement à l'ADN double brin, et lorsque le colorant est lié à l'ADN en cours d'amplification, il émet de la fluorescence. La quantité de fluorescence émise est directement proportionnelle à la quantité d'ADN amplifié pendant la réaction de PCR.

L'ADN est extrait à partir de l'échantillon biologique d'intérêt (sol) à l'aide d'un kit d'extraction (DNeasy PowerSoil kit ©QIAGEN). L'échantillon peut être de l'ADN génomique, de l'ARN qui sera converti en ADN complémentaire (ADNc), ou de l'ADN plasmidique. Le mélange réactionnel de la qPCR contient l'ADN cible à amplifier, des amorces spécifiques à la séquence cible, une ADN polymérase thermostable (généralement la Taq polymérase), des nucléotides (dNTPs) et des tampons réactionnels. Le colorant SYBR Green est également inclus dans le mélange réactionnel. S'en suivent différentes phases de qPCR[27,28] (Figure 12) :

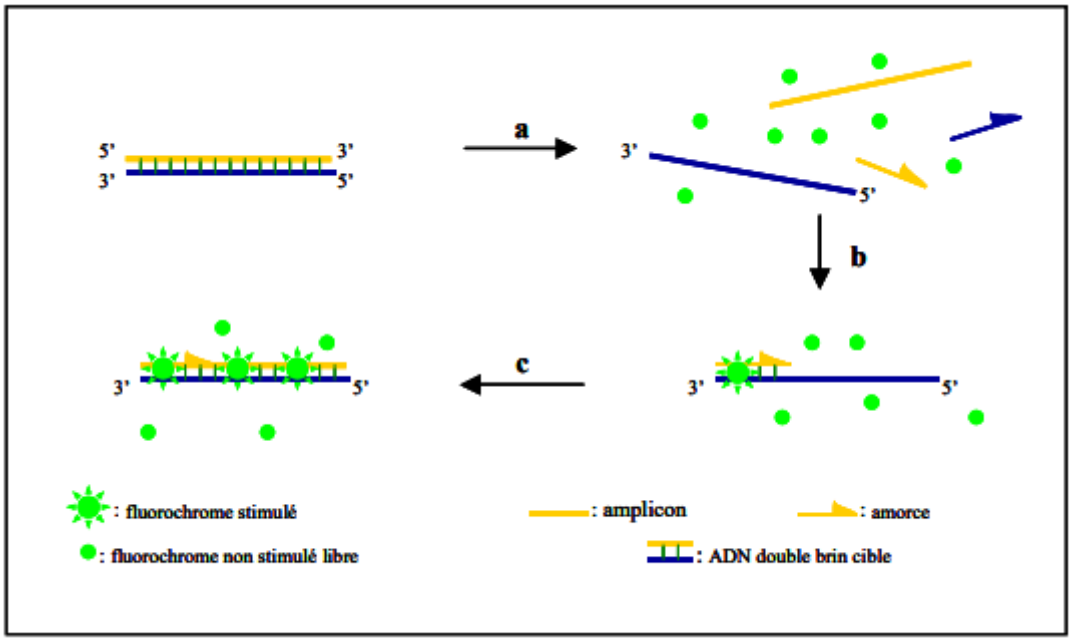

Figure 12: Schéma du principe d'une qPCR (d'après Poitras et Houde[27])

- phase de dénaturation (a) : le mélange réactionnel est chauffé à une température élevée (généralement 95°C) pour dénaturer l'ADN double brin en brins simples,

- phase d'hybridation (b) : la température est abaissée (généralement entre 50°C et 60°C) pour permettre l'hybridation des amorces spécifiques à la séquence cible sur l'ADN simple brin,

- phase d'élongation ou de polymérisation (c) : la température est augmentée à une valeur optimale pour l'activité de la polymérase (généralement entre 72°C et 75°C). La polymérase synthétise un nouveau brin d'ADN complémentaire à partir des amorces spécifiques, ce qui entraîne l'amplification de la séquence cible. Pendant la réaction d'amplification, le colorant SYBR Green se lie spécifiquement à l'ADN double brin nouvellement synthétisé. Lorsque le colorant se lie à l'ADN et émet de la fluorescence. La quantité de fluorescence émise augmente au fur et à mesure que l'ADN cible est amplifié. Les données de fluorescence sont collectées à chaque cycle d'amplification. Une courbe d'amplification est générée, qui représente la quantité d'ADN cible en fonction du nombre de cycles d'amplification. La quantité d'ADN cible est quantifiée en utilisant des étalons standards de concentration d'ADN connue[27,28].

La technologie basée sur le SYBR Green présente certains avantages et inconvénients. Contrairement à l'utilisation de sondes fluorescentes, cette technologie ne nécessite pas de conception particulière de sondes, car sa spécificité dépend entièrement des amorces utilisées[29]. De plus, elle n'est pas affectée par les mutations dans l'ADN cible qui pourraient influencer l'hybridation des sondes spécifiques[30]. Grâce à sa capacité à se lier à n'importe quelle molécule d'ADN double brin, le SYBR Green offre une certaine polyvalence, car il peut détecter plusieurs produits d'amplification dans la même réaction (séquence réactionnelle). Cependant, cette méthode présente également des limites : (I) étant donné que l'ADN double brin total émet des signaux, il devient difficile de s'assurer de la spécificité des amplicons en cours de réaction, et il est difficile de discriminer différents amplicons dans le cas de multiplexage, (II) le mauvais appariement (mis-primering), qui génère souvent des bandes d'ADN superflues observables sur un gel d'électrophorèse, peut conduire à des faux positifs ou à une surestimation de la quantification et (III) l'émission de fluorescence peut être influencée par la masse moléculaire de l'ADN amplifié, de sorte qu'un amplicon plus long fixera davantage de molécules

fluorescentes par rapport à un amplicon plus court dans la même réaction[29]. Malgré ces limites, la technologie SYBR Green reste largement utilisée pour de nombreuses applications en qPCR en raison de sa facilité d'utilisation et de sa polyvalence. Les extractions d'ADN du sol et la qPCR ont été réalisées au laboratoire d'écologie fonctionnelle et environnement par Melissa SONTAG (Toulouse, France).

Bibliographie (chapitre 2):

(1) Brunauer, S.; Emmett, P. H.; Teller, E. Adsorption of Gases in Multimolecular Layers. *J. Am. Chem. Soc.* **1938**, *60* (2), 309–319. https://doi.org/10.1021/ja01269a023.
(2) Raman, C. V.; Krishnan, K. S. A New Type of Secondary Radiation. *Nature* **1928**, *121* (3048), 501–502. https://doi.org/10.1038/121501c0.
(3) Mulvaney, S. P.; Keating, C. D. Raman Spectroscopy. *Anal. Chem.* **2000**, *72* (12), 145–158. https://doi.org/10.1021/a10000155.
(4) Dresselhaus, M. S.; Dresselhaus, G.; Saito, R.; Jorio, A. Raman Spectroscopy of Carbon Nanotubes. *Physics Reports* **2005**, *409* (2), 47–99. https://doi.org/10.1016/j.physrep.2004.10.006.
(5) Nguyen, Q. Mise au point d'un spéctromètre à l'échelle nanoscopique et son application. phdthesis, Ecole Polytechnique X, 2008. https://pastel.hal.science/pastel-00004206 (accessed 2023-08-02).
(6) Winey, M.; Meehl, J. B.; O'Toole, E. T.; Giddings, T. H. Conventional Transmission Electron Microscopy. *MBoC* **2014**, *25* (3), 319–323. https://doi.org/10.1091/mbc.e12-12-0863.
(7) *NC3100™*. Nanocyl. https://www.nanocyl.com/product/nc3100/ (accessed 2023-09-12).
(8) Boulinguiez, B.; Bouzaza, A.; Merabet, S.; Wolbert, D. Photocatalytic Degradation of Ammonia and Butyric Acid in Plug-Flow Reactor: Degradation Kinetic Modeling with Contribution of Mass Transfer. *Journal of Photochemistry and Photobiology A: Chemistry* **2008**, *200* (2), 254–261. https://doi.org/10.1016/j.jphotochem.2008.08.005.
(9) Ferrandon, O.; Bouabane, H.; Mazet, M. Contribution à l'étude de la validité de différents modèles, utilisés lors de l'adsorption de solutés sur charbon actif. *rseau* **1995**, *8* (2), 183–200. https://doi.org/10.7202/705218ar.
(10) Özcan, A. S.; Erdem, B.; Özcan, A. Adsorption of Acid Blue 193 from Aqueous Solutions onto Na–Bentonite and DTMA–Bentonite. *Journal of Colloid and Interface Science* **2004**, *280* (1), 44–54. https://doi.org/10.1016/j.jcis.2004.07.035.
(11) Ding, C.; Cheng, W.; Wang, X.; Wu, Z.-Y.; Sun, Y.; Chen, C.; Wang, X.; Yu, S.-H. Competitive Sorption of Pb(II), Cu(II) and Ni(II) on Carbonaceous Nanofibers: A Spectroscopic and Modeling Approach. *Journal of Hazardous Materials* **2016**, *313*, 253–261. https://doi.org/10.1016/j.jhazmat.2016.04.002.
(12) Fiyadh, S. S.; AlSaadi, M. A.; Jaafar, W. Z.; AlOmar, M. K.; Fayaed, S. S.; Mohd, N. S.; Hin, L. S.; El-Shafie, A. Review on Heavy Metal Adsorption Processes by Carbon Nanotubes. *Journal of Cleaner Production* **2019**, *230*, 783–793. https://doi.org/10.1016/j.jclepro.2019.05.154.
(13) Wang, J.; Guo, X. Adsorption Isotherm Models: Classification, Physical Meaning, Application and Solving Method. *Chemosphere* **2020**, *258*, 127279. https://doi.org/10.1016/j.chemosphere.2020.127279.
(14) Weber, T. W.; Chakravorti, R. K. Pore and Solid Diffusion Models for Fixed-Bed Adsorbers. *AIChE Journal* **1974**, *20* (2), 228–238. https://doi.org/10.1002/aic.690200204.
(15) Özcan, A.; Öncü, E. M.; Özcan, A. S. Kinetics, Isotherm and Thermodynamic Studies of Adsorption of Acid Blue 193 from Aqueous Solutions onto Natural Sepiolite. *Colloids and Surfaces A: Physicochemical and Engineering Aspects* **2006**, *277* (1), 90–97. https://doi.org/10.1016/j.colsurfa.2005.11.017.
(16) Lowell, S.; Shields, J. E. *Powder Surface Area and Porosity*, 3rd edition.; Springer: London ; New York, 1991.
(17) Brunauer, S.; Deming, L. S.; Deming, W. E.; Teller, E. On a Theory of the van Der Waals Adsorption of Gases. *J. Am. Chem. Soc.* **1940**, *62* (7), 1723–1732. https://doi.org/10.1021/ja01864a025.
(18) Ho, Y. S.; McKay, G. Pseudo-Second Order Model for Sorption Processes. *Process Biochemistry* **1999**, *34* (5), 451–465. https://doi.org/10.1016/S0032-9592(98)00112-5.
(19) Benson, S.; Lennard, C.; Maynard, P.; Roux, C. Forensic Applications of Isotope Ratio Mass Spectrometry—A Review. *Forensic Science International* **2006**, *157* (1), 1–22. https://doi.org/10.1016/j.forsciint.2005.03.012.

(20) Muccio, Z.; P. Jackson, G. Isotope Ratio Mass Spectrometry. *Analyst* **2009**, *134* (2), 213–222. https://doi.org/10.1039/B808232D.
(21) Bourdiol, F. Évaluation de l'écotoxicité de Nanotubes de Carbone En Milieu Aquatique à l'aide Du Modèle Amphibien Xenopus Laevis : Synthèse, Protocoles d'exposition, Détection et Dosage, 2019. http://www.theses.fr/17945739X (accessed 2019-06-13).
(22) Fahrni, C. J. Biological Applications of X-Ray Fluorescence Microscopy: Exploring the Subcellular Topography and Speciation of Transition Metals. *Current Opinion in Chemical Biology* **2007**, *11* (2), 121–127. https://doi.org/10.1016/j.cbpa.2007.02.039.
(23) Berger, P.; Revel, G. Nuclear microprobe. Applications; Microsonde nucleaire. Applications. *Techniques de l'Ingenieur. Analyse et Caracterisation* **2005**, *P3*.
(24) Hou, X.; Amais, R. S.; Jones, B. T.; Donati, G. L. Inductively Coupled Plasma Optical Emission Spectrometry. In *Encyclopedia of Analytical Chemistry*; John Wiley & Sons, Ltd, 2021; pp 1–29. https://doi.org/10.1002/9780470027318.a5110.pub4.
(25) *Spectrophotmétrie d'émission par plasma à couplage induit —*. https://chimieanalytique.com/spectrophotmetrie-icp/ (accessed 2023-08-16).
(26) Gessner, M. O. Ergosterol as a Measure of Fungal Biomass. In *Methods to Study Litter Decomposition: A Practical Guide*; Bärlocher, F., Gessner, M. O., Graça, M. A. S., Eds.; Springer International Publishing: Cham, 2020; pp 247–255. https://doi.org/10.1007/978-3-030-30515-4_27.
(27) Poitras, E.; Houde, A. La PCR En Temps Réel: Principes et Applications. *Reviews in Biology and Biotechnology* **2003**, *2*, 2–11.
(28) Livak, K.; Schmittgen, T. Analysis of Relative Gene Expression Data Using Real-Time Quantitative PCR. *Methods (San Diego, Calif.)* **2002**, *25*, 402–408. https://doi.org/10.1006/meth.2001.1262.
(29) Bustin, S. A. Absolute Quantification of MRNA Using Real-Time Reverse Transcription Polymerase Chain Reaction Assays. *Journal of Molecular Endocrinology* **2000**, *25* (2), 169–193. https://doi.org/10.1677/jme.0.0250169.
(30) Mackay, I. M.; Arden, K. E.; Nitsche, A. Real-Time PCR in Virology. *Nucleic Acids Research* **2002**, *30* (6), 1292–1305. https://doi.org/10.1093/nar/30.6.1292.

Chapitre 3 : Caractérisation des interactions NMC et ETM en milieux simplifiés

Depuis la découverte des interactions entre NMC et ETM, l'intérêt des scientifiques n'a cessé de s'accroitre afin de mieux les comprendre. D'ailleurs, le nombre de publication avec les mots clés « trace metal » and « carbon nanotube » / « graphene » a considérablement augmenté depuis 2010 (Figure 13).

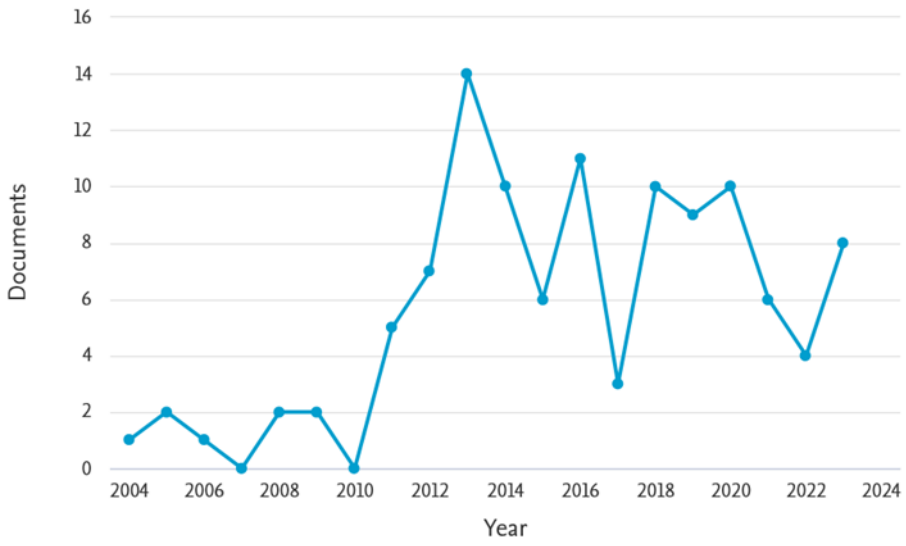

Figure 13: Graphique représentant les documents contenant les mots clés clés « trace metal » et « carbon nanotube » ou « graphene » depuis 2004 à nos jours

Ainsi, des études dans des milieux simplifiés (milieux aqueux) faisant intervenir un NMC comme adsorbant et un métal comme adsorbat ont été menées afin de déterminer de quelle manière : 1) les propriétés intrinsèques des NMC (surface spécifique (SSA), degré d'oxydation et nombre de parois) et 2) les conditions expérimentales (concentrations relatives de NMC et d'ETM, nature de l'ETM, pH du milieu et durée de contact) influencent l'adsorption des ETM à la surface des NMC. Comme pour toutes les premières approches dans un sujet de recherche émergent, les études ont été réalisées dans des systèmes les plus "simplifiés" possibles, de manière à maîtriser pleinement la compréhension des résultats obtenus et pour ensuite comprendre comment optimiser l'adsorption des ETM pour les développements industriels et passer à une étape supérieure dans l'utilisation des NMC. Dès lors, l'utilisation des NMC s'affirmant davantage, le besoin de compréhension des interactions NMC/ETM

dans des systèmes plus complexes régis par des questions environnementales/écotoxicologiques se fait de plus en plus ressentir. C'est dans ce mouvement que les expériences de ce chapitre ont été réalisées.

Les ETM peuvent se retrouver en concentrations anormalement élevées et ce, simultanément pour plusieurs ETM dans l'environnement et en particulier dans les agrosystèmes. Il a donc été décidé de travailler dans un système multi-spécifique en ETM. De plus, puisque le Cu, Zn, Pb et Cd sont les éléments les plus préoccupants pour l'environnement, car souvent signalés comme étant à l'origine de la contamination du sol, de l'eau et des réseaux trophiques[1], ce sont ces 4 ETM qui ont été choisis pour les expériences d'adsorption.

Les modèles théoriques qui décrivent le comportement d'adsorption des ETM à la surface des NMC dans des systèmes mono-métalliques ont été largement utilisés au cours des 20 dernières années, offrant ainsi suffisamment de recul sur leur validité pour décrire ces phénomènes. Toutefois, ces modèles ont été peu employés pour décrire le comportement d'adsorption des ETM sur les NMC dans des systèmes multi-métalliques. Deux expériences utilisant un modèle d'isotherme et de cinétique d'adsorption ont été réalisées pour s'assurer de leur validité dans des systèmes multi-spécifiques en ETM.

Des NMC aux propriétés intrinsèques différentes ont été utilisés afin de confirmer ou non les hypothèses proposées et les connaissances acquises issues des 20 dernières années de recherche à savoir que les propriétés intrinsèques des NMC ainsi que les paramètres du milieux (pH, temps de contact, nature de l'ETM, etc) régissent les interactions entre NMC et ETM.

En outre, les composés du sol contenus dans la solution du sol, tels que les argiles et la MO, qui forment le complexe argilo-humique possédant un important pouvoir adsorbant et un rôle biologique fondamental pour la nutrition des êtres vivants[2], sont susceptibles d'entrer en compétition d'adsorption avec les NMC. Il est donc essentiel de comprendre de quelle manière se déroule l'adsorption des ETM dans un système présentant à la fois des NMC et des composés du sol tels que

les argiles et la MO, et ainsi d'envisager ce qu'il pourrait se produire dans les écosystèmes et les répercussions sur le vivant. Dans ce contexte, une première expérience avec des NTC, un cocktail d'ETM et de la MO, a été menée afin de mieux comprendre le rôle de la MO sur l'adsorption des ETM à la surface des NMC. Dans un deuxième temps, deux solutions de sols aux propriétés texturales et aux concentrations en MO contrastées ont servi de milieux expérimentaux pour évaluer leur influence sur l'adsorption des ETM sur les NMC.

RESULTATS PRINCIPAUX

Les expériences menées dans ce chapitre ont permis de confirmer que les quantités d'adsorption des ETM en surface des NMC dépendent fortement du pH du milieu et que la nature des interactions (chimiosorption ou physiosorption) était certainement fonction du pH du milieu. Les modèles de Langmuir et de pseudo-second ordre demeurent adaptés pour caractériser l'adsorption des ETM lorsqu'ils sont en mélange dans le milieu. Selon le degré d'oxydation du NMC, la nature des liaisons est probablement différente : à savoir davantage de physisorption pour des NMC non oxydés et de chimiosorption pour des NMC oxydés. Il s'est avéré que le Cu et Pb s'adsorbent davantage sur les NMC oxydés que le Cd et Zn, alors qu'aucune affinité ne semble mise en évidence pour des NMC non oxydés. La présence de MO diminue l'adsorption des ETM qui ont le plus d'affinité pour les sites d'adsorption (Cu et Pb). Les composés contenus dans la solution de sol ne semblent pas modifier l'adsorption des ETM en surface des NMC mais comme attendu ajoutent beaucoup de variabilité dans les résultats.

Ces données seront particulièrement intéressantes à mobiliser pour tenter d'expliquer les résultats obtenus dans la suite de ce travail doctoral dans les expériences de transfert et de toxicité dans les agrosystèmes.

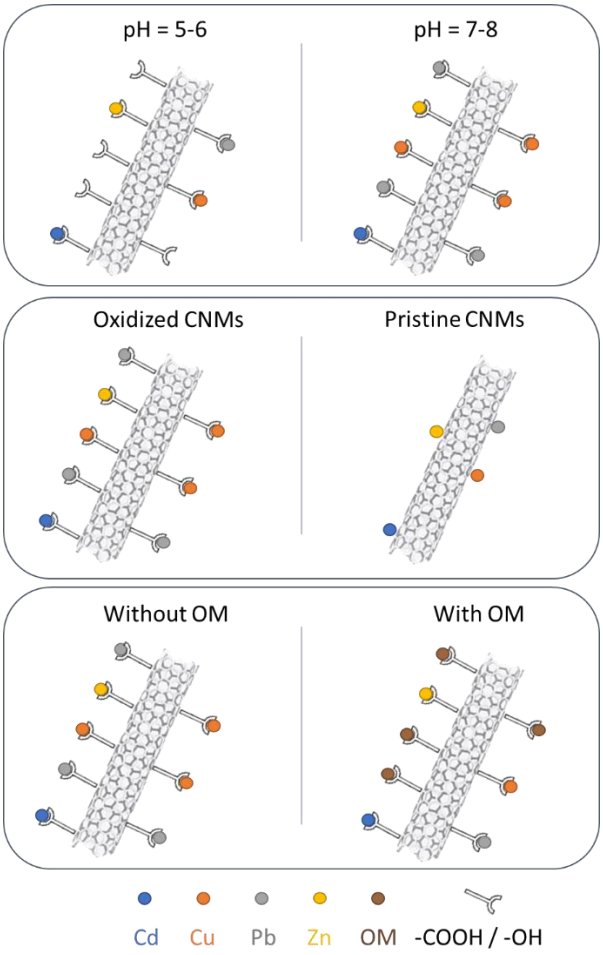

Figure 14: Schéma récapitulatif des principaux résultats du chapitre n°3 (OM = Organic Matter, CNMs = nanomatériaux carbonés)

Competitive adsorption on carbon based nanomaterials of a mixture of cadmium, copper, lead and zinc and influence of environmental parameters

Mathieu Leroy[1,2], Morgan Legnani[2], Emmanuel Flahaut[2*], Camille Larue[1*]

[1]Laboratoire écologie fonctionnelle et environnement, Université de Toulouse, CNRS, Toulouse, France, [2] CIRIMAT, Université de Toulouse, CNRS, Université Toulouse 3 - Paul Sabatier, 118 Route de Narbonne, 31062 Toulouse cedex 9 - France

*Corresponding authors: emmanuel.flahaut@univ-tlse3.fr; +00-33-(0)5-61-55-69-70; camille.larue@ensat.fr; +00-33-(0)5 34-32-37-55

Keywords: carbon-based nanomaterials, graphene oxide, metals, organic matter, cocktail

1. Introduction

Human activity leads to an always increasing use and environmental release of many contaminants. As such, the effect of contaminant mixtures (cocktail) is a major topic to date because interactions among contaminants could modify transfer and toxicity on organisms composing natural ecosystems, making risks more difficult to evaluate. To improve risk assessment strategies, we need, as a first step, to initiate studies in simplified environments to understand the interactions that exist among contaminants and to identify what are the effects of different environmental parameters on these interactions.

Among contaminants exhibiting strong interaction potential, emerging contaminants such as carbonaceous nanomaterials (CNM) and historical contaminants such as metals are particularly interesting to investigate from an environmental point of view since both contaminants can accumulate and coexist, in particular in agrosystems. Indeed, they tend to accumulate in sewage sludge which is applied as fertilizer in agrosystems[1] making soil contamination one of the most pressing concerns in the debate about food security and food safety in Europe[2] and globally[3]. In terms of concentrations, models predict that the concentration of CNM in biosolids could reach up to 10 mg.kg^{-}

[1] while in natural soil it could be up to 0.01 mg kg^{-1} [4]. Another study calculated that carbon nanotube (CNT) concentrations in European agricultural soils treated with sewage sludge could increase annually by 74 $ng.kg^{-1}$[1], especially because of their potential application as nanofertilizers[5] or nanopesticides[6], or even as decontaminant agent[7–10]. Concerning metals, they are found in agrosystems for several other reasons such as atmospheric deposition, irrigation with wastewater or polluted water, introduction of livestock manure, metallo-pesticides or herbicides, and phosphate-based fertilizers[11,12]. Governments decided to regulate heavy metal concentrations by setting maximum allowable thresholds in agricultural soils up to 1-3, 50-140, 30-75, 50-300, 150-300 and 1-1.5 $mg.kg^{-1}$ for Cd, Cu, Ni, Pb, Zn and Hg, respectively[13].

Some studies investigated metal adsorption onto CNM in aqueous media in the previous decade and concluded that it depends on the CNM properties (especially oxidation state and specific surface area (SSA)), the CNM/metal ratio, the contact time and organic matter (OM) concentration[14]. To date, most studies focused on the adsorption of one single metallic ion onto CNM, but this type of system is not environmentally relevant because it does not consider the diversity of metals present simultaneously in ecosystems, and their competition for adsorption sites[14]. Indeed the few studies on that topic highlighted changes when metal were present as mixture. Ding et al. showed that adsorption equilibrium for Pb, Cu or Ni added individually with an adsorbent was decreased when they were added simultaneously[15]. This trend was confirmed in different studies for other metal(loid)s[16–21] so that sequences of affinities can be drawn up and thus highlight different metal affinities for adsorption sites. Salam *et al.*[16] reported the following affinity sequence Cu>Zn>Pb>Cd for multi-walled CNT (MWCNT) while Sitko *et al.*[19] and Li *et al.*[20] found Pb>Cu>Cd>Zn for graphene oxide (GO) and oxidized MWCNT. In addition, most studies were carried out with industrial development as perspective, without environmental relevance, in particular on CNM concentrations, which were in excess in comparison with metal concentrations.

Additionally, agrosystems are composed of many components which can modify CNM/metal interactions. For example, OM could modify the adsorption of metal[22–24] but the mechanisms are still unknown. Soil structure (grain arrangement) and granulometry (grain size) could modify contaminant transport and thus metal adsorption onto CNM[25–27]. Very few studies characterized soil component influence on CNM/metal interactions and more are needed considering that ecotoxicity data available in the literature show either an increase[28–36] or a decrease[28,31,33,34,37,38] of metal(loid)s transfer into organisms due to CNM addition.

This work aimed at (1) investigating the competitive adsorption of Cd(II), Cu(II), Pb(II) and Zn(II) on oxidized-double walled CNT (o-DWNCTs) at different environmentally relevant pH values ranging from 5 to 8 and with the establishment of isotherms and kinetics profiles, (2) comparing metal adsorption on o-DWCNT with other adsorbents (pristine DWCNT, pristine and oxidized-MWCNT, GO and, activated carbon (AC)) to clarify the influence of CNM intrinsic property influence and (3) exploring o-DWCNT/metal interactions in natural soil solution coming from soil with contrasting properties.

The results obtained here will bring a valuable contribution towards a better understanding of the interactions among contaminants in natural environment and their impacts on both transfer and toxicity of such contaminants.

2. Material and methods

2.1 Materials

Carbon nanotubes were synthesized at Centre inter-universitaire de Recherche et d'Ingénierie des Matériaux (CIRIMAT, Toulouse, France). For synthesis, the carbon source was methane or ethanol for DWCNT and MWCNT, respectively[39]. The elemental composition of the catalyst ($Mg_{0.99}Co_{0.0075}Mo_{0.0025}O$) was the same for both syntheses but in the case of MWCNT, it was prepared by impregnation of MgO powder by a solution of the relevant amounts of Cobalt(II) nitrate and ammonimum heptamolybdate (instead of combustion synthesis in the case of DWCNT). After 1h of

stirring (magnetic barrel), the suspension was frozen by immersion in liquid nitrogen. After freeze-drying, the resulting powder was calcined in air at 450°C for 1h. Combustion chemical vapor deposition (CCVD) synthesis was performed by heating at 5°/min in nitrogen atmosphere (50 sccm) from room temperature to 300°C. At that temperature, ethanol was introduced by bubbling the nitrogen in a gas washing bottle filled with ethanol. When the temperature reached 850°C, a 30-minute dwell time was observed before cooling down to room temperature at 5°/min. When the temperature was back to 300°C, the introduction of ethanol was stopped, and nitrogen alone was used. In both cases (DWCNT and MWCNT), as-prepared composite powders were processed with an aqueous HCl solution to dissolve the catalytic support and isolate the CNT. The protocol applied for oxidation of CNM was as follows: after washing with deionized water, a wet sample corresponding to an equivalent dry-weight of 100 mg CNT was introduced into a 250 mL flask with 100 mL of 3M HNO_3. The mixture was sonicated in an ultrasonic bath for 10 min before heating in reflux conditions at 130°C for 24h and finally cooled down to room temperature and filtered using a polypropylene membrane (Merck Millipore, 0.45 µm). Activated Carbon (AC), commercial MWCNT (8CNT) and GO were obtained from KURARAY CO., LTD., Nanocyl SA and Antolin Group, respectively. More information about adsorbate characteristics may be found in Table 6 and SI Figure S1 and S2.

Stock solutions of Cd(II), Cu(II), Pb(II) and Zn(II) were prepared by dissolving $Cd(NO_3)_2 \cdot 4H_2O$, $Cu(NO_3)_2 \cdot 2.5H_2O$, $Pb(NO_3)_2$ and $Zn(NO_3)_2 \cdot 6H_2O$ (98% purity, Sigma-Aldrich, USA) in ultrapure water.

Two types of contrasted soil were studied. The first one is a loamy sand soil (LUFA-Speyer) named Lufa 2.1 sieved to 2 mm with 86.0% of sand, 12.6% of loam and 1.4% of clay. It contained 0.58 wt. % of organic carbon, 0.04 wt. % of nitrogen, with a pH of 5.0 ± 0.1 and a cation exchange capacity of 2.9 ± 0.2 meq.100g^{-1}. The second soil is a clayey soil (Lufa 6S) sieved to 2 mm with 22.4% of sand, 35.1% of loam and 42.5% of clay. It contained 1.50% of organic carbon, 0.17% of nitrogen, with a pH of 7.3 ± 0.1 and a cation exchange capacity of 18.7 ± 1.2 meq.100g^{-1}. Soil solutions were prepared by adaptation of the standard AFNOR NF EN 12457-4[40]. Briefly, 100 g of soil were placed in 1L of ultrapure water, shaken at

180 RPM for 24 hours and then filtered at 20 µm. Initial pH value of each solution was not adjusted and their elemental composition is available in SI Figure S3. The cocktail of metals (1 mM of Cd(II), Cu(II), Pb(II) and Zn(II)) and o-DWCNT (10 $mg.L^{-1}$) was then added to these soil solutions . After prepared, pH of soils solutions was 4.3 ± 0.2 and 5.7 ± 0.2 for Lufa 2.1 and Lufa 6S respectively.

2.2. CNM characterization techniques

Transmission Electron Microscopy (TEM) was used to assess the length and diameter of CNM (JEOL TEM 1400; 120 kV, Centre de microcaractérisation Raimond Castaing, UMS3623, Toulouse). The SSA was determined using Brunauer-Emmett-Teller (BET) method (Micrometrics Flow Sorb II 2300; 2h degassing at 100°C in N_2 and adsorption of nitrogen gas at the temperature of liquid nitrogen; measurement accuracy ± 3%). Raman characteristics were analyzed to get information on the structural quality of the CNM used at λ = 633 nm (Labram HR800 Horiba Yvon Jobin). The proportion of carbon and oxygen contained in CNM were determined with organic micro-analyzers (total combustion at 1050°C under helium/oxygen flux for C and N dosage; total pyrolysis at 1080°C under nitrogen flux for O dosage; SCA CNRS Lyon) and were provided from Liné thesis which studied the same CNM as in this work[41].

Table 6: Characteristics (Length, diameter, specific surface area, Id/Ig and % of C and O) of CNM (graphene oxide (GO), oxidized double-walled CNT (o-DWCNT), oxidized multi-walled CNT (o-MWCNT), double-walled CNT (DWCNT), commercial pristine MWCNT (8CNT) and activated carbon (AC)) used in this study. Measure correspond to the average of 3 values. Thickness of AC and GO were not provided. % of C and O for AC were not dtermined.

Materials	Lenght (µm)	Diameter/ Thickness (nm)	Specific surface area ($m_2.g^{-1}$)	Id/Ig	% of C	% of O
AC	5 to 20	-	1500-1800	1.21	-	-
DWCNT	1 to 100	2.1 ± 0.7	854	0.23	89.7	2.2
8CNT	< 1.5	10.2 ± 1.1	229	1.87	91.8	1.2
GO	0.2 to 8.0	-	228	1.09	69.0	31.0
o-DWCNT	1 to 100	2.1 ± 0.7	218	0.23	76.9	17.2
o-MWCNT	1 to 20	24.2 ± 8.6	60	1.31	93.2	6.8

2.3. Adsorption experiments

Preliminary tests were conducted in order to select relevant conditions for adsorption experiments. In order to get closer to environmentally relevant conditions**,** it has been decided to work in saturated metal concentrations compared to CNM adsorption capabilities. *i.e.* 1 mM for each metal and 10 $mg.L^{-1}$ for CNM. Four metals were selected for batch adsorption experiments (Cd, Cu, Pb and Zn: 1mM for Cd = 112.41 $mg.L^{-1}$, for Cu = 63.54 $mg.L^{-1}$, for Pb = 207.2 $mg.L^{-1}$ and for Zn = 65.38 $mg.L^{-1}$) due to their toxicity and environmental monitoring. First results showed that metal adsorption was the highest at pH = 7, 3 hours and these conditions were thus selected for batch adsorptions. To test the effects of CNM characteristics (SSA, diameter, surface oxidation), metal adsorption onto pristine DWCNT, pristine MWCNT and commercial pristine (8CNT), o-MWCNT, GO and AC were compared to o-DWCNT. To investigate the effect of pH and OM on metal adsorption onto o-DWCNT, relevant environmental conditions were selected and fixed on a pH ranging from 5 to 8[42] and two concentration of OM as 10 and 20 $mg.L^{-1}$.

The experimental design was the same for all batch adsorption experiments. Briefly, before introducing 50 ml of the metal cocktail solution in an erlenmeyer (V = 100 ml), the initial pH values were recorded and adjusted to 7 if needed with a few drops of 10 M NaOH solution to limit dilution. Then, CNM (10 $mg.L^{-1}$, 500 µL) were introduced in experimental units (together with OM in one experiment) and the suspensions were placed under shaking on an orbital shaker plate at 200 rpm during 3 hours (excepted for kinetics experiments) at room temperature (18.3 ± 0.9 °C). Samples were then centrifuged at 4000 rpm (20°C) for 5 min. Finally, samples were filtered on 0.45 µm polypropylene filtration membrane (LABO MODERNE). Control experiments were performed in each case in the absence of CNM. Parameters of each experiment are summarized in Table 7.

Table 7: Summary of adsorption experiment parameters (H = Hours, OM = organic matter, o-DWCNT= oxidized double walled carbon nanotube, o-MWCNT= oxidized multi walled carbon nanotube, AC = activated carbon, 8CNT = commercial pristine MWCNT, GO = graphen oxide).

Tested parameter	CNM nature and concentration	Metal nature and concentration	Other component nature and concentration	pH solution	Contact Time
pH	o-DWCNT 10 mg.L^{-1}	Mixture of 4 metals (Cd(II), Cu(II), Pb(II) and Zn(II)), all at 1 mM	-	5.0, 6.0, 7.0, 8.0	3 H
Elemental ratio	o-DWCNT 10 mg.L^{-1}	Mixture of 4 metals (Cd(II), Cu(II), Pb(II) and Zn(II)), all at 0.1, 0.2, 0.5, 0.7, 1.0, 2.0, 2.5, 4 or 8 mM (but range concentration was selected for every metals for isotherm modelling, see Figure 15).	-	7.0	3 H
Kinetics	o-DWCNT 10 mg.L^{-1}	Mixture of 4 metals (Cd(II), Cu(II), Pb(II) and Zn(II)), all at 1 mM	-	7.0	10, 20, 40, 60, 90, 120, 180, and 360 min
OM	o-DWCNT 10 mg.L^{-1}	Mixture of 4 metals (Cd(II), Cu(II), Pb(II) and Zn(II)), all at 1 mM	OM = 0, 10 or 20 mg.L^{-1}	7.0	3 H
CNM type	DWCNT, o-DWCNT, o-MWCNT, GO, 8CNT, AC 10 mg.L^{-1}	Mixture of 4 metals (Cd(II), Cu(II), Pb(II) and Zn(II)), all at 1 mM	-	7.0	3 H
Soil solution	o-DWCNT 10 mg.L^{-1}	2.1 and 6S soil solution + mixture of 4 metals (Cd(II), Cu(II), Pb(II) and Zn(II)), all at 1 mM	-	Without metals : 2.1 = 7.5, 6S = 7.3 With metals : 2.1 = 4.3, 6S = 5.7	3 H

The effect of the ratio o-DWCNT/metal concentration was modelled thanks to Langmuir isotherm using the following equation (1):

$$(1)\ Langmuir:\ q_e = k_L q_m C_e / (1 + k_L C_e)$$

where q_e and q_m (mM.g^{-1}) represent equilibrium and maximum adsorption capacities, respectively; C_e (mM.L^{-1}) the equilibrium aqueous concentration; k_L (L.mM^{-1}) the equilibrium constant.

For isotherm modelling, 0.1-4 mM range concentration of Cd and Zn, 0.2-4 mM for Pb and 0.1-2.5mM for Cu were used due to metals precipitation.

Kinetics experiment was described by diffusion models such as the pseudo-second-order following this equation (2)[43]:

$$(2)\ Pseudo\ second\ order:\ q_t = k_2 q_e^2 t / (t k_2 q_e + 1)$$

where q_t and q_e are the adsorption capacities (mM.g^{-1}) at time t and equilibrium and k_2 (g.mM.min^{-1}) is the constant rate of the pseudo-second order.

2.4. Analytical measurements

Samples were diluted in 3% HNO_3 before elemental analysis by ICP-AES (ARCOS FHX22, AMETEK Spectral).

2.5. Modelling and statistical analyses

Modelling was performed on Microsoft Excel 2019 version 1808.

All presented data have been transformed as follows (example for Cd):

Cd adsorption for replicate n°1 = mean of Cd concentration of five replicates without CNM - Cd concentration for replicate n°1 with CNM.

Then, adsorption concentrations ($mM.g^{-1}$) obtained were corrected with CNM concentration in the sample to obtain for each ion used in experiments: $\frac{\text{ions concentration (mM)}}{\text{g of CNM}}$.

All statistical analyses were performed on RStudio software (version 3.4.1). First, 1-way ANOVAs were performed on adsorption data to test the effects of each parameters investigated in batch adsorption experiments (metal concentration, pH, time contact, OM concentration, soil solutions). The normality, independence and homoscedasticity of the residues were checked using Shapiro, Durbin-Watson and Breusch-Pagan tests, respectively. Data were transformed to log or square root if one of the three conditions of validity was not met. A non-parametric Kruskal-Wallis test was performed in case of failed transformations.

Precipitations forms of Cd, Cu, Pb and Zn according to pH value and Pourbaix diagrams are available in SI Figure S4, S6, S7, S8, S9 and S10. They were made in Visual Minteq 3.1.

3. Results and discussion

3.1 Influence of the pH

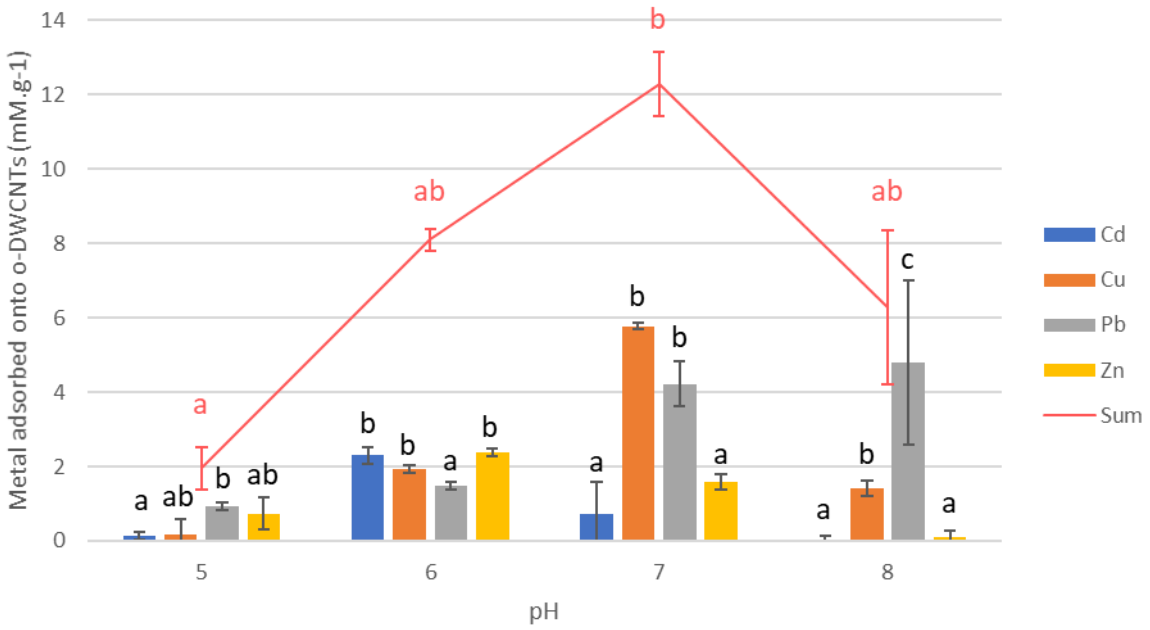

Figure 14: Metal (Cd, Cu, Pb and Zn) adsorbed onto o-DWCNT depending on the pH (o-DWCNT concentration: 10 mg.L^{-1}, metal concentrations: 1 mM. Contact time: 3 hours, temperature: 18.3 ± 0.9 °C). Same lowercase letters indicate treatments that do not differ significantly following 1 way ANOVA. ANOVA has been performed within a pH value (p-value > 0.05; n=5)

Figure 14 shows the effect of pH on the adsorption of Cd, Cu, Pb and Zn onto o-DWCNT in a multi-metallic system. First, cumulative metal adsorption onto o-DWCNT increases with pH with a maximum adsorption reached at pH = 7 up to 12.29 mM.g^{-1}, before decreasing at higher pH = 8 down to 6.28 mM.g^{-1}. This result is in agreement with the general trend found in the literature in which metal adsorption depends on the solution pH, similarly in single metal system[44–50,19] and in multi-metallic system[15,16,20]. In particular, Salam *et al.*[16] highlighted a maximum adsorption for Cu and Pb onto MWCNT at pH = 6, while it was not reached for Cd and Zn in the tested pH range (pH range: 3 to 9)[16]. Our present results could suggest that metals were more precipitated in aqueous solution around pH = 8 as suggested by Minteq modelling (SI Figure S4) and because their adsorption started to decrease at this pH but it was not the case (concentrations of TME in samples at pH = 8: Cd_{pH8}= 0.99 mM, Cu_{pH8}= 0.99 mM, Pb_{pH8}= 0.87, Zn_{pH8}= 0.96 mM).

Then, metals were not adsorbed in the same proportions at the tested pH points. Indeed, two metal adsorption patterns could be defined according to the pH range : (i) in the range pH = 5 to 6, metal

adsorption was low (around 1-2 mM.g^{-1}) and very similar among metals, and (ii) for higher pH, metal adsorption was higher (more than 5 and 4 mM.g^{-1} for Cu and Pb, respectively) and metal dependent so that adsorption sequences could be defined at the maximal adsorption pH (pH = 7) as following Cu ≈ Pb > Cd ≈ Zn sequence, while it was Pb > Cu > Cd ≈ Zn at pH = 8.

Salam *et al.*[16] obtained different patterns, where Cu was already more adsorbed onto MWCNT starting from pH = 5 than other metals (Cd, Pb and Zn). Also, at pH = 7, they highlighted the following sequence : Cu > Zn > Pb > Cd, while Sitko *et al.*[19] found a similar sequence as ours (Pb > Cu > Cd > Zn) with GO. On one hand, it is likely that the mechanisms of adsorption differ for an oxidized material and a raw material. Indeed, oxidized materials due to the presence of -COOH and -OH groups could favour adsorption based on ionic and electrostatic interactions, while it would be more of physical nature for raw materials[8,14,50–53], thus explaining the differences observed in the adsorption sequences mentioned above. On the other hand, adsorption phenomenon seems also related to the point of zero charge of CNM such as when pH > pH_{PZC}, cation adsorption is higher due to the electrostatic interactions between the cations and the negative surface charge of CNM and when pH ≤ pH_{PZC}, cation adsorption is lower due to the neutralization of the surface charge of CNM, or even the presence of repulsive positive charges[14]. In our case, the pH_{pzc} for o-DWNCTs used in this experiment was not reached within a pH range from 2 to12 (SI, Figure S5). Our results suggest that Cu(II) and Pb(II) ions show more affinity for the adsorption sites than Cd(II) and Zn(II). Also, the change in affinity sequence at pH = 7 (Cu ≈ Pb > Cd ≈ Zn) and pH = 8 (Pb > Cu > Cd ≈ Zn) could reveal that Pb(II) has more affinity for adsorption sites at pH = 8 than Cu(II).

Regarding the median value of pH in agricultural soils in Europe (pH = 5.8)[54], metals would be weakly adsorbed and in similar proportion. However, in the environment, and in particular in agrosystems, it has been proven that sewage sludge application (main entry pathway for CNM) increases soil pH[55], which according to our results could reinforce the adsorption of metals on the surface of o-DWCNT. Indeed, sewage sludge application could increase agricultural soil pH at pH = 7 or 8 where metal

adsorption followed affinity sequences described here. In parallel, sewage sludge application increases metal availability and thus their adsorption behaviour and potential toxicity.

3.2. Isotherms

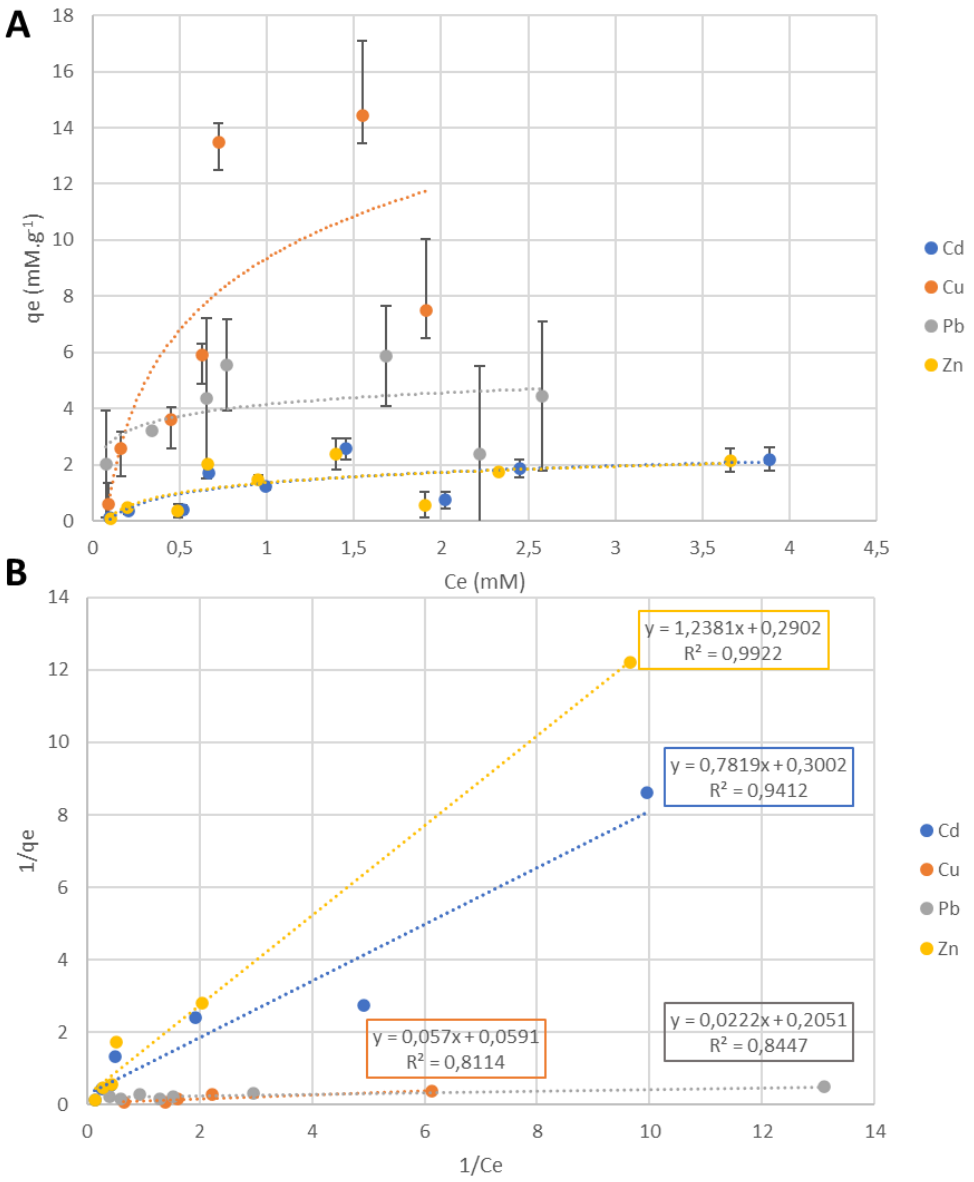

C

	Intercept	Slope	q_{max}	q_{exp}	K_L	R_L	R^2
Cd	0.30	0.08	3.33	1.24	3.84	0.03	0.94
Cu	0.06	0.06	16.92	13.48	1.04	0.09	0.81
Pb	0.21	0.02	4.88	5.55	9.24	0.01	0.84
Zn	0.29	1.24	3.45	1.49	0.23	0.30	0.99

Figure 15: Multi-metallic Langmuir non-linear isotherm (A), linear isotherm (B) and Langmuir adsorption isotherm constants (C) for Cd, Cu, Pb and Zn with o-DWCNT (o-DWCNT concentration: 10 mg.L^{-1}, metal concentrations for isotherm modelling: 0.1-4 mM for Cd and Zn, 0.2-4 mM for Pb and 0.1-2.5mM for Cu, pH: 7, contact time: 3 hours, temperature: 18.3 ± 0.9 °C), qe: metal quantity adsorbed onto o-DWCNT (mM.g^{-1}), Ce: equilibrium aqueous concentration (mM), q_{max}: maximal quantity of metal adsorbed onto o-DWCNT at the equilibrium calculated by Langmuir model (mM.g^{-1}), q_{exp}: experimental quantity of metal adsorbed onto o-DWCNT at the equilibrium (mM.g^{-1}), K_L= adsorption equilibrium constant, R_L : separation factor, R^2 : correlation coefficient)

Non-linear and linear Langmuir isotherm models were applied to simulate and understand the adsorption mechanism of metal ions (Cd(II), Cu(II), Pb(II) and Zn(II)) on o-DWCNT (Figure 15, SI Figure S11). Due to metal precipitation, concentration range used to build Langmuir isotherms was selected specifically for each metal. It should be remembered that one of the basic assumptions for the use of this model is not respected, since it characterizes the adsorption of a gas on a solid surface. In our case, however, it is used to characterize adsorption at the solid-liquid interface. Although the latter is not respected, this model has been used since it is commonly used in the literature in this case and offers a good description of the data.

First, it can be noticed that the sorption isotherms fitted better for Cd(II), Pb(II) and Zn(II) than for Cu(II) as correlation coefficients were > 0.90 while it was 0.81 for Cu(II). This is probably due to the fact that equilibrium was not reached only for Cu(II) in our exposure conditions as it is the first metal that precipitates in the medium (SI, Figure S4, S7 and S10). Despite this, the four correlation coefficients and the fit between the Langmuir model and the experimental values are satisfactory because > 0.80. In mono-metallic system, the mean R^2 (R^2 = 0.97) of studies reviewed in Leroy *et al.*[14] was higher than in multi-metallic system, which suggests that one metal interacts with another such that they can (I) co-precipitate and/or (II) modify the adsorption behaviour of other metals. A meta-analysis of adsorption data in mono-metallic systems available in the literature would therefore makes it possible to anticipate what would happen in multi-metallic systems on adsorption sequence affinity but did not provided the real metals quantity adsorbed (because not realized with several metals at the same time). According to the linear Langmuir fit (Figure 15B) which allows to establish the value of q_{max} (Figure 15C), we can see that the equilibrium was reached at values close to those indicated on non-linear Langmuir representation for the four metals, which are 16.92, 4.88, 3.45 and 3.33 $mM.g^{-1}$ for Cu(II), Pb(II), Zn(II) and Cd(II) with linear model and around 14.00, 4.60, 2.10 and 2.10 $mM.g^{-1}$ for Cu(II), Pb(II), Zn(II) and Cd(II) with non-linear model respectively. The q_{max} adsorption coincided well with the experimental adsorption (q_{exp}) with q_{exp} up to 13.48, 5.55, 1.49, 1.24 $mM.g^{-1}$ for Cu(II), Pb(II), Zn(II) and Cu(II), respectively. The separation factor R_L of Langmuir model (Figure 15C), which reveals whether

the adsorption is irreversible ($R_L = 0$), favourable ($0< R_L <1$), linear ($R_L = 1$) or unfavourable ($R_L >1$)[56] indicates that adsorption was favourable for all metals studied. In addition, K_L (Figure 15C) which corresponds to the extent of the interaction between the adsorbate and the surface such that the larger the value of K_L, the stronger the interaction between the adsorbate and the adsorbent, reveals the following adsorbate/adsorbent interaction sequence Pb>Cd>Cu>Zn. It is the combination of K_L and R_L that establishes q_{max}, hence the adsorption affinity sequence (reflected with q_{max}).

To explain this affinity sequence, Sitko *et al.*[19] suggested that this order is in agreement with metal electronegativity and the first stability constant of the associated metal hydroxide ($Me^{2+} + OH^- \leftrightarrow Me(OH)^+$; log K1 = 7.82, 7.0, 4.17, 4.4 for $Pb(OH)^+$, $Cu(OH)^+$, Cd- $(OH)^+$ and $Zn(OH)^+$, respectively)[19,57] and carboxylic acid ($Me^{2+} + CA^- \leftrightarrow Me(CA)^+$; log K1 = 2.52, 2.16, 1.5 and 1.5 for $Pb(CA)^+$, $Cu(CA)^+$, $Cd(CA)^+$ and $Zn(CA)^+$, respectively). Although Sitko et al.[19] hypothesis is a step in the right direction, it does not, on its own, fully explain the results we have observed. Additionally, this sequence also fits with what we highlighted in mono-metallic systems in our review paper (Leroy *et al.*[14]) with the following sequence based on q_{max} values for oxidized CNT: Pb(II) > Ni(II) > Cu(II) ≥ Cd(II) > Hg(II) ≥ Cr(II) ≥ Zn(II)[14]. By confronting the results obtained here and those gathered in our recent review (Leroy *et al.*[14]), it seems that the simultaneous presence of metallic species of different nature in solution does not modify the affinity of metals for the adsorption sites pre-established in mono-metallic systems (at least when the concentrations of the different ions is low or in the same range and in the solubility range).

It has been evaluated that sewage sludge application increases the heavy metal contamination risks in this order Cu > Pb > Zn > Cd[58], which is the same than the adsorption sequence shown here. Comparing the limits of metal concentrations in European soils at the range 6 < pH < 7 (Cd: 1-3 $mg.kg^{-1}$, Cu: 50-140 $mg.kg^{-1}$, Pb: 50-300 $mg.kg^{-1}$ and Zn: 150-300 $mg.kg^{-1}$)[13] and metal concentrations at 1mM in this study at pH = 7 (1 mM of Cd: 112.41 $mg.L^{-1}$, 1 mM of Cu: 63.546 $mg.L^{-1}$, 1 mM of Pb: 207.23 $mg.L^{-1}$ and

1 mM of Zn: 65.38 mg.L^{-1}), it would be expected that the quantities of metals adsorbed on the NMC surface would follow the same order as the affinity sequence defined in our study.

3.3. Kinetics

A

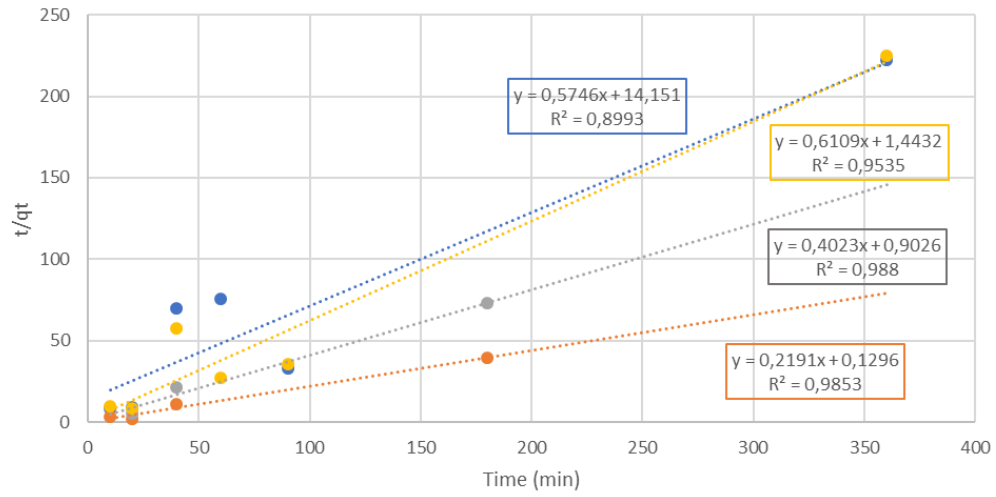

B

	Intercept	Slope	qe	k_2	R^2
Cd	14.15	0.57	1.75	0.02	0.90
Cu	0.13	0.22	4.55	0.37	0.99
Pb	0.90	0.40	2.50	0.18	0.99
Zn	1.44	0.61	1.64	0.26	0.95

Figure 16: Multi-metallic non-linear pseudo-second order (A) and pseudo-second order constants (B) for Cd, Cu, Pb and Zn with o-DWCNT (o-DWCNT concentration: 10 mg.L^{-1}, metal concentrations: 1 mM for Cd, Cu, Pb and Zn, pH: 7, contact time: 10 to 360 min^{-1}, temperature: 18.3 ± 0.9 °C, qe: metal quantity adsorbed onto o-DWCNT calculated by pseudo-second order model (mM.g^{-1}), qt: total quantity of metals adsorbed onto o-DWCNT, k_2= constant rate of the pseudo-second-order (g.mM.min^{-1}), R^2 : correlation coefficient)

Figure 16A displays the kinetic of adsorption with pseudo-second order linear representation with t/qt as a function of time which permits to deduce some kinetics parameters (Figure 16B). First, adsorption kinetics of metal mixture were well translated by pseudo-second order model as correlation coefficients were > 0.9. Second order rate constant (k_2) was different from metal to metal, reaching 0.37, 0.26, 0.18 and 0.02 g.mM^{-1}.min^{-1} for Cu(II), Zn(II), Pb(II) and Cd(II), respectively. However, metal quantity at the equilibrum (qe) followed the previously determined, order as Cu(II) > Pb(II) > Cd(II) ≥ Zn (II) (sections 3.1. and 3.2 with quantity of metals adsorbed up to 4.55, 2.50, 1.75 and 1.64 mM.g^{-1}, respectively). It is important to note that in this experiment, the initial Cu(II) and Pb(II) concentrations

in samples did not reach 1 mM (0.46 and 0.60, respectively) as for the other metals (Cd(II) and Zn(II)) probably due to dysfunctions on pHmeter calibration when increasing the pH value of stock solutions at the beginning of experiment. Yet it is repeatedly observed that an increase in the initial concentration of the metals decreases the adsorption rate constant k_2[16,59,21], does this mean that the k_2 values for Cu and Pb are more overvalued than those for Cd and Zn. As seen through the Langmuir isotherm modelling, Pb(II) had a stronger interaction with the surface of o-DWCNT (K_L) than Zn(II), which could explain why more Pb(II) was adsorbed onto the surface of o-DWCNT at equilibrium even though its k_2 was smaller. Indeed, it is likely that Zn(II) adsorbs faster than Pb(II), but due to the higher interaction strength of Pb(II), this ion takes over the adsorption sites where Zn(II) was first located on the surface of o-DWCNT, as it has been observed by Tan *et al.*[18]. Compared to the literature, our k_2 results (Cd(II) = 1.10^{-6}, Cu(II) = $1.85.10^{-6}$, Pb (II) = 9.10^{-6} and Zn(II) $1.3.10^{-6}$ $g.mol^{-1}.min^{-1}$) were a bit lower than Sitko *et al.*[19] who found $9.79.10^{-5}$, $2.52.10^{-4}$, $4.34.10^{-5}$ and $7.19.10^{-4}$ $g.mol^{-1}.min^{-1}$ for Cd(II), (Cu(II), Pb(II) and Zn(II), respectively but the experimental conditions were different (Sitko *et al.*[19] : pH = 5, MWCNT = 0.1 $g.L^{-1}$, metals = 5 $mg.L^{-1}$).

3.4. CNM type

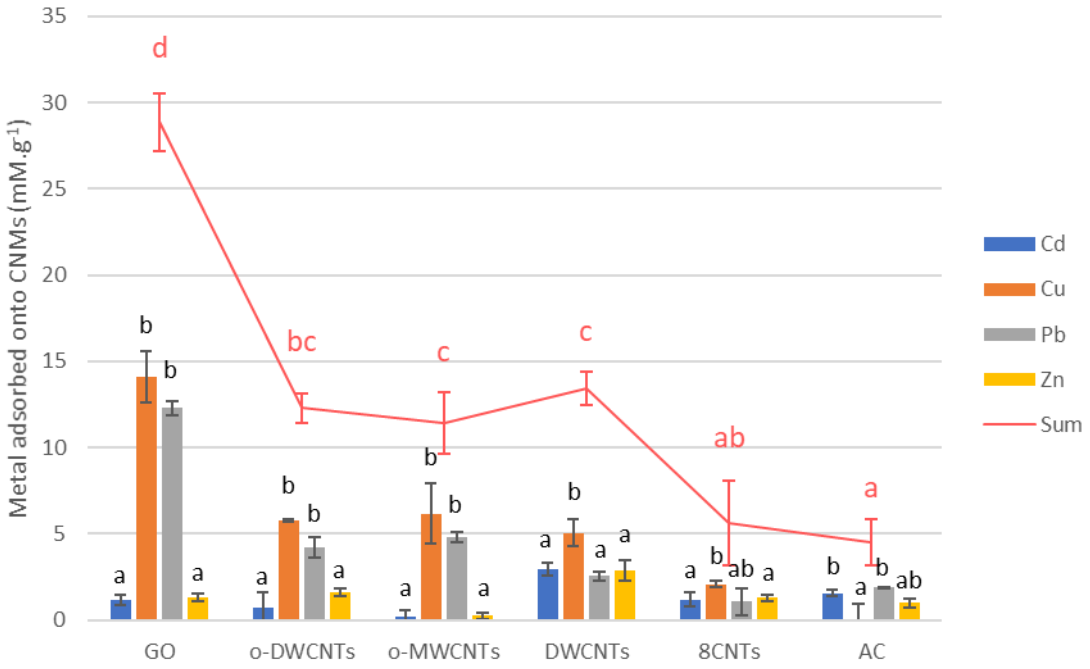

Figure 17: Metals (Cd, Cu, Pb and Zn) adsorbed onto different carbon based nanomaterials: graphene oxide (GO), oxidized double-walled CNT (o-DWCNT), oxidized multi-walled CNT (o-MWCNT), pristine double-walled CNT (DWCNT), commercial pristine MWCNT (8CNT) and activated carbon (AC) using a multi-metallic solution (CNM concentration: 10 mg.L^{-1}, metal concentrations: 1 mM, pH: 7, contact time: 3 hours, temperature: 18.3 ± 0.9 °C). Same lowercase letters indicate treatments that do not differ significantly within a CNM type following 1 way ANOVA. ANOVA was based on the same CNM types (p-value > 0.05; n=5)

First, concerning cumulative metal adsorption onto CNM, 3 groups could be distinguished (Figure 17): one with a significantly higher adsorption level for GO (28.86 mM.g^{-1}), another group with average adsorption for o-DWCNT, o-MWCNT and DWCNT (12.29, 11.43 and 13.41 mM.g^{-1}, respectively) and a last one with a lower adsorption level for 8CNT and AC (5.64 and 4.50 mM.g^{-1}, respectively). These 3 groups seems to be established by the combination of several factors as CNM SSA and oxidation degree.

The level of oxidation plays a key role in adsorption mechanisms as demonstrated by the two adsorption patterns observed. The first pattern applied for oxidized CNM with a high adsorption level with a mean of cumulative adsorption for oxidized CNM up to 17.52 mM.g^{-1} and with a clear affinity sequence for metal adsorption for GO, o-DWCNT and o-MWCNT following Cu(II) = Pb(II) > Cd(II) = Zn(II) (14.08/12.28 > 1.17/1.33 mM.g^{-1} for GO, 5.77/4.22 > 1.58/0.71 mM.g^{-1} for o-DWCNT and 6.17/4.82 > 0.25/0.19 mM.g^{-1} for o-MWCNT).

The second pattern observed for pristine CNM displayed lower mean of cumulative adsorption with on average 7.85 $mM.g^{-1}$ and quasi-similar level of adsorption among metals with on average 3.35, 1.41 and 1.13 $mM.g^{-1}$ for all metals adsorbed on DWCNT, 8CNT and AC, respectively. As mentioned above, this could be related to different mechanisms of adsorption between oxidized materials and pristine materials. Indeed, oxidized materials due to the presence of -COOH and -OH groups could favour adsorption through chemical and electrostatic interactions while it would be more of physical nature for raw materials[8,14,50–53].

The number of layers (directly related with the SSA), is also a factor that could explain the differences of adsorption among CNM. Indeed, it has been observed in the literature that an increase in the number of layers reduces the adsorption of metals to nanomaterial surfaces, for nanomaterials with a similar oxidation levels[60,61]. Here, in the case of graphene (GO), most interaction sites for pollutants are present at the top and bottom faces (sites located at the edge may play a marginal role) that is why all the surface of that monolayer graphene is available for adsorption[62,63]. On the other hand, multilayer graphene and MWCNT have lower SSA as their internal layers are little or not accessible by adsorbates[62].

In the environment, it is very unlikely that the oxidation state of CNM increases but reduction may however be easier which would reduce CNM adsorption capabilities. However, in the industry, oxidized CNM are more used than other CNM due to their properties.

3.5. OM

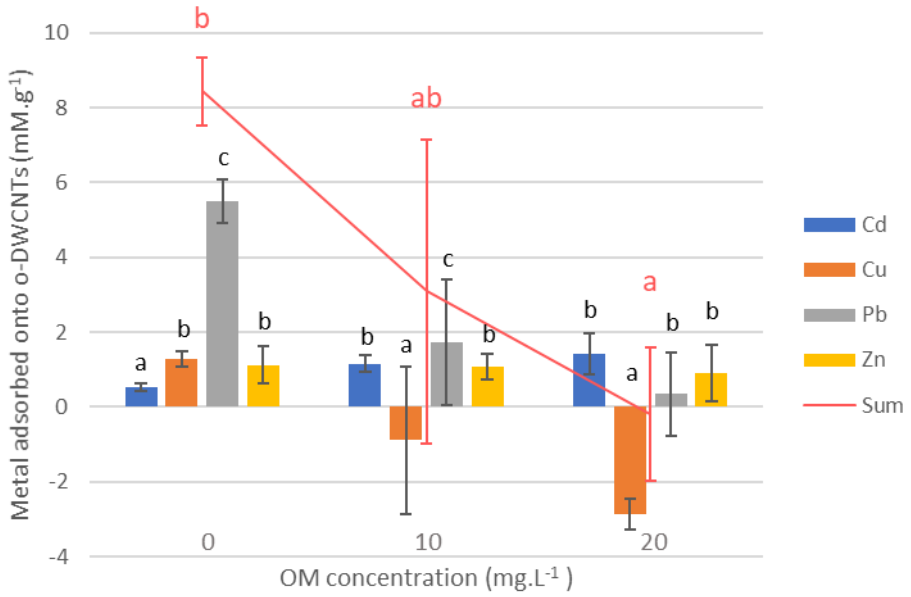

Figure 18: Metals (Cd, Cu, Pb and Zn) adsorbed onto o-DWCNT using a multi-metallic solution according to OM concentration in the medium (o-DWCNT concentration: 10 mg.L^{-1}, metal concentrations 1 mM, pH: 7, contact time: 3 hours, temperature: 18.3 ± 0.9 °C, OM: Organic Matter). Same lowercase letters indicate treatments that do not differ significantly following 1 way ANOVA. ANOVA was performed within a same OM concentration (p-value > 0.05; n=5)

Cumulative metal adsorption onto o-DWCNT decreased with OM concentration (Figure 18). It was significantly lower at 20 mg.L^{-1} compared to control with -0.20 and 8.43 mM.g^{-1}, respectively. Whatever, the OM concentration, adsorptions of Cd(II) and Zn(II) were similar ranging from 0.5 to 1 mM.g^{-1} while it was different for Pb(II) and Cu(II). Indeed, Pb and Cu adsorption decreased following OM increase, leading to adsorption values ranging from 5.5 without OM to 1.7 and 0.35 mM.g^{-1} with the addition of 10 and 20 mg.L^{-1} of OM, respectively and for Cu(II) ranging from 1.3 without OM to -0.9 and -2.9 mM.g^{-1} with the addition of 10 and 20 mg.L^{-1} of OM. These results suggest that there are more Cu(II) and Pb(II) in experimental units with o-DWCNT than in experimental units without o-DWCNT implying that OM decreased the adsorption of Pb(II) and Cu(II) on the surface of o-DWCNT in a dose-dependent manner. One hypothesis is that OM adsorbed on the adsorption sites (-OH and -COOH) of o-DWCNT for which Pb(II) and Cu(II) have a more pronounced affinity than Cd(II) and Zn(II). Some examples in the literature reported contrasting results, with OM addition favouring Pb(II) and Cu(II) adsorption onto MWCNT[22,24]. These discrepancies could be explained by the fact that pH conditions were different (Lin et al.[22] pH = 5 and Sheng et al.[24] pH = 4-10) leading to different

interactions among CNT, OM and metals. In addition, Sheng et al.[24] also demonstrated a decrease of Cu adsorption onto MWCNT when pH > 7.5, supporting pH influence on CNT/OM/metal interactions. Additionally, the nature of OM could also influence interactions and conducted to disparities in metal adsorption results.

Surprisingly, some of adsorption results were negative, one explanation is that metallic ions (Cu(II) and Pb(II)) could interact with the OM in control conditions which would lead to their solubilisation in the medium. The addition of CNT in the medium could modify these interactions leading to adsorption of the OM on CNT surface and thus to a better stabilisation of the ions in the medium. For example, during the adsorption of OM on the surface of CNT, H^+ may be released into the aqueous medium, which could interact with Cu and Pb in particular, increasing their solubility in the medium. In our case, no metals were adsorbed onto OM (see SI Figure S12).

In France, the great plains of intensive cultivation contained 1 to 2% of OM[64] which corresponds to concentration tested in our experiment. It suggest thus that Metal adsorption would be limited in agricultural soil. Although weak, the adsorption of OM on o-DWCNT could gradually decrease its availability for decomposers and consequently decreases the minerals present in the soil available for the food web of agrosystems.

3.6. Soil solution

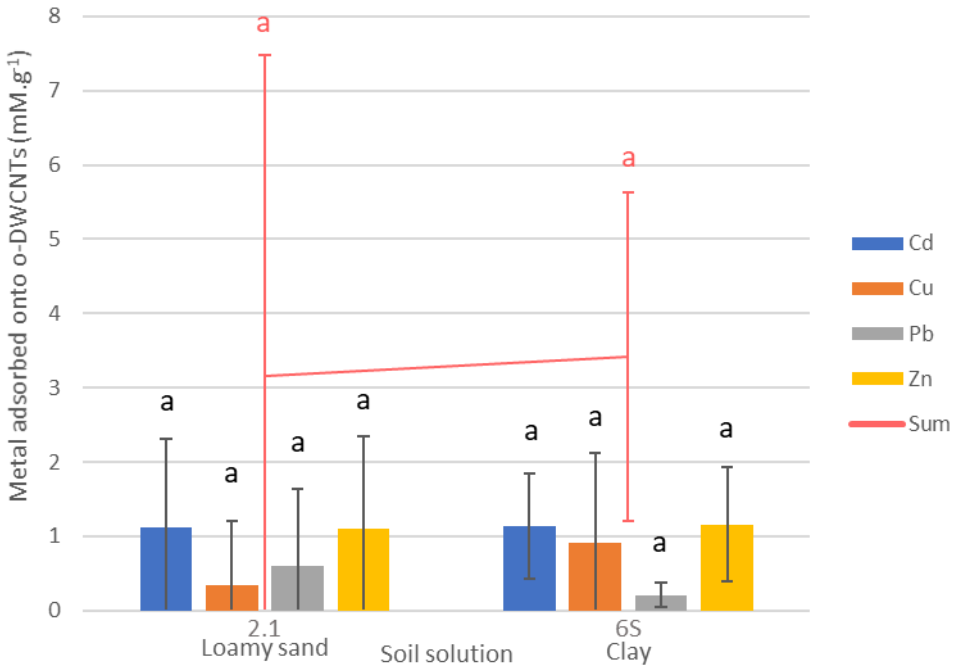

Figure 19: Metals (Cd(II), Cu(II), Pb(II) and Zn(II)) adsorbed onto o-DWCNT using a multi-metallic solution diluted in two different soil solutions (o-DWCNT concentration: 10 mg.L^{-1}, metal concentrations 1 mM, $pH_{2.1}$: 4.3, pH_{6S}: 5.7, contact time: 3 hours, temperature: 18.3 ± 0.9 °C). Same lowercase letters indicate treatments that do not differ significantly (p-value > 0.05; n=5)

The cumulative metal adsorption onto o-DWCNT was not different between soil solution tested (on average 3.15 and 3.41 mM.g^{-1} for 2.1 and 6S soil solution, respectively) and among metals (with on average 1.12, 0.33, 0.60 and 1.10 mM.g^{-1} for Cd(II), Cu(II), Pb(II) and Zn(II), respectively for 2.1 soil solution and 1.14, 0.91, 0.20 and 1.16, respectively for Cd(II), Cu(II), Pb(II) and Zn(II) for 6S soil solution (Figure 19). Compared to adsorption in pH experiment at the same pH value (pH = 5), adsorption were in the same order of magnitude (adsorption in ultrapure water at pH_5 = 1.96 mM.g^{-1}) and with no specific preferential adsorption which reveals that in our conditions, soil components contain in soil solution did not modified the adsorption behaviour of the four metals. However, it is interesting to note that a much higher standard deviation was visible in this set of experiment; this can be explained by metal precipitation induced by soil solution components as demonstrated by the fact that Cu(II) and Pb(II) concentrations reached 0.93 mM for the two metals in 2.1 soil solution but were lower with 0.45 and 0.11 mM for Cu(II) and Pb(II), respectively in 6S soil solution (instead of 1 mM).

The granulometry of upper agricultural soil horizons in France[65] is a mix between loamy and clayey soil (somewhere in between the two soil used in this experiment) suggesting that the adsorption behaviour of metals on the surface of CNT should be similar whatever soil granulometry, with similar adsorption levels of Cd(II), Cu(II), Pb(II) and Zn(II).

4. General conclusion

Regarding the average agricultural soil properties as soil pH (pH = 5.8), OM concentration (1-2%) and granulometry (equilibrium between loamy and clayey soil) and CNM/metal ratio (with metals in excess in comparison with CNM), the results of this present work suggest equivalent adsorption of Cd(II), Cu(II), Pb(II) and Zn(II) on the surface of CNT, with rather low values (1-2 mM). Also, Cu and Pb adsorption could decrease with higher OM concentration. According to these results, pH and OM are the two physico-chemical parameters that most modify the adsorption behaviour of metals on the surface of CNT. In addition, many compounds such as pesticides, herbicides and others are simultaneously present in agrosystems, coumpounds which could also adsorbed onto CNT[66] and modified metal adsorption behaviour. Further studies combining physico-chemistry and ecotoxicology data are needed to better understand CNM/metal interactions and their impacts on transfer and toxicity in ecosystems.

Acknowledgements

The authors would like to acknowledge the Région Occitanie, Toulouse Federal University (under research programme NANOMETAGRO), and EC2CO program CARBOSTRESS (CNRS-INSU) for their funding support. We also thank Frédéric Candaudap and Frédéric Julien, R&D engineers on the FBiI (ICP-AES) and PAPC (physico-chemical analysis) platforms of Laboratoire Ecologie Fonctionnelle et Environnement. Finally, the authors thank Marie-Claire Barthélémy, Roman Teisserenc, Anne-Marie Galibert, Brigitte Soula, Joséphine Leflaive and Mathilde Clavier for their valuable technical help and scientific discussions.

Bibliography (article: Competitive adsorption on carbon based nanomaterials of a mixture of cadmium, copper, lead and zinc and influence of environmental parameters):

(1) Gottschalk, F.; Sun, T.; Nowack, B. Environmental Concentrations of Engineered Nanomaterials: Review of Modeling and Analytical Studies. *Environmental Pollution* **2013**, *181*, 287–300. https://doi.org/10.1016/j.envpol.2013.06.003.

(2) SEC_2006_620.Pdf. https://ec.europa.eu/environment/archives/soil/pdf/SEC_2006_620.pdf (accessed 2020-11-27).

(3) Kong, X. China Must Protect High-Quality Arable Land. *Nature* **2014**, *506* (7486), 7. https://doi.org/10.1038/506007a.

(4) Holden, P. A.; Klaessig, F.; Turco, R. F.; Priester, J. H.; Rico, C. M.; Avila-Arias, H.; Mortimer, M.; Pacpaco, K.; Gardea-Torresdey, J. L. Evaluation of Exposure Concentrations Used in Assessing Manufactured Nanomaterial Environmental Hazards: Are They Relevant? *Environ. Sci. Technol.* **2014**, *48* (18), 10541–10551. https://doi.org/10.1021/es502440s.

(5) Butt, B. Z.; Naseer, I. Nanofertilizers. In *Nanoagronomy*; Javad, S., Ed.; Springer International Publishing: Cham, 2020; pp 125–152. https://doi.org/10.1007/978-3-030-41275-3_8.

(6) Paramo, L. A.; Feregrino-Pérez, A. A.; Guevara, R.; Mendoza, S.; Esquivel, K. Nanoparticles in Agroindustry: Applications, Toxicity, Challenges, and Trends. *Nanomaterials* **2020**, *10* (9), 1654. https://doi.org/10.3390/nano10091654.

(7) Agasti, N.; Gautam, V.; Priyanka; Manju; Pandey, N.; Genwa, M.; Meena, P. L.; Tandon, S.; Samantaray, R. Carbon Nanotube Based Magnetic Composites for Decontamination of Organic Chemical Pollutants in Water: A Review. *Applied Surface Science Advances* **2022**, *10*, 100270. https://doi.org/10.1016/j.apsadv.2022.100270.

(8) Perreault, F.; Faria, A. F. de; Elimelech, M. Environmental Applications of Graphene-Based Nanomaterials. *Chem. Soc. Rev.* **2015**, *44* (16), 5861–5896. https://doi.org/10.1039/C5CS00021A.

(9) Yadav, A.; Bagotia, N.; Sharma, A. K.; Kumar, S. Advances in Decontamination of Wastewater Using Biomass-Basedcomposites: A Critical Review. *Science of The Total Environment* **2021**, *784*, 147108. https://doi.org/10.1016/j.scitotenv.2021.147108.

(10) Xu, J.; Cao, Z.; Zhang, Y.; Yuan, Z.; Lou, Z.; Xu, X.; Wang, X. A Review of Functionalized Carbon Nanotubes and Graphene for Heavy Metal Adsorption from Water: Preparation, Application, and Mechanism. *Chemosphere* **2018**, *195*, 351–364. https://doi.org/10.1016/j.chemosphere.2017.12.061.

(11) Nagajyoti, P. C.; Lee, K. D.; Sreekanth, T. V. M. Heavy Metals, Occurrence and Toxicity for Plants: A Review. *Environ Chem Lett* **2010**, *8* (3), 199–216. https://doi.org/10.1007/s10311-010-0297-8.

(12) Rai, P. K.; Lee, S. S.; Zhang, M.; Tsang, Y. F.; Kim, K.-H. Heavy Metals in Food Crops: Health Risks, Fate, Mechanisms, and Management. *Environment International* **2019**, *125*, 365–385. https://doi.org/10.1016/j.envint.2019.01.067.

(13) *EUR-Lex - 01986L0278-20180704 - FR - EUR-Lex*. https://eur-lex.europa.eu/legal-content/FR/TXT/?uri=CELEX%3A01986L0278-20180704 (accessed 2020-11-27).

(14) Leroy, M.; Flahaut, E.; Larue, C. Carbon Based Nanomaterial Interactions with Metals and Metalloids in Terrestrial Environment: A Review. *Carbon* **2023**, *206*, 325–339. https://doi.org/10.1016/j.carbon.2023.02.047.

(15) Ding, C.; Cheng, W.; Wang, X.; Wu, Z.-Y.; Sun, Y.; Chen, C.; Wang, X.; Yu, S.-H. Competitive Sorption of Pb(II), Cu(II) and Ni(II) on Carbonaceous Nanofibers: A Spectroscopic and Modeling Approach. *Journal of Hazardous Materials* **2016**, *313*, 253–261. https://doi.org/10.1016/j.jhazmat.2016.04.002.

(16) Salam, M. A.; Al-Zhrani, G.; Kosa, S. A. Simultaneous Removal of Copper(II), Lead(II), Zinc(II) and Cadmium(II) from Aqueous Solutions by Multi-Walled Carbon Nanotubes. *Comptes Rendus Chimie* **2012**, *15* (5), 398–408. https://doi.org/10.1016/j.crci.2012.01.013.

(17) Alimohammady, M.; Jahangiri, M.; Kiani, F.; Tahermansouri, H. Highly Efficient Simultaneous Adsorption of Cd(II), Hg(II) and As(III) Ions from Aqueous Solutions by Modification of Graphene

Oxide with 3-Aminopyrazole: Central Composite Design Optimization. *New J. Chem.* **2017**, *41* (17), 8905–8919. https://doi.org/10.1039/C7NJ01450C.

(18) Tan, P.; Hu, Y.; Bi, Q. Competitive Adsorption of Cu2+, Cd2+ and Ni2+ from an Aqueous Solution on Graphene Oxide Membranes. *Colloids and Surfaces A: Physicochemical and Engineering Aspects* **2016**, *509*, 56–64. https://doi.org/10.1016/j.colsurfa.2016.08.081.

(19) Sitko, R.; Turek, E.; Zawisza, B.; Malicka, E.; Talik, E.; Heimann, J.; Gagor, A.; Feist, B.; Wrzalik, R. Adsorption of Divalent Metal Ions from Aqueous Solutions Using Graphene Oxide. *Dalton Trans.* **2013**, *42* (16), 5682–5689. https://doi.org/10.1039/C3DT33097D.

(20) Li, Y.-H.; Ding, J.; Luan, Z.; Di, Z.; Zhu, Y.; Xu, C.; Wu, D.; Wei, B. Competitive Adsorption of Pb2+, Cu2+ and Cd2+ Ions from Aqueous Solutions by Multiwalled Carbon Nanotubes. *Carbon* **2003**, *41* (14), 2787–2792. https://doi.org/10.1016/S0008-6223(03)00392-0.

(21) Lu, C.; Liu, C.; Su, F. Sorption Kinetics, Thermodynamics and Competition of Ni2+ from Aqueous Solutions onto Surface Oxidized Carbon Nanotubes. *Desalination* **2009**, *249* (1), 18–23. https://doi.org/10.1016/j.desal.2009.06.009.

(22) Lin, D.; Tian, X.; Li, T.; Zhang, Z.; He, X.; Xing, B. Surface-Bound Humic Acid Increased Pb2+ Sorption on Carbon Nanotubes. *Environmental Pollution* **2012**, *167*, 138–147. https://doi.org/10.1016/j.envpol.2012.03.044.

(23) Tian, X.; Li, T.; Yang, K.; Xu, Y.; Lu, H.; Lin, D. Effect of Humic Acids on Physicochemical Property and Cd(II) Sorption of Multiwalled Carbon Nanotubes. *Chemosphere* **2012**, *89* (11), 1316–1322. https://doi.org/10.1016/j.chemosphere.2012.05.082.

(24) Sheng, G.; Li, J.; Shao, D.; Hu, J.; Chen, C.; Chen, Y.; Wang, X. Adsorption of Copper(II) on Multiwalled Carbon Nanotubes in the Absence and Presence of Humic or Fulvic Acids. *Journal of Hazardous Materials* **2010**, *178* (1–3), 333–340. https://doi.org/10.1016/j.jhazmat.2010.01.084.

(25) Kasel, D.; Bradford, S. A.; Šimůnek, J.; Pütz, T.; Vereecken, H.; Klumpp, E. Limited Transport of Functionalized Multi-Walled Carbon Nanotubes in Two Natural Soils. *Environmental Pollution* **2013**, *180*, 152–158. https://doi.org/10.1016/j.envpol.2013.05.031.

(26) Lu, Y.; Yang, K.; Lin, D. Transport of Surfactant-Facilitated Multiwalled Carbon Nanotube Suspensions in Columns Packed with Sized Soil Particles. *Environmental Pollution* **2014**, *192*, 36–43. https://doi.org/10.1016/j.envpol.2014.05.008.

(27) Cornelis, G.; Hund-Rinke, K.; Kuhlbusch, T.; Brink, N. van den; Nickel, C. Fate and Bioavailability of Engineered Nanoparticles in Soils: A Review. *Critical Reviews in Environmental Science and Technology* **2014**, *44* (24), 2720–2764. https://doi.org/10.1080/10643389.2013.829767.

(28) Hu, X.; Kang, J.; Lu, K.; Zhou, R.; Mu, L.; Zhou, Q. Graphene Oxide Amplifies the Phytotoxicity of Arsenic in Wheat. *Scientific Reports* **2014**, *4* (1), 6122. https://doi.org/10.1038/srep06122.

(29) Li, J.; Wu, F.; Fang, Q.; Wu, Z.; Duan, Q.; Li, X.; Ye, W. The Mutual Effects of Graphene Oxide Nanosheets and Cadmium on the Growth, Cadmium Uptake and Accumulation in Rice. *Plant Physiology and Biochemistry* **2020**, *147*, 289–294. https://doi.org/10.1016/j.plaphy.2019.12.034.

(30) Gao, M.; Yang, Y.; Song, Z. Effects of Graphene Oxide on Cadmium Uptake and Photosynthesis Performance in Wheat Seedlings. *Ecotoxicology and Environmental Safety* **2019**, *173*, 165–173. https://doi.org/10.1016/j.ecoenv.2019.01.093.

(31) Zhao, L.; Guan, X.; Yu, B.; Ding, N.; Liu, X.; Ma, Q.; Yang, S.; Yilihamu, A.; Yang, S.-T. Carboxylated Graphene Oxide-Chitosan Spheres Immobilize Cu2+ in Soil and Reduce Its Bioaccumulation in Wheat Plants. *Environment International* **2019**, *133*, 105208. https://doi.org/10.1016/j.envint.2019.105208.

(32) He, Y.; Qian, L.; Zhou, K.; Hu, R.; Huang, M.; Wang, M.; Zhao, G.; Liu, Y.; Xu, Z.; Zhu, H. Graphene Oxide Promoted Cadmium Uptake by Rice in Soil. *ACS Sustainable Chem. Eng.* **2019**, *7* (12), 10283–10292. https://doi.org/10.1021/acssuschemeng.8b06823.

(33) Gong, X.; Huang, D.; Liu, Y.; Zeng, G.; Wang, R.; Xu, P.; Zhang, C.; Cheng, M.; Xue, W.; Chen, S. Roles of Multiwall Carbon Nanotubes in Phytoremediation: Cadmium Uptake and Oxidative Burst in Boehmeria Nivea (L.) Gaudich. *Environ. Sci.: Nano* **2019**, *6* (3), 851–862. https://doi.org/10.1039/C8EN00723C.

(34) Leroy, M.; Pey, B.; Jassey, V. E. J.; Liné, C.; Elger, A.; Probst, A.; Flahaut, E.; Silvestre, J.; Larue, C. Interactive Effects of Metals and Carbon Nanotubes in a Microcosm Agrosystem. *Journal of Hazardous Materials* **2022**, *431*, 128613. https://doi.org/10.1016/j.jhazmat.2022.128613.
(35) Manjate, E.; Ramos, S.; Almeida, C. M. R. Potential Interferences of Microplastics in the Phytoremediation of Cd and Cu by the Salt Marsh Plant Phragmites Australis. *Journal of Environmental Chemical Engineering* **2020**, *8* (2), 103658. https://doi.org/10.1016/j.jece.2020.103658.
(36) Li, M.; Liu, Y.; Xu, G.; Wang, Y.; Yu, Y. Impacts of Polyethylene Microplastics on Bioavailability and Toxicity of Metals in Soil. *Science of The Total Environment* **2021**, *760*, 144037. https://doi.org/10.1016/j.scitotenv.2020.144037.
(37) Gao, M.; Xu, Y.; Chang, X.; Dong, Y.; Song, Z. Effects of Foliar Application of Graphene Oxide on Cadmium Uptake by Lettuce. *Journal of Hazardous Materials* **2020**, *398*, 122859. https://doi.org/10.1016/j.jhazmat.2020.122859.
(38) Dong, Y.; Gao, M.; Song, Z.; Qiu, W. Microplastic Particles Increase Arsenic Toxicity to Rice Seedlings. *Environmental Pollution* **2020**, *259*, 113892. https://doi.org/10.1016/j.envpol.2019.113892.
(39) Flahaut, E.; Bacsa, R.; Peigney, A.; Laurent, C. Gram-Scale CCVD Synthesis of Double-Walled Carbon Nanotubes. *Chem. Commun.* **2003**, No. 12, 1442–1443. https://doi.org/10.1039/B301514A.
(40) AFNOR. NF EN 12457-4. AFNOR editions 2002. https://www.boutique.afnor.org/fr-fr/norme/nf-en-124574/caracterisation-des-dechets-lixiviation-essai-de-conformite-pour-lixiviatio/fa104284/20762 (accessed 2023-01-24).
(41) Liné, C. Evaluation of Parameters Influencing Plant Response to Carbon Nanotube Contamination. These de doctorat, Toulouse, INPT, 2019. http://www.theses.fr/2019INPT0082 (accessed 2021-07-06).
(42) GisSol. *Gis Sol » Le pHeau des horizons de surface (0-30 cm) des sols de France*. https://www.gissol.fr/donnees/cartes/le-pheau-des-horizons-de-surface-0-30-cm-des-sols-de-france-2421 (accessed 2023-07-25).
(43) Xu, J.; Cao, Z.; Zhang, Y.; Yuan, Z.; Lou, Z.; Xu, X.; Wang, X. A Review of Functionalized Carbon Nanotubes and Graphene for Heavy Metal Adsorption from Water: Preparation, Application, and Mechanism. *Chemosphere* **2018**, *195*, 351–364. https://doi.org/10.1016/j.chemosphere.2017.12.061.
(44) Ren, X.; Chen, C.; Nagatsu, M.; Wang, X. Carbon Nanotubes as Adsorbents in Environmental Pollution Management: A Review. *Chemical Engineering Journal* **2011**, *170* (2), 395–410. https://doi.org/10.1016/j.cej.2010.08.045.
(45) Rao, G. P.; Lu, C.; Su, F. Sorption of Divalent Metal Ions from Aqueous Solution by Carbon Nanotubes: A Review. *Separation and Purification Technology* **2007**, *58* (1), 224–231. https://doi.org/10.1016/j.seppur.2006.12.006.
(46) Marques, P. A. S. S.; Rosa, M. F.; Pinheiro, H. M. PH Effects on the Removal of Cu2+, Cd2+ and Pb2+ from Aqueous Solution by Waste Brewery Biomass. *Bioprocess Engineering* **2000**, *23* (2), 135–141. https://doi.org/10.1007/PL00009118.
(47) Fu, F.; Wang, Q. Removal of Heavy Metal Ions from Wastewaters: A Review. *Journal of Environmental Management* **2011**, *92* (3), 407–418. https://doi.org/10.1016/j.jenvman.2010.11.011.
(48) Di, Z.-C.; Li, Y.-H.; Luan, Z.-K.; Liang, J. Adsorption of Chromium(VI) Ions from Water by Carbon Nanotubes. *Adsorption Science & Technology* **2004**, *22* (6), 467–474. https://doi.org/10.1260/0263617042879537.
(49) Di, Z.-C.; Ding, J.; Peng, X.-J.; Li, Y.-H.; Luan, Z.-K.; Liang, J. Chromium Adsorption by Aligned Carbon Nanotubes Supported Ceria Nanoparticles. *Chemosphere* **2006**, *62* (5), 861–865. https://doi.org/10.1016/j.chemosphere.2004.06.044.
(50) Moradi, O. The Removal of Ions by Functionalized Carbon Nanotube: Equilibrium, Isotherms and Thermodynamic Studies. *Chemical and Biochemical Engineering Quarterly* **2011**, *25* (2), 229–240.

(51) Vuković, G. D.; Marinković, A. D.; Čolić, M.; Ristić, M. Đ.; Aleksić, R.; Perić-Grujić, A. A.; Uskoković, P. S. Removal of Cadmium from Aqueous Solutions by Oxidized and Ethylenediamine-Functionalized Multi-Walled Carbon Nanotubes. *Chemical Engineering Journal* **2010**, *157* (1), 238–248. https://doi.org/10.1016/j.cej.2009.11.026.
(52) Chen, P. H.; Hsu, C.-F.; Tsai, D. D.-W.; Lu, Y.-M.; Huang, W.-J. Adsorption of Mercury from Water by Modified Multi-Walled Carbon Nanotubes: Adsorption Behaviour and Interference Resistance by Coexisting Anions. *Environmental Technology* **2014**, *35* (15), 1935–1944. https://doi.org/10.1080/09593330.2014.886627.
(53) Gupta, A.; Vidyarthi, S. R.; Sankararamakrishnan, N. Enhanced Sorption of Mercury from Compact Fluorescent Bulbs and Contaminated Water Streams Using Functionalized Multiwalled Carbon Nanotubes. *Journal of Hazardous Materials* **2014**, *274*, 132–144. https://doi.org/10.1016/j.jhazmat.2014.03.020.
(54) Fabian, C.; Reimann, C.; Fabian, K.; Birke, M.; Baritz, R.; Haslinger, E. GEMAS: Spatial Distribution of the PH of European Agricultural and Grazing Land Soil. *Applied Geochemistry* **2014**, *48*, 207–216. https://doi.org/10.1016/j.apgeochem.2014.07.017.
(55) de Soto, I. S.; Zamanian, K.; Urmeneta, H.; Enrique, A.; Virto, I. 25 Years of Continuous Sewage Sludge Application vs. Mineral Fertilizers on a Calcareous Soil Affected PH but Not Soil Carbonates. *Frontiers in Soil Science* **2022**, *2*.
(56) Davodi, B.; Jahangiri, M. Determination of Optimum Conditions for Removal of As (III) and As (V) by Polyaniline/Polystyrene Nanocomposite. *Synthetic Metals* **2014**, *194*, 97–101. https://doi.org/10.1016/j.synthmet.2014.04.020.
(57) Dastgheib, S. A.; Rockstraw, D. A. A Model for the Adsorption of Single Metal Ion Solutes in Aqueous Solution onto Activated Carbon Produced from Pecan Shells. *Carbon* **2002**, *40* (11), 1843–1851. https://doi.org/10.1016/S0008-6223(02)00037-4.
(58) Achkir, A.; Aouragh, A.; El Mahi, M.; Lotfi, E. M.; Labjar, N.; EL Bouch, M.; Ouahidi, M. L.; Badza, T.; Farhane, H.; EL Moussaoui, T. Implication of Sewage Sludge Increased Application Rates on Soil Fertility and Heavy Metals Contamination Risk. *Emerging Contaminants* **2023**, *9* (1), 100200. https://doi.org/10.1016/j.emcon.2022.100200.
(59) Bullen, J. C.; Saleesongsom, S.; Gallagher, K.; Weiss, D. J. A Revised Pseudo-Second-Order Kinetic Model for Adsorption, Sensitive to Changes in Adsorbate and Adsorbent Concentrations. *Langmuir* **2021**, *37* (10), 3189–3201. https://doi.org/10.1021/acs.langmuir.1c00142.
(60) Lu, C.; Chiu, H.; Liu, C. Removal of Zinc(II) from Aqueous Solution by Purified Carbon Nanotubes: Kinetics and Equilibrium Studies. *Ind. Eng. Chem. Res.* **2006**, *45* (8), 2850–2855. https://doi.org/10.1021/ie051206h.
(61) Lu, C.; Chiu, H. Adsorption of Zinc(II) from Water with Purified Carbon Nanotubes. *Chemical Engineering Science* **2006**, *61* (4), 1138–1145. https://doi.org/10.1016/j.ces.2005.08.007.
(62) Sitko, R.; Zawisza, B.; Malicka, E. Graphene as a New Sorbent in Analytical Chemistry. *TrAC Trends in Analytical Chemistry* **2013**, *51*, 33–43. https://doi.org/10.1016/j.trac.2013.05.011.
(63) Zhao, J.; Wang, Z.; White, J. C.; Xing, B. Graphene in the Aquatic Environment: Adsorption, Dispersion, Toxicity and Transformation. *Environ. Sci. Technol.* **2014**, *48* (17), 9995–10009. https://doi.org/10.1021/es5022679.
(64) *Gis Sol » Le stock de carbone organique dans les 30 premiers centimètres des sols de France métropolitaine*. https://www.gissol.fr/donnees/cartes/le-stock-de-carbone-organique-dans-les-30-premiers-centimetres-des-sols-de-france-metropolitaine-1487 (accessed 2023-08-28).
(65) *Gis Sol » La texture des horizons supérieurs du sol en France métropolitaine*. https://www.gissol.fr/donnees/cartes/la-texture-des-horizons-superieurs-du-sol-en-france-metropolitaine-1883 (accessed 2023-08-28).
(66) Pyrzynska, K. Carbon Nanotubes as Sorbents in the Analysis of Pesticides. *Chemosphere* **2011**, *83* (11), 1407–1413. https://doi.org/10.1016/j.chemosphere.2011.01.057.

5. Supporting information

Competitive adsorption on carbon based nanomaterials of a mixture of cadmium, copper, lead and zinc and influence of environmental parameters

Mathieu Leroy[1,2], Morgan Legnani[2], Emmanuel Flahaut[2*], Camille Larue[1*]

[1]Laboratoire écologie fonctionnelle et environnement, Université de Toulouse, CNRS, Toulouse, France, [2] CIRIMAT, Université de Toulouse, CNRS, Université Toulouse 3 - Paul Sabatier, 118 Route de Narbonne, 31062 Toulouse cedex 9 - France

*Corresponding authors: emmanuel.flahaut@univ-tlse3.fr; +00-33-(0)5-61-55-69-70; camille.larue@ensat.fr; +00-33-(0)5 34-32-37-55

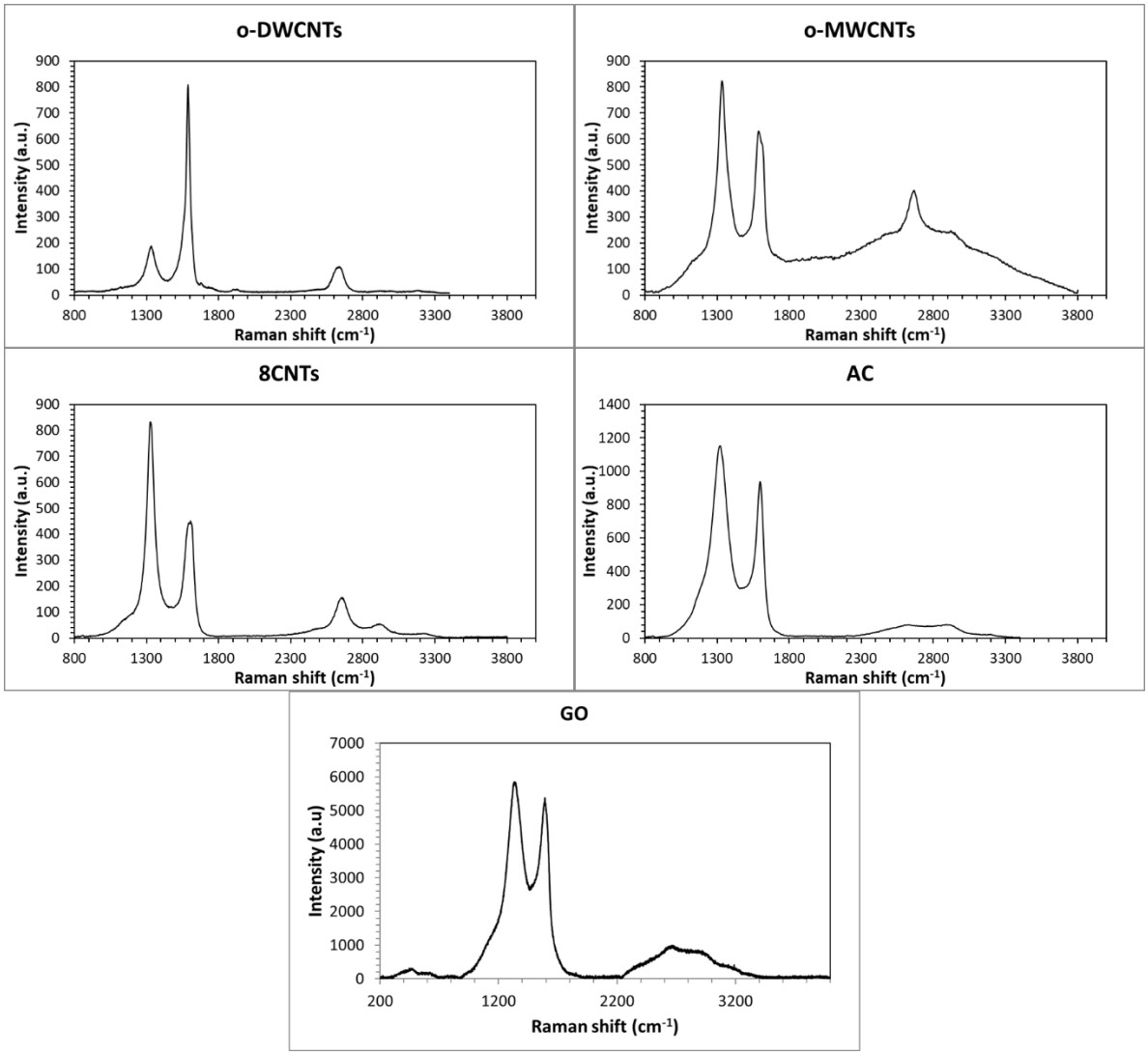

Figure S15 : Representative Raman spectra for o-DWCNT, o-MWCNT, 8CNT, AC and GO (λ = 633 nm)

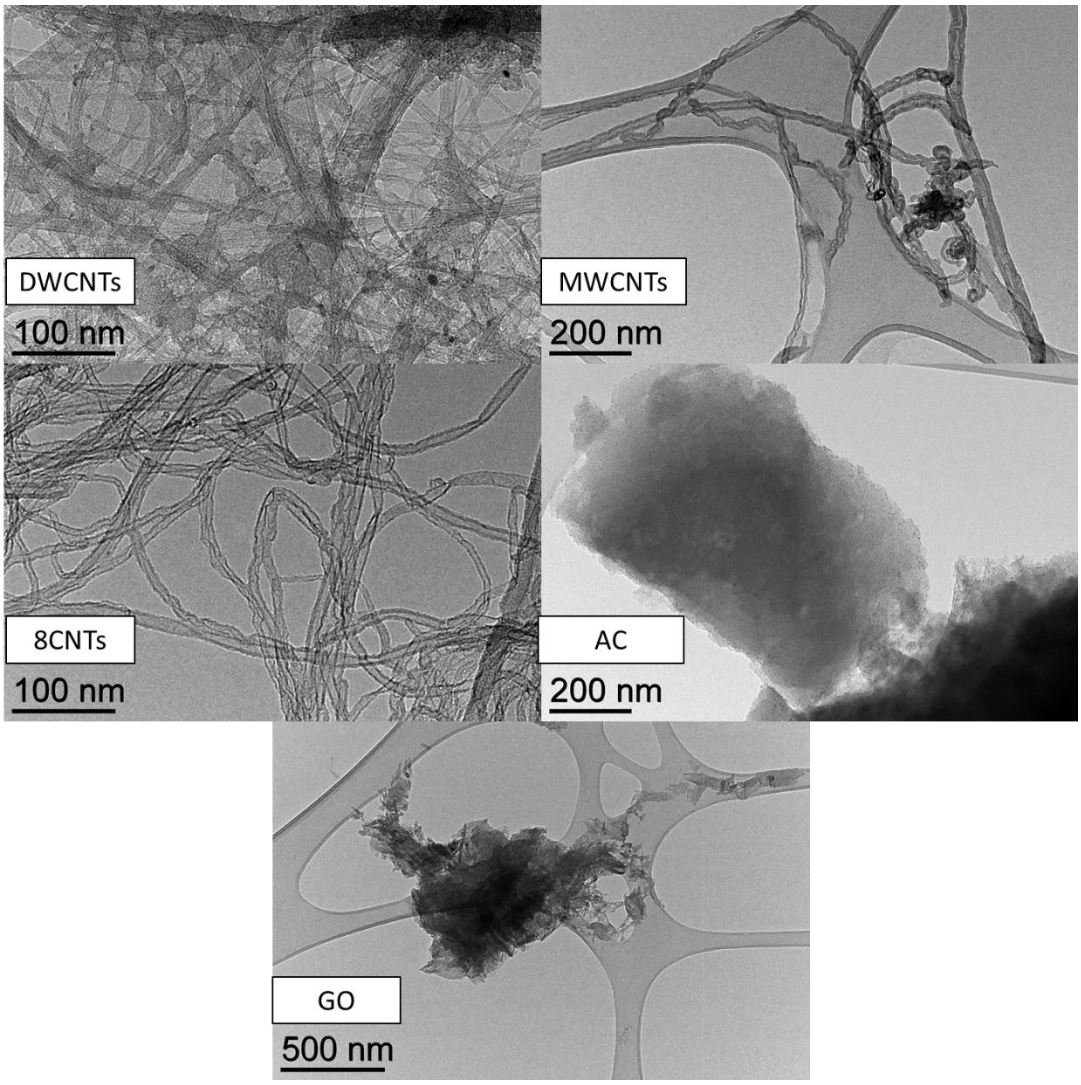

Figure S2 : Transmission Electronic Microscopy observations for DWCNT, MWCNT, 8CNT, AC and GO

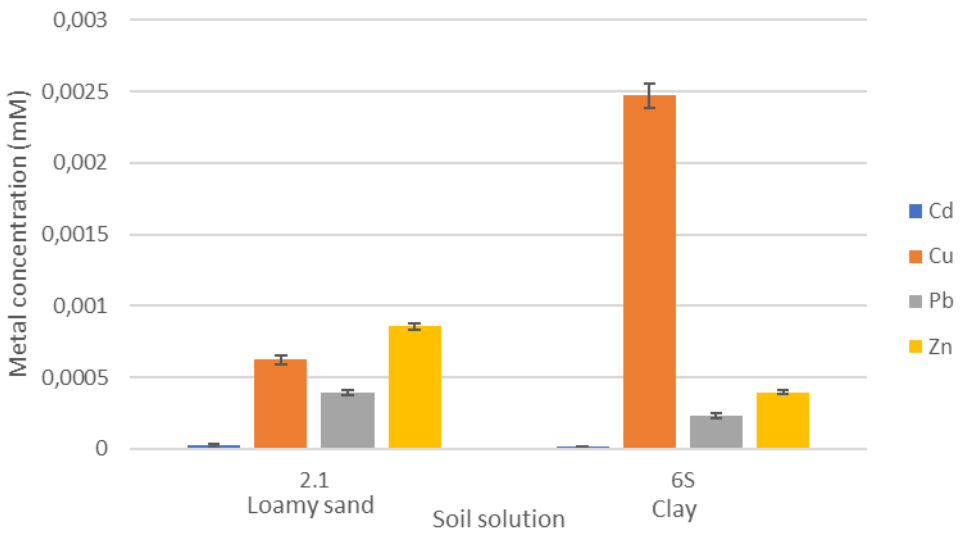

Figure S3: Cd, Cu, Pb and Zn concentrations contained in solution of loamy sand (Lufa 2.1) and clayey (Lufa 6S) soil ($pH_{2.1}$ = 7.50, pH_{6s} = 7.28) before to add 1mM of Cd, Cu, Pb and Zn

A

Mineral	log IAP	Sat. Index (=log IAP - log Ks)	Stoichiometry and mineral components												
Cd(OH)2(s)	6.839	-7.204	1	Cd+2	2	H2O	-2	H+1							
Cu(OH)2(s)	6.838	-2.676	1	Cu+2	2	H2O	-2	H+1							
Litharge	6.838	-6.128	1	Pb+2	1	H2O	-2	H+1							
Massicot	6.838	-6.333	1	Pb+2	1	H2O	-2	H+1							
Pb(OH)2(s)	6.838	-1.558	-2	H+1	1	Pb+2	2	H2O							
Pb2O(OH)2(s)	13.676	-12.514	2	Pb+2	3	H2O	-4	H+1							
PbO:0.3H2O(s)	6.838	-6.142	-2	H+1	1	Pb+2	1.33	H2O							
Tenorite(am)	6.838	-1.925	1	Cu+2	1	H2O	-2	H+1							
Tenorite(c)	6.838	-1.075	1	Cu+2	-2	H+1	1	H2O							
Zincite	6.839	-4.769	1	Zn+2	1	H2O	-2	H+1							
Zn(OH)2 (am)	6.839	-5.996	1	Zn+2	2	H2O	-2	H+1							
Zn(OH)2 (beta)	6.839	-5.265	1	Zn+2	2	H2O	-2	H+1							
Zn(OH)2 (delta)	6.839	-5.005	1	Zn+2	-2	H+1	2	H2O							
Zn(OH)2 (epsilon)	6.839	-5.026	1	Zn+2	2	H2O	-2	H+1							
Zn(OH)2 (gamma)	6.839	-5.240	1	Zn+2	2	H2O	-2	H+1							

B

Mineral	log IAP	Sat. Index (=log IAP - log Ks)	Stoichiometry and mineral components												
Cd(OH)2(s)	8.839	-5.203	1	Cd+2	2	H2O	-2	H+1							
Cu(OH)2(s)	8.823	-0.691	1	Cu+2	2	H2O	-2	H+1							
Litharge	8.833	-4.133	1	Pb+2	1	H2O	-2	H+1							
Massicot	8.833	-4.339	1	Pb+2	1	H2O	-2	H+1							
Pb(OH)2(s)	8.832	0.436	-2	H+1	1	Pb+2	2	H2O							
Pb2O(OH)2(s)	17.665	-8.525	2	Pb+2	3	H2O	-4	H+1							
PbO:0.3H2O(s)	8.833	-4.147	-2	H+1	1	Pb+2	1.33	H2O							
Tenorite(am)	8.823	0.060	1	Cu+2	1	H2O	-2	H+1							
Tenorite(c)	8.823	0.909	1	Cu+2	-2	H+1	1	H2O							
Zincite	8.839	-2.768	1	Zn+2	1	H2O	-2	H+1							
Zn(OH)2 (am)	8.839	-3.995	1	Zn+2	2	H2O	-2	H+1							
Zn(OH)2 (beta)	8.839	-3.265	1	Zn+2	2	H2O	-2	H+1							
Zn(OH)2 (delta)	8.839	-3.005	1	Zn+2	-2	H+1	2	H2O							
Zn(OH)2 (epsilon)	8.839	-3.026	1	Zn+2	2	H2O	-2	H+1							
Zn(OH)2 (gamma)	8.839	-3.239	1	Zn+2	2	H2O	-2	H+1							

C

Mineral	log IAP	Sat. Index (=log IAP - log Ks)	Stoichiometry and mineral components												
Cd(OH)2(s)	10.848	-3.195	1	Cd+2	2	H2O	-2	H+1							
Cu(OH)2(s)	10.380	0.867	1	Cu+2	2	H2O	-2	H+1							
Litharge	10.776	-2.190	1	Pb+2	1	H2O	-2	H+1							
Massicot	10.776	-2.395	1	Pb+2	1	H2O	-2	H+1							
Pb(OH)2(s)	10.776	2.379	-2	H+1	1	Pb+2	2	H2O							
Pb2O(OH)2(s)	21.552	-4.638	2	Pb+2	3	H2O	-4	H+1							
PbO:0.3H2O(s)	10.776	-2.204	-2	H+1	1	Pb+2	1.33	H2O							
Tenorite(am)	10.380	1.617	1	Cu+2	1	H2O	-2	H+1							
Tenorite(c)	10.380	2.467	1	Cu+2	-2	H+1	1	H2O							
Zincite	10.846	-0.762	1	Zn+2	1	H2O	-2	H+1							
Zn(OH)2 (am)	10.846	-1.989	1	Zn+2	2	H2O	-2	H+1							
Zn(OH)2 (beta)	10.846	-1.258	1	Zn+2	2	H2O	-2	H+1							
Zn(OH)2 (delta)	10.846	-0.998	1	Zn+2	-2	H+1	2	H2O							
Zn(OH)2 (epsilon)	10.846	-1.019	1	Zn+2	2	H2O	-2	H+1							
Zn(OH)2 (gamma)	10.846	-1.233	1	Zn+2	2	H2O	-2	H+1							

D

Mineral	log IAP	Sat. Index (=log IAP - log Ks)	Stoichiometry and mineral components												
Cd(OH)2(s)	12.861	-1.182	1	Cd+2	2	H2O	-2	H+1							
Cu(OH)2(s)	11.181	1.668	1	Cu+2	2	H2O	-2	H+1							
Litharge	12.099	-0.867	1	Pb+2	1	H2O	-2	H+1							
Massicot	12.099	-1.073	1	Pb+2	1	H2O	-2	H+1							
Pb(OH)2(s)	12.099	3.702	-2	H+1	1	Pb+2	2	H2O							
Pb2O(OH)2(s)	24.198	-1.992	2	Pb+2	3	H2O	-4	H+1							
PbO:0.3H2O(s)	12.099	-0.881	-2	H+1	1	Pb+2	1.33	H2O							
Tenorite(am)	11.182	2.418	1	Cu+2	1	H2O	-2	H+1							
Tenorite(c)	11.182	3.268	1	Cu+2	-2	H+1	1	H2O							
Zincite	12.806	1.199	1	Zn+2	1	H2O	-2	H+1							
Zn(OH)2 (am)	12.806	-0.029	1	Zn+2	2	H2O	-2	H+1							
Zn(OH)2 (beta)	12.806	0.702	1	Zn+2	2	H2O	-2	H+1							
Zn(OH)2 (delta)	12.806	0.962	1	Zn+2	-2	H+1	2	H2O							
Zn(OH)2 (epsilon)	12.806	0.941	1	Zn+2	2	H2O	-2	H+1							
Zn(OH)2 (gamma)	12.806	0.727	1	Zn+2	2	H2O	-2	H+1							

Figure S4: Minteq precipitation modelling in the case of multi-metallic solution composed of Cd, Cu, Pb and Zn at 1 mM and pH = 5 (A), pH = 6 (B), pH = 7 (C) and pH = 8 (D). Negative Saturation index (Sat. index) presented in blue color indicates compounds that do not precipitate at the corresponding pH value. Red color indicates compounds precipitated at the corresponding pH value.

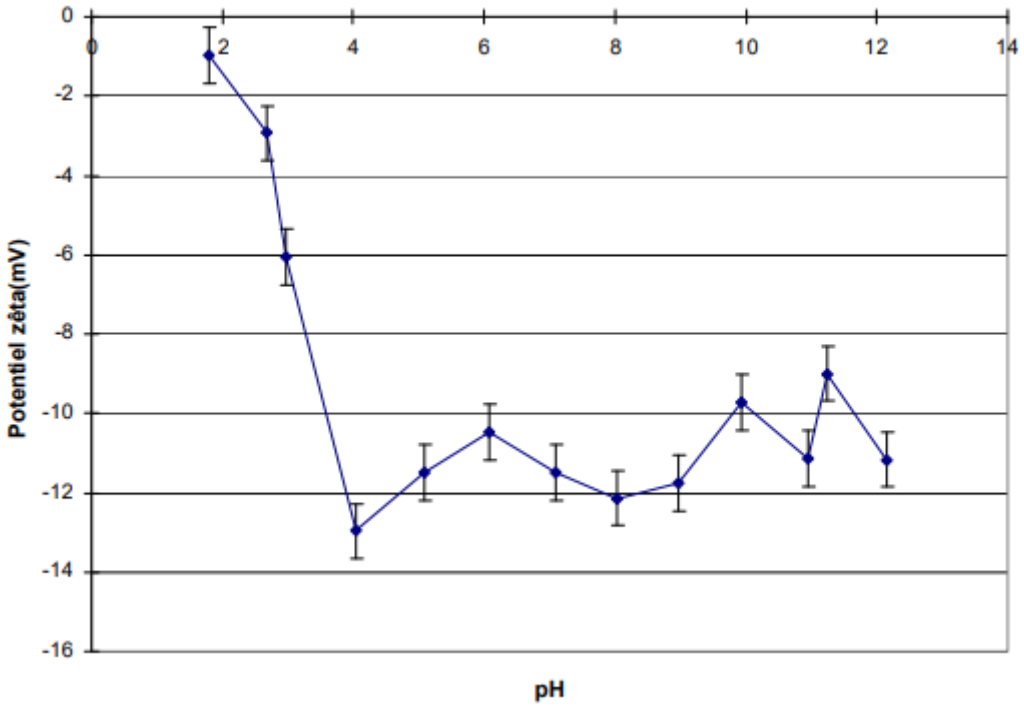

Figure S5: Variation with pH of the zeta potential of an aqueous suspension of o-DWCNT (data from Zhang Bin, Master 2 report supervised by Emmanuel Flahaut)

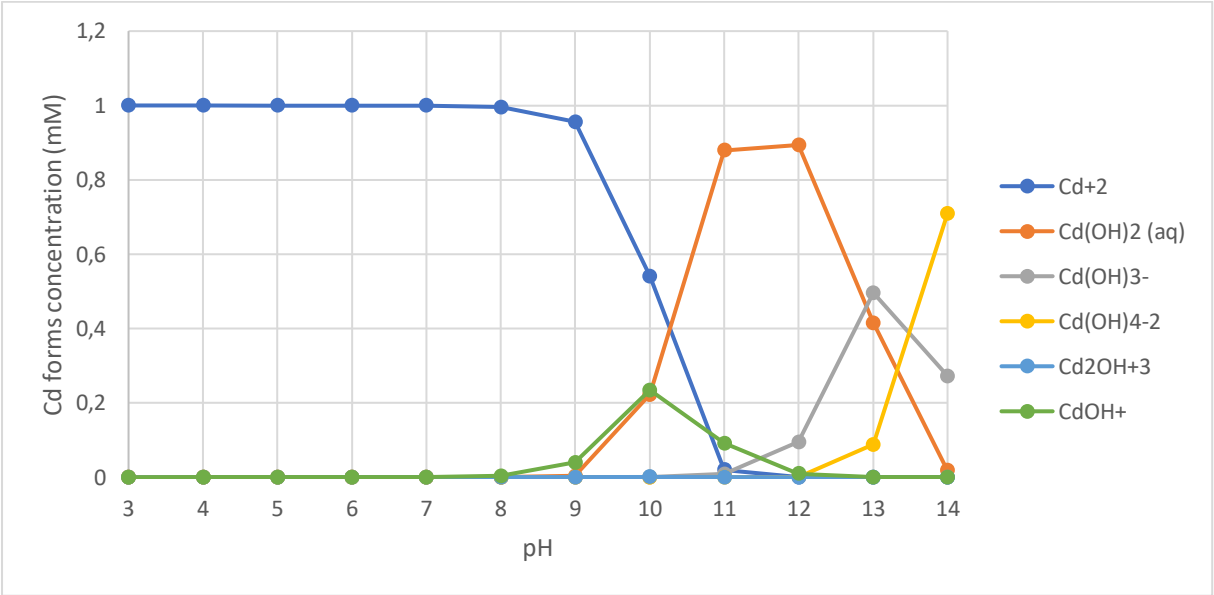

Figure S6: Pourbaix diagram showing the different forms of Cd depending on the pH

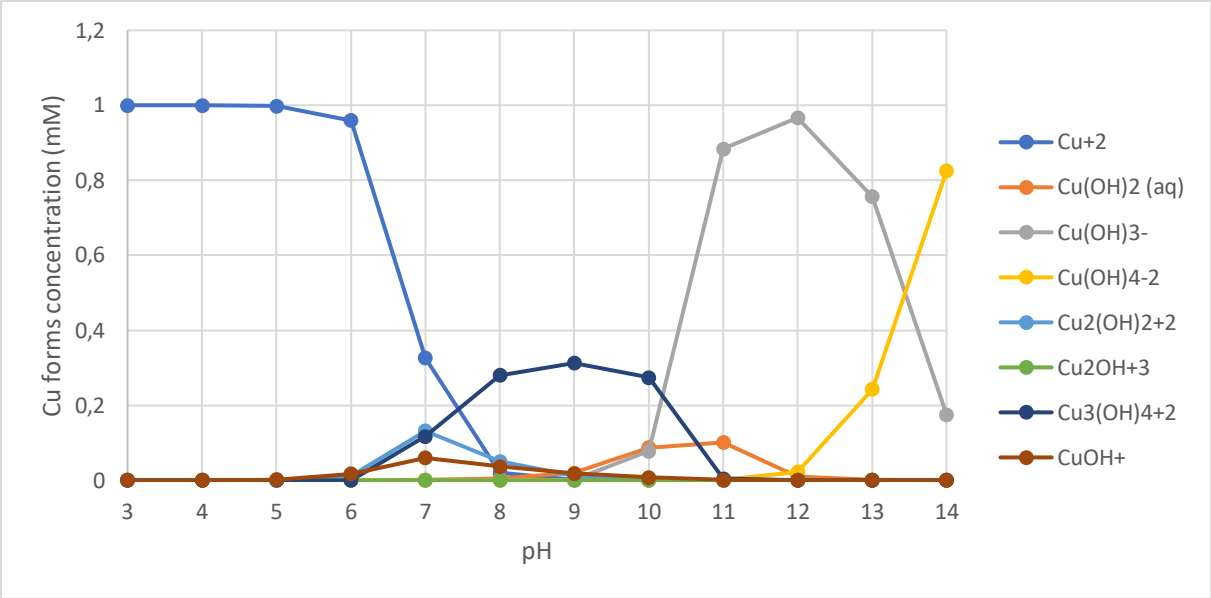

Figure S7: Pourbaix diagram showing the different forms of Cu depending on the pH

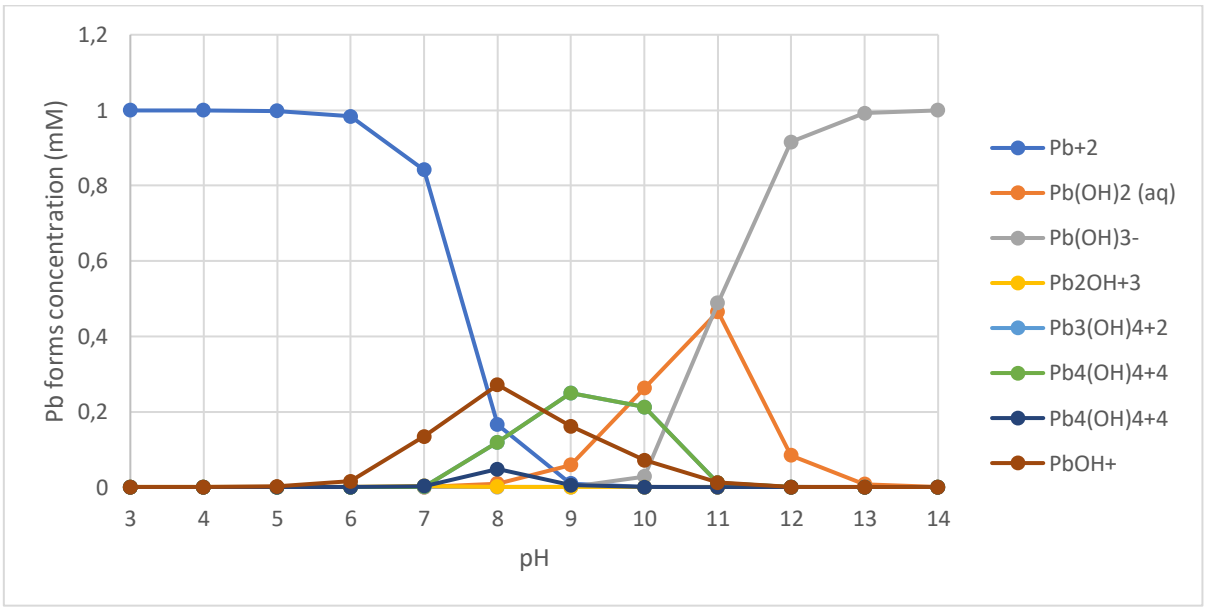

Figure S8: Pourbaix diagram showing the different forms of Pb depending on the pH

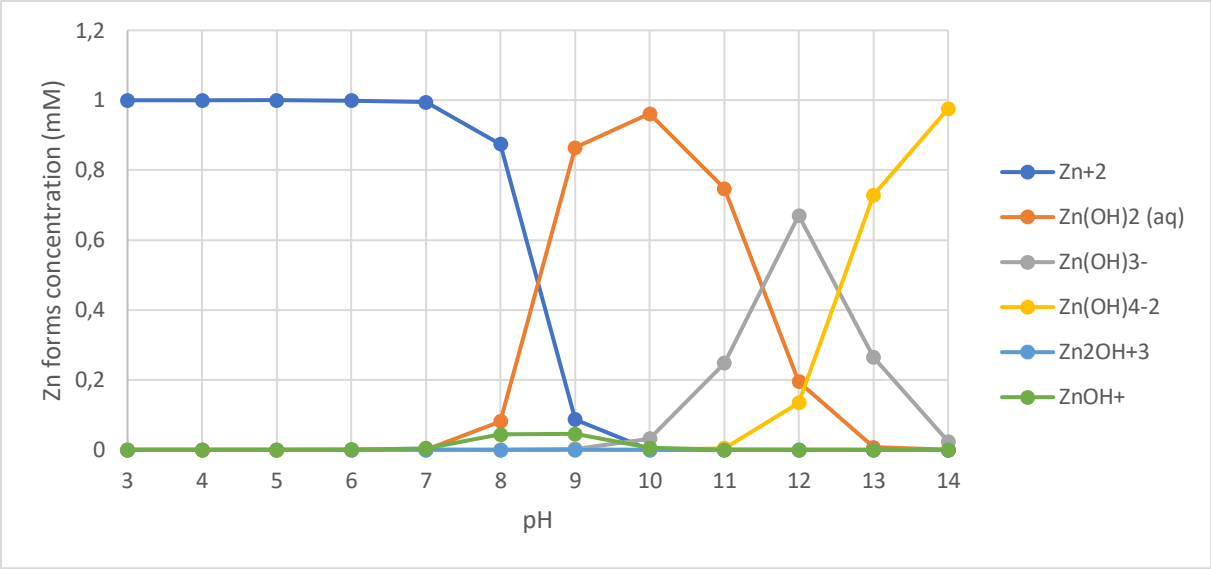

Figure S9: Pourbaix diagram showing the different forms of Zn depending on the pH

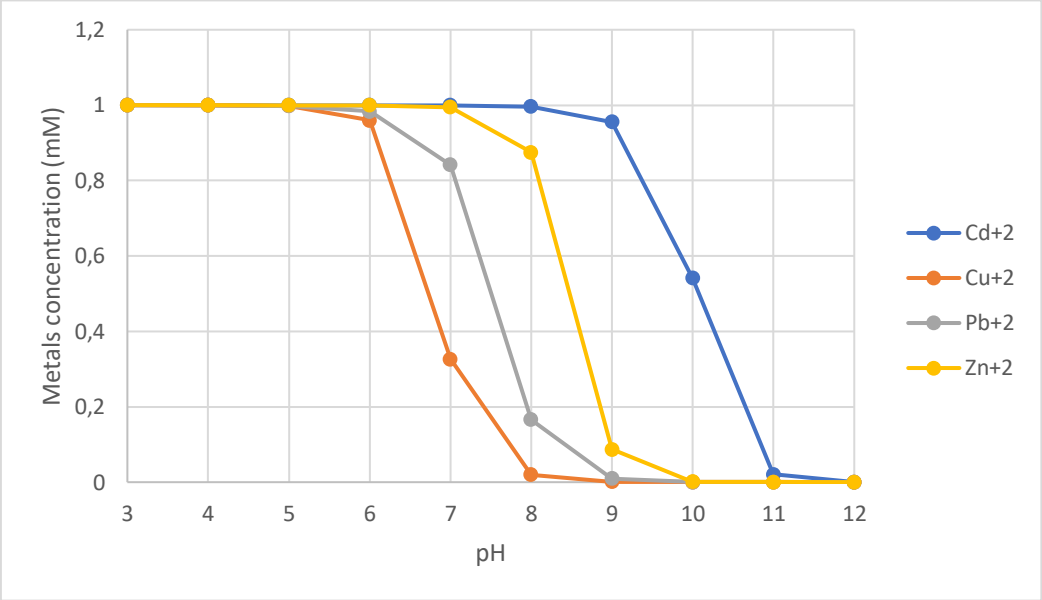

Figure S10: Cd^{2+}, Cu^{2+}, Pb^{2+} and Zn^{2+} concentration in a pH range from 3 to 12

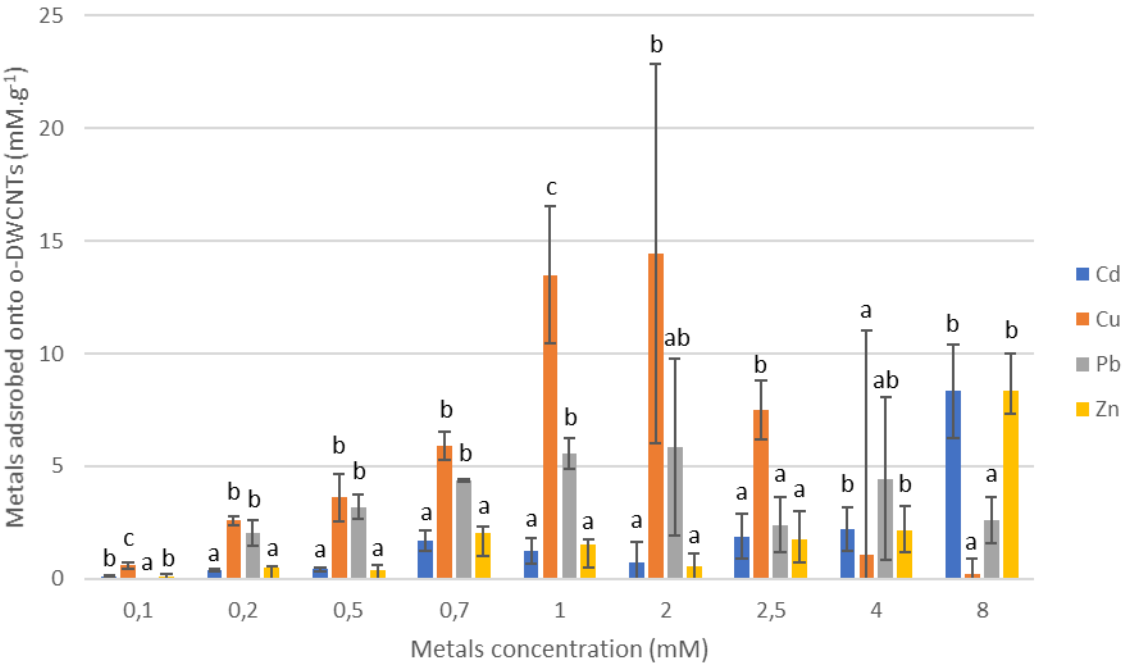

Figure S11: Data used to build Langmuir isotherm in the case of multi-metallic solution composed of Cd, Cu, Pb and Zn with o-DWCNT (o-DWCNT concentration: 10 mg.L^{-1}, metal concentrations: from 0.1 to 8 mM. pH: 7, contact time: 3 hours, temperature: 18.3 ± 0.9 °C). Same lowercase letters indicate treatments that do not differ significantly (p-value > 0.05; n=5). For isotherm modelling, 0.1-4 mM range concentration of Cd and Zn were used, 0.2-4 mM forPb and 0.1-2.5mM for Cu.

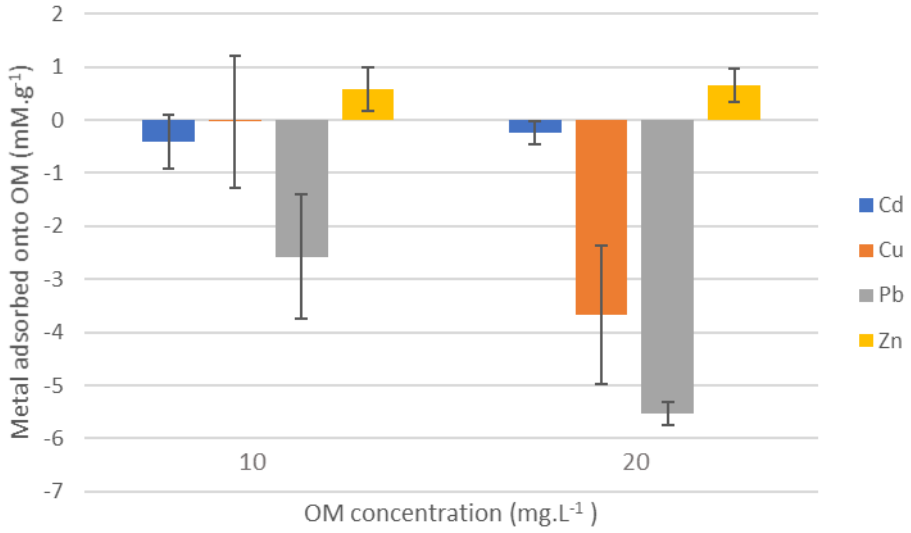

Figure S162: Adsorption of Cd, Cu, Pb and Zn onto organic matter (OM) for tested concentrations. To calculate metals adsorption, same procedure was followed as to calculate metals adsorption onto CNM

Chapitre 4 : Mise en évidence des impacts d'une contamination monospécifique en NTC sur un agrosystème

Des recherches sur la toxicité des NMC sur les organismes ont été menées ces dernières années, offrant un corpus de connaissances scientifiques non négligeable. Toutefois, la majorité des études se font par une approche à l'échelle de l'individu ce qui ne permet pas de présumer des réponses d'un écosystème à un contaminant. Ainsi, des approches plus larges avec l'utilisation d'écomarqueurs qui rendent compte du fonctionnement de l'écosystème doivent être mises en place. En parallèle, à l'issue des avancées théoriques en écologie, des indicateurs intégratifs des fonctions écosystémiques ont vu le jour qui tendent à être de plus en plus utilisés en écotoxicologie. Ainsi, afin de combler le manque de connaissance sur les impacts d'une contamination en NMC sur les services et fonctions d'un agrosystème, une étude a été réalisée dans ce sens combinant des biomarqueurs à l'échelle individuelle, et des écomarqueurs à l'échelle de l'écosystème qui ont ensuite été intégrés à l'aide d'un indicateur émergent en écologie : l'indice de mulitfonctionnalité

Parmi les fonctions ciblées, une attention particulière a été portée sur celles reliées aux cycles biogéochimiques du carbone (C) et de l'azote (N) de par leurs prévalences dans les agrosystèmes par rapport aux autres éléments ainsi que pour l'importance des implications que pourraient avoir des perturbations de ces cycles sur l'environnement plus global[1,2]. En effet, des gaz à effets de serres tels que le CO_2, le CH_4 et le N_2O font partie des cycles biogéochimiques de ces deux éléments et une augmentation de leurs émissions pourrait avoir des conséquences dramatiques pour la planète puisque la production alimentaire contribue à hauteur de 30% de l'empreinte écologique de la civilisation humaine (notamment via l'apport d'engrais organiques et inorganiques azotés)[3].

Un focus spécial a aussi été porté sur le cycle de l'eau. Le récent changement du régime des précipitations et des pénuries aiguës d'eau combinés à une demande accrue de nourriture ont profondément modifié la disponibilité de la ressource en eau pour les agrosystèmes. Dans de telles circonstances, il convient de prévoir les effets des contaminants émergents sur cette ressource et en

particulier sur l'efficience des cultures à utiliser cette ressource en eau. En effet, des études ont mis en évidence que les nanomatériaux provoquaient des signes d'un stress hydrique chez les végétaux[8,9].

Dans ce contexte, l'étude a porté sur l'impact d'une contamination en NTC sur le cycle du C en mesurant l'abondance bactérienne, la décomposition de la MO, la concentration en chlorophylle contenue dans les feuilles des plantes ainsi que leur rendement quantique et l'émission de CO_2 et CH_4 au niveau du système. Pour le cycle du N, l'impact de la contamination en NTC sur l'abondance des taxons bactériens reliés à la nitrification (gènes *amoA-AOA* et gène *amoA-AOB*) et à la dénitrification (gènes *nirK* et *nosZ*) a été analysé. Le cycle de l'eau a été approximé par l'étude de la teneur en eau des plantes ainsi que par les échanges d'H_2O dans le système.

Pour rendre compte de l'impact toxicologique sur les plantes et le rendement des agrosystèmes, les composés phénoliques, tanins et flavonoïdes et la production de biomasse d'une plante d'intérêt agricole (mais) ont été étudiés.

Enfin, de manière à avoir une approche intégrative et multifonctionnelle, les différentes fonctions ont été insérées dans un unique index qui renseigne sur la multifonctionnalité de l'agrosystème. De cette façon, il a été possible d'obtenir une vision plus globale de l'impact des NTC sur l'agrosystème. Cette analyse a été couplée à une modélisation par équations structurelles afin de rendre compte de la prépondérance de chaque variable et de leurs inter-relations.

PRINCIPAUX RESULTATS

Les résultats des expériences de ce chapitre ont montré des effets contrastés des NTC sur l'agrosystème, dépendants de la concentration en NTC dans le sol. Avec l'ajout de 0.1 $mg.kg^{-1}$, l'abondance bactérienne du sol et la concentration en chlorophylle, tannins et composés phénoliques dans les feuilles de maïs ont été diminuées. Malgré la diminution de l'abondance bactérienne et de la chlorophylle, aucune modification de la décomposition de la litière et d'émission de CO_2 et CH_4 respectivement n'ont été détectées. La diminution des tannins et composés phénoliques pourraient diminuer la capacité du maïs à réagir face aux stress environnementaux. Avec l'ajout de 10 $mg.kg^{-1}$ de CNT, l'abondance bactérienne du sol, les copies de gène des archées impliquées dans le processus de nitrification (*amoA*-AOA) et la décomposition de la litière ont été augmentées. L'augmentation de l'abondance bactérienne du sol pourrait être responsable d'une augmentation du processus de décomposition. Cette augmentation de la décomposition pourrait elle-même être responsable d'une libération accrue d'amonium, qui est le cation à l'origine du processus de nitrification, et être responsable de l'augmentation d'une partie des communautés de bactéries nitrifiantes. Chez le maïs, la concentration chlorophyllienne des feuilles a diminué et la teneur en eau du maïs augmenté, ce qui pourrait être dû à une obstruction du transfert de l'eau par les NTC au niveau des racines. La multifonctionnalité de l'écosystème a été diminué avec l'ajout de 0.1 $mg.kg^{-1}$ et augmenté avec l'ajout de 10 $mg.kg^{-1}$.

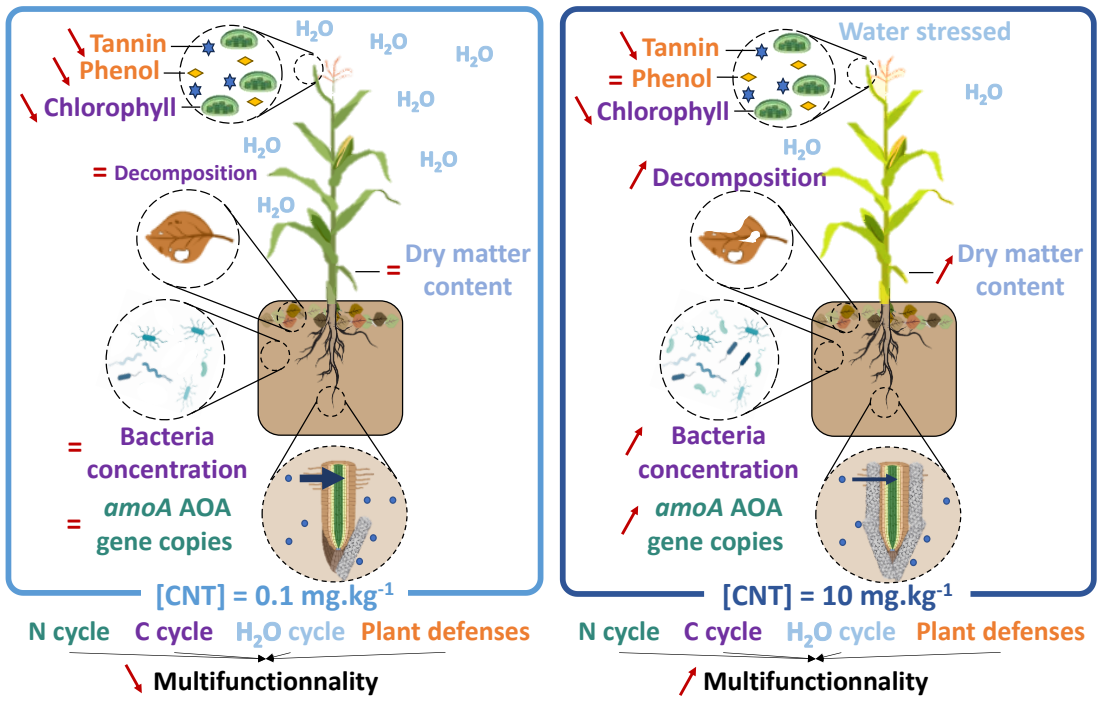

Figure 20: Schéma synthétique des principaux résultats du chapitre 4

Bibliographie (chapitre 4):

(1) Sauerbeck, D. R. CO2 Emissions and C Sequestration by Agriculture – Perspectives and Limitations. *Nutrient Cycling in Agroecosystems* **2001**, *60* (1), 253–266. https://doi.org/10.1023/A:1012617516477.
(2) Cassman, K. G.; Dobermann, A.; Walters, D. T. Agroecosystems, Nitrogen-Use Efficiency, and Nitrogen Management. *ambi* **2002**, *31* (2), 132–140. https://doi.org/10.1579/0044-7447-31.2.132.
(3) Banerjee, A.; Jhariya, M. K.; Meena, R. S.; Yadav, D. K. Ecological Footprints in Agroecosystem: An Overview. In *Agroecological Footprints Management for Sustainable Food System*; Banerjee, A., Meena, R. S., Jhariya, M. K., Yadav, D. K., Eds.; Springer: Singapore, 2021; pp 1–23. https://doi.org/10.1007/978-981-15-9496-0_1.
(4) Sainju, U. M.; Ghimire, R.; Pradhan, G. P.; Rigobelo, E. C.; Serra, A. P. Nitrogen Fertilization I: Impact on Crop, Soil, and Environment. In *Nitrogen Fixation*; IntechOpen, 2019. https://doi.org/10.5772/intechopen.86028.
(5) Nicholson, F. A.; Smith, S. R.; Alloway, B. J.; Carlton-Smith, C.; Chambers, B. J. An Inventory of Heavy Metals Inputs to Agricultural Soils in England and Wales. *Science of The Total Environment* **2003**, *311* (1), 205–219. https://doi.org/10.1016/S0048-9697(03)00139-6.
(6) Nagajyoti, P. C.; Lee, K. D.; Sreekanth, T. V. M. Heavy Metals, Occurrence and Toxicity for Plants: A Review. *Environmental Chemistry Letters* **2010**, *8* (3), 199–216. https://doi.org/10.1007/s10311-010-0297-8.
(7) *Toxic Metals in Soil-Plant Systems*; Ross, S., Ed.; Wiley: Chichester, West Sussex, England ; New York, 1994.
(8) Alp, F. N.; Ozfidan-Konakci, C.; Yildiztugay, E.; Arikan, B.; Elbasan, F.; Ozmen, M.; Kucukoduk, M. Multi-Walled Carbon Nanotubes Influence on Gas Exchange, Redox Reaction and Antioxidant System in Zea Mays Exposed to Excessive Copper. *J Plant Growth Regul* **2021**. https://doi.org/10.1007/s00344-021-10503-2.
(9) Izad, A. I.; Ibrahim, M. H.; Abdullah, C. A. C.; Zain, N. A. M. Growth, Leaf Gas Exchange and Secondary Metabolites of Orthosiphon Stamineus as Affected by Multiwall Carbon Nanotubes Application. *Annual Research & Review in Biology* **2018**, 1–13. https://doi.org/10.9734/ARRB/2018/38113.

Carbon nanotube impacts on geochemical cycles in an agrosystem: an integrative approach

Leroy Mathieu[1,2], Melissa Sontag[1], Jassey Vincent E.J.[1], Silvestre Jérôme[1], Barret Maialen[1], Flahaut Emmanuel[2], Larue Camille[1*]

[1]Laboratoire Ecologie Fonctionnelle et Environnement, Université de Toulouse, CNRS, Toulouse, France,

[2]CIRIMAT, Université de Toulouse, CNRS, INPT, UPS, UMR CNRS-UPS-INP N°5085, Université Toulouse 3 Paul Sabatier, Bât. CIRIMAT, 118, route de Narbonne, 31062 Toulouse cedex 9, France

* corresponding author: Avenue de l'Agrobiopole, F-31326 Castanet-Tolosan. camille.larue@cnrs.fr

Abstract

Since the discovery of the potential of carbon nanotubes (CNT) in agriculture to improve crop yield, many studies have been conducted to understand which effects CNT could have on agrosystem components. However, to date, very little is known about their impacts on ecosystem functions such as biogeochemical cycles or primary production and consequently on the multifunctionality of agrosystems. In this study, we aimed at understanding the impact of CNT in microcosms including soil bacteria and a crop plant (maize) with a special focus on H_2O, C and N cycles. After a 6-week exposure, bacterial concentration was decreased by 51% in soils exposed to 0.1 $mg.kg^{-1}$ while the organic matter decomposition rate was enhanced with the addition of 10 $mg.kg^{-1}$ of CNT. A dose dependent increase of nitrifier abundance was found with archaeal *amoA* copy numbers reaching +145% in soils exposed to 10 $mg.kg^{-1}$ of CNT. Maize exposed to 0.1 $mg.kg^{-1}$ of CNT had in average 34%, 18% and 15% lower chlorophyll, tannin and phenolic compounds, respectively but no impact was detected on the biomass production. Maize plants were water-stressed after exposure to 10 $mg.kg^{-1}$ of CNT with a significant 17% increase of the dry matter compared to unexposed maize. As a result, the multifunctionality of the agrosystem was significantly decreased at 0.1 $mg.kg^{-1}$ while it increased at 10 $mg.kg^{-1}$.

Keywords: bacteria, crop, emerging contaminant, gas exchange, nanomaterial, water stress

Highlights

- CNT impact on agrosystem was assessed by an integrative approach: organism to “ecosystem”.
- CNT disrupted C cycle by increasing bacteria number and litter decomposition rate.
- H_2O cycle changed at both organism (plant dry matter) and ecosystem (gas exchange) scales.

1. Introduction

Nanotechnology feeds the hopes of several research domains due to its many potential applications. Indeed, nanotechnology seems to be an important lever to the convergence of knowledge and technology for the benefit of the society and could be an opportunity for progress in the twenty-first century[1]. In order to develop nanotechnology, production and use of nanomaterials have increased over the years[2]. Among nanomaterials, a particular attention from industries is focused on carbon nanotubes (CNT) because of their remarkable physical, electronical and chemical properties[3], and mainly because they can combine several of them. Consequently, CNT are now found in products such as electronics, tires or sport equipments[4], and subsequently end up into the environment during their journey from production to recyling[5]. In addition, they tend to accumulate in sewage sludge used as fertilizer in agriculture[5] and modelling predicts that concentration of carbonaceous nanomaterials in biosolids could reach up to 10 $mg.kg^{-1}$ while in natural soil it could be up to 0.01 $mg.kg^{-1}$ [6]. Furthermore, CNT might be used as nano-fertilizer as their application on plants (for biofuel applications) and crops leads to increased yield according to several studies[7,8]. Thus, their concentration in ecosystems, in particular in agrosystems, will possibly increase in the future and their effects on this type of ecosystems need to be further examined in order to ensure a sustainable use of CNT.

According to the literature, CNT have contrasted impacts on plants[8]. They can act on plants from the germination stage with an activation of this process[9–12]. Furthermore, upon exposure, growth of plants was reported either increased, or decreased or even unmodified (based on root systems, biomass production, number of flowers and fruits)[8,13]. When toxicity was detected, it has been mostly associated with an overproduction of reactive oxygen species (ROS), antioxidant enzymatic activities, necrotic lesions of cells and leaf tissues as well as root and leaf morphological changes, decreased chlorophyll, and programmed cell death[14–17]. Additionally, CNT can also influence gas exchanges of plants with their environment. For example, CNT exposure at 250 $mg.L^{-1}$ increased carbon (C) assimilation rate of *Zea mays* and also decreased stomatal conductance and transpiration rate possibly as a result of H_2O use modulation[18]. The same results were observed on *Orthosiphon stamineus* with

a decrease in transpiration rate, stomatal conductance and net photosynthesis following a dose dependent relationship with the increase of CNT concentration (0, 700, 1400 and 2100 mg.L^{-1})[19]. Plants were also water-stressed as demonstrated by the positive correlation between water use efficiency and CNT concentration[19]. At lower concentrations (25 mg.L^{-1} and 54 mg.L^{-1}) no effects of CNT exposure were observed on *Arabidopsis thaliana* on ambient photosynthetic rate, stomatal conductance, transpiration, intrinsic water use efficiency and instantaneous water use efficiency[20]. It is also worth mentioning that these reported studies were performed in hydroponics which is not a realistic exposure scenario for agrosystems. Also, the effect of CNT on crops seems to be species dependent with maize being especially sensitive[21].

In parallel, interactions of CNT with micro-organisms have also been investigated. Microscopy observations have evidenced that CNT can interact with bacterial cell membranes; they can disrupt integrity of the membrane structure by oxidative stress and/or physical damage[22–25]. In addition, most studies have reported a decrease in soil microbial activity following exposure to CNT[26–29] and a loss of viability[25,26,30]. Furthermore, CNT and other carbon nanomaterial application can also cause changes in microbial community structure[26,29,31,32] . Finally, microbial functions such as organic matter decomposition, nitrogen (N) cycle and CO_2 fixation could be modified[33–36].

If the impact of CNT in single-organism exposure condition has been studied so far, very little has been done at the ecosystem scale. However, having a functional overview of contaminant impacts at this scale is of tremendous importance as plant/soil micro-organism interactions drive multiple processes and functions supporting ecosystem services such as food production[37]. In particular, aboveground-belowground interactions drive biogeochemical cycles (C, N, P) through several processes such as photosynthesis, mineralisation, nitrogen fixation, nitrification, denitrification, among others[37]. One way to tackle this gap of knowledge is the use of multifunctionality score as developed in ecology[38–40]. This score provides an easily interpretable measure of the ability of different entities composing an

ecosystem (bacteria and plants, for example) to sustain multiple functions simultaneously by gathering the selected functions in an index[41].

The objective of this study was thus to investigate the impacts of CNT at both the organism (crop plant) or community (micro-organisms) scales and at the microcosm scale by implementing a multifunctionality score. More specifically, after exposure to CNT their toxicity was assessed on (1) the overall abundance of bacteria using flow cytometry, (2) the organic matter decomposition process using tea bags, (3) the abundance of microbial communities related to N cycle by quantifying marker genes by qPCR , (4) the plant development (height, biomass, foliar surface area, dry matter content) (5) the plant physiology (photosynthetic pigment and secondary metabolite concentrations by spectrophotometry) and (6) gas exchanges of the system (CO_2, H_2O, CH_4). From these different variables, the impact of CNT on ecosystem functioning was determined by an integrative approach using multifunctionality scores.

2. Material and methods

2.1. CNT synthesis and characterization

CNT were synthesized at the Interuniversity Center of Materials Research and Engineering (CIRIMAT, Toulouse University) and characterized using transmission electron microscopy (JEOL 1400F, operated at 120 kV,), Raman spectroscopy (Labram HR 800 Yvon Jobin equipped with a He laser at 633 nm) (Figure S1). In brief, catalyst powder prepared by citric combustion was introduced in an alumina boat, boat itself placed at the center of a quartz reactor. The powder was first heated at 1000°C in an atmosphere containing at a speed of 5°C.min^{-1} then cooled down until 120°C at a speed of 5°C.min^{-1}; finally the reactor was flushed with nitrogen (N_2). MWCNT were first extracted from the nanocomposite powder by processing in an aqueous solution of HCl, then washed to neutrality using deionised water. Then, the wet nanotubes were oxidised in 3M HNO_3 by refluxing them at 130°C for 24h. Finally, the oxidized MWCNT were washed to neutrality using deionised water and used wet. For

specific surface area (SSA) assessment, the MWCNT were freeze-dried. They were oxidized multiwalled CNT (MWCNT) with length varying from 1 to 20 µm, an average diameter of 22.5 ± 5.0 nm and a specific surface area of 60 $m^2.g^{-1}$. CNT were suspended in deionised water at 100 $mg.L^{-1}$ and homogenized for 15 min in an ultrasonic bath before use.

CNT were characterized using transmission electron microscopy (JEOL 1400F, operated at 120 kV,), Raman spectroscopy (Labram HR 800 Yvon Jobin equipped with a He laser at 633 nm) and BET method (on freeze-dried samples). They were oxidized multiwalled CNT (MWCNT) with length varying from 1 to 20 µm, an average diameter of 22.5 ± 5.0 nm (Figure S1) and a specific surface area of 60 $m^2.g^{-1}$. CNT were suspended in deionised water at 100 $mg.L^{-1}$ and homogenized for 15 min in an ultrasonic bath before use.

2.2. Soil characterization and contamination

The experiment was performed with a sandy soil (LUFA-Speyer 2.1) sieved to 2 mm with 86.0% of sand, 12.6% of loam and 1.4% of clay. It contained 0.58 wt. % of organic carbon, 0.04 wt. % of nitrogen, with a pH of 5.0 ± 0.1 and a cation exchange capacity of 2.9 ± 0.2 $meq.100g^{-1}$. More details on soil characteristics are available in supporting information (Tables S1 and S2). Soils were contaminated by the addition of the required volume of CNT suspension to reach a final concentration of 0.1 or 10 $mg.kg^{-1}$ dry soil while maintaining the water holding capacity at 25%; the first concentration being close to environmentally predicted concentrations[6] and the second one representing a worst-case scenario (use of nano-fertilizer, for instance). They were then mixed manually for 10 min every day for a week to ensure that CNT were homogeneously distributed in the soil.

2.3. Microcosm set-up

Three hundred grams of soil were distributed in each microcosm (L = 45 cm, D = 10 cm). A tea-bag (©Lipton green tea sencha, 1.13 ± 0.32 g) was introduced after the addition of 50 g of soil in each

microcosm to study organic matter decomposition. Prior to introduction, tea bags were infused in water at 90°C to remove tea molecules which could have induced bias in microbial community behaviour, dried at 70°C during 48 h and weighted. One seed of *Zea mays* L. subsp. mays was added, plants were watered *ad libitum*. For each condition (CNT concentration of 0, 0.1 and 10 $mg.kg^{-1}$), microcosms were replicated five times with a total of 15 microcosms. The experiment lasted for 6 weeks in an environmental chamber with controlled parameters (10 h/14 h day/night cycle, 24°/18 °C and a hygrometry rate of 85%).

2.4. Bacterial abundance, litter decomposition and functional genes

After exposure, bacterial abundance was determined by collecting 1 g of previously homogenized dried soil placed in a tube with 5 mL of Formol 4% until further analysis. After 2 hours of stirring at 150 RPM and a centrifugation step at 6000 RPM, the sample supernatant containing bacteria was filtered at 10 µm to remove suspended matter coarse particles. Then, 1 mL of supernatant was stained with SYBR Green I (0.1 x final concentration) and incubated in the dark for 15 minutes. Finally, the samples were analysed by flow cytometry (Guava, Merck, United States) at a medium speed of 2 $\mu L.s^{-1}$ and a count rate not exceeding 1000 events s^{-1} to determine bacterial cell concentrations in each microcosm.

To study litter decomposition (C cycle), tea bags were removed and weighted after the 6 weeks of exposure which permitted to calculate a decomposition average rate as follows:

$$\text{Decomposition rate} = \frac{Mi - Mf}{Duration\ of\ exposure}$$

where Mi and Mf represent initial and final mass (mg dry weight) of the tea bag and duration of exposure is expressed in days.

Finally, the abundance of selected genes indicators for N cycling (nitrification and denitrification) was analysed by qPCR [42]. To summarize, after DNA isolation from contaminated soil using the extraction DNeasy PowerSoil kit ©QIAGEN, the total abundance of soil bacteria was measured by targeting the

universal 16S rRNA gene. The following genes related to N cycle were quantified: ammonia monooxygenase A gene (*amoA*) of ammonia oxidizing archaea (AOA) and ammonia oxidizing bacteria (AOB), nitrite reductase (*nirK*) and nitrous oxide reductase (*nosZ*) genes. The same experimental procedure as described in Vijayaraj *et al.*[43] was used. Results were expressed relative to the initial gene abundances at the beginning of experiment to account for initial variability among microcosms (Figure S2; absolute results after exposure are also available in Figure S3).

2.5. Plant morphology and metabolism

Upon exposure, indicators of C cycle and biomass production were gathered through the determination of the effective quantum yield of maize plants (Diving-Pam underwater fluorometer, Walz, United Kingdom), the height, the fresh and dry biomasses and the leaf surface area (using Image J software). Part of the leaf biomass was oven-dried (60°C until constant weight) to determine elemental concentrations by ICP-AES (see section 2.7). The remaining biomass was used fresh for methanol-based extraction to quantify photosynthetic pigments (chlorophyll a and b) and secondary metabolites *i.e.* total phenolic compounds, flavonoids and tannins as described in Leroy et al.[44].

2.6. Gas measurements and analysis

When plants were sufficiently high (*i.e.* sixth week), H_2O, CO_2 and CH_4 exchanges were recorded every second for 3 minutes. To do so, an airtight flux chamber (V = 0.06 m^3) was connected to a trace gas analyser (LI-7810, ©LI-COR inc, United States).

Net ecosystem exchange of CO_2 (NEE) was measured using a transparent chamber and a LED light while ecosystem CO_2 respiration (RECO) was measured using a darkened chamber. Gross primary productivity (GPP: CO_2 uptake as a result of photosynthesis), was calculated as the difference between NEE and RECO.

The slope of gas concentration was calculated and used to determine CO2 flux rates ($mg_{gaz}.m^{-2}.h^{-1}$). using R software and the "flux"[45] and "gasfluxes"[46] packages[46]. For NEE, calculations used an exponential nonlinear function to calculate the change in the concentration in the chamber over time[47]. RECO was calculated using linear regression of gas concentrations in the chamber over time. The same was done with H_2O and CH_4 to obtain fluxes in presence of light and in the dark. Positive values for the CO_2 and CH_4 fluxes indicate C release from the system while negative values indicate C uptake by the mesocosm.

2.7. Sample preparation and chemical analysis by ICP-AES

Soil samples went through a pre-digestion step overnight in 3 ml of concentrated HNO_3. Then, both plant and soil samples were digested using 1 ml of a mix of HNO_3 and HCl (3:1 v/v) and 1 ml of H_2O_2 in a close vessel in a microwave system (MARS 2, ©CEM corporation, USA: ramp time: 20-25 min; holding time: 10 min; temperature: 190 °C). After digestion, a filtration step (0.45 µm) was added for soil samples. Digested samples were then diluted in 5% HNO_3 before analysis on an ICP-AES (ARCOS FHX22, ©AMETEK Spectral, United States) along with control samples (blanks with only chemicals)

2.8. Statistical analyses

For statistical analyses, 1-way ANOVAs were performed on the toxicity endpoints to test the effects of the addition of CNT. The normality, independence and homoscedasticity of the residues were checked using Shapiro, Durbin-Watson and Breusch-Pagan tests, respectively. Data were transformed to log or square root if one of the three conditions of validity was not met. A non-parametric Kruskal-Wallis test was performed in the case of failed transformations. All statistical analyses were performed on RStudio software (version 3.4.1). Principal component analyses (PCA) were performed on the elemental concentrations in plants to assess the impact of CNT on plant nutrition.

Major and representatives functions were selected to reflect agrosystem viability and services. Following selection, we ended up with functions related to carbon dynamic (i.e. GPP and CH_4 emission with light and in darkness and litter decomposition), H_2O emission (with light and in darkness), bacteria population (bacteria concentration and the number of ARN 16S gene copies), N cycle (as number of *nosZ*, *nirK*, *AmoA-AOA* and *AmoA-AOB* gene copies), agricultural yield (as plant biomass), plant defenses (as total phenolic compound and tannin concentrations) and photosynthesis capabilities (as quantic yield and total chlorophyll concentrations) were standardized and implemented in a unique Z-score, an index representing the multifunctionality of the ecosystem as described by Delgado-Baquerizo et al.[38]. Negative Z-score indicated a low multifunctionality and positive Z-score a high multifunctionality of the considered agrosystem.

3. Results

3.1. Microbial responses to CNT exposure

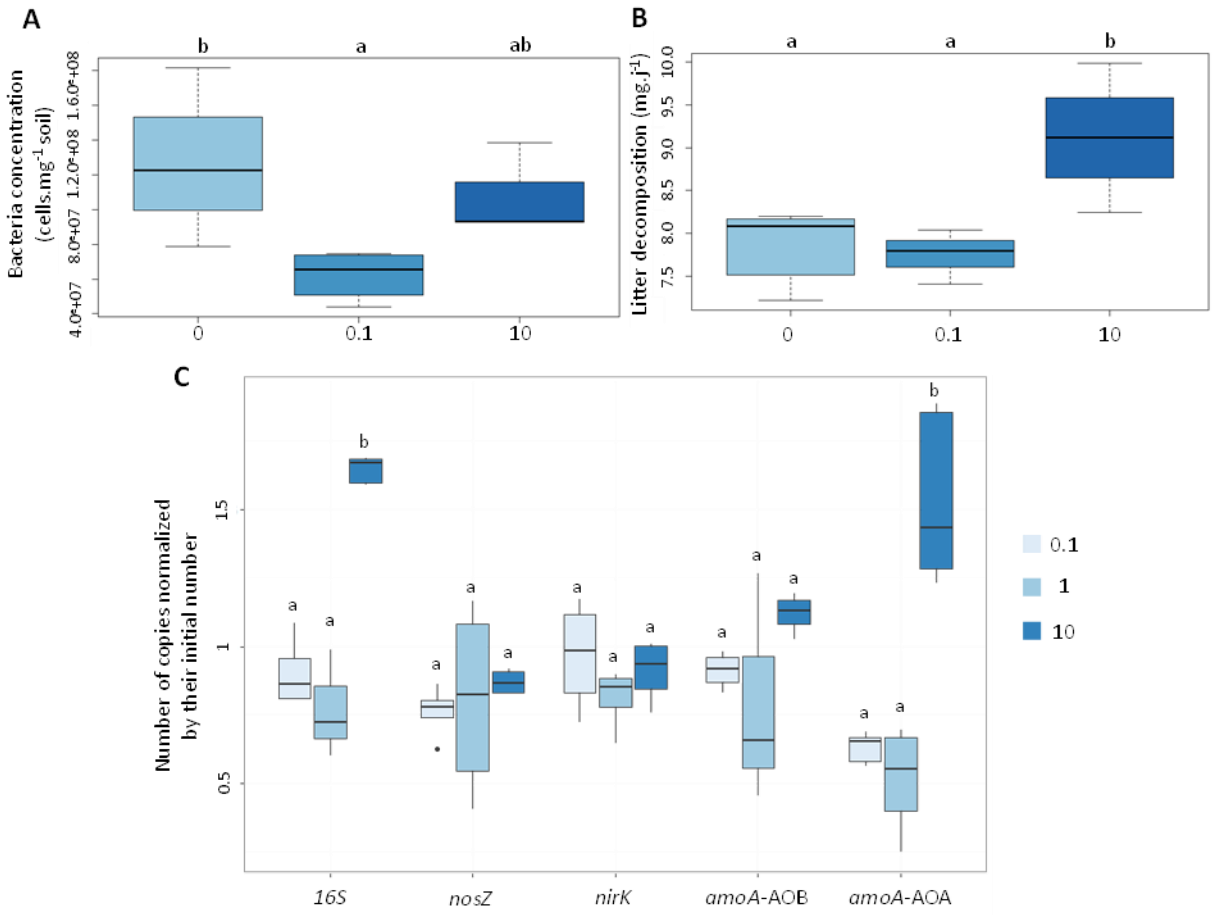

Figure 21: Bacteria concentration determined by flow cytometry (A), decomposition of litter (B), gene copy quantification for selected genes involved in N cycle: nosZ , nirK, amoA-AOB and amoA-AOA by qPCR (normalized by the initial number of gene copies) for the 3 CNT modalities (0 = 0 mg.kg^{-1}, 0.1 = 0.1 mg.kg^{-1}, 10 = 10 mg.kg^{-1}) after a 6-week exposure in soil. Same lowercase letters indicate treatments that do not differ significantly (p-value > 0.05) following an ANOVA or a Kruskal-Wallis test (n = 5).

Bacterial abundance decreased by 51% in soils exposed to 0.1 mg.kg^{-1} of CNT when compared to control soils ($p_{bacteria\ concentration}$ = 0.04, Figure 21A) as revealed by flow cytometry, while no effect was found with the addition of 10 mg.kg^{-1}. Decomposition rate of the litter was faster in soils exposed to 10 mg.kg^{-1} of CNT compared to the other conditions ($p_{litter\ decomposition}$ < 0.01) with on average 9.1 mg.j^{-1} *vs*. 7.8 mg.j^{-1} (Figure 21B). In soils exposed to 10 mg.kg^{-1} of CNT, the dynamics of 16S rRNA and *amoA*-AOA gene abundances exhibited significant differences ($p_{ARN\ 16S}$ < 0.01 and $p_{AmoaA\text{-}AOA}$ < 0.01, Figure 21C), with a 80% and 145% increase while both gene abundances tended to decrease in control conditions.

For these two genes, no difference was found at 0.1 mg.kg^{-1} (Figure 21C). No significant difference was found for *nosZ*, *nirK* and *amoA*-AOB gene copies with on average 0.80, 0.90 and 0.97 across conditions, respectively (p_{nosZ} = 0.76, p_{nirK} = 0.39, $p_{amoA\text{-}AOB}$ = 0.13, Figure 21C).

3.2. Crop plant response to CNT exposure

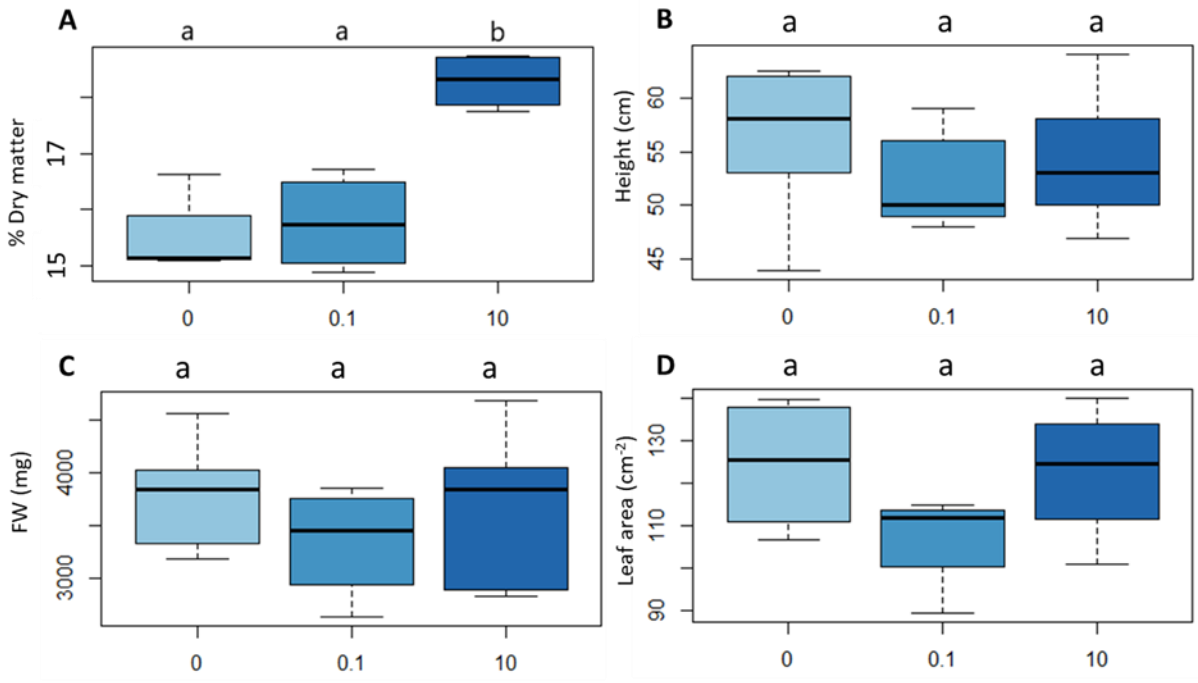

Figure 22: Plant morphological parameter assessment: dry weight/ fresh weight proportion (% of dry matter) (A), height (B), fresh weight (FW, C), and leaf area (D) of maize exposed for 6 weeks in soil contaminated with 3 CNT modalities (0 = 0 mg.kg^{-1}, 0.1 = 0.1 mg.kg^{-1}, 10 = 10 mg.kg^{-1}). Same lowercase letters indicate treatments that do not differ significantly (p-value > 0.05) following an ANOVA (n = 5).

At the end of exposure, the proportion of dry weight was higher for plants exposed to 10 mg.kg^{-1} of CNT with on average +17.4% compared to control plants ($p_{\%DW}$ < 0.01, Figure 22A). No significant difference was found on the other growth parameters tested, height, FW and leaf area with on average 54.23 cm, 3.54 g and 126.34 cm^2, respectively whatever the condition (p_{height} = 0.7, p_{FW} = 0.6, $p_{leaf\ area}$ = 0.5, Figure 22 B-C-D).

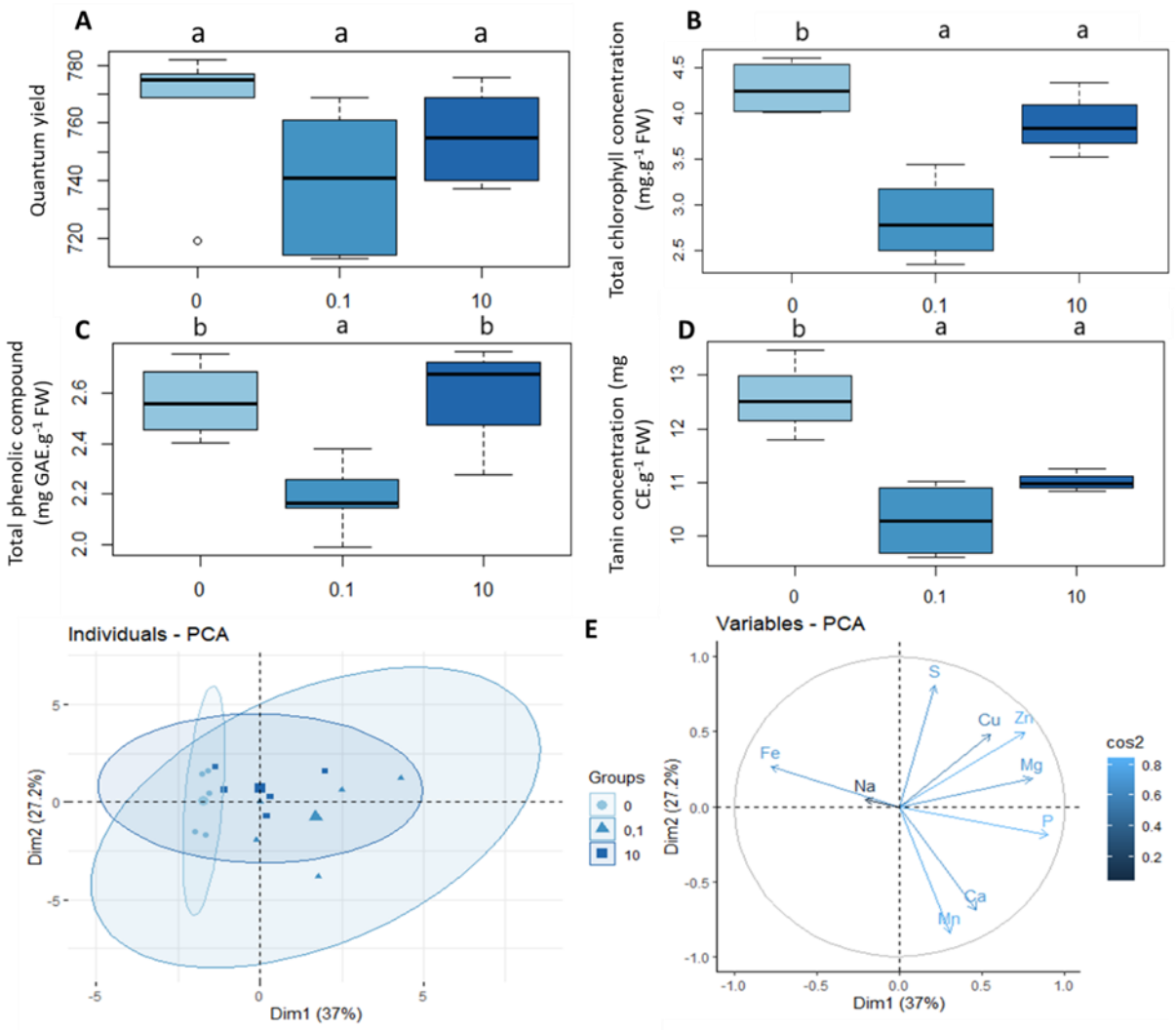

Figure 23: Quantum yield (A), total chlorophyll (B), total phenolic compounds (C), tannin concentration (D) and principal component analysis (PCA, E) on the micro- and macro-nutrient content (Ca, Cu, Fe, Cu, Mg, Mn, Na, P, S, Zn) represented by individuals and correlation circle graphs for maize leaves exposed to the 3 CNT modalities (0 = 0 mg.kg^{-1}, 0.1 = 0.1 mg.kg^{-1}, 10 = 10 mg.kg^{-1}) after a 6-week exposure in soil. Cos2 corresponds to the level of variable contributions (elements) to dimensions 1 and 2. Same lowercase letters indicate treatments that do not differ significantly (p-value > 0.05) following an ANOVA (n = 5).

At the metabolic level, no difference on the quantum yield was detected between maize grown on control soils and those exposed to CNT ($p_{quantum\ yield}$ = 0.3, Figure 23A). However, the concentration of total chlorophyll was on average 34% and 9% lower in maize exposed to 0.1 and 10 of mg.kg^{-1} CNT than in maize in control condition ($p_{Chlorophyll}$ < 0.01, Figure 23B). Furthermore, phenolic compounds decreased by 15% when exposed to 0.1 mg.kg^{-1} of CNT compared to control condition ($p_{phenolic\ compounds}$ < 0.01, Figure 23C). Similarly, maize exposed to the two CNT concentrations (0.1 and 10 mg.kg^{-1}) decreased by 18% their tannin content in leaves compared to control soils (p_{tannin} = 0.01, Figure 23D).

CNT exposure did not seem to impact plant mineral nutrition. Indeed, the PCA on maize leaf elemental composition (Ca, Cu, Fe, Mg, Mn, Na, P, S, Zn) after exposure displayed similar features for all three conditions (Figure 23E, Table S3).

3.3. Gas exchange

At the 6th week of exposure, the NEE, RECO and CH_4 (in light and dark conditions) were similar whatever the CNT concentration with on average 0.04 and 0.07 $mg_{CO2}.m^{-2}.h^{-1}$ and -0.004 and -0.002 $mg_{CH4}.m^{-2}.h^{-1}$ respectively (p_{NEE} = 0.6, p_{RECO} = 0.2, $p_{CH4\ Light}$ = 0.4, $p_{CH4\ darkness}$ = 0.9, Figure 24A-B-E-F). Additionally, the GPP was also similar whatever the CNT concentration with on average -0.16 $mg_{CO2}.m^{-2}.h^{-1}$ (p_{GPP} = 0.7, Figure S4). In contrast, the emission of H_2O in microcosms measured with light (*i.e* the evapotranspiration gathering both leaf transpiration and soil evaporation) was around twice lower in the presence of CNT at the two concentrations studied than in controls with on average 16.4 and 37.2 $mg_{H2O}.m^{-2}.h^{-1}$, respectively ($p_{H2O\ light}$ < 0.01, Figure 24C). This was not the case without light: the emission of H_2O was on average 10.5 $mg_{H2O}.m^{-2}.h^{-1}$ whatever the CNT concentration ($p_{H2O\ dark}$ = 0.16, Figure 24D).

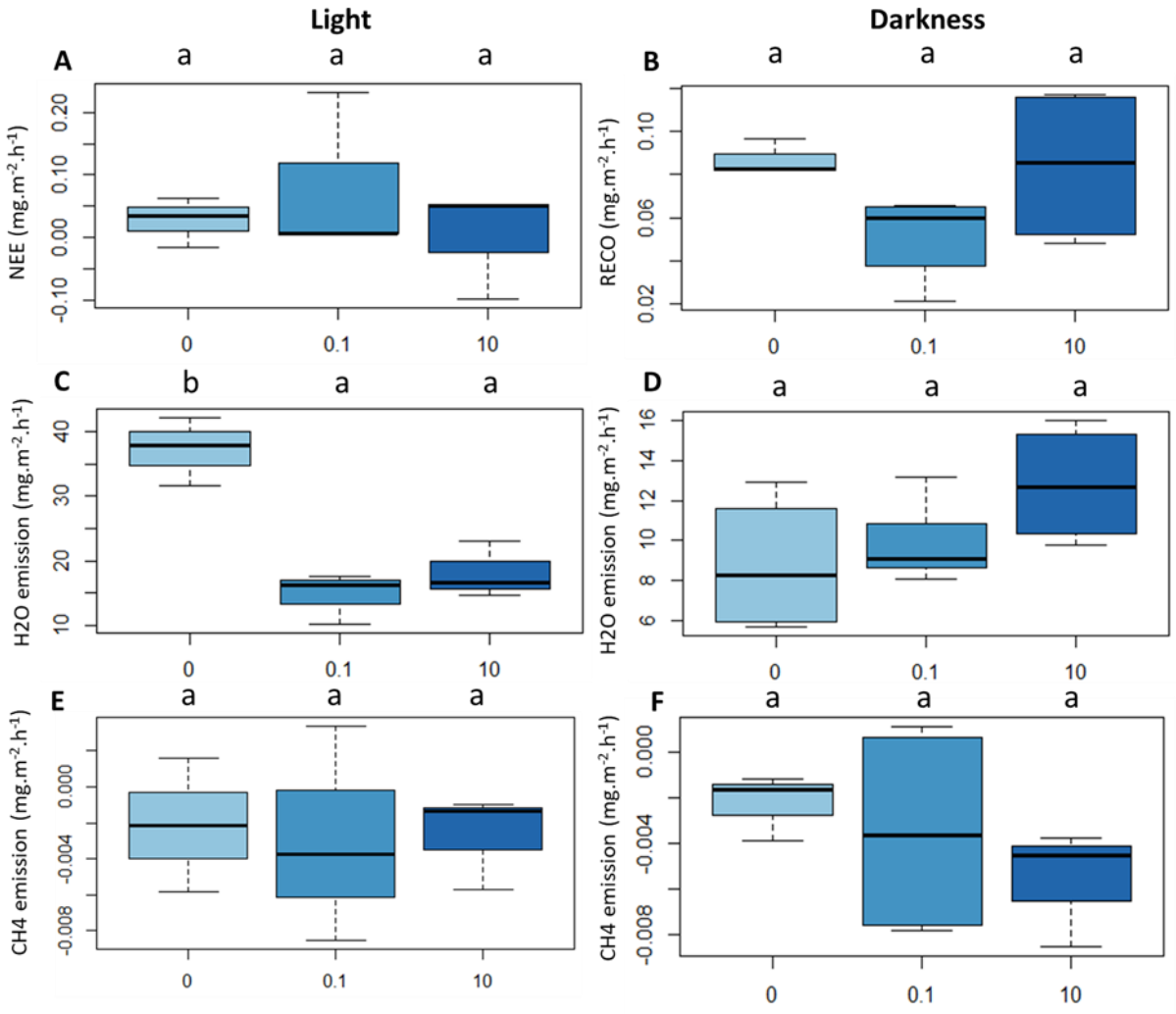

Figure 24: Net ecosystem exchange (NEE, A), ecosystem respiration (RECO,B), H_2O emission measured in presence of light (C) and in darkness (D) and CH_4 emission measured in presence of light (E) and in darkness (F) for microcosms exposed to the 3 CNT modalities (0 = 0 mg.kg^{-1}, 0.1 = 0.1 mg.kg^{-1}, 10 = 10 mg.kg^{-1}) after a 6-week exposure. Same lowercase letters indicate treatments that do not differ significantly (p-value > 0.05) following an ANOVA and Kruskal-Wallis (CH_4 in darkness) (n = 5).

3.4. Multifunctionality

The ecosystem multifunctionality was found to be decreased from 0.13 ± 0.07 in control condition to -0.38 ± 0.15 with the addition of 0.1 mg.kg^{-1} CNT while the addition of 10 mg.kg^{-1} led to a significant increase of the multifunctionality index up to 0.36 ± 0.09 (p < 0.001, Figure 25).

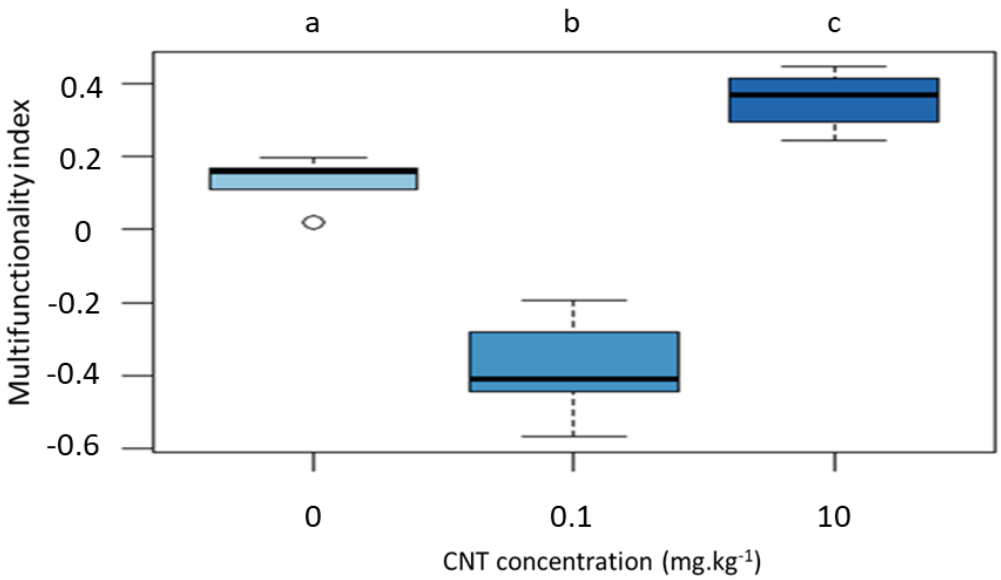

Figure 25: Multifunctionality index of microcosms exposed to the 3 CNT modalities (0 = 0 mg.kg^{-1}, 0.1 = 0.1 mg.kg^{-1}, 10 = 10 mg.kg^{-1}) after a 6-week exposure. Same lowercase letters indicate treatments that do not differ significantly (p-value > 0.05) following an ANOVA (n=5).

4. Discussion

4.1. Impacts of CNT on C cycle

Organic matter decomposition was 17% faster with the addition of 10 mg.kg^{-1} of CNT compared to control microcosms. This result might be related to the increase in the relative number of universal 16S rRNA gene copies (+80%) suggesting an increase in bacteria population at this same condition. Differences between rRNA 16S and bacteria concentration counted by flow cytometry could reveal that non-viable gene copies were counted in the qPCR as already demonstrated in the litterature[48,49]. However, at the lowest CNT concentration (0.1 mg.kg^{-1}), bacteria abundance was decreased accordingly to flow cytometry analysis. In parallel, plant photosynthesis did not seem to be impacted (visible trend of a decrease in the quantum yield of exposed maize, although not significant) even though there was a significant decrease in total chlorophyll pigments for plants exposed to CNT. The development of plants (biomass production and height) was also not impacted after 6 weeks of exposure.

In the literature, it has been reported in different articles that nanomaterials can increase organic matter decomposition process[50,51]. A study with similar exposure duration (56 days) highlighted the same increase in 16S rRNA copies in the presence of CNT (both single-walled CNT and multi-walled CNT) at 10 and 50 $g.kg^{-1}$[52]. In addition, the higher toxicity of CNT at lower concentrations has already been evidenced with similar reduction of microbial biomass after exposure to carbon nanomaterials such as graphene[29,53], graphene oxide[29,53,54] and CNT[28,29]. The homo and hetero-agglomeration of CNT in soil might explain this effect[44]. Despite the decrease in bacteria concentration at 0.1 $mg.kg^{-1}$ of CNT, no effect on decomposition potential was noticeable suggesting that decomposition was maybe compensated by others decomposers such as fungus. As proposed by Evariste et al.[51] in aquatic systems, the presence of carbon nanomaterials[55,56] and other nanoparticles[50] at low concentration may increase fungus development and thus stimulate decomposition activity due to their role as decomposers.

Interestingly, the difference detected at the organisms and community levels (bacteria population and chlorophyll pigments) did not lead to any significant difference in gas exchange (CO_2 and CH_4) at the microcosm level, suggesting some compensation mechanisms at this scale.

4.2. Impacts of CNT on N cycle

The quantification of genes involved in the nitrogen cycle showed an increase in *amoA*-AOA gene copies up to 145% in soils exposed to 10 $mg.kg^{-1}$ of CNT compared to the control. The similar trend was noticeable on *amoA*-AOB gene copies, suggesting a dose-dependent induction of the nitrifier bacterial communities. In the literature, a study demonstrated a similar increase in *amoA*-AOA and *amoA*-AOB gene abundances after 120 days of 0.5 $mg.L^{-1}$ and 5 $mg.L^{-1}$ exposure to GO in constructed wetlands, while the increase was only significant for *amoA*-AOA gene abundance after exposure to 0.5 $mg.L^{-1}$ after 30 days[35]. In contrast, in another study after 180 days of wastewater exposure, the addition of carbon-based nanomaterials (single-walled CNT, multi-walled CNT and fullerene, 10 and 1000 $\mu g.L^{-1}$)

led to the decline of the relative abundance of *Nitrosomonas* which is the dominant ammonia oxidizing bacteria[34,57] and is mainly responsible for the oxidation of ammonia to nitrate[34,58,59]. Different parameters such as exposure media, the physico-chemical characteristics of nanomaterials or different initial microbial communities could explain the discrepancies among studies[60]. In our case, the increase of litter decomposition could induce an increased ion NH4+ release which is the substrate of nitrifiers and could explain increases observed on nitrifiers communities. However, there was no impacts of CNT exposure on denitrifier communities (*nosZ* and *nirK*).

These different results suggest that the population of nitrifiers could be favored under chronic exposure to carbon nanomaterials compared to denitrifiers (*nosZ* and *nirK* genes unchanged abundance). This nitrification potential increase could lead to enhanced nitrate release and could thus result in higher plant uptake and therefore higher growth along the life cycle. Indeed in our study, CNT exposure resulted in a decrease in chlorophyll concentration. If no significant impact was detected on quantum yield and biomass after a six-week exposure, it would be interesting to assess these parameters after a full plant life-cycle exposure. This highlights also the interest of working with microcosm to be able to investigate cascading effects of a contaminant on an organism assemblage.

4.3. Impacts of CNT on H_2O cycle

Concerning maize, the dry matter content was on average 17.4% higher for plants exposed to 10 $mg.kg^{-1}$ of CNT compared to control plants suggesting a decrease in water content. In the literature, Mondal *et al*.[16] evidenced similar results on *Brassica juncea* with an increase in DW/FW ratio after exposure to CNT and oxidized CNT at 2.3 and 23 $\mu g.L^{-1}$, respectively[16]. This dry matter content increase has been demonstrated to be a stress response[62,63]. It can be also correlated with a decrease in some secondary metabolites in maize exposed to CNT confirming the fact that plants are suffering stress conditions. Decrease in secondary metabolites such as phenolic compounds and tannins could impair plant

defense capabilities as they are implied in many stress defense mechanisms such as high light, low temperatures, pathogen infection, herbivores, nutrient deficiency and exposure to metals[64,65].

Alternatively, this decreased water content in maize may also be associated with CNT water adsorption capabilities, decreasing water bioavailability for maize[66,67].

However, the dry mater content results obtained in this study do not follow the general trend observed in the literature which described an increase in water content with CNT exposure[8,18,68,69]. However, as demonstrated by Line *et al*. crop species have very contrasted response to the exposure to CNT, which can partly be explained by different plant characteristics (morphology and/or physiology)[21].

The results related to water use obtained at the plant organism scale were confirmed at the ecosystem scale with a decrease in H_2O flux in light condition in the microcosms exposed to CNT. It might be related with a decreased stomatal opening in water-stressed CNT-exposed maize. Indeed, several studies demonstrated a dose-dependent decrease in stomatal conductance with the concentration of CNT in *Orthosiphon stamineus*[19] and *Zea mays*[18].

4.4. Impacts of CNT on agrosystem multifunctionality

The multifunctionality of agrosystems was decreased with 0.1 $mg.kg^{-1}$ and increase with 10 $mg.kg^{-1}$ of CNT addition corresponding that functions of agrosystem were less efficient and more efficient respectively. Lozano et al.[70] observed a decrease in multifunctionality index up to -60% due to the exposure to microplastics (4 $g.kg^{-1}$). In the same study, authors observed the same increase in decomposition as in this work, suggesting that the decomposition process is not an an indicator following the trend of the multifunctionality index, certainly because this type of process could be compensated. In the same work, Lozano et al.[70] showed that β-glucosidase activity was the most important indicator to describe multifunctionnality of the ecosystem.

In conclusion, despite some articles of the literature suggesting that CNT could be used as fertilizer to increase crop production, our results obtained using an integrative approach in microcosms

demonstrated an impairment of some of the major geochemical cycles with consequences both at the organism and at the ecosystem level.

Acknowledgement

This work was supported by the Région Occitanie, Toulouse Federal University, and EC2CO program CARBOSTRESS (CNRS-INSU). Authors are thankful to the FBiI and PAPC platforms of the laboratory for functional ecology and environment for ICP-AES analysis and soil physico-chemical characterization, respectively. We are also grateful to Morgan Légnani for CNT synthesis and Laure Gandois for providing the LICOR instrument.

Bibliography (article: Carbon nanotube impacts on geochemical cycles in an agrosystem: an integrative approach) :

(1) Roco, M. C.; Bainbridge, W. S. The New World of Discovery, Invention, and Innovation: Convergence of Knowledge, Technology, and Society. *J Nanopart Res* **2013**, *15* (9), 1946. https://doi.org/10.1007/s11051-013-1946-1.

(2) Piccinno, F.; Gottschalk, F.; Seeger, S.; Nowack, B. Industrial Production Quantities and Uses of Ten Engineered Nanomaterials in Europe and the World. *J Nanopart Res* **2012**, *14* (9), 1109. https://doi.org/10.1007/s11051-012-1109-9.

(3) O'Connell, M. J. *Carbon Nanotubes: Properties and Applications*; CRC Press, 2018.

(4) *Search Database - The Nanodatabase*. https://nanodb.dk/en/search-database/ (accessed 2023-07-06).

(5) Gottschalk, F.; Sun, T.; Nowack, B. Environmental Concentrations of Engineered Nanomaterials: Review of Modeling and Analytical Studies. *Environmental Pollution* **2013**, *181*, 287–300. https://doi.org/10.1016/j.envpol.2013.06.003.

(6) Holden, P. A.; Klaessig, F.; Turco, R. F.; Priester, J. H.; Rico, C. M.; Avila-Arias, H.; Mortimer, M.; Pacpaco, K.; Gardea-Torresdey, J. L. Evaluation of Exposure Concentrations Used in Assessing Manufactured Nanomaterial Environmental Hazards: Are They Relevant? *Environ. Sci. Technol.* **2014**, *48* (18), 10541–10551. https://doi.org/10.1021/es502440s.

(7) Rudakiya, D.; Patel, Y.; Chhaya, U.; Gupte, A. Carbon Nanotubes in Agriculture: Production, Potential, and Prospects. In *Nanotechnology for Agriculture: Advances for Sustainable Agriculture*; Panpatte, D. G., Jhala, Y. K., Eds.; Springer: Singapore, 2019; pp 121–130.

(8) Liné, C.; Larue, C.; Flahaut, E. Carbon Nanotubes: Impacts and Behaviour in the Terrestrial Ecosystem - A Review. *Carbon* **2017**, *123*, 767–785. https://doi.org/10.1016/j.carbon.2017.07.089.

(9) Oleszczuk, P.; Jośko, I.; Xing, B. The Toxicity to Plants of the Sewage Sludges Containing Multiwalled Carbon Nanotubes. *Journal of Hazardous Materials* **2011**, *186* (1), 436–442. https://doi.org/10.1016/j.jhazmat.2010.11.028.

(10) Ratnikova, T. A.; Podila, R.; Rao, A. M.; Taylor, A. G. *Tomato Seed Coat Permeability to Selected Carbon Nanomaterials and Enhancement of Germination and Seedling Growth*. The Scientific World Journal. https://doi.org/10.1155/2015/419215.

(11) Lahiani, M. H.; Chen, J.; Irin, F.; Puretzky, A. A.; Green, M. J.; Khodakovskaya, M. V. Interaction of Carbon Nanohorns with Plants: Uptake and Biological Effects. *Carbon* **2015**, *81*, 607–619. https://doi.org/10.1016/j.carbon.2014.09.095.

(12) Lahiani, M. H.; Dervishi, E.; Ivanov, I.; Chen, J.; Khodakovskaya, M. Comparative Study of Plant Responses to Carbon-Based Nanomaterials with Different Morphologies. *Nanotechnology* **2016**, *27* (26), 265102. https://doi.org/10.1088/0957-4484/27/26/265102.

(13) Wang, Q.; Li, C.; Wang, Y.; Que, X. Phytotoxicity of Graphene Family Nanomaterials and Its Mechanisms: A Review. *Front. Chem.* **2019**, *7*. https://doi.org/10.3389/fchem.2019.00292.

(14) Lin, C.; Fugetsu, B.; Su, Y.; Watari, F. Studies on Toxicity of Multi-Walled Carbon Nanotubes on Arabidopsis T87 Suspension Cells. *Journal of Hazardous Materials* **2009**, *170* (2), 578–583. https://doi.org/10.1016/j.jhazmat.2009.05.025.

(15) Shen, C.-X.; Zhang, Q.-F.; Li, J.; Bi, F.-C.; Yao, N. Induction of Programmed Cell Death in Arabidopsis and Rice by Single-Wall Carbon Nanotubes. *American Journal of Botany* **2010**, *97* (10), 1602–1609. https://doi.org/10.3732/ajb.1000073.

(16) Mondal, A.; Basu, R.; Das, S.; Nandy, P. Beneficial Role of Carbon Nanotubes on Mustard Plant Growth: An Agricultural Prospect. *J Nanopart Res* **2011**, *13* (10), 4519. https://doi.org/10.1007/s11051-011-0406-z.

(17) Begum, P.; Fugetsu, B. Phytotoxicity of Multi-Walled Carbon Nanotubes on Red Spinach (Amaranthus Tricolor L) and the Role of Ascorbic Acid as an Antioxidant. *Journal of Hazardous Materials* **2012**, *243*, 212–222. https://doi.org/10.1016/j.jhazmat.2012.10.025.
(18) Alp, F. N.; Ozfidan-Konakci, C.; Yildiztugay, E.; Arikan, B.; Elbasan, F.; Ozmen, M.; Kucukoduk, M. Multi-Walled Carbon Nanotubes Influence on Gas Exchange, Redox Reaction and Antioxidant System in Zea Mays Exposed to Excessive Copper. *J Plant Growth Regul* **2021**. https://doi.org/10.1007/s00344-021-10503-2.
(19) Izad, A. I.; Ibrahim, M. H.; Abdullah, C. A. C.; Zain, N. A. M. Growth, Leaf Gas Exchange and Secondary Metabolites of Orthosiphon Stamineus as Affected by Multiwall Carbon Nanotubes Application. *Annual Research & Review in Biology* **2018**, 1–13. https://doi.org/10.9734/ARRB/2018/38113.
(20) Voleti, R. Effects of Low Concentrations of Carbon Nanotubes on Growth and Gas Exchange in Arabidopsis Thaliana. *MSU Graduate Theses* **2015**.
(21) Liné, C.; Manent, F.; Wolinski, A.; Flahaut, E.; Larue, C. Comparative Study of Response of Four Crop Species Exposed to Carbon Nanotube Contamination in Soil. *Chemosphere* **2021**, *274*, 129854. https://doi.org/10.1016/j.chemosphere.2021.129854.
(22) Jackson, P.; Jacobsen, N. R.; Baun, A.; Birkedal, R.; Kühnel, D.; Jensen, K. A.; Vogel, U.; Wallin, H. Bioaccumulation and Ecotoxicity of Carbon Nanotubes. *Chem Cent J* **2013**, *7*, 154. https://doi.org/10.1186/1752-153X-7-154.
(23) Zheng, X.; Su, Y.; Chen, Y.; Wan, R.; Li, M.; Wei, Y.; Huang, H. Carboxyl-Modified Single-Walled Carbon Nanotubes Negatively Affect Bacterial Growth and Denitrification Activity. *Sci Rep* **2014**, *4*. https://doi.org/10.1038/srep05653.
(24) Hu, W.; Peng, C.; Luo, W.; Lv, M.; Li, X.; Li, D.; Huang, Q.; Fan, C. Graphene-Based Antibacterial Paper. *ACS Nano* **2010**, *4* (7), 4317–4323. https://doi.org/10.1021/nn101097v.
(25) Giraud, L.; Tourrette, A.; Flahaut, E. Carbon Nanomaterials-Based Polymer-Matrix Nanocomposites for Antimicrobial Applications: A Review. *Carbon* **2021**. https://doi.org/10.1016/j.carbon.2021.06.002.
(26) Jin, L.; Son, Y.; DeForest, J. L.; Kang, Y. J.; Kim, W.; Chung, H. Single-Walled Carbon Nanotubes Alter Soil Microbial Community Composition. *Sci. Total Environ.* **2014**, *466–467*, 533–538. https://doi.org/10.1016/j.scitotenv.2013.07.035.
(27) Chung, H.; Son, Y.; Yoon, T. K.; Kim, S.; Kim, W. The Effect of Multi-Walled Carbon Nanotubes on Soil Microbial Activity. *Ecotoxicology and Environmental Safety* **2011**, *74* (4), 569–575. https://doi.org/10.1016/j.ecoenv.2011.01.004.
(28) Jin, L.; Son, Y.; Yoon, T. K.; Kang, Y. J.; Kim, W.; Chung, H. High Concentrations of Single-Walled Carbon Nanotubes Lower Soil Enzyme Activity and Microbial Biomass. *Ecotoxicology and Environmental Safety* **2013**, *88*, 9–15. https://doi.org/10.1016/j.ecoenv.2012.10.031.
(29) Ge, Y.; Priester, J. H.; Mortimer, M.; Chang, C. H.; Ji, Z.; Schimel, J. P.; Holden, P. A. Long-Term Effects of Multiwalled Carbon Nanotubes and Graphene on Microbial Communities in Dry Soil. *Environ. Sci. Technol.* **2016**, *50* (7), 3965–3974. https://doi.org/10.1021/acs.est.5b05620.
(30) Chung, H.; Son, Y.; Yoon, T. K.; Kim, S.; Kim, W. The Effect of Multi-Walled Carbon Nanotubes on Soil Microbial Activity. *Ecotoxicology and Environmental Safety* **2011**, *74* (4), 569–575. https://doi.org/10.1016/j.ecoenv.2011.01.004.
(31) Kerfahi, D.; Tripathi, B. M.; Singh, D.; Kim, H.; Lee, S.; Lee, J.; Adams, J. M. Effects of Functionalized and Raw Multi-Walled Carbon Nanotubes on Soil Bacterial Community Composition. *PLOS ONE* **2015**, *10* (3), e0123042. https://doi.org/10.1371/journal.pone.0123042.
(32) Evariste, L.; Braylé, P.; Mouchet, F.; Silvestre, J.; Gauthier, L.; Flahaut, E.; Pinelli, E.; Barret, M. Graphene-Based Nanomaterials Modulate Internal Biofilm Interactions and Microbial Diversity. *Front. Microbiol.* **2021**, *12*. https://doi.org/10.3389/fmicb.2021.623853.
(33) Wu, F.; You, Y.; Werner, D.; Jiao, S.; Hu, J.; Zhang, X.; Wan, Y.; Liu, J.; Wang, B.; Wang, X. Carbon Nanomaterials Affect Carbon Cycle-Related Functions of the Soil Microbial Community and the

Coupling of Nutrient Cycles. *Journal of Hazardous Materials* **2020**, *390*, 122144. https://doi.org/10.1016/j.jhazmat.2020.122144.
(34) Yang, X.; He, Q.; Guo, F.; Sun, X.; Zhang, J.; Chen, Y. Impacts of Carbon-Based Nanomaterials on Nutrient Removal in Constructed Wetlands: Microbial Community Structure, Enzyme Activities, and Metabolism Process. *Journal of Hazardous Materials* **2021**, *401*, 123270. https://doi.org/10.1016/j.jhazmat.2020.123270.
(35) Yan, C.; Huang, J.; Wang, Y.; Lin, X.; Cao, C.; Qian, X. Assessment on the Treatment of Nitrogen Contaminant by Constructed Wetland Exposed to Different Concentrations of Graphene Oxide. *Journal of Cleaner Production* **2022**, *338*, 130567. https://doi.org/10.1016/j.jclepro.2022.130567.
(36) Das, P.; Davis, K.; Penton, C. R.; Westerhoff, P.; Bi, Y. Impacts of Graphitic Nanofertilizers on Nitrogen Cycling in a Sandy, Agricultural Soil. *J Nanopart Res* **2022**, *24* (6), 120. https://doi.org/10.1007/s11051-022-05500-9.
(37) Barbault, R. *Ecologie Generale*; Dunod, 2008.
(38) Delgado-Baquerizo, M.; Maestre, F. T.; Reich, P. B.; Jeffries, T. C.; Gaitan, J. J.; Encinar, D.; Berdugo, M.; Campbell, C. D.; Singh, B. K. Microbial Diversity Drives Multifunctionality in Terrestrial Ecosystems. *Nat Commun* **2016**, *7* (1), 10541. https://doi.org/10.1038/ncomms10541.
(39) Maestre, F. T.; Quero, J. L.; Gotelli, N. J.; Escudero, A.; Ochoa, V.; Delgado-Baquerizo, M.; García-Gómez, M.; Bowker, M. A.; Soliveres, S.; Escolar, C.; García-Palacios, P.; Berdugo, M.; Valencia, E.; Gozalo, B.; Gallardo, A.; Aguilera, L.; Arredondo, T.; Blones, J.; Boeken, B.; Bran, D.; Conceição, A. A.; Cabrera, O.; Chaieb, M.; Derak, M.; Eldridge, D. J.; Espinosa, C. I.; Florentino, A.; Gaitán, J.; Gatica, M. G.; Ghiloufi, W.; Gómez-González, S.; Gutiérrez, J. R.; Hernández, R. M.; Huang, X.; Huber-Sannwald, E.; Jankju, M.; Miriti, M.; Monerris, J.; Mau, R. L.; Morici, E.; Naseri, K.; Ospina, A.; Polo, V.; Prina, A.; Pucheta, E.; Ramírez-Collantes, D. A.; Romão, R.; Tighe, M.; Torres-Díaz, C.; Val, J.; Veiga, J. P.; Wang, D.; Zaady, E. Plant Species Richness and Ecosystem Multifunctionality in Global Drylands. *Science* **2012**, *335* (6065), 214–218. https://doi.org/10.1126/science.1215442.
(40) Liu, Y.-R.; Delgado-Baquerizo, M.; Trivedi, P.; He, J.-Z.; Wang, J.-T.; Singh, B. K. Identity of Biocrust Species and Microbial Communities Drive the Response of Soil Multifunctionality to Simulated Global Change. *Soil Biology and Biochemistry* **2017**, *107*, 208–217. https://doi.org/10.1016/j.soilbio.2016.12.003.
(41) Lefcheck, J. S.; Byrnes, J. E. K.; Isbell, F.; Gamfeldt, L.; Griffin, J. N.; Eisenhauer, N.; Hensel, M. J. S.; Hector, A.; Cardinale, B. J.; Duffy, J. E. Biodiversity Enhances Ecosystem Multifunctionality across Trophic Levels and Habitats. *Nat Commun* **2015**, *6* (1), 6936. https://doi.org/10.1038/ncomms7936.
(42) Simonin, M.; Richaume, A.; Guyonnet, J. P.; Dubost, A.; Martins, J. M. F.; Pommier, T. Titanium Dioxide Nanoparticles Strongly Impact Soil Microbial Function by Affecting Archaeal Nitrifiers. *Sci Rep* **2016**, *6* (1), 33643. https://doi.org/10.1038/srep33643.
(43) Vijayaraj, V.; Liné, C.; Cadarsi, S.; Salvagnac, C.; Baqué, D.; Elger, A.; Barret, M.; Mouchet, F.; Larue, C. Transfer and Ecotoxicity of Titanium Dioxide Nanoparticles in Terrestrial and Aquatic Ecosystems: A Microcosm Study. *Environ. Sci. Technol.* **2018**, *52* (21), 12757–12764. https://doi.org/10.1021/acs.est.8b02970.
(44) Leroy, M.; Pey, B.; Jassey, V. E. J.; Liné, C.; Elger, A.; Probst, A.; Flahaut, E.; Silvestre, J.; Larue, C. Interactive Effects of Metals and Carbon Nanotubes in a Microcosm Agrosystem. *Journal of Hazardous Materials* **2022**, *431*, 128613. https://doi.org/10.1016/j.jhazmat.2022.128613.
(45) Jurasinski, G.; Koebsch, F.; Guenther, A.; Beetz, S. *Flux Rate Calculation from Dynamic Closed Chamber Measurements*; 2022.
(46) Fuss, R.; Hueppi, R.; function (version 0.3.1)), A. R. P. (for code copied from the not-exported H. H. fit1. *Gasfluxes: Greenhouse Gas Flux Calculation from Chamber Measurements*; 2020.
(47) Kutzbach, L.; Schneider, J.; Sachs, T.; Giebels, M.; Nykänen, H.; Shurpali, N. J.; Martikainen, P. J.; Alm, J.; Wilmking, M. CO_2 Flux Determination by Closed-Chamber Methods Can Be Seriously

Biased by Inappropriate Application of Linear Regression. *Biogeosciences* **2007**, *4* (6), 1005–1025. https://doi.org/10.5194/bg-4-1005-2007.
(48) Josephson, K. L.; Gerba, C. P.; Pepper, I. L. Polymerase Chain Reaction Detection of Nonviable Bacterial Pathogens. *Applied and Environmental Microbiology* **1993**, *59* (10), 3513–3515. https://doi.org/10.1128/aem.59.10.3513-3515.1993.
(49) Kralik, P.; Ricchi, M. A Basic Guide to Real Time PCR in Microbial Diagnostics: Definitions, Parameters, and Everything. *Frontiers in Microbiology* **2017**, *8*.
(50) Du, J.; Qv, W.; Niu, Y.; Yuan, S.; Zhang, L.; Yang, H.; Zhang, Y. Co-Exposures of Acid Rain and ZnO Nanoparticles Accelerate Decomposition of Aquatic Leaf Litter. *Journal of Hazardous Materials* **2022**, *426*, 128141. https://doi.org/10.1016/j.jhazmat.2021.128141.
(51) Evariste, L.; Mottier, A.; Lagier, L.; Cadarsi, S.; Barret, M.; Sarrieu, C.; Soula, B.; Mouchet, F.; Flahaut, E.; Pinelli, E.; Gauthier, L. Assessment of Graphene Oxide Ecotoxicity at Several Trophic Levels Using Aquatic Microcosms. *Carbon* **2020**, *156*, 261–271. https://doi.org/10.1016/j.carbon.2019.09.051.
(52) Wu, F.; You, Y.; Zhang, X.; Zhang, H.; Chen, W.; Yang, Y.; Werner, D.; Tao, S.; Wang, X. Effects of Various Carbon Nanotubes on Soil Bacterial Community Composition and Structure. *Environmental Science & Technology* **2019**. https://doi.org/10.1021/acs.est.8b06909.
(53) Liu, S.; Zeng, T. H.; Hofmann, M.; Burcombe, E.; Wei, J.; Jiang, R.; Kong, J.; Chen, Y. Antibacterial Activity of Graphite, Graphite Oxide, Graphene Oxide, and Reduced Graphene Oxide: Membrane and Oxidative Stress. *ACS Nano* **2011**, *5* (9), 6971–6980. https://doi.org/10.1021/nn202451x.
(54) Chung, H.; Kim, M. J.; Ko, K.; Kim, J. H.; Kwon, H.; Hong, I.; Park, N.; Lee, S.-W.; Kim, W. Effects of Graphene Oxides on Soil Enzyme Activity and Microbial Biomass. *Science of The Total Environment* **2015**, *514*, 307–313. https://doi.org/10.1016/j.scitotenv.2015.01.077.
(55) Yang, H.; Feng, S.; Ma, Q.; Ming, Z.; Bai, Y.; Chen, L.; Yang, S.-T. Influence of Reduced Graphene Oxide on the Growth, Structure and Decomposition Activity of White-Rot Fungus Phanerochaete Chrysosporium. *RSC Advances* **2018**, *8* (9), 5026–5033. https://doi.org/10.1039/C7RA12364G.
(56) Xie, J.; Ming, Z.; Li, H.; Yang, H.; Yu, B.; Wu, R.; Liu, X.; Bai, Y.; Yang, S.-T. Toxicity of Graphene Oxide to White Rot Fungus Phanerochaete Chrysosporium. *Chemosphere* **2016**, *151*, 324–331. https://doi.org/10.1016/j.chemosphere.2016.02.097.
(57) Liang, Z.; Tu, Q.; Su, X.; Yang, X.; Chen, J.; Chen, Y.; Liu, C.; Li, H.; He, Q. Formation, Extracellular Polymeric Substances and Microbial Community of Aerobic Granules Enhanced by Microbial Flocculant Compared with Poly-Aluminum Chloride. *Journal of Cleaner Production* **2019**, *220*, 544–552. https://doi.org/10.1016/j.jclepro.2019.02.180.
(58) Song, P.; Huang, G.; Hong, Y.; An, C.; Xin, X.; Zhang, P. A Biophysiological Perspective on Enhanced Nitrate Removal from Decentralized Domestic Sewage Using Gravitational-Flow Multi-Soil-Layering Systems. *Chemosphere* **2020**, *240*, 124868. https://doi.org/10.1016/j.chemosphere.2019.124868.
(59) Zheng, X.; Chen, Y.; Wu, R. Long-Term Effects of Titanium Dioxide Nanoparticles on Nitrogen and Phosphorus Removal from Wastewater and Bacterial Community Shift in Activated Sludge. *Environ. Sci. Technol.* **2011**, *45* (17), 7284–7290. https://doi.org/10.1021/es2008598.
(60) Leroy, M.; Flahaut, E.; Larue, C. Carbon Based Nanomaterial Interactions with Metals and Metalloids in Terrestrial Environment: A Review. *Carbon* **2023**, *206*, 325–339. https://doi.org/10.1016/j.carbon.2023.02.047.
(61) Beeckman, F.; Motte, H.; Beeckman, T. Nitrification in Agricultural Soils: Impact, Actors and Mitigation. *Current Opinion in Biotechnology* **2018**, *50*, 166–173. https://doi.org/10.1016/j.copbio.2018.01.014.
(62) Tollenaar, M.; Deen, W.; Echarte, L.; Liu, W. Effect of Crowding Stress on Dry Matter Accumulation and Harvest Index in Maize. *Agronomy Journal* **2006**, *98* (4), 930–937. https://doi.org/10.2134/agronj2005.0336.

(63) Turhan, E.; Eris, A. Changes of Micronutrients, Dry Weight, and Chlorophyll Contents in Strawberry Plants Under Salt Stress Conditions. *Communications in Soil Science and Plant Analysis* **2005**, *36* (7–8), 1021–1028. https://doi.org/10.1081/CSS-200050418.
(64) Lattanzio, V. Phenolic Compounds: Introduction. In *Natural Products: Phytochemistry, Botany and Metabolism of Alkaloids, Phenolics and Terpenes*; 2013; pp 1543–1580. https://doi.org/10.1007/978-3-642-22144-6_57.
(65) War, A. R.; Paulraj, M. G.; Ahmad, T.; Buhroo, A. A.; Hussain, B.; Ignacimuthu, S.; Sharma, H. C. Mechanisms of Plant Defense against Insect Herbivores. *Plant Signaling & Behavior* **2012**, *7* (10), 1306–1320. https://doi.org/10.4161/psb.21663.
(66) Chen, Z.; Zhao, J.; Cao, J.; Zhao, Y.; Huang, J.; Zheng, Z.; Li, W.; Jiang, S.; Qiao, J.; Xing, B.; Zhang, J. Opportunities for Graphene, Single-Walled and Multi-Walled Carbon Nanotube Applications in Agriculture: A Review. *Crop Design* **2022**, *1* (1), 100006. https://doi.org/10.1016/j.cropd.2022.100006.
(67) Striolo, A.; Chialvo, A. A.; Gubbins, K. E.; Cummings, P. T. Water in Carbon Nanotubes: Adsorption Isotherms and Thermodynamic Properties from Molecular Simulation. *J. Chem. Phys.* **2005**, *122* (23), 234712. https://doi.org/10.1063/1.1924697.
(68) Martínez-Ballesta, M. C.; Zapata, L.; Chalbi, N.; Carvajal, M. Multiwalled Carbon Nanotubes Enter Broccoli Cells Enhancing Growth and Water Uptake of Plants Exposed to Salinity. *Journal of Nanobiotechnology* **2016**, *14* (1), 42. https://doi.org/10.1186/s12951-016-0199-4.
(69) Tiwari, D. K.; Dasgupta-Schubert, N.; Villaseñor Cendejas, L. M.; Villegas, J.; Carreto Montoya, L.; Borjas García, S. E. Interfacing Carbon Nanotubes (CNT) with Plants: Enhancement of Growth, Water and Ionic Nutrient Uptake in Maize (Zea Mays) and Implications for Nanoagriculture. *Appl Nanosci* **2014**, *4* (5), 577–591. https://doi.org/10.1007/s13204-013-0236-7.
(70) Lozano, Y. M.; Aguilar-Trigueros, C. A.; Onandia, G.; Maaß, S.; Zhao, T.; Rillig, M. C. Effects of Microplastics and Drought on Soil Ecosystem Functions and Multifunctionality. *Journal of Applied Ecology* **2021**, *58* (5), 988–996. https://doi.org/10.1111/1365-2664.13839.

5. Supporting information

Carbon nanotube impacts on geochemical cycles in an agrosystem: an integrative approach

Leroy Mathieu[1,2], Jassey Vincent E.J.[1], Flahaut Emmanuel [2], Silvestre Jérôme[1], Barret Maialen[1], Melissa Sontag1, Larue Camille[1]

[1]Laboratoire Ecologie Fonctionnelle et Environnement, Université de Toulouse, CNRS, Toulouse, France, [2]CIRIMAT, Université de Toulouse, CNRS, INPT, UPS, UMR CNRS-UPS-INP N°5085, Université Toulouse 3 Paul Sabatier, Bât. CIRIMAT, 118, route de Narbonne, 31062 Toulouse cedex 9, France

2. Material and Methods

2.1. CNT synthesis and characterization

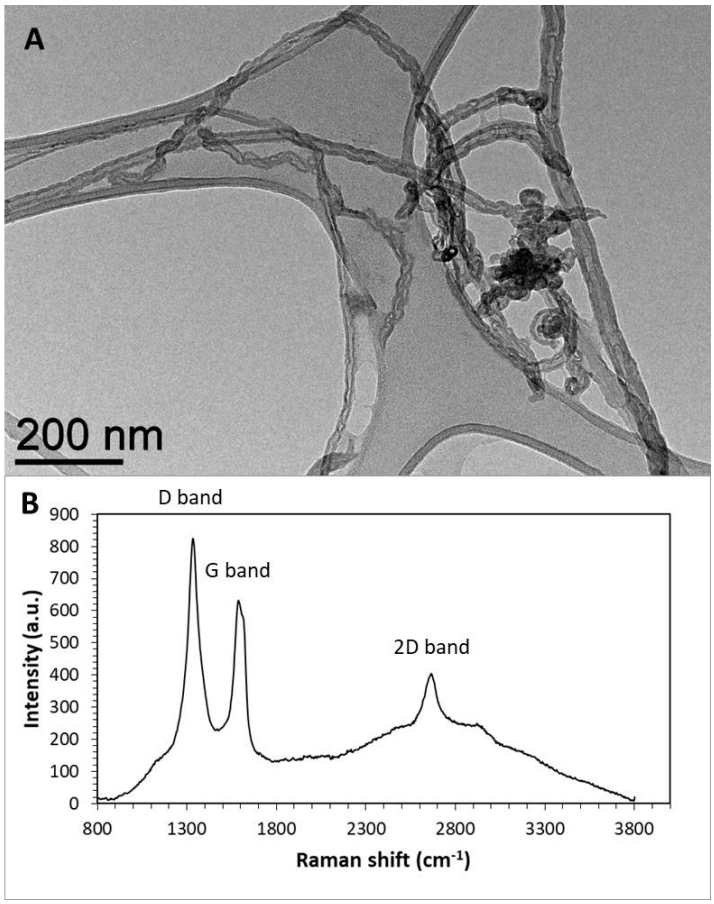

Figure S1: CNT characterization (A) observed by transmission electron microscope (A) and CNT powder Raman scattering spectrum obtained using a 633 nm wavelength laser

2.2. Soil characterization and contamination

Table S2: Soil physico-chemical characterization after exposure. Average and standard deviation for clay, silt, sand, C/N, N, organic C (Corg) and pH for the 3 CNT modalities (0 = 0 mg kg^{-1}, 0.1 = 0.1 mg kg^{-1}, 10 = 10 mg kg^{-1}). Same lowercase letters indicate treatments that do not differ significantly (p-value > 0.05) following an ANOVA (pH, loam, C/N, N and C) or Kruskal-Wallis test (clay, sand and Corg) (n = 5)

CNT concentration	pH	Clay (%)	Silt (%)	Sand (%)	Corg (%)	N (%)	C (%)	C/N
0	5.1 ± 0.1 **a**	1.5 ± 0.1 **a**	12.7 ± 0.6 **a**	85.8 ± 0.6 **a**	1.3 ± 0.2 **a**	0.04 ± 0.005 **a**	0.5 ± 0.1 **a**	13.4 ± 0.9 **a**
0.1	5.0 ± 0.1 **a**	1.4 ± 0.1 **a**	11.6 ± 1.0 **a**	87.0 ± 1.0 **a**	1.3 ± 0.04 **a**	0.04 ± 0.006 **a**	0.5 ± 0.1 **a**	14.0 ± 0.7 **a**
10	5.0 ± 0.1 **a**	1.2 ± 0.1 **a**	13.5 ± 1.2 **a**	85.3 ± 1.2 **a**	1.5 ± 0.1 **a**	0.04 ± 0.004 **a**	0.58 ± 0.04 **a**	14.1 ± 0.4 **a**

Table S3: Soil elemental concentrations quantified by ICP-AES after exposure for the 3 CNT modalities (0 = 0 mg kg^{-1}, 0.1 = 0.1 mg kg^{-1}, 10 = 10 mg kg^{-1}). Same lowercase letters indicate treatments that do not differ significantly (p-value > 0.05) following an ANOVA (B, Ca, Cd, Fe, Mg, Mn, Ni, P, Pb and Zn) or Kruskal-Wallis test (Cu, Na and S) (n = 5)

CNT concentration	B	Ca	Cd	Cu	Fe	Mg
0	5.29 ± 0.7 **a**	1408.34 ± 99.2 **a**	0.02 ± 0.004 **a**	0.73 ± 0.02 **a**	13.26 ± 0.66 **ab**	815.57 ± 9.5 **a**
0.1	5.63 ± 0.4 **a**	1518.58 ± 91.3 **a**	0.02 ± 0.004 **a**	0.72 ± 0.09 **a**	11.32 ± 0.35 **a**	966.15 ± 94.3 **b**
10	7.96 ± 0.5 **b**	1427.63 ± 55.2 **a**	0.02 ± 0.005 **a**	0.7 ± 0.04 **a**	14.15 ± 0.71 **b**	961.84 ± 42.5 **b**
Mn	**Na**	**Ni**	**P**	**Pb**	**S**	**Zn**
24.77 ± 4.3 **a**	20.37 ± 3.4 **ab**	0.13 ± 0.02 **b**	1321.83 ± 50.6 **a**	1.02 ± 1.02 **a**	186.73 ± 24.7 **a**	7.08 ± 1.6 **a**
29.59 ± 4.4 **a**	17.27 ± 2.6 **a**	0.12 ± 0.02 **ab**	1815.95 ±160.6 **b**	0.89 ± 0.1 **a**	188.67 ± 19.2 **a**	11.58 ± 2.5 **a**
24.93 ± 3.6 **a**	32.79 ± 5.5 **b**	0.09 ± 0.02 **a**	1402.91 ± 163.1 **a**	1.04 ± 0.1 **a**	164.25 ± 92 **a**	10.98 ± 1.6 **a**

2.4. Bacterial abundance, litter decomposition and microbial communities

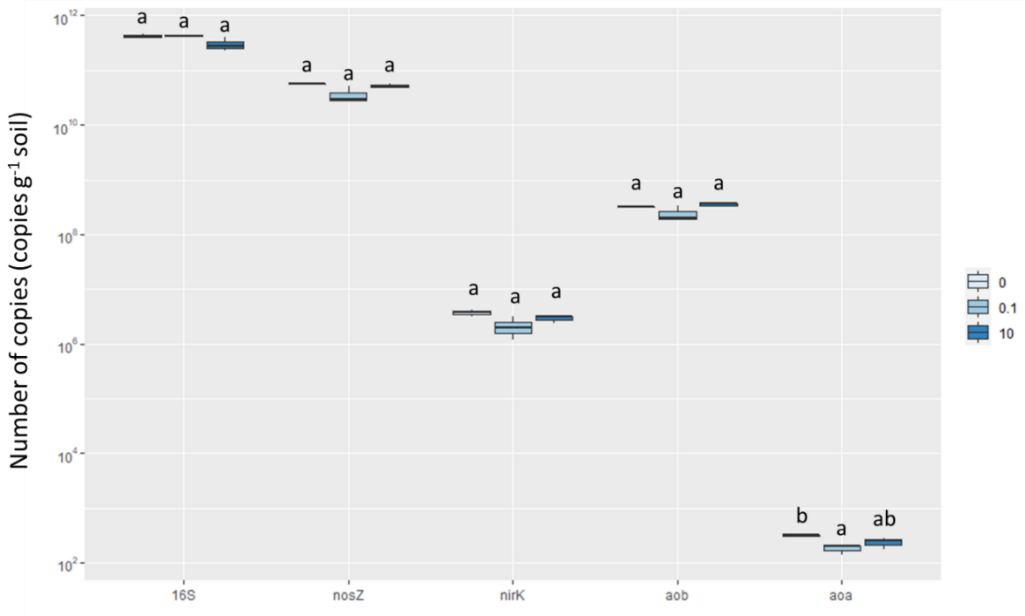

Figure S2: rRNA 16S, nosZ, nirK, aob and aoa number of copies at the beginning of experiment for the 3 CNT modalities (0 = 0 mg.kg^{-1}, 0.1 = 0.1 mg.kg^{-1}, 10 = 10 mg.kg^{-1}) as determined by qPCR. Same lowercase letters indicate treatments that do not differ significantly (p-value > 0.05) following an ANOVA.

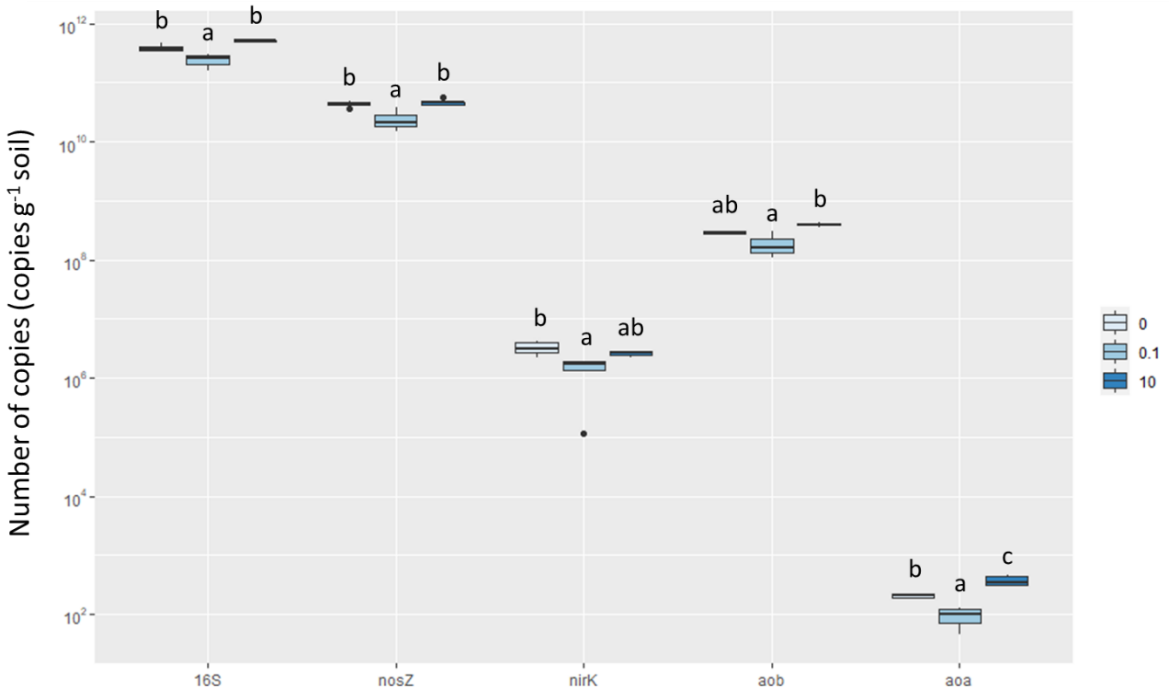

Figure S3: rRNA 16S, nosZ, nirK, aob and aoa number of copies at the end of experiment for the 3 CNT modalities (0 = 0 mg.kg^{-1}, 0.1 = 0.1 mg.kg^{-1}, 10 = 10 mg.kg^{-1}) as determined by qPCR. Same lowercase letters indicate treatments that do not differ significantly (p-value > 0.05) following an ANOVA.

2.5. Phytotoxicity parameters

The photochemical efficiency of photosystem II was determined by spectrofluorometry[1] on the basis of the effective quantum yield (EQY) $\phi_{PSII} = (F_m' - F_t)/F_m' = \Delta F/F_m'$ (F_m' is the steady state maximum fluorescence measured after a saturating pulse and F_t the steady-state fluorescence level after a period of constant actinic light) without dark adaptation using a portable field device (Diving-PAM, Walz, Germany). The DLC-8 leaf clips were used to keep a constant distance between the leaf and the optical fiber.

For other biomarkers, dry leaf material was ground twice in a ball mill for 1.5 minutes. 50 mg of this material was placed in a 2 ml microplate with 96 wells filled with 1.5 ml of 95% methanol. The plate was mixed for 2 min, incubated in the dark at 4°C for 24 and 48 h respectively, for chlorophyll a and b and secondary metabolites (phenolic compounds, flavonoids and tannins). After incubation and

centrifugation (5 min at 4500 rpm), chlorophyll a and b were measured by transferring 100 µl of the supernatant to new microplates and measuring absorbance at 470, 652 and 666 nm.

For phenolic compounds, 200 µl reaction mixture contained 20 µl supernatant, 40 µl Folin reagent (10% v/v) and 0.10 mM sodium hydrogen carbonate ($NaHCO_3$). The mixture was allowed to stand for 2 hours at room temperature for colour development. Then the absorbance was measured at 760 nm.

Flavonoids was determined with the reaction mixture (final volume 200 µL) contained 25 µL of methanolic extract, 7.25 µM sodium nitrite ($NaNO_2$), 0.11 µM aluminium chloride ($AlCl_3$) and 0.02 mM sodium hydroxide (NaOH). The mixture was homogenised for 1 minute and the absorbance was measured at 595 nm. For tannins, the reaction mixture (final volume of 100 µl) contained 50 µl of methanolic extract and 6.57 µmol of vanillin[2]. The mixture was left in the dark for 15 minutes and the absorbance was measured at 500 nm.

The concentrations of phenolic, flavonoid and tannin compounds were calculated using standard gallic acid and catechin curves, respectively.

3.2. Crop endpoints

Table S3: Elemental concentrations in maize leaves for the 3 CNT modalities (0 = 0 mg.kg^{-1}, 0.1 = 0.1 mg.kg^{-1}, 10 = 10 mg.kg^{-1}) after a six week-exposure in soil. Same lowercase letters indicate treatments that do not differ significantly (p-value > 0.05) following an ANOVA (B, Ca, Cd, Fe, Mg, Mn, Ni, P, Pb and Zn) or Kruskal-Wallis test (C, Na and S) (n = 5)

CNT concentration	B	Ca	Cd	Cu	Fe	Mg
0	4.85 ± 0.7 a	1238.9 ± 91.6 a	0.01 ± 0.002 a	0.61 ± 0.02 a	5.83 ± 0.6 b	811.39 ± 8.0 a
0.1	5.53 ± 0.4 a	1370.59 ± 90.3 a	0.012 ± 0.002 a	0.61 ± 0.1 a	3.97 ± 0.1 a	962.24 ± 93.4 b
10	7.92 ± 0.5 b	1274.4 ± 63.5 a	0.01 ± 0.003 a	0.59 ± 0.1 a	5.27 ± 0.5 b	957.5 ± 42.6 b
Mn	**Na**	**Ni**	**P**	**Pb**	**S**	**Zn**
20.22 ± 3.8 a	16.0 ± 2.9 ab	0.12 ± 0.03 a	1321.06 ± 44.4 b	0.07 ± 0.005 a	189.71 ± 23.2 a	6.62 ± 1.5 a
24.72 ± 4.4 a	12.44 ± 3.0 a	0.11 ± 0.02 a	1812.48 ± 160.3 a	0.12 a	186.92 ± 19.0 a	11.18 ± 2.5 b
19.66 ± 3.8 a	27.93 ± 5.8 b	0.09 ± 0.02 a	1399.51 ± 163.2 b	0.13 ± 0.1 a	203.52 ± 15.6 a	10.45 ± 1.7 b

3.3. Gaz exchange

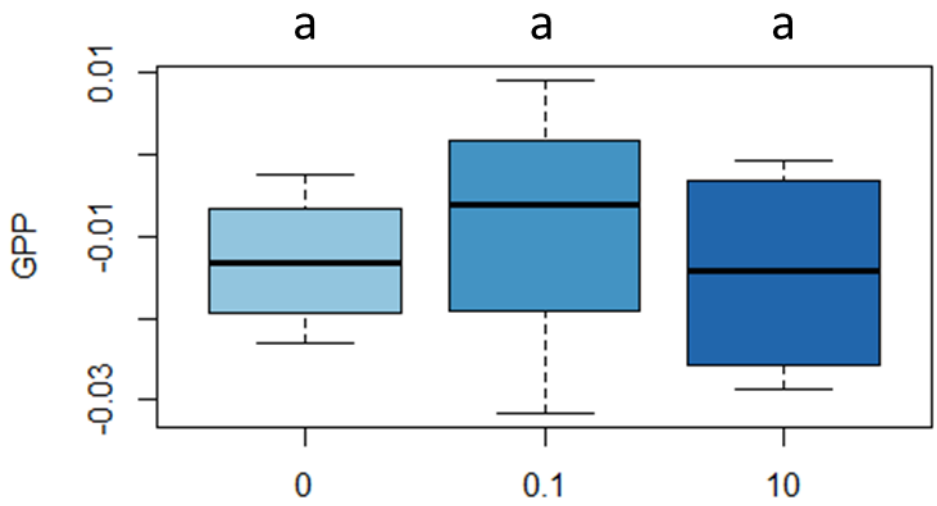

Figure S4: Gross Primary Production (GPP) of microcosms for the 3 CNT modalities (0 = 0 mg.kg^{-1}, 0.1 = 0.1 mg.kg^{-1}, 10 = 10 mg.kg^{-1}). Same lowercase letters indicate treatments that do not differ significantly (p-value > 0.05) following an ANOVA.

Bibliography (Supporting Information article : Carbon nanotube impacts on geochemical cycles in an agrosystem: an integrative approach) :

(1) Genty, B.; Briantais, J.-M.; Baker, N. R. The Relationship between the Quantum Yield of Photosynthetic Electron Transport and Quenching of Chlorophyll Fluorescence. *Biochimica et Biophysica Acta (BBA) - General Subjects* **1989**, *990* (1), 87–92. https://doi.org/10.1016/S0304-4165(89)80016-9.

(2) El Euch, S. K.; Bouajila, J.; Bouzouita, N. Chemical Composition, Biological and Cytotoxic Activities of Cistus Salviifolius Flower Buds and Leaves Extracts. *Industrial Crops and Products* **2015**, *76*, 1100–1105. https://doi.org/10.1016/j.indcrop.2015.08.033.

Chapitre 5 : Caractérisation des impacts d'une co-contamination en NTC et ETM sur un agrosystème

Depuis l'émergence de l'intérêt porté sur les impacts sur les écosystèmes naturels des différentes substances que l'Homme émet en raison de ses activités, de nombreuses questions de recherches ont vu le jour afin de caractériser au mieux ces impacts. La conduite concomitante d'études en laboratoire et *in situ* est le levier de recherche en écotoxicologie qui permet à la fois d'envisager et de constater les impacts de ces substances. En raison de la nature des conditions expérimentales qui diffèrent entre les approches en laboratoire et *in situ*, les résultats en termes de transfert et de toxicité des substances peuvent varier et mener à des conclusions quelque peu différentes. Notamment, la multiplicité toujours plus importante des substances dans les écosystèmes s'avère être un facteur essentiel à considérer en raison des interactions entre substances qui peuvent se produire et des modifications de transfert et de toxicité qui en résultent[1–5]. De plus, ces substances, une fois intégrées dans les écosystèmes, peuvent se voir modifier au cours du temps et ainsi se comporter différemment qu'au début de leur émission. L'impact de cette transformation ou vieillissement des substances doit être étudié afin de mieux caractériser le risque lié à la dissémination des contaminants.

A ce jour, l'évaluation des risques écologiques des mélanges de substances repose sur l'hypothèse de l'additivité des risques induits individuellement par chacune des substances, il convient de renforcer les connaissances sur les interactions entre substances ainsi que leur modulation écotoxicologique (synergie et antagonisme, entre autres) afin d'amorcer un changement de paradigme. On sait depuis longtemps que les ETM seuls en laboratoire et *in situ* sont toxiques et le corpus scientifique tend à montrer la même chose pour les NTC, dans une moindre mesure. D'ailleurs, les résultats du chapitre 4 ont mis en évidence des altérations de différentes fonctions des agrosystèmes après exposition aux NTC seuls. De plus, on sait que ces deux contaminants peuvent interagir du fait des phénomènes d'adsorption possibles dans des conditions environnementales (*cf*. chapitre 3). Dès lors, ce chapitre propose d'étudier les effets de substances en mélange dont les interactions sont avérées, à savoir les

NTC et les ETM, sur des agrosystèmes ainsi que l'effet du vieillissement de ces contaminants. Deux types de vieillissement ont été envisagés : (i) en ajoutant un mélange d'ETM et de NTC dans un sol « standard » (Lufa Speyer) et en le laissant vieillir pendant 2 ans et (ii) en utilisant un sol historiquement contaminé en ETM (ancien site industriel de MetalEurop) et en ajoutant des NTC.

Pour le premier design expérimental et fort de l'expérience acquise au cours de la précédente expérimentation, les cycles du C et du N ont une nouvelle fois été étudiés à travers le suivi de l'émission de CO_2 à l'échelle du microcosme, de l'abondance des taxons bactériens liés aux processus de nitrification et dénitrification, de la décomposition de la MO et de la concentration en chlorophylle contenue dans les feuilles des plantes. Les biomarqueurs métaboliques tels que les composés phénoliques et tanins et la production de biomasse de la plante (monocotylédone : *Zea mays* L. subsp.mays) ont aussi été étudiés afin de renseigner sur la toxicité de la co-contamination de la plante d'intérêt agronomique.

Afin de vérifier les hypothèses émises sur les effets des NTC sur le cycle de l'eau et la décomposition de la MO, la transpiration foliaire et l'abondance des champignons du sol ainsi que le suivi des activités enzymatiques liées aux cycles du C et du N ont été suivies.

Dans un second temps, les effets d'une contamination historique en ETM et de l'ajout de NTC ont été étudiés en ajoutant un maillon trophique avec la présence de vers de terre (*Eisenia fetida*) en plus des bactéries natives et d'une plante d'intérêt agronomique (dicotylédone : *Lactuca sativa*). Cette expérience a été menée au cours du stage de fin d'étude (master 2) réalisé en 2019. L'article écrit et publié au cours de la thèse n'est pas intégré dans le manuscrit puisque ce travail n'a pas été réalisé au cours des années de thèse mais, compte tenu de sa complémentarité et de sa pertinence vis-à-vis du projet doctoral il est cité et recommandé de le consulter par l'intermédiaire du lien ci-contre :

https://www.sciencedirect.com/science/article/pii/S0304389422004010?casa_token=j28nqzt2NVMAAAAA:Upc7FY5SJ607T1KRALKvw5qVA05S8wehydoWztWoHipJRKPXXB54YyA2XZc4w0qz9rsKnS6FrPI

Leroy, M.; Pey, B.; Jassey, V. E. J.; Liné, C.; Elger, A.; Probst, A.; Flahaut, E.; Silvestre, J.; Larue, C. Interactive Effects of Metals and Carbon Nanotubes in a Microcosm Agrosystem. *Journal of Hazardous Materials* **2022**, *431*, 128613. https://doi.org/10.1016/j.jhazmat.2022.128613.

PRINCIPAUX RESULTATS

Expérience 1: Après une exposition de 8 semaines, l'abondance des communautés fongiques et la décomposition de la matière organique ont été diminué avec l'ajout de 0.025 $mg.kg^{-1}$ de NTC tandis que l'activité enzymatique lié au cycle du carbone (pyranosidase) a été augmenté à la même concentration. L'exposition aux ETM n'a eu que peu d'effets sur les marqueurs des processus du sol (communautés fongiques, activités enzymatiques liés au carbone, azote et phosphore et decomposition de la litière). Chez le maïs, l'ajout de NTC dans le milieu n'a pas modifié le transfert des ETM. L'ajout de 0.025 $mg.kg^{-1}$ de NTC a diminué la transpiration du maïs (16%) et bien que pas statistiquement mis en évidence, la teneur en matière sèche du maïs a été augmenté à la même concentration (22%) ce qui témoigne d'un stress hydrique. D'ailleurs, les composés phénoliques, connus pour être impliqué dans la réponse au stress hydrique à été augmenté (30%). L'ajout des ETM dans le sol à uniquement diminué la biomasse du maïs. A l'échelle de l'écosystèmes, la respiration ainsi que la productivité primaire ont été diminué en raison de l'exposition des ETM. En revanche, aucune modification n'a été observé sur l'émission de CO_2 avec l'ajout de NTC. Le vieillissement du sol tend à atténuer les effets toxiques imposés par les NTC. De nombreuses interactions ont été mises en évidence sur l'activité enzymatique lié au carbone (pyranosidase), la decomposition de la litière, la transpiration et la concentration en composés phénoliques. Pour tous ces marqueurs, des effets antagonistes sont à l'oeuvre.

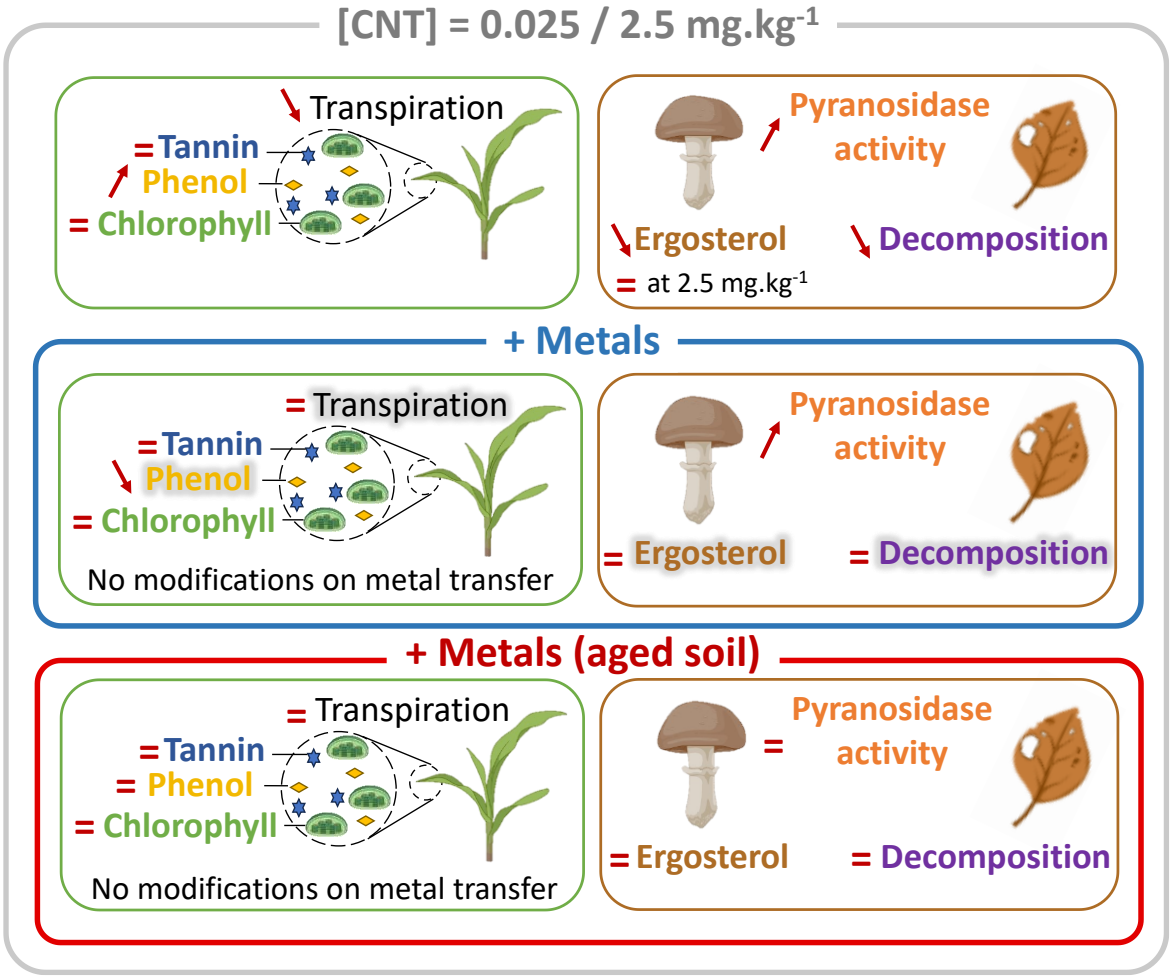

Figure 26 : Schéma récapitulatif des principaux résultats issus de l'expérience du chapitre 5. Si aucune indication n'est présente, alors les résultats des marqueurs étudiés aux concentrations de 0.025 et 2.5 mg.kg^{-1} de NTC sont similaires. Sinon, une indiactaion est ajoutée pour délivrer les résultats obtenus à chacue des concentrations. Les marqueurs aux éclats grisés sont ceux pour lesquels de l'antagonisme a été identifié.

Expérience 2 (stage M2): Après une exposition de 6 semaines, aucun effet toxique de l'ajout de NTC dans des sols historiquement contaminés par des ETM (Cd, Pb et Zn) n'a été détectée sur la concentration bactérienne ou la croissance des vers de terre. Cependant, dans la laitue, un effet interactif entre les NTC et les ETM a été mis en évidence : dans le sol contenant les concentrations élevées d'ETM, l'ajout de 0,1 mg kg^{-1} de NTC a entraîné une perte de biomasse (-22%) et une augmentation de la concentration en flavonoïdes (+27%). Parallèlement, l'ajout de NTC a eu des effets différents sur l'absorption des éléments dans les feuilles de laitue, probablement en rapport avec la teneur en MO du sol. Pour les vers de terre, l'ajout de 10 mg kg^{-1} de NTC a entraîné une augmentation du transfert d'éléments tissulaires dans le cas du sol à plus forte teneur en MO (Pb : + 34 % et Zn : + 25 %).

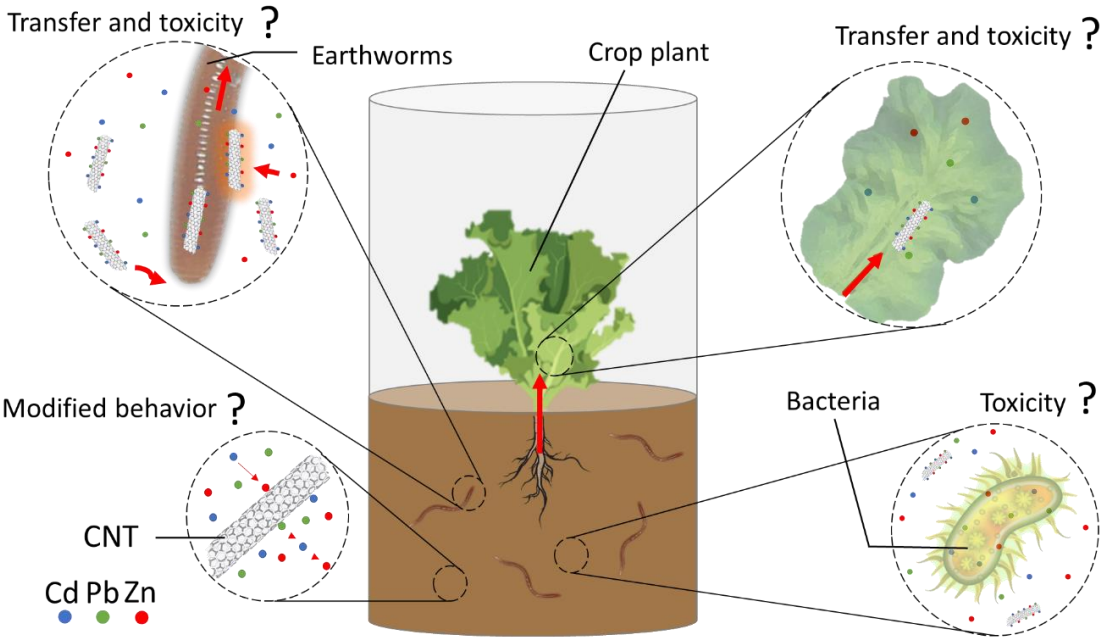

Figure 27: Schéma récapitulatif des principaux résultats issus de l'expérience réalisée au cours du stage de M2

Bibliographie (chapitre 5):

(1) Leroy, M.; Flahaut, E.; Larue, C. Carbon Based Nanomaterial Interactions with Metals and Metalloids in Terrestrial Environment: A Review. *Carbon* **2023**, *206*, 325–339. https://doi.org/10.1016/j.carbon.2023.02.047.

(2) Anderson, T. D.; Zhu, K. Y. Synergistic and Antagonistic Effects of Atrazine on the Toxicity of Organophosphorodithioate and Organophosphorothioate Insecticides to Chironomus Tentans (Diptera: Chironomidae). *Pesticide Biochemistry and Physiology* **2004**, *80* (1), 54–64. https://doi.org/10.1016/j.pestbp.2004.06.003.

(3) Folt, C. L.; Chen, C. Y.; Moore, M. V.; Burnaford, J. Synergism and Antagonism among Multiple Stressors. *Limnology and Oceanography* **1999**, *44* (3part2), 864–877. https://doi.org/10.4319/lo.1999.44.3_part_2.0864.

(4) Holmstrup, M.; Bindesbøl, A.-M.; Oostingh, G. J.; Duschl, A.; Scheil, V.; Köhler, H.-R.; Loureiro, S.; Soares, A. M. V. M.; Ferreira, A. L. G.; Kienle, C.; Gerhardt, A.; Laskowski, R.; Kramarz, P. E.; Bayley, M.; Svendsen, C.; Spurgeon, D. J. Interactions between Effects of Environmental Chemicals and Natural Stressors: A Review. *Science of The Total Environment* **2010**, *408* (18), 3746–3762. https://doi.org/10.1016/j.scitotenv.2009.10.067.

(5) Pavlaki, M. D.; Pereira, R.; Loureiro, S.; Soares, A. M. V. M. Effects of Binary Mixtures on the Life Traits of Daphnia Magna. *Ecotoxicology and Environmental Safety* **2011**, *74* (1), 99–110. https://doi.org/10.1016/j.ecoenv.2010.07.010.

Assessing the impact of a mixture of carbon nanotube and metals and their aging on agrosystems

Leroy Mathieu[1,2], Jassey Vincent E.J.[1], Barret Maialen[1], Silvestre Jérôme [1], Flahaut Emmanuel [2], Larue Camille[1]

[1]Laboratoire écologie fonctionnelle et environnement, Université de Toulouse, CNRS, Toulouse, France, [2]CIRIMAT, Université de Toulouse, CNRS, INPT, UPS, UMR CNRS-UPS-INP N°5085, Université Toulouse 3 Paul Sabatier, Bât. CIRIMAT, 118, route de Narbonne, 31062 Toulouse cedex 9, France

1. Introduction

To date, Ecological Risk Assessment (ERA) for a mixture of contaminants is based on the assumption of the additivity of the risk induced by the substances considered alone. However for more than one decade, it has been recognized that contaminants could interact together modifying their respective transfer and toxicological effects[1–5]. Furthermore, actual ERA guidance on conventional chemicals suffers from insufficient methods to consider the specific interactions of nanomaterials with other abiotic and biotic systems[6,7].

Agrosystems are particularly sensitive receptacles for multiple contaminants especially due to cultural practices and their intensification[8–11]. For instance, the continuous spreading of chemical fertilizers and sewage sludge for fertilization have progressively led to the accumulation of Trace Metal Elements (TME) into agrosystems[8]. In addition, it has been recognized that mining and industrial activities have brought TME, possibly entering agroecosystems by dry and wet deposit[8]. Over time, other emerging chemicals have been introduced into agrosystems such as micro-nano-plastics[12] and other engineered nanomaterials such as carbon nanomaterials[10] (CNMs) that also tend to accumulate in sewage sludge[10,12,13]. Thus, models forecast up to 10 $mg.kg^{-1}$ of CNMs in biosolids while in natural soil it could be up to 0.01 $mg.kg^{-1}$ [14]. Public authorities are monitoring and limiting the amount of few identified contaminants in agrosystems (mostly, TME, and some organic contaminants) to ensure food safety[15] while ignoring so far emerging contaminants such as nanomaterials.

Recently, scientists showed that CNMs can adsorb TME onto their surface[1,16–19]. This phenomenon raises question about the influence of CNMs on TME transfer and toxicity. Indeed, there are many examples in the literature reporting an increase[20–28] or a decrease[20,23,25,26,29,30] in TME transfer from soil to crops upon CNM application followed by the mitigation of TME toxicity (synergic effects[20,22] or antagonist effects[29,31]). In particular, Chen et al.[32] observed a decrease in As concentration in *Solanum nigrum L.* stem (-25%) and leaf (-34%) upon addition of 100 $mg.kg^{-1}$ of multi-walled carbon nanotubes (MWCNT) highlighting an antagonist effect; these same MWCNT promoted an increase in molecules implied in oxidative stress chain (malondialdehyde and proline)[32]. A similar study observed the opposite results (synergic effect) with an enhancement of As uptake upon addition of GO (going from 19.9% in the control condition to 24.6% and 32.1% in the presence of GO concentrations of 0.1 and 1 $mg.L^{-1}$, respectively) and also led to an enhanced decrease in dry biomass of roots and shoots, chlorophyll and rubisco concentrations[22]. Additionally, Zhao *et al.*[23] observed a decrease in Cu concentration in roots and stems by 60% and 67% (resp.) with the addition of 5 $mg.L^{-1}$ GO compared to Cu single contamination, but did not observe interactive effects on growth (biomass, root, stem and leaf lengths) and cellular parameters (photosynthesis, transpiration and stomatal conductance)[23].

In addition, the influence of contaminant aging has already been highlighted for TME[33] with for instance a modeling study predicting that total soil metal concentrations yielding 10% inhibition in freshly amended soils were up to two orders of magnitude smaller than those in corresponding aged soils or field-contaminated soils. However, the impact of ageing on nanomaterial transfer and toxicity is still very scarce not mentioning the impact on nanomaterial interactions with other contaminants. Some authors evidenced contrasted impact of aging processes on CNT toxicity on plants; root growth inhibition was differentially impacted according to CNT nominal diameter: it was reduced following CNT aging in sludge for a diameter < 10 nm whereas it was increased for CNT with a diameter ranging from 40 to 60 nm[34]. Furthermore, it has been shown that natural aging (simulated by dielectric barrier discharge plasma reactor) could modify CNT structure: decreased specific surface area, increased

defects, distorted structure and addition of oxygen-containing functional groups at the surface enhancing their adsorption capacity du to UV and reactive oxygen species (ROS)[35].

In this context, this work based on an integrative approach including both abiotic and biotic components of agrosystems assessed the impact and transfer of a cocktail of contaminants (CNT and TME) fresh or after a two-year aging step in the soil at the individual level on crop plant (growth, dry weight/fresh weight (DW/FW), transpiration, chlorophyll, phenolic compound and tannin concentrations), at the community level on fungi (ergosterol concentration) and on soil bacteria (soil enzymatic activities) but also at the ecosystem level (organic matter decomposition, gas exchange).

2. Material and methods

2.1. CNT synthesis and characterization

Multi-walled CNT were synthesized at the Interuniversity Center of Materials Research and Engineering (CIRIMAT, Toulouse University). Briefly, catalyst powder ($Mg_{0.99}Co_{0.0075}Mo_{0.0025}O$) prepared by citric combustion was introduced in an alumina boat placed at the center of a quartz reactor. Powder was first heated at 1000°C at a speed of 5°C.min^{-1} then cooled down until 120°C at a speed of 5°C.min^{-1}. Then, the reactor was flushed with nitrogen (N_2) at room temperature during 20 min. CNT were functionalized by adding 100 mg of wet CNT to 100 mL of 3M HNO_3 in a 250 mL flask. The mixture was sonicated in an ultrasonic bath during 10 min and the suspension was then heated in reflux conditions at 130°C for 24h, then cooled down to room temperature and filtered through a polypropylene membrane (Merk Millipore, 0.45 µm) leading to oxidized multi-walled CNT with length varying from 1 to 20 µm, an average diameter of 24.2 ± 8.6 nm and a specific surface area of 60 m².g^{-1} (Figure 28). Finally, CNT were dispersed in ultrapure water at 100 mg.L^{-1} and homogenized for 15 min in an ultrasonic bath immediately before use.

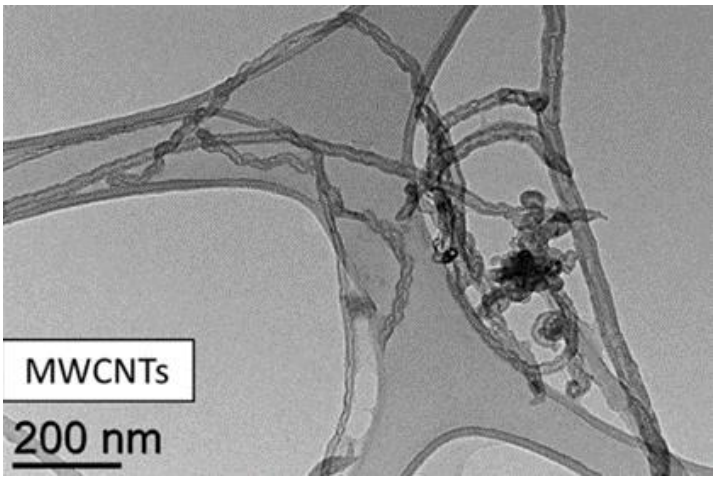

Figure 28: Transmission Electronic Microscopy observation of MWCNT used in this study

2.2. Soil characterization and contamination

A loamy sand soil (LUFA-Speyer 2.1) sieved to 2 mm with 82.1% of sand, 16.8% of loam and 1.1% of clay was used. It contained 0.58 % of organic carbon, 0.05 wt. % of nitrogen, had a pH of 4.6 ± 0.1 and a cation exchange capacity of 2.9 ± 0.2 meq.100g^{-1}. Soils were contaminated by the addition of the required volume of CNT suspension to reach a final concentration of 0.025 or 2.5 mg.kg^{-1} dry soil; the first concentration being close to environmentally predicted concentrations[14] and the second one representing a worst case scenario (use of nanofertiliser, for instance). Additionally, part of the soils were contaminated with Cd, Pb and Zn at 3.8, 104.8 and 71.3 mg.kg^{-1}, respectively with solutions of $CdSO_4 \cdot H_2O$, $Pb(NO_3)_2$, and $Zn(NO_3)_2 \cdot 6H_2O$ (98% purity, Sigma) corresponding to their acceptable concentration limits in European soils[36]. They were then mixed manually for 10 min every day for a week to ensure that CNT and TME were homogeneously distributed in the soil. Aged soils were placed in a dark room at 4°C during 2 years. More information about soil characterization in Table SI 1 and 2.

2.3. Experimental set-up

In each experimental unit (L = 45 cm, D = 10 cm), 300 g of soil were distributed. To study organic matter decomposition, a tea-bag (Lipton green tea sencha, 1079.4 ± 27.7 g) was introduced after the addition of 50 g of soil in each microcosm. One seed of *Zea mays* L. subsp. mays was added in the first two

centimeters. Several exposure modalities were implemented to test the impact of CNT concentration (0, 0.025 and 2.5 mg.kg^{-1}), contamination aging status (freshly added "F" *vs.* aged for 2 years "A") and the addition of TME (addition "M") leading to 9 exposure conditions with 5 biological replicates each (45 microcosms). The experiment lasted for 8 weeks in an environmental chamber with controlled parameters (14 h/10 h day/night cycle, 24°/18 °C and a hygrometry rate of 85%).

2.4. Enzymatic activities, fungal abundance and litter decomposition

After exposure, four soil enzymatic activities were studied as β-glucopyranosidase (pyranosidase, C cycle), β-glucosaminadine (4-MUF-NAG, C cycle), 4-MUB-phosphatase (phosphatase, P cycle) and L-Leucine 7 amino-4-methylcoumarin (leucine aminopeptidse, N cycle), (Sigma-Aldrich®). Three grams of fresh soil were ground in 50 mL of 0.1 M $CaCl_2$ solution with 0.05 % Tween 80 and 20 g polyvinylpolypyrrolidone and shaken for 90 min on a reciprocal shaker (150 rpm). Then, samples were centrifuged (10,000 g for 5 min at 4 °C), the supernatant was filtered (0.45 µm) and concentrated in a cellulose dialysis tube (10 kDa molecular mass cut-off) covered with polyethylene glycol. The concentrated enzymatic extract was recovered in 10 mL (1/10 of the initial volume) phosphate buffer (pH = 5.6; a pH close to field conditions)[37]. For each sample, four pseudo-replicates were incubated in microwells with 22.8 µL of enzymatic extract and 150 µL of fluorescein substrate. In addition, control assays were performed for each sample to account for enzymatic quenching: four pseudo-replicate wells were incubated with 22.8 µL of boiled enzymatic extract (3 h at 90 °C) and 150 µL of fluorescein substrate. Microplates were incubated 3 h at 25 °C in the dark and fluorescence intensity was measured at 490 nm for excitation and 523 nm for emission (BioTek SynergyMX). Potential fluorescein diacetate (FDA) enzymatic activity was calculated in nmol of product degraded per hour and normalized per gram of fresh soil (nmol h^{-1} g^{-1} f.wt).

Ergosterol concentration was determined according to Gesner[38]. To summarize, a first step of hot methanol extraction was performed on soil samples, followed by a solid-phase extraction, and the

purification and quantification of ergosterol by high-performance liquid chromatography (HPLC) with UV detection at 282 nm.

To study litter decomposition, tea bags were weighted before their introduction in the experimental unit and after the 8 weeks of exposure, which permitted to calculate a decomposition rate index as follows:

$$\text{Decomposition rate} = \frac{Mi - Mf}{Duration\ of\ exposure}$$

where the decomposition rate represents litter decomposition ($mg.days^{-1}$), Mi and Mf represent initial and final mass (mg) of tea bag, respectively and duration of exposure is expressed in days.

2.5. Plant morphology and metabolism

After exposure, fresh and dry biomasses were determined. Part of the leaf biomass was oven-dried (60°C) to measure elemental concentrations by ICP-AES (see section 2.7). The remaining biomass was used fresh for methanol-based extraction to quantify photosynthetic pigments (chlorophyll a and b) and secondary metabolites (*i.e.* total phenolic compounds, flavonoids and tannins) as described in Leroy et al.[26]. Transpiration of maize leaf was measured by LI-1600 (LICOR).

2.6. Gas exchange measurements and analysis

At the end of exposure, microcosms were placed in an airtight chamber (V = 7385.28 cm^3) connected to a gas analyzer (SBA-5 CO2 gas analyzer, PPsystems). The evolution of CO_2 concentration contained in the chamber was analyzed for 5 minutes for each microcosm. The slope of gas concentration evolution was calculated and used to determine fluxes ($mg_{gaz}.m^{-2}.h^{-1}$). For each measurement, the first 60 seconds were removed to avoid potential manipulation artifact influence.

Net ecosystem exchanges (NEE) were measured with the transparent chamber, whereas ecosystem respiration (RECO) was assessed using overshadowed “dark” chamber. CO_2 flux data transformation

was performed with RStudio software (version 3.4.1) using the packages "flux"[39] and "gasfluxes"[40] to obtain RECO and NEE data[41]. For NEE, calculations used an exponential nonlinear function to calculate the change in the concentration in the chamber over time[42]. The negative values of NEE indicate a loss of carbon and the positive ones a carbon uptake. RECO was calculated using a linear regression of gas concentrations in the chamber over time. Difference between NEE and RECO traduces the Gross Primary Production (GPP).

2.7. Sample preparation and chemical analysis by ICP-AES

Soil and plants samples (500 mg) were added to 3 ml concentrated HNO_3 overnight. Then, 1 ml of a mix of HNO_3 and $HClO_4$ (3:1 v/v) (only for soil samples) and 1 ml of H_2O_2 were added before introducing the samples in a microwave system (MARS 2, CEM corporation, Matthews, NC, USA) to perform digestion (ramp time: 20-25 min; holding time: 10 min; temperature: 190 °C). For soil, a filtration step (0.45 µm, polypropylene membrane) was added. Digested samples were then diluted to reach 5% HNO_3 in samples before analysis on an ICP-AES (ARCOS FHX22, AMETEK Spectral) along with control samples (blanks with only chemicals).

2.8. Statistical analyses

For statistical analyses, first, 3-way ANOVAs were performed on the toxicity endpoints to test the effects of TME, CNT and soil aging. The normality, independence and homoscedasticity of the residues were checked using Shapiro, Durbin-Watson and Breusch-Pagan tests, respectively. Data were transformed to log or square root if one of the three conditions of validity was not met. A non-parametric Kruskal-Wallis test was performed in the case of failed transformations. All statistical analyses were performed on RStudio software (version 3.4.1).

3. Results

3.1. Mixture and aging impact on belowground processes

3.1.1. Fungi

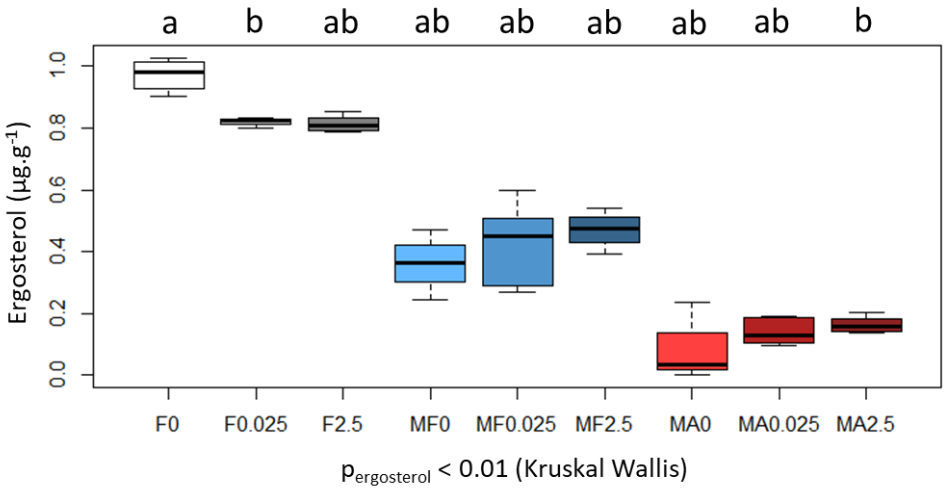

Figure 29: Ergosterol concentration in soil for the 9 exposure modalities (F0, F0.025, F2.5: Fresh soils (F) without TME and with 0, 0.025 and 2.5 mg.kg^{-1}of CNT; MF0, MF0.025, MF2.5: TME Fresh soils (MF) with 0, 0.025 and 2.5 mg.kg^{-1}of CNT; MA0, MA0.025, MA2.5: TME aged soils (MA) with 0, 0.025 and 2.5 mg.kg^{-1} of CNT) after 8 weeks of exposure. Same lowercase letters indicate treatments that do not differ significantly (p-value > 0.05) following a Kruskal Wallis test (n=5).

Although there was nearly a factor 3 between ergosterol concentration in control soil (no TME) and in soil exposed to TME with values of 0.87 and 0.27 µg.g^{-1}, respectively, no statistical difference could be detected (Figure 29). However, there was a significant decrease after CNT addition with soils exposed to 0.025 mg.kg^{-1} CNT without TME containing 16% less ergosterol than control ($p_{Ergosterol}$ < 0.01). Ergosterol concentrations after the contaminant aging step were overall lower than when exposed to freshly added contaminants (-80%).

Finally, no interactions between CNT/TME and CNT/soil aging were detected on ergosterol concentration in soils.

3.1.2. Soil enzymatic activities

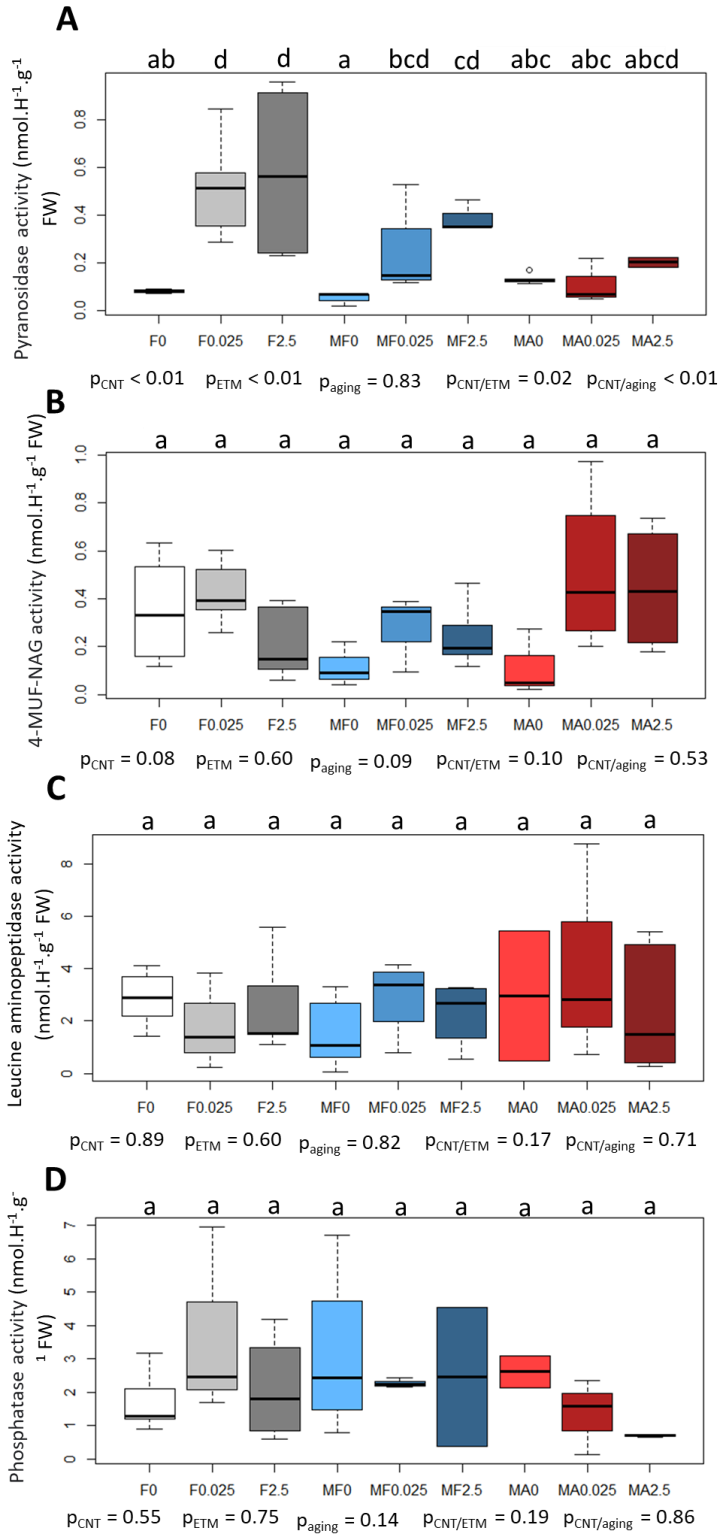

Figure 30: (A) Pyranosidase, (B) 4-MUF-NAG, (C) Leucine amino-peptidase and (D) Phosphatase activity for the 9 exposure modalities (F0, F0.025, F2.5: Fresh soils (F) without TME and with 0, 0.025 and 2.5 mg.kg^{-1}of CNT; MF0, MF0.025, MF2.5: TME Fresh soils (MF) with 0, 0.025 and 2.5 mg.kg^{-1} of CNT; MA0, MA0.025, MA2.5: TME aged soils (MA) with 0, 0.025 and 2.5 mg.kg^{-1}of CNT) after 8 weeks of exposure. Same lowercase letters indicate treatments that do not differ significantly (p-value > 0.05) following a 3-way ANOVA (n=5).

Only pyranosidase activity was modified by the exposure conditions. TME addition led to a decrease of 54% of the enzymatic activity in comparison with soil unexposed to TME ($p_{pyranosidase} < 0.01$, Figure 30A). On the opposite, CNT addition enhanced the enzymatic activity with a 240% and 356% increase in soil exposed to 0.025 and 2.5 mg.kg^{-1} of CNT in comparison with soil unexposed to CNT ($p_{pyranosidase} < 0.01$). However, no impact of the aging step was detected ($p_{pyranosidase} = 0.83$). An interaction between CNT and TME was visible through a decrease of 53% of the enzymatic activity in soil exposed to CNT and TME in comparison with soil exposed only to CNT ($p_{pyranosidase} = 0.02$). Finally, a CNT and soil aging interaction was detected for this soil enzyme with an activity that was 66% higher in fresh soils exposed to CNT than in aged soils exposed to CNT ($p_{pyranosidase} < 0.01$).

For the three other enzymes, glucosimiadine (C cycle), phosphatase (P cycle) and leucyl-aminopeptidase (N cycle) no significant effect were detected (Figure 30B, 3C, 3D).

3.1.3. Organic matter decomposition

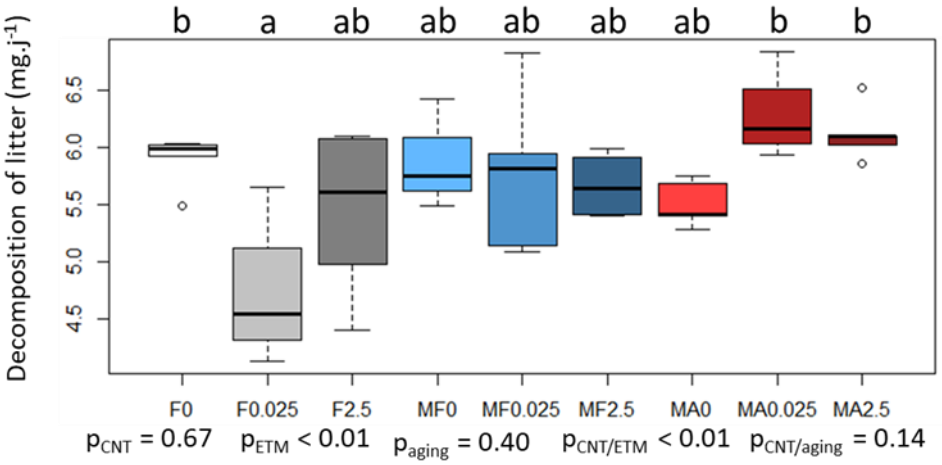

Figure 31: Litter decomposition in soil for the 9 exposure modalities (F0, F0.025, F2.5: Fresh soils (F) without TME and with 0, 0.025 and 2.5 mg.kg^{-1}of CNT; MF0, MF0.025, MF2.5: TME Fresh soils (MF) with 0, 0.025 and 2.5 mg.kg^{-1} of CNT; MA0, MA0.025, MA2.5: TME aged soils (MA) with 0, 0.025 and 2.5 mg.kg^{-1} of CNT) after 8 weeks of exposure. Same lowercase letters indicate treatments that do not differ significantly (p-value > 0.05) following a 3-way ANOVA (n=5).

Litter decomposition was higher up to 9% for microcosm exposed to TME than in those unexposed to TME ($p_{Decomposition\ of\ litter} < 0.01$, Figure 31) but there was no significant effect of CNT addition ($p_{Decomposition}$

$_{\text{of litter}}$ = 0.68) and no effect of the aging process ($p_{\text{Decomposition of litter}}$ = 0.40). An interaction was detected indicating that the decomposition was 19% faster in soil exposed to CNT and TME together than in soil exposed only to CNT ($p_{\text{4-MUB-N-acetyl-β-glucopyranosidase}}$ < 0.01).

3.2. Impact on plant development, metabolism and elemental transfer

3.2.1. Crop TME transfer

Cd, Pb and Zn concentration in maize leaves were significantly higher in maize exposed to TME with on average 2.10, 56.28 and 41.14 mg.kg^{-1}, respectively than in those unexposed with on average 0.002, 0.97 and 14.90 mg.kg^{-1}, respectively (p < 0.01 for the three elements, Figure 32). There was no CNT nor soil aging effects on TME transfer from soil to maize and no interactive effects among factors.

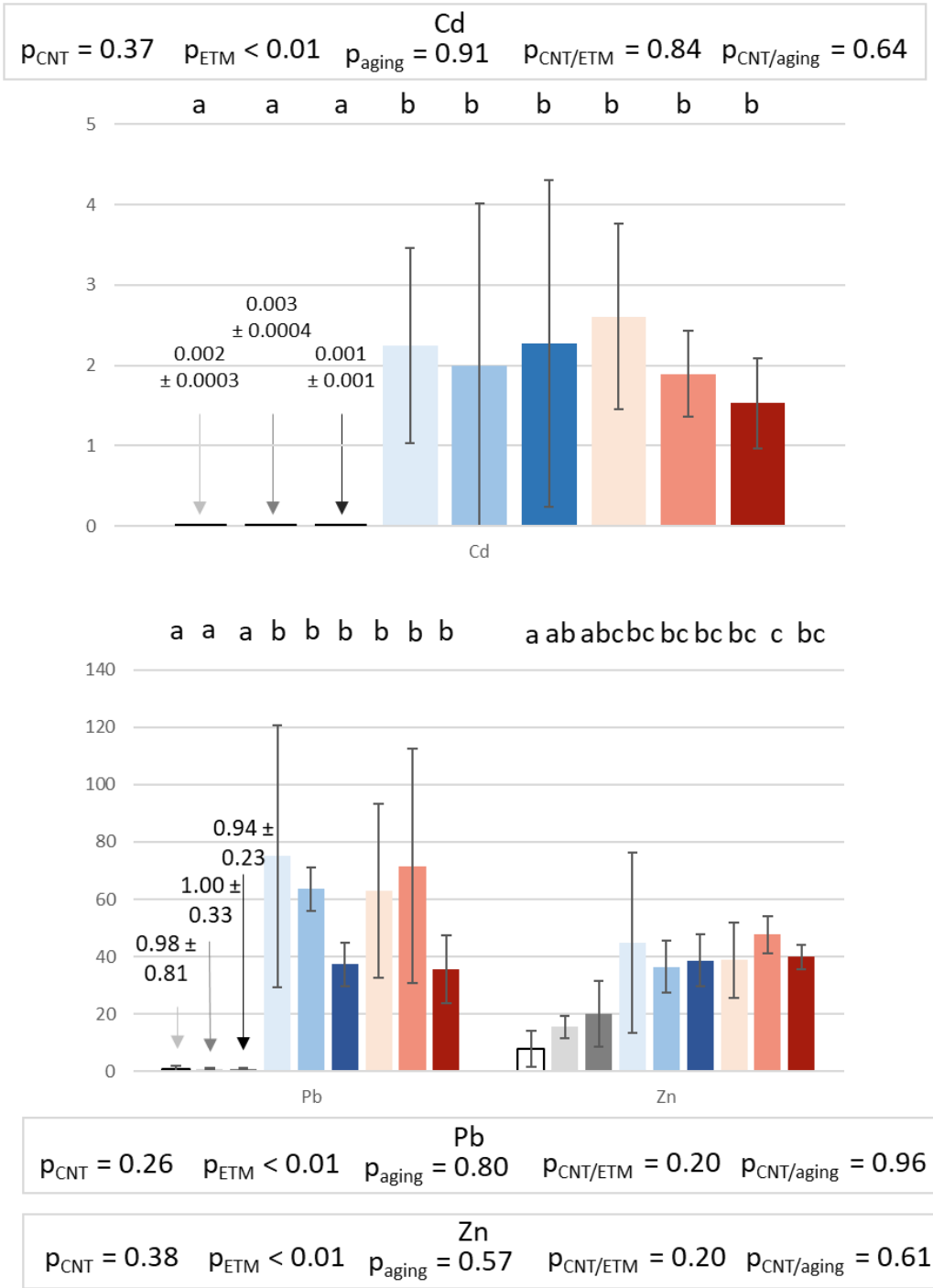

Figure 32: Cd, Pb and Zn concentration in maize leaves grown in the 9 exposure modalities (F0, F0.025, F2.5: Fresh soils (F) without TME and with 0, 0.025 and 2.5 mg.kg^{-1}of CNT; MF0, MF0.025, MF2.5: TME Fresh soils (MF) with 0, 0.025 and 2.5 mg.kg^{-1} of CNT; MA0, MA0.025, MA2.5: TME aged soils (MA) with 0, 0.025 and 2.5 mg.kg^{-1} of CNT) after 8 weeks of exposure. Same lowercase letters indicate treatments that do not differ significantly (p-value > 0.05) following a 3-way ANOVA (n=5).

3.2.2. Toxicity of CNT and TME on crop

The addition of TME led to a significant decrease of maize biomass (-52%, $p_{Biomass} < 0.01$, Figure 33A), and total phenolic compounds (-56%, $p_{phenolic} < 0.01$, Figure 33B) while it enhanced tannin concentration (+52%, $p_{tanin} < 0.01$, Figure 33C).

Likewise, CNT addition impacted maize metabolism with a decreased in leaf transpiration rate (-16%, $p_{Transpiration} < 0.01$, Figure 33C). Phenol and tannin concentrations were also impacted but with opposite effects compared to TME addition: phenol was significantly increased (+30%, $p_{Phenolic} < 0.01$, Figure 33B) while tannin was decreased (-19%, $p_{tanin} < 0.01$, Figure 33C).

The contamination aging step globally led to a decrease of both transpiration rate (-13%, $p_{Transpiration} < 0.01$, Figure 33C) and chlorophyll concentration in leaves (-41% $p_{Chlorophyll} < 0.01$, Figure 33C).

Some interactive effects were detected between CNT and TME such as maize exposed to CNT alone experienced a 168% increase in total phenolic compounds while maize exposed to both CNT and TME underwent through a 24% decreased of the same molecule ($p_{Phenolic} < 0.01$, Figure 33B). Likewise, for the transpiration rate, TME addition seemed to mitigate the impact of CNT: the transpiration rate decreased of 26% after addition of CNT alone while it decreased only of 9% with the addition of both TME and CNT ($p_{Transpiration} < 0.01$, Figure 33C).

The DW/FW was not different among modalities exposure with an average 0.14 (Figure 33B).

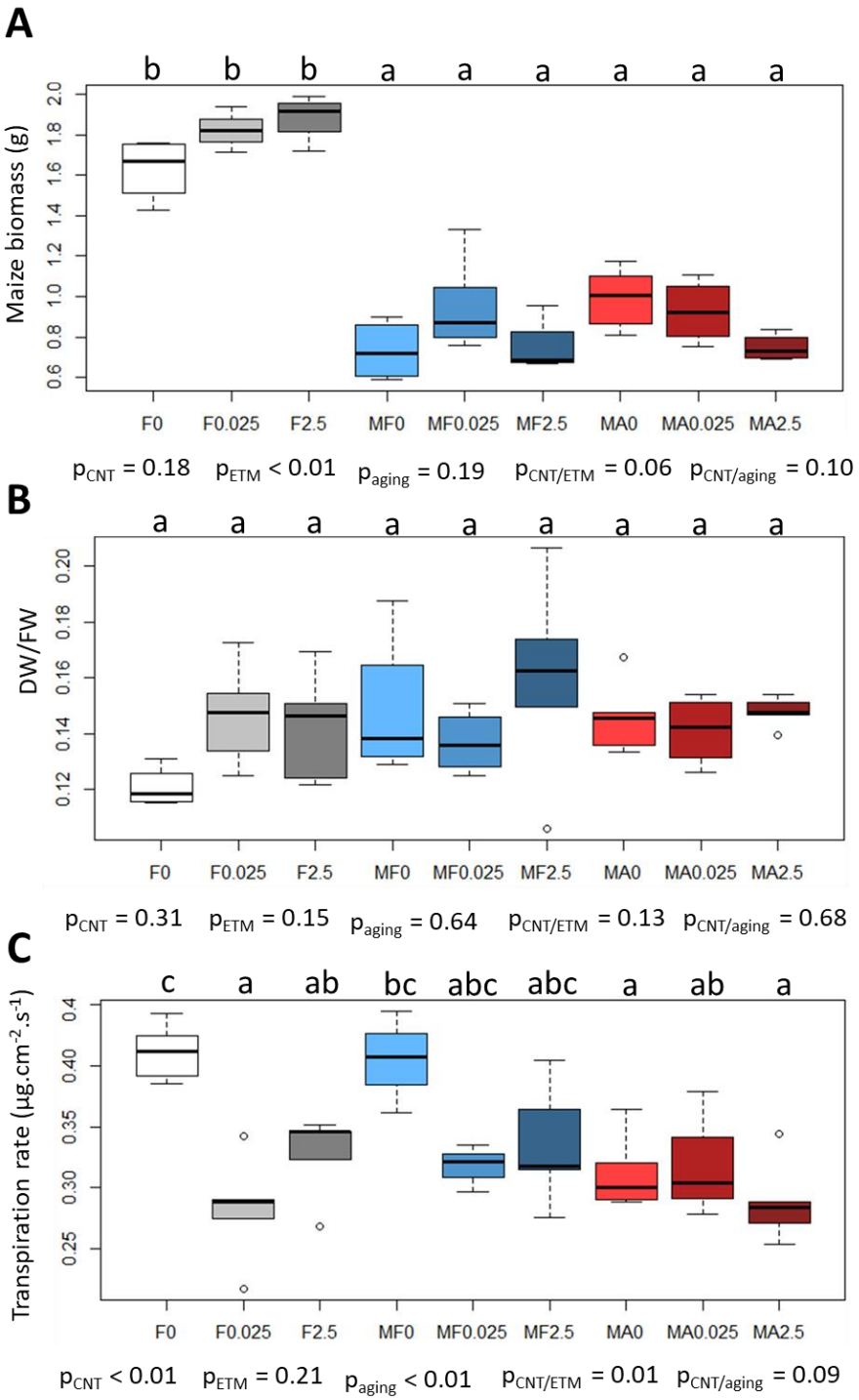

Figure 33: (A) Maize biomass, (B) DW/FW and (C) transpiration of maize leaves grown in the 9 exposure modalities (F0, F0.025, F2.5: Fresh soils (F) without TME and with 0, 0.025 and 2.5 mg.kg^{-1} of CNT; MF0, MF0.025, MF2.5: TME Fresh soils (MF) with 0, 0.025 and 2.5 mg.kg^{-1} of CNT; MA0, MA0.025, MA2.5: TME aged soils (MA) with 0, 0.025 and 2.5 mg.kg^{-1} of CNT) after 8 weeks of exposure. Same lowercase letters indicate treatments that do not differ significantly (p-value > 0.05) following a Kruskal Wallis (A) or a 3 way ANOVA (B and C, n=5).

CNT and soil aging interactions were also detected for phenolic compounds indicating that maize exposed to fresh soils with CNT had 42% more phenolic compounds than maize unexposed to CNT

while it was only 2% more for maize exposed to aged soils ($p_{Phenolic} < 0.01$, Figure 34B). Likewise, a CNT/soil aging interaction was detected for tannin concentration so that maize exposed to fresh soils with CNT had 24% less phenolic compounds than control plants while it was decreased by 10% for maize exposed to CNT in aged soils ($p_{Phenolic} < 0.01$, Figure 34B).

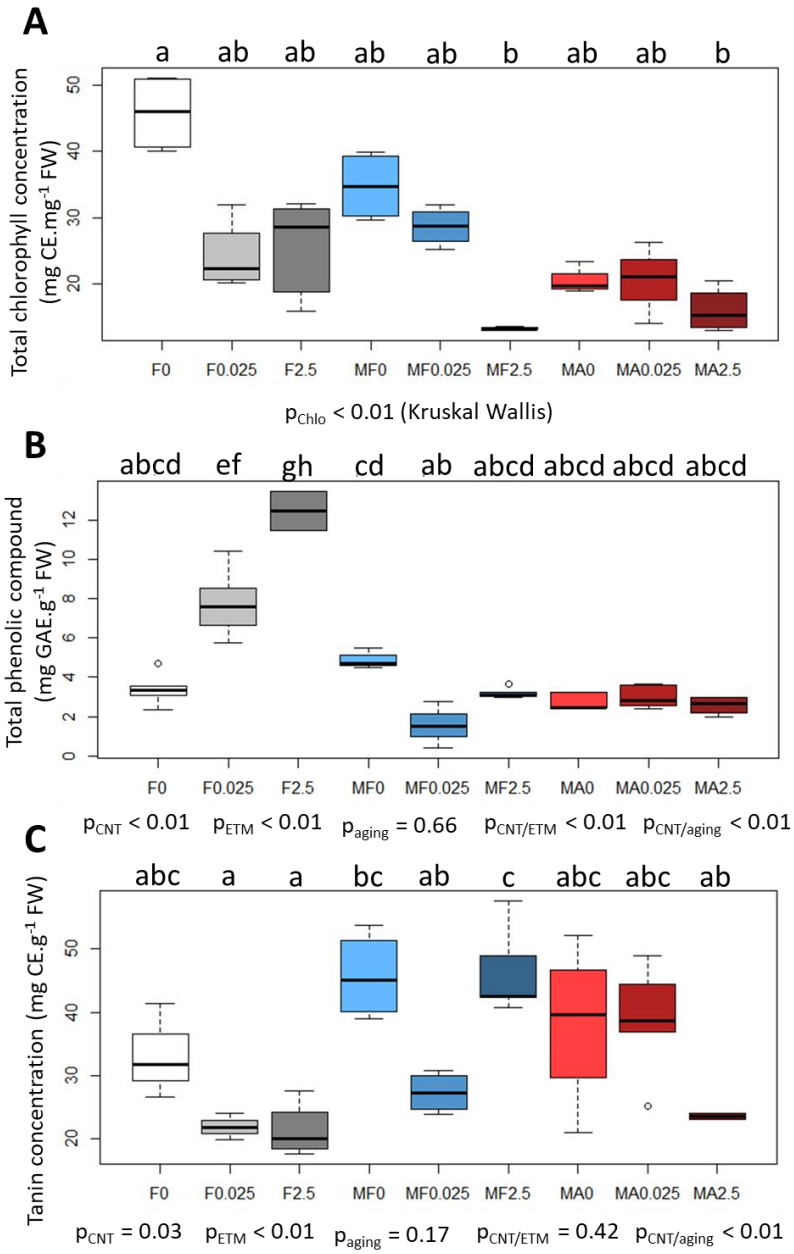

Figure 34: Total chlorophyll (A), total phenolic compound (B) and tannin (C) concentrations in maize leaves exposed to the 9 exposure modalities (F0, F0.025, F2.5: Fresh soils (F) without TME and with 0, 0.025 and 2.5 mg.kg^{-1} of CNT; MF0, MF0.025, MF2.5: TME Fresh soils (MF) with 0, 0.025 and 2.5 mg.kg^{-1} of CNT; MA0, MA0.025, MA2.5: TME aged soils (MA) with 0, 0.025 and 2.5 mg.kg^{-1} of CNT) after 8 weeks of exposure. Same lowercase letters indicate treatments that do not differ significantly (p-value > 0.05) following a Kruskal Wallis (A) or a 3 way ANOVA (B and C, n=5).

3.3. Gas exchange

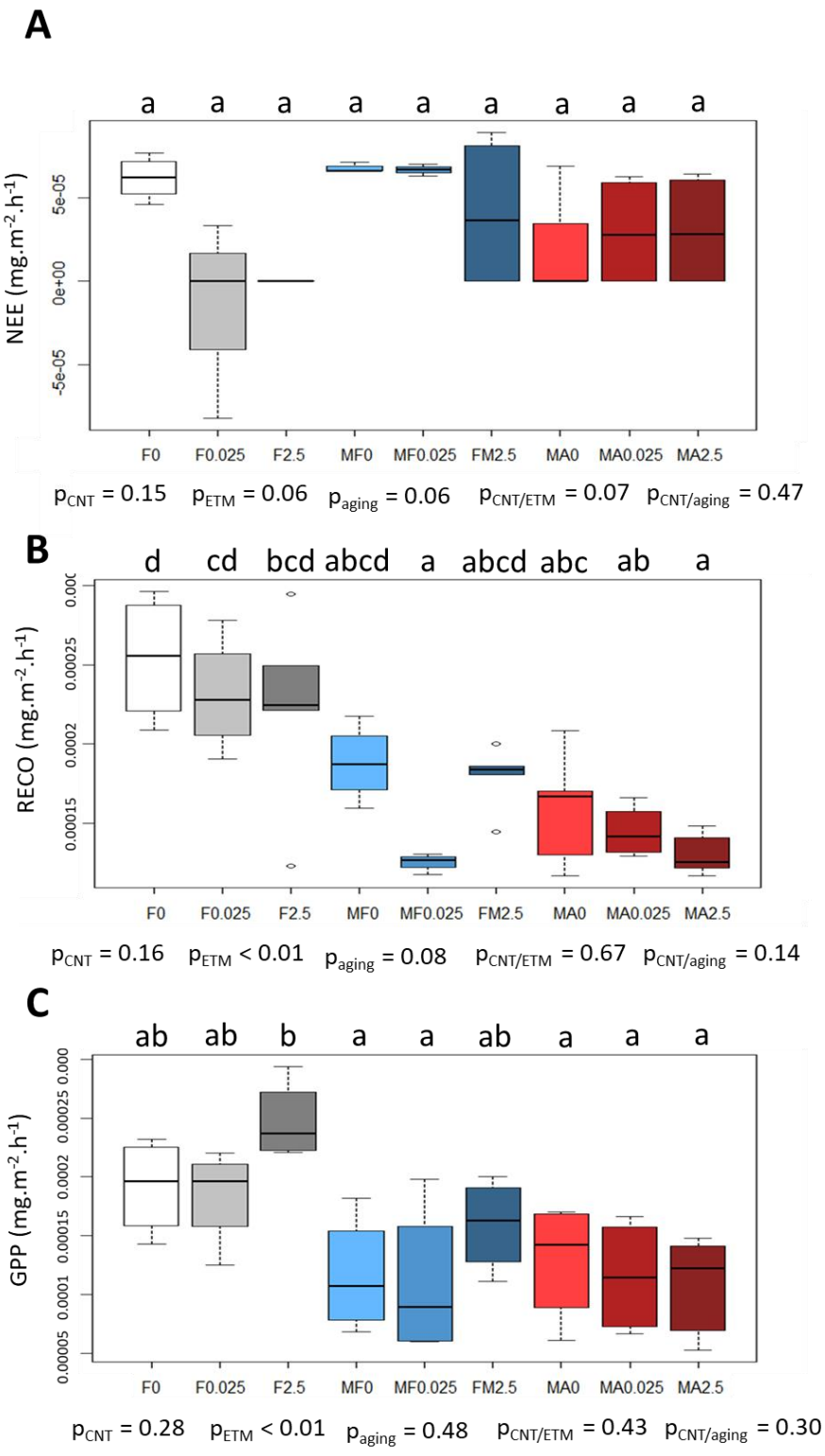

Figure 35: NEE (A), RECO (B) and GPP (C) of microcosms exposed to the 9 modalities (F0, F0.025, F2.5: Fresh soils (F) without TME and with 0, 0.025 and 2.5 mg.kg^{-1} of CNT; MF0, MF0.025, MF2.5: TME Fresh soils (MF) with 0, 0.025 and 2.5 mg.kg^{-1} of CNT; MA0, MA0.025, MA2.5: TME aged soils (MA) with 0, 0.025 and 2.5 mg.kg^{-1} of CNT) after 8 weeks of exposure. Same lowercase letters indicate treatments that do not differ significantly (p-value > 0.05) following a 3-way ANOVA (n=5).

TME addition had a significant effect on RECO and GPP where a 33% and 41% decrease were detected for microcosms in these conditions but not on NEE (p_{NEE} = 0.06, p_{RECO} < 0.01, p_{GPP} < 0.01, Figure 35A-B-C). There was no effect of CNT addition on NEE, RECO and GPP (p_{NEE} = 0.15, p_{RECO} = 0.16, p_{GPP} = 0.28).

Likewise, no interactive effects among the three factors were detected on these gas exchange parameters.

4. Discussion

4.1. CNT exposure impacts

According to the results obtained, the fungal populations of the soil were sensitive to CNT contamination unlike bacteria. Indeed, after 8 weeks of exposure, there was a 16% reduction of the ergosterol concentration in the soil following the application of 0.025 mg.kg^{-1} of CNT revealing an acute toxicity of CNT on fungal populations. This decrease could explained the 9% decrease seen on litter decomposition at 0.025 mg.kg^{-1} of CNT. In a previous study, the addition of 0.1 mg.kg^{-1} had decreased bacteria abundance in the soil but the decomposition of the litter was not impacted (chapter 4). At the time, it was assumed that fungal communities would functionally compensate for litter decomposition, but the results obtained here do not support this hypothesis. Also, the addition of 10 mg.kg^{-1} in our previous study increased litter decomposition. At the same time, the enzymatic activity of β-glucopyranosidase involved in the carbon cycle was increased with the addition of 0.025 and 2.5 mg.kg^{-1} in the soil. A pattern emerges whereby CNT toxicity to soil communities is more pronounced at low concentrations (0.025 mg.kg^{-1}), which is seen from a functional point of view by a concomitant decrease in litter decomposition, offset by higher activity at 0.1 mg.kg^{-1} and then increased at higher concentrations (2.5 and 10 mg.kg^{-1}) as less toxic to soil communities. Rodrigues *et al.*[43] observed a modification of the structure of fungal communities after 14 days following an exposure to 250 and 500 mg.kg^{-1} of SWCNT revealing CNT toxicity at high concentrations, in contrast to our study. However, CNT properties could explain this difference because our CNT was oxidized while it was not the case in

Rodrigues *et al.*[43] study. Oxidized CNT are known to be more reactive thanks to their surface functional groups, which may explain why oxidized CNT are more toxic than pristine CNT ones[44].

Regarding enzymatic activities, only pyranosidase activity (implied in C cycle) was modified after CNT exposure with a dose dependent pattern as 240% and 356% increase with 0.025 and 2.5 $mg.kg^{-1}$ respectively. Most of the results in the literature describe a decrease in the soil enzymatic activities following exposure to nanomaterials[44,45]. It has been observed that certain enzymes may be involved in the degradation of nanomaterials when they are present in the environment, which could reveal a reaction of microbial communities to reduce the toxicity induced by nanomaterials[46]. It can be hypothesized in our study that populations tolerant to nanomaterials may have an increased activity following the exogenous supply of carbon in the soil by the addition of nanomaterials.

Concerning water use efficiency in the system, in a previous study (chapter 4), the addition of 10 $mg.kg^{-1}$ of CNT increased the dry matter content of maize up (17%). Although not significant in this study, a similar trend was observed with an increase of up to 22% and 18% of the dry matter content after exposure at 0.025 and 2.5 $mg.kg^{-1}$ of CNT, respectively. Likewise, in the literature Mondal *et al*.[47] observed a 91% increase of the dry matter content in *Brassica juncea* with 2.3 $\mu g.mL^{-1}$ of oxidized MWCNT. This behavior can be related to a concomitant decreased of the transpiration rate (- 16% at 0.025 $mg.kg^{-1}$ of CNT) which could revealed the water stress imposed by CNT addition in soil. Presumably, CNT exposure causes water stress in these plants which could be prevented by further closing stomata in order to limit water loss. In addition, several clues in the literature reveal that water stress in plants is correlated with an increase in the concentration of phenolic compounds because they could be involved in water regulation through auxin biosynthesis and transport[48–51]. In this present work, maize exposed to CNT had a total phenolic compound concentration increase of 30%. Finally, this effect visible at the plant level scale has also been detected at the ecosystem scale (see chapter 4) with a decrease in H_2O emission as a result of exposure to 0.1 and 10 $mg.kg^{-1}$ of CNT.

Additionally, plant exposure to CNT decreased tannin concentration by 19%, a metabolite implied in several stress defense mechanisms such as high light, low temperatures, pathogen infection, herbivores, nutrient deficiency and exposure to metals[52,53]. Defense capabilities of maize could in the long term be less efficient due to CNT exposure.

4.2. TME exposure impacts

No differences were detected for TME addition on fungal population despite soil exposed to TME had 69% less ergosterol than unexposed of TME. The statistical test used to assess differences in these results was a non-parametric test as the data were non-parametric which could explain the lower power to detect significant differences. Thus, these results suggest an acute toxicity of TME on fungal populations with the application of Cd, Pb and Zn which was worsen in aged soils. These results are in agreement with the literature as toxicity of metals on fungal communities is well known[54,55] and detected through DNA damage, inhibition of transcription and cell division, disruption of membrane integrity and protein denaturation[54,55].

Pyranosidase (implied in C cycle) was the only enzyme affected by TME addition with a decrease of the activity. A meta-analysis with 671 observations demonstrates that Pb, Zn, Cd, Cu and As contamination could reduce the activities of all enzymes including pyranosidase corroboring our results. Interestingly, authors observed much stronger impact of TME on living microorganisms and their endoenzymes than on extracellular enzymes as studied in our work because these last ones can be stabilized on clay minerals and organic matter. This hypothesis could be an explanation why there were no modifications detected for the other tested enzymes.

On maize development, experiment conducted in the present study revealed an acute toxicity of TME on the biomass which was reduced by 52%, as already demonstrated in the literature[56]. At the metabolic level, the addition of metals to fresh soil reduced the concentration of total phenolic

compounds in maize leaves by 56% and increased the concentration of tannins by 52%. These results are also in agreement with those of the literature[57,58].

In parallel, as expected, Cd, Pb and Zn concentrations in maize leaves were significantly higher in maize exposed to TME than in those unexposed. However, CNT did not modified TME transfer as it was observed in previous study on lettuce (experiments 2 of chapter 5). In the literature, there are some examples in which CNT increase or decrease TME transfer and there are some examples in which CNT did not modified TME transfer[1]. These differences on TME transfer with CNT addition in the medium could be partly explained by plant species or soil type. More investigations are needed to respond to these hypotheses.

TME contamination increased the NEE while it decreased the RECO and the GPP respectively. The decrease in GPP following TME contamination can reduce the carbon sequestration capacity of agrosystems. In addition, with regard to the TME concentrations of the contaminated soils compared to the limits fixed by the authorities (our study: Cd = 3.72, Pb = 104.21, Zn = 74.55, limits: Cd = 2, Pb = 100, Zn = 300 $mg.kg^{-1}$), it is advisable to be particularly vigilant when it comes to the monitoring and surveillance of metal concentrations and greenhouse gas emissions from agrosystems.

4.3. Aging of contaminant impacts

Although not statistically evident, the abundance of fungi in aged soils was drastically reduced (80%). Rodrigues *et al.*[43] did not observed any modification on the structure of fungal communities after a one-year exposure of SWCNT and MWCNT to 1 $g.kg^{-1}$, while they observed similar decrease with only CNT exposure as our study. In addition, they observed similar trend as contaminant ageing reduced CNT toxicity. Since belowground communities have varying degrees of tolerance to CNT[44], it seems that the least tolerant populations decline rapidly after exposure to CNTs, while the most tolerant populations may persist over the long term.

The reduction in contaminant toxicity due to soil ageing was also observed for maize transpiration.

Aging of contaminants mitigate toxicity of contaminants only on pyranosidase activity, probably for the same reason as proposed for fungal communities.

Also, similar mitigation was observed on chlorophyll, phenolic compounds and tannin concentration in maize leaves.

However, mitigation of contaminants toxicity did not produced effects on microcosm gas emissions.

One hypothesis that could explain the attenuation of contaminant toxicity as soils age is that contaminants may become less bioavailable over time. Also, due to the high adsorption capacity of CNT, it is likely that over time substances will adsorb, thus limiting their toxicity.

4.4. Co-contaminants impacts

Interactions between CNT and TME were observed for several of the biomarkers studied, namely β-glucopyranosidase activity, litter decomposition, transpiration and total phenol concentration. In all these cases, an antagonistic effect was observed, i.e. the effect caused by CNT exposure alone was decreased when the organisms were exposed to both contaminants (CNT and TME). However, this effect was not transferable at the ecosystem scale (at least considering the ecomarkers used here) as no interactions were detected on gas exchange. In the literature[1], 64% of the studies focusing on the ecotoxicity of a mixture of contaminants containing both carbon based nanomaterials and TME demonstrated interactive effects as well; half of them highlighting antagonist effect as this present work and the other half synergistic effects. It would be interesting to carry out a more in depth analysis of these results in the light of those obtained in this PhD work to investigate if soil pH and OM content could explain why in some cases the interactions led to synergistic or antagonist effects.

Acknowledgement

This work was supported by the Région Occitanie, Toulouse Federal University under the NANOMETAGRO research project, and by EC2CO program under the project CARBOSTRESS (CNRS-INSU). Authors are thankful to the FBiI and PAPC platforms of the laboratory for functional ecology and environment for ICP-AES analysis and soil physico-chemical characterization, respectively. We are also grateful to Morgan Légnani for CNT synthesis and Antoine Lecerf for providing the SBA instrument.

Bibliography (article: Assessing the impact of a mixture of carbon nanotube and metals and their aging on agrosystems):

(1) Leroy, M.; Flahaut, E.; Larue, C. Carbon Based Nanomaterial Interactions with Metals and Metalloids in Terrestrial Environment: A Review. *Carbon* **2023**, *206*, 325–339. https://doi.org/10.1016/j.carbon.2023.02.047.

(2) Anderson, T. D.; Zhu, K. Y. Synergistic and Antagonistic Effects of Atrazine on the Toxicity of Organophosphorodithioate and Organophosphorothioate Insecticides to Chironomus Tentans (Diptera: Chironomidae). *Pesticide Biochemistry and Physiology* **2004**, *80* (1), 54–64. https://doi.org/10.1016/j.pestbp.2004.06.003.

(3) Folt, C. L.; Chen, C. Y.; Moore, M. V.; Burnaford, J. Synergism and Antagonism among Multiple Stressors. *Limnology and Oceanography* **1999**, *44* (3part2), 864–877. https://doi.org/10.4319/lo.1999.44.3_part_2.0864.

(4) Holmstrup, M.; Bindesbøl, A.-M.; Oostingh, G. J.; Duschl, A.; Scheil, V.; Köhler, H.-R.; Loureiro, S.; Soares, A. M. V. M.; Ferreira, A. L. G.; Kienle, C.; Gerhardt, A.; Laskowski, R.; Kramarz, P. E.; Bayley, M.; Svendsen, C.; Spurgeon, D. J. Interactions between Effects of Environmental Chemicals and Natural Stressors: A Review. *Science of The Total Environment* **2010**, *408* (18), 3746–3762. https://doi.org/10.1016/j.scitotenv.2009.10.067.

(5) Pavlaki, M. D.; Pereira, R.; Loureiro, S.; Soares, A. M. V. M. Effects of Binary Mixtures on the Life Traits of Daphnia Magna. *Ecotoxicology and Environmental Safety* **2011**, *74* (1), 99–110. https://doi.org/10.1016/j.ecoenv.2010.07.010.

(6) Schwirn, K.; Voelker, D.; Galert, W.; Quik, J.; Tietjen, L. Environmental Risk Assessment of Nanomaterials in the Light of New Obligations Under the REACH Regulation: Which Challenges Remain and How to Approach Them? *Integrated Environmental Assessment and Management* **2020**, *16* (5), 706–717. https://doi.org/10.1002/ieam.4267.

(7) Meesters, J. A.; Veltman, K.; Hendriks, A. J.; van de Meent, D. Environmental Exposure Assessment of Engineered Nanoparticles: Why REACH Needs Adjustment. *Integrated Environmental Assessment and Management* **2013**, *9* (3), e15–e26. https://doi.org/10.1002/ieam.1446.

(8) He, Z. L.; Yang, X. E.; Stoffella, P. J. Trace Elements in Agroecosystems and Impacts on the Environment. *Journal of Trace Elements in Medicine and Biology* **2005**, *19* (2), 125–140. https://doi.org/10.1016/j.jtemb.2005.02.010.

(9) Koul, B.; Taak, P. Soil Pollution: Causes and Consequences. In *Biotechnological Strategies for Effective Remediation of Polluted Soils*; Koul, B., Taak, P., Eds.; Springer: Singapore, 2018; pp 1–37. https://doi.org/10.1007/978-981-13-2420-8_1.

(10) Abd-Elsalam, K. A. 1 - Carbon Nanomaterials: 30 Years of Research in Agroecosystems. In *Carbon Nanomaterials for Agri-Food and Environmental Applications*; Abd-Elsalam, K. A., Ed.; Micro and Nano Technologies; Elsevier, 2020; pp 1–18. https://doi.org/10.1016/B978-0-12-819786-8.00001-3.

(11) Ng, E.-L.; Huerta Lwanga, E.; Eldridge, S. M.; Johnston, P.; Hu, H.-W.; Geissen, V.; Chen, D. An Overview of Microplastic and Nanoplastic Pollution in Agroecosystems. *Science of The Total Environment* **2018**, *627*, 1377–1388. https://doi.org/10.1016/j.scitotenv.2018.01.341.

(12) Okeke, E. S.; Okoye, C. O.; Atakpa, E. O.; Ita, R. E.; Nyaruaba, R.; Mgbechidinma, C. L.; Akan, O. D. Microplastics in Agroecosystems-Impacts on Ecosystem Functions and Food Chain. *Resources, Conservation and Recycling* **2022**, *177*, 105961. https://doi.org/10.1016/j.resconrec.2021.105961.

(13) Gottschalk, F.; Sun, T.; Nowack, B. Environmental Concentrations of Engineered Nanomaterials: Review of Modeling and Analytical Studies. *Environmental Pollution* **2013**, *181*, 287–300. https://doi.org/10.1016/j.envpol.2013.06.003.

(14) Holden, P. A.; Klaessig, F.; Turco, R. F.; Priester, J. H.; Rico, C. M.; Avila-Arias, H.; Mortimer, M.; Pacpaco, K.; Gardea-Torresdey, J. L. Evaluation of Exposure Concentrations Used in Assessing Manufactured Nanomaterial Environmental Hazards: Are They Relevant? *Environ. Sci. Technol.* **2014**, *48* (18), 10541–10551. https://doi.org/10.1021/es502440s.
(15) Moolenaar, S. W. Sustainable Management of Heavy Metals in Agro-Ecosystems. **1998**.
(16) Addo Ntim, S.; Mitra, S. Adsorption of Arsenic on Multiwall Carbon Nanotube–Zirconia Nanohybrid for Potential Drinking Water Purification. *Journal of Colloid and Interface Science* **2012**, *375* (1), 154–159. https://doi.org/10.1016/j.jcis.2012.01.063.
(17) Tofighy, M. A.; Mohammadi, T. Adsorption of Divalent Heavy Metal Ions from Water Using Carbon Nanotube Sheets. *Journal of Hazardous Materials* **2011**, *185*, 140–147. https://doi.org/10.1016/j.jhazmat.2010.09.008.
(18) Moradi, O. The Removal of Ions by Functionalized Carbon Nanotube: Equilibrium, Isotherms and Thermodynamic Studies. *Chemical and Biochemical Engineering Quarterly* **2011**, *25* (2), 229–240.
(19) Moradi, O.; Zare, K. Adsorption of Pb(II), Cd(II) and Cu(II) Ions in Aqueous Solution on SWCNTs and SWCNT –COOH Surfaces: Kinetics Studies. *Fullerenes, Nanotubes and Carbon Nanostructures* **2011**, *19* (7), 628–652. https://doi.org/10.1080/1536383X.2010.504955.
(20) Hu, X.; Kang, J.; Lu, K.; Zhou, R.; Mu, L.; Zhou, Q. Graphene Oxide Amplifies the Phytotoxicity of Arsenic in Wheat. *Scientific Reports* **2014**, *4* (1), 6122. https://doi.org/10.1038/srep06122.
(21) Li, J.; Wu, F.; Fang, Q.; Wu, Z.; Duan, Q.; Li, X.; Ye, W. The Mutual Effects of Graphene Oxide Nanosheets and Cadmium on the Growth, Cadmium Uptake and Accumulation in Rice. *Plant Physiology and Biochemistry* **2020**, *147*, 289–294. https://doi.org/10.1016/j.plaphy.2019.12.034.
(22) Gao, M.; Yang, Y.; Song, Z. Effects of Graphene Oxide on Cadmium Uptake and Photosynthesis Performance in Wheat Seedlings. *Ecotoxicology and Environmental Safety* **2019**, *173*, 165–173. https://doi.org/10.1016/j.ecoenv.2019.01.093.
(23) Zhao, L.; Guan, X.; Yu, B.; Ding, N.; Liu, X.; Ma, Q.; Yang, S.; Yilihamu, A.; Yang, S.-T. Carboxylated Graphene Oxide-Chitosan Spheres Immobilize Cu2+ in Soil and Reduce Its Bioaccumulation in Wheat Plants. *Environment International* **2019**, *133*, 105208. https://doi.org/10.1016/j.envint.2019.105208.
(24) He, Y.; Qian, L.; Zhou, K.; Hu, R.; Huang, M.; Wang, M.; Zhao, G.; Liu, Y.; Xu, Z.; Zhu, H. Graphene Oxide Promoted Cadmium Uptake by Rice in Soil. *ACS Sustainable Chem. Eng.* **2019**, *7* (12), 10283–10292. https://doi.org/10.1021/acssuschemeng.8b06823.
(25) Gong, X.; Huang, D.; Liu, Y.; Zeng, G.; Wang, R.; Xu, P.; Zhang, C.; Cheng, M.; Xue, W.; Chen, S. Roles of Multiwall Carbon Nanotubes in Phytoremediation: Cadmium Uptake and Oxidative Burst in Boehmeria Nivea (L.) Gaudich. *Environ. Sci.: Nano* **2019**, *6* (3), 851–862. https://doi.org/10.1039/C8EN00723C.
(26) Leroy, M.; Pey, B.; Jassey, V. E. J.; Liné, C.; Elger, A.; Probst, A.; Flahaut, E.; Silvestre, J.; Larue, C. Interactive Effects of Metals and Carbon Nanotubes in a Microcosm Agrosystem. *Journal of Hazardous Materials* **2022**, *431*, 128613. https://doi.org/10.1016/j.jhazmat.2022.128613.
(27) Manjate, E.; Ramos, S.; Almeida, C. M. R. Potential Interferences of Microplastics in the Phytoremediation of Cd and Cu by the Salt Marsh Plant Phragmites Australis. *Journal of Environmental Chemical Engineering* **2020**, *8* (2), 103658. https://doi.org/10.1016/j.jece.2020.103658.
(28) Li, M.; Liu, Y.; Xu, G.; Wang, Y.; Yu, Y. Impacts of Polyethylene Microplastics on Bioavailability and Toxicity of Metals in Soil. *Science of The Total Environment* **2021**, *760*, 144037. https://doi.org/10.1016/j.scitotenv.2020.144037.
(29) Gao, M.; Xu, Y.; Chang, X.; Dong, Y.; Song, Z. Effects of Foliar Application of Graphene Oxide on Cadmium Uptake by Lettuce. *Journal of Hazardous Materials* **2020**, *398*, 122859. https://doi.org/10.1016/j.jhazmat.2020.122859.

(30) Dong, Y.; Gao, M.; Song, Z.; Qiu, W. Microplastic Particles Increase Arsenic Toxicity to Rice Seedlings. *Environmental Pollution* **2020**, *259*, 113892. https://doi.org/10.1016/j.envpol.2019.113892.
(31) Gao, M.; Chang, X.; Yang, Y.; Song, Z. Foliar Graphene Oxide Treatment Increases Photosynthetic Capacity and Reduces Oxidative Stress in Cadmium-Stressed Lettuce. *Plant Physiology and Biochemistry* **2020**, *154*, 287–294. https://doi.org/10.1016/j.plaphy.2020.06.021.
(32) Chen, X.; Wang, J.; Hayat, K.; Zhang, D.; Zhou, P. Small Structures with Big Impact: Multi-Walled Carbon Nanotubes Enhanced Remediation Efficiency in Hyperaccumulator Solanum Nigrum L. under Cadmium and Arsenic Stress. *Chemosphere* **2021**, *276*, 130130. https://doi.org/10.1016/j.chemosphere.2021.130130.
(33) Smolders, E.; Oorts, K.; Van Sprang, P.; Schoeters, I.; Janssen, C. R.; McGrath, S. P.; Mclaughlin, M. J. Toxicity of Trace Metals in Soil as Affected by Soil Type and Aging After Contamination: Using Calibrated Bioavailability Models to Set Ecological Soil Standards. *Environmental Toxicology and Chemistry* **2009**, *28* (8), 1633–1642. https://doi.org/10.1897/08-592.1.
(34) Oleszczuk, P.; Jośko, I.; Xing, B. The Toxicity to Plants of the Sewage Sludges Containing Multiwalled Carbon Nanotubes. *Journal of Hazardous Materials* **2011**, *186* (1), 436–442. https://doi.org/10.1016/j.jhazmat.2010.11.028.
(35) Zhao, X.; Liu, H.; Yan, Z.; Song, C. Aging of Carbon Nanotubes Increases Their Adsorption towards Tetracycline. *Water* **2022**, *14* (17), 2731. https://doi.org/10.3390/w14172731.
(36) *EUR-Lex - 01986L0278-20180704 - FR - EUR-Lex*. https://eur-lex.europa.eu/legal-content/FR/TXT/?uri=CELEX%3A01986L0278-20180704 (accessed 2020-11-27).
(37) Jassey, V. E. J.; Chiapusio, G.; Mitchell, E. A. D.; Binet, P.; Toussaint, M.-L.; Gilbert, D. Fine-Scale Horizontal and Vertical Micro-Distribution Patterns of Testate Amoebae Along a Narrow Fen/Bog Gradient. *Microb Ecol* **2011**, *61* (2), 374–385. https://doi.org/10.1007/s00248-010-9756-9.
(38) Gessner, M. O. Ergosterol as a Measure of Fungal Biomass. In *Methods to Study Litter Decomposition: A Practical Guide*; Bärlocher, F., Gessner, M. O., Graça, M. A. S., Eds.; Springer International Publishing: Cham, 2020; pp 247–255. https://doi.org/10.1007/978-3-030-30515-4_27.
(39) Gerald Jurasinski. *Flux Rate Calculation from Dynamic Closed Chamber Measurements*; 2014.
(40) Roland Fuss. *Greenhouse Gas Flux Calculation from Chamber Measurement*; 2023.
(41) Fuss, R.; Hueppi, R.; function (version 0.3.1)), A. R. P. (for code copied from the not-exported H. H. fit1. *Gasfluxes: Greenhouse Gas Flux Calculation from Chamber Measurements*; 2020.
(42) Kutzbach, L.; Schneider, J.; Sachs, T.; Giebels, M.; Nykänen, H.; Shurpali, N. J.; Martikainen, P. J.; Alm, J.; Wilmking, M. CO_2 Flux Determination by Closed-Chamber Methods Can Be Seriously Biased by Inappropriate Application of Linear Regression. *Biogeosciences* **2007**, *4* (6), 1005–1025. https://doi.org/10.5194/bg-4-1005-2007.
(43) Rodrigues, D. F.; Jaisi, D. P.; Elimelech, M. Toxicity of Functionalized Single-Walled Carbon Nanotubes on Soil Microbial Communities: Implications for Nutrient Cycling in Soil. *Environ. Sci. Technol.* **2013**, *47* (1), 625–633. https://doi.org/10.1021/es304002q.
(44) Shrestha, B.; Acosta-Martinez, V.; Cox, S. B.; Green, M. J.; Li, S.; Cañas-Carrell, J. E. An Evaluation of the Impact of Multiwalled Carbon Nanotubes on Soil Microbial Community Structure and Functioning. *Journal of Hazardous Materials* **2013**, *261*, 188–197. https://doi.org/10.1016/j.jhazmat.2013.07.031.
(45) Jin, L.; Son, Y.; Yoon, T. K.; Kang, Y. J.; Kim, W.; Chung, H. High Concentrations of Single-Walled Carbon Nanotubes Lower Soil Enzyme Activity and Microbial Biomass. *Ecotoxicology and Environmental Safety* **2013**, *88*, 9–15. https://doi.org/10.1016/j.ecoenv.2012.10.031.
(46) Chen, M.; Qin, X.; Zeng, G. Biodegradation of Carbon Nanotubes, Graphene, and Their Derivatives. *Trends in Biotechnology* **2017**, *35* (9), 836–846. https://doi.org/10.1016/j.tibtech.2016.12.001.

(47) Mondal, A.; Basu, R.; Das, S.; Nandy, P. Beneficial Role of Carbon Nanotubes on Mustard Plant Growth: An Agricultural Prospect. *J Nanopart Res* **2011**, *13* (10), 4519. https://doi.org/10.1007/s11051-011-0406-z.
(48) Gaspar, T.; Bastin, M.; Leyh, C. Composés phénoliques, acide β-indolacétique et activité auxines-oxydasique. *Bulletins de l'Académie Royale de Belgique* **1964**, *50* (1), 799–815. https://doi.org/10.3406/barb.1964.65029.
(49) Clérivet, A.; Alami, I.; Breton, F.; Garcia, D.; Sanier, C. Les Composés Phénoliques et La Résistance Des Plantes Aux Agents Pathogènes. *Acta Botanica Gallica* **1996**, *143* (6), 531–538. https://doi.org/10.1080/12538078.1996.10515350.
(50) Babenko, L. M.; Smirnov, O. E.; Romanenko, K. O.; Trunova, O. K.; Kosakivska, I. V. Phenolic Compounds in Plants: Biogenesis and Functions. *Ukrainian Biochemical Journal* **2019**, *91* (3), 5–18.
(51) Effects of an Increase in Levels of Phenolic Compounds on the Auxin Content and Growth of Lycopersicum Esculentum. *Zeitschrift für Pflanzenphysiologie* **1979**, *92* (1), 33–38. https://doi.org/10.1016/S0044-328X(79)80150-6.
(52) Lattanzio, V. Phenolic Compounds: Introduction. In *Natural Products: Phytochemistry, Botany and Metabolism of Alkaloids, Phenolics and Terpenes*; 2013; pp 1543–1580. https://doi.org/10.1007/978-3-642-22144-6_57.
(53) War, A. R.; Paulraj, M. G.; Ahmad, T.; Buhroo, A. A.; Hussain, B.; Ignacimuthu, S.; Sharma, H. C. Mechanisms of Plant Defense against Insect Herbivores. *Plant Signaling & Behavior* **2012**, *7* (10), 1306–1320. https://doi.org/10.4161/psb.21663.
(54) Baath, E. Effects of Heavy Metals in Soil on Microbial Processes and Populations (a Review). *Water, Air, and Soil Pollution* **1989**, *47* (3–4), 335–379. https://doi.org/10.1007/BF00279331.
(55) Giller, K. E.; Witter, E.; McGrath, S. P. Heavy Metals and Soil Microbes. *Soil Biology and Biochemistry* **2009**, *41* (10), 2031–2037. https://doi.org/10.1016/j.soilbio.2009.04.026.
(56) Goyal, D.; Yadav, A.; Prasad, M.; Singh, T. B.; Shrivastav, P.; Ali, A.; Dantu, P. K.; Mishra, S. Effect of Heavy Metals on Plant Growth: An Overview. In *Contaminants in Agriculture: Sources, Impacts and Management*; Naeem, M., Ansari, A. A., Gill, S. S., Eds.; Springer International Publishing: Cham, 2020; pp 79–101. https://doi.org/10.1007/978-3-030-41552-5_4.
(57) Kopittke, P. M.; Blamey, F. P. C.; Asher, C. J.; Menzies, N. W. Trace Metal Phytotoxicity in Solution Culture: A Review. *Journal of Experimental Botany* **2010**, *61* (4), 945–954. https://doi.org/10.1093/jxb/erp385.
(58) Gall, J. E.; Boyd, R. S.; Rajakaruna, N. Transfer of Heavy Metals through Terrestrial Food Webs: A Review. *Environ Monit Assess* **2015**, *187* (4), 201. https://doi.org/10.1007/s10661-015-4436-3.

5. Supporting Information

Assessing the impact of a mixture of carbon nanotube and metals and their aging on agrosystems

Leroy Mathieu[1,2], Jassey Vincent E.J.[1], Barret Maialen[1], Silvestre Jérôme [1], Flahaut Emmanuel [2], Larue Camille[1]

[1]Laboratoire écologie fonctionnelle et environnement, Université de Toulouse, CNRS, Toulouse, France, [2]CIRIMAT, Université de Toulouse, CNRS, INPT, UPS, UMR CNRS-UPS-INP N°5085, Université Toulouse 3 Paul Sabatier, Bât. CIRIMAT, 118, route de Narbonne, 31062 Toulouse cedex 9, France

2. Material and methods

2.2. Soil characterization and contamination

Table S1 : Soil physico-chemical characterization after exposure. Average and standard deviation for clay, silt, sand, pH, organic C (C) for the 9 exposure modalities (F0, F0.025, F2.5: Fresh soils (F) without TME and with 0, 0.025 and 2.5 mg.kg^{-1}of CNT; MF0, MF0.025, MF2.5: TME Fresh soils (MF) with 0, 0.025 and 2.5 mg.kg^{-1}of CNT; MA0, MA0.025, MA2.5: TME aged soils (MA) with 0, 0.025 and 2.5 mg.kg^{-1} of CNT). Same lowercase letters indicate treatments that do not differ significantly (p-value > 0.05) following a 3-way ANOVA test (n=5).

Soil	Clay	Silt	Sand	pH	C
F0	0.86 ± 0.22 **ab**	13.9 ± 1.35 **a**	85.24 ± 1.52 **a**	4.06 ± 0.18 **a**	1.34 ± 0.03 **bc**
F0.025	0.77 ± 0.09 **a**	16.14 ± 1.58 **ab**	84.04 ± 2.6 **ab**	4.96 ± 0.28 **b**	1.2 ± 0.03 **a**
F2.5	0.98 ± 0.17 **abc**	16.71 ± 1.64 **ab**	82.31 ± 1.76 **ab**	4.56 ± 0.09 **bc**	1.27 ± 0.02 **ab**
MF0	1.04 ± 0.18 **abc**	19.02 ± 0.18 **b**	79.94 ± 0.18 **b**	4.21 ± 0.2 **ac**	1.33 ± 0.06 **bc**
MF0.025	1.07 ± 0.15 **abc**	16.53 ± 0.46 **ab**	82.4 ± 0.51 **ab**	4.3 ± 0.06 **abc**	1.5 ± 0.09 **d**
MF2.5	1.14 ± 0.12 **bc**	17.16 ± 0.88 **ab**	81.7 ± 0.99 **ab**	4.26 ± 0.08 **ac**	1.4 ± 0.05 **cd**
MA0	1.2 ± 0.16 **bc**	17.31 ± 1.94 **ab**	81.49 ± 2.05 **ab**	4.41 ± 0.05 **abc**	1.37 ± 0.06 **bc**
MA0.025	1.31 ± 0.13 **c**	17.36 ± 1.41 **ab**	81.34 ± 1.51 **ab**	4.42 ± 0.02 **abc**	1.43 ± 0.05 **cd**
MA2.5	1.14 ± 0.19 **bc**	17.12 ± 2.2 **ab**	79.8 ± 2.37 **b**	4.33 ± 0.23 **ac**	1.41 ± 0.06 **cd**

Table S2: Elemental conentrations (B, Ca, Cd, Cu, Fe, K, Mg, Mn, Na, P, Pb, S Zn) in soil for the 9 exposure modalities (F0, F0.025, F2.5: Fresh soils (F) without TME and with 0, 0.025 and 2.5 mg.kg^{-1}of CNT; MF0, MF0.025, MF2.5: TME Fresh soils (MF) with 0, 0.025 and 2.5 mg.kg^{-1}of CNT; MA0, MA0.025, MA2.5: TME aged soils (MA) with 0, 0.025 and 2.5 mg.kg^{-1} of CNT). Same lowercase letters indicate treatments that do not differ significantly (p-value > 0.05) following a 3-way ANOVA test (n=5).

	B	Ca	Cd	Cu	Fe	K	Mg	Mn	Na	P	Pb	S	Zn
CTRL F	3.09 ± 1.1 **ab**	2798.34 ± 696.3 **a**	0.03 ± 0.01 **a**	0.76 ± 0.1 **a**	594.45 ± 45.7 **a**	148.4 ± 21.9 **a**	90.21 ± 9 **a**	31.63 ± 2.8 **a**	27.14 ± 11.3 **a**	57 ± 5.5 **a**	3.47 ± 0.3 **a**	21.78 ± 7.8 **a**	3.29 ± 0.3 **a**
NTC 0.1 F	4.93 ± 0.5 **ab**	1694.94 ± 116.6 **ab**	0.03 ± 0.005 **ab**	0.84 ± 0.05 **ab**	597.33 ± 29.5 **a**	148.17 ± 13.6 **a**	92.19 ± 2.5 **a**	32.87 ± 2.8 **a**	35.41 ± 6.1 **a**	53.15 3.4 **a**	3.53 ± 0.2 **ac**	27.45 ± 6.3 **a**	3.47 ± 0.2 **ac**
NTC 10 F	1.7 ± 0.2 **b**	1653.13 ± 74.9 **b**	0.03 ± 0.01 **a**	0.78 ± 0.09 **ab**	586.82 ± 50.6 **a**	134.37 ± 17.8 **a**	86.3 ± 7.4 **a**	32.68 ± 3.5 **a**	23.62 ± 4.6 **a**	57.26 ± 4.9 **a**	3.71 ± 0.6 **ac**	23.7 ± 5.7 **a**	3.64 ± 0.5 **ac**
ETM F	4.4 ± 0.5 **ab**	1703.34 ± 78.6 **ab**	2.28 ± 0.7 **ab**	1.02 ± 0.1 **b**	591.06 ± 75.3 **a**	147.71 ± 13.3 **a**	93.58 ± 15.4 **a**	38.59 ± 8.2 **a**	25.77 ± 9.3 **a**	59.36 ± 5.5 **a**	119.51 ± 23.3 **bc**	17.96 ± 3 **a**	85.01 ± 34.5 **bc**
ETM/NTC 0.1 F	5.48 ± 0.2 **a**	1764.74 ± 69.6 **ab**	5.19 ± 0.6 **b**	0.97 ± 0.03 **ab**	619.5 ± 80.94 **a**	163.07 ± 23.8 **a**	110.07 ± 3.4 **a**	38.41 ± 5.5 **a**	31.12 ± 3.6 **a**	56.42 ± 3.8 **a**	116.86 ± 4.5 **b**	19.8 ± 1.1 **a**	49.28 ± 8.9 **abc**
ETM/NTC 10 F	5.18 ± 0.6 **ab**	1666.4 ± 96.6 **b**	4.08 ± 0.8 **ab**	0.86 ± 0.07 **ab**	566.612 ± 40.3 **a**	144.61 ± 9.6 **a**	90.68 ± 6.51 **a**	33.7 ± 3 **a**	24.86 ± 4.1 **a**	55.75 ± 4.6 **a**	102.11 ± 6.6 **abc**	17.63 ± 1.3 **a**	43.95 ± 4.4 **abc**
ETM A	5.26 ± 0.5 **ab**	1784.19 ± 50.6 **ab**	4.12 ± 0.4 **ab**	0.9 ± 0.05 **ab**	618.29 ± 31.61 **a**	172.12 ± 19.2 **a**	108.64 ± 8.71 **a**	39.8 ± 3.8 a	36.08 ± 6.7 **a**	55.49 ± 2.3 **a**	107.96 ± 5.5 **abc**	21.38 ± 2.8 **a**	54.94 ± 5.3 **abc**
ETM/NTC 0.1 A	5.12 ± 0.8 **ab**	1753.56 ± 102.2 **ab**	3.11 ± 0.8 **ab**	0.82 ± 0.05 **ab**	591.55 ± 29.97 **a**	162.92 ± 16.8 **a**	99.74 ± 9.65 **a**	34.84 ± 5.4 **a**	27.31 ± 8 **a**	54.31 ± 2.8 **a**	93.6 ± 8.4 **abc**	19.82 ± 2.6 **a**	100.52 ± 35.6 **b**
ETM/NTC 10 A	4.57 ± 0.3 **ab**	1708.43 ± 33.9 **ab**	3.92 ± 0.3 **ab**	0.79 ± 0.05 **ab**	574.22 ± 35.21 **a**	153.08 ± 18.6 **a**	102.18 ± 3.75 **a**	37.03 ± 0.9 **a**	32.23 ± 2 **a**	52.5 ± 3.6 **a**	88.97 ± 3.5 **abc**	21.17 ± 2.2 **a**	93.97 ± 68 **abc**

Chapitre 6 : Caractérisation du transfert de NTC et ETM au sein d'un réseau trophique reconstitué

Afin d'établir l'écotoxicité d'une substance pour les écosystèmes, les écotoxicologues utilisent un indicateur simple pour rendre compte de la teneur de la substance rapportée à une masse donnée, communément appelé concentration. Or, les substances émergentes et en particulier les CNM se confrontent à des défis de détection qui permettent très difficilement d'établir la concentration de la substance dans une matrice environnementale carbonée. En effet, le contaminant et la matrice étant tous les 2 composés de carbone, il s'avère alors difficile de quantifier ces nanomatériaux d'autant plus quand on travaille aux concentrations environnementalement attendues (c'est-à-dire faibles).

Des innovations techniques ont émergé ces 10 dernières années afin de détecter les CNM dans le vivant et de quantifier leur transfert pour déterminer pleinement leur potentielle toxicité en fonction de leur concentration. Parmi les innovations proposées pour détecter les CNM, l'enrichissement des CNM en isotopes stables ou radioactifs (^{13}C et ^{14}C, par exemple) semble être une méthode intéressante[1–4]. Par exemple, Petersen et al. ont réussi à détecter des NTC chez le ver de terre grâce à un enrichissement en ^{14}C. Mais l'utilisation de cet isotope radioactif, même s'il est efficace, présente des contraintes à la fois financières (précurseur extrêmement cher) et techniques (besoin de disposer de laboratoires « chauds » équipés d'une chambre de croissance). Ainsi, dans de précédents tests issus de la thèse de Liné (Liné, 2019[5]), les NTC ont été dopés avec du ^{13}C. Mais avec un enrichissement à 17%, ces NTC n'avaient pas donné de résultats concluants, certainement en raison de l'enrichissement qui n'était assez élevé pour permettre leur détection. L'enrichissement des NTC par du Pb encapsulé à l'intérieur des tubes a aussi été testé par Camille Larue et Emmanuel Flahaut, mais dans ce cas, c'est la digestion acide des NTC pour libérer et doser le Pb qui s'est avérée problématique. Aussi, d'autres techniques ont été proposées avec des techniques d'observations optiques[4,6,7], Raman[8] et de chauffage induit par micro-ondes[9] qui doivent encore être développées afin de fournir des résultats probants.

Outre le manque dans la détection et la caractérisation des concentrations des CNM dans des matrices biologiques, les études qui cherchent à établir le transfert des CNM le long des réseaux trophiques sont à ce jour peu représentées dans la littérature scientifique. Chae et An. (2020) ont étudié le transfert de nanoplatsiques le long d'une chaine trophique reconstituée et ont confirmé le transfert trophique de nanoplastiques par fluorescence des sols vers les haricots mungo (*Vigna radiata*) puis vers les escargots géants africains (*Achatina fulica*)[10]. L'étude du transfert de nanoparticule d'argent depuis la laitue jusqu'aux escargots (*Achatina fulica*) a révélé des facteurs de transfert trophique de 2,0 à 5,9 dans le corps mou des escargots avec une bioamplification importante des nanoparticules d'argent. Ainsi, il semble que l'escargot soit un modèle biologique enclin au transfert trophique de nanoparticules. La caractérisation du transfert par voie trophique est plus que nécessaire afin de 1) caractériser l'exposition réelle en NMC pour les organismes dépendant des agrosystèmes et 2) garantir la sécurité sanitaire. D'autres incertitudes accompagnent l'étude de cette voie d'exposition notamment celle liée à la possibilité d'un effet « cheval de Troie » pour d'autres contaminants tels que les ETM en raison des interactions entre ces deux substances qui ont été étudiées dans les précédents chapitres.

Ici, un design expérimental plus complexe a été mis en place, avec l'utilisation d'un consommateur primaire sensible et considéré comme sentinelle pour la surveillance des ETM[11] en raison de ces deux voies d'exposition (trophique via l'ingestion de laitue ou environnementale via le contact avec un sol contaminé combinant exposition dermique et par voie orale) afin d'approfondir les connaissances sur l'écotoxicité de substances en mélange. Une attention particulière a été portée dans ce chapitre sur la synthèse et la quantification du transfert de NTC fortement enrichis en ^{13}C (100%) le long d'un réseau trophique reconstitué.

Résultats principaux :

La synthèse de NTC dopés à 100% en ^{13}C a permis de révéler une signature isotopique significativement différente dans les parties aériennes de la laitue après exposition à une dose de 10 mg.kg^{-1} pendant 2 semaines (Figure 1), pouvant révéler que les NTC s'accumulent dans ces parties. Bien que non statistiquement mise en évidence, une tendance a l'accumulation de NTC dans la glande digestive de l'escargot par voie trophique a été observée. L'exposition conjointe en NTC et ETM a augmenté le transfert de Zn dans les feuilles de laitues. De la même manière, l'ajout de 10 mg.kg^{-1} de NTC a augmenté le transfert de Cu dans la glande digestive de l'escargot par le la voie d'exposition par le sol. Aucune toxicité n'a été observé sur la biomasse des escargots aussi bien par exposition individuelle des NTC et ETM que par exposition conjointe, quel que soit la voie d'exposition (exposition trophique vs exposition par le sol). Les résultats de ce chapitre offrent de plus amples informations quant au transfert des NTC le long d'une chaine trophique et quant à la modification du transfert des ETM par les NTC chez la laitue et l'escargot.

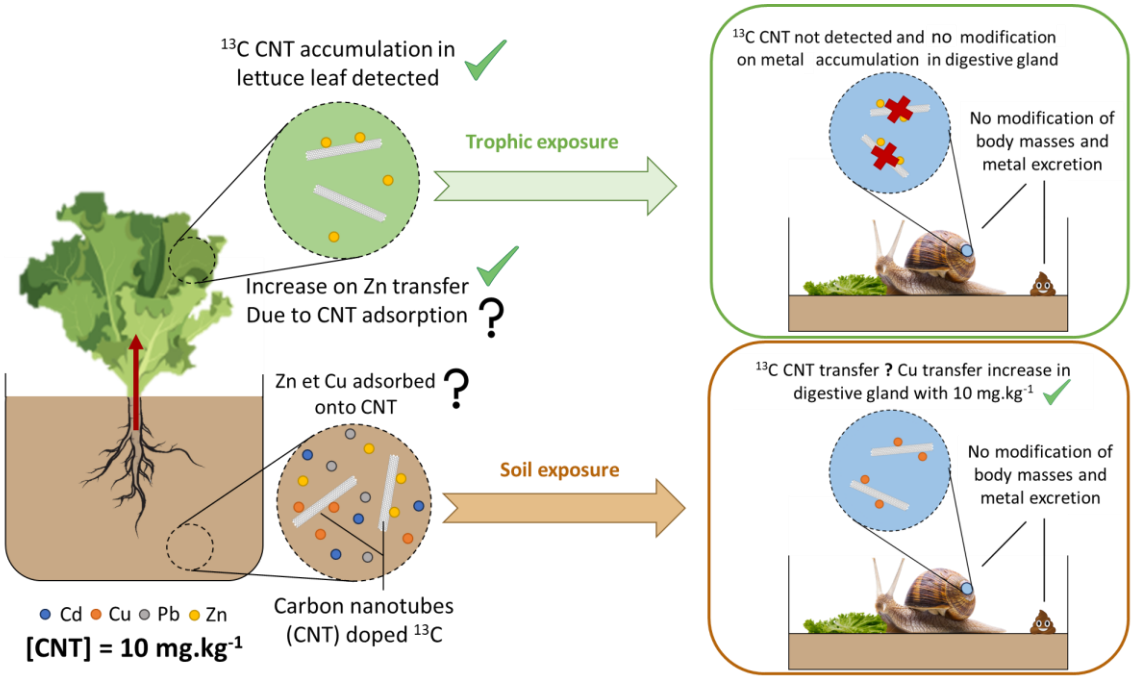

Figure 36: Schéma bilan des principaux résultats du chapitre 6

Bibliographie (chapitre 6):

(1) Petersen, E. J.; Huang, Q.; Weber, Jr., Walter J. Bioaccumulation of Radio-Labeled Carbon Nanotubes by Eisenia Foetida. *Environ. Sci. Technol.* **2008**, *42* (8), 3090–3095. https://doi.org/10.1021/es071366f.
(2) Petersen, E. J.; Huang, Q.; Weber, W. J. Ecological Uptake and Depuration of Carbon Nanotubes by Lumbriculus Variegatus. *Environ Health Perspect* **2008**, *116* (4), 496–500. https://doi.org/10.1289/ehp.10883.
(3) Ferguson, P. L.; Chandler, G. T.; Templeton, R. C.; DeMarco, A.; Scrivens, W. A.; Englehart, B. A. Influence of Sediment−Amendment with Single-Walled Carbon Nanotubes and Diesel Soot on Bioaccumulation of Hydrophobic Organic Contaminants by Benthic Invertebrates. *Environ. Sci. Technol.* **2008**, *42* (10), 3879–3885. https://doi.org/10.1021/es702830b.
(4) Larue, C.; Pinault, M.; Czarny, B.; Georgin, D.; Jaillard, D.; Bendiab, N.; Mayne-L'Hermite, M.; Taran, F.; Dive, V.; Carrière, M. Quantitative Evaluation of Multi-Walled Carbon Nanotube Uptake in Wheat and Rapeseed. *Journal of Hazardous Materials* **2012**, *227–228*, 155–163. https://doi.org/10.1016/j.jhazmat.2012.05.033.
(5) Liné, C. Evaluation of Parameters Influencing Plant Response to Carbon Nanotube Contamination. These de doctorat, Toulouse, INPT, 2019. http://www.theses.fr/2019INPT0082 (accessed 2021-07-06).
(6) Chen, G.; Qiu, J.; Liu, Y.; Jiang, R.; Cai, S.; Liu, Y.; Zhu, F.; Zeng, F.; Luan, T.; Ouyang, G. Carbon Nanotubes Act as Contaminant Carriers and Translocate within Plants. *Scientific Reports* **2015**, *5*, 15682. https://doi.org/10.1038/srep15682.
(7) Martínez-Ballesta, M. C.; Zapata, L.; Chalbi, N.; Carvajal, M. Multiwalled Carbon Nanotubes Enter Broccoli Cells Enhancing Growth and Water Uptake of Plants Exposed to Salinity. *Journal of Nanobiotechnology* **2016**, *14* (1), 42. https://doi.org/10.1186/s12951-016-0199-4.
(8) Khodakovskaya, M. V.; Kim, B.-S.; Kim, J. N.; Alimohammadi, M.; Dervishi, E.; Mustafa, T.; Cernigla, C. E. Carbon Nanotubes as Plant Growth Regulators: Effects on Tomato Growth, Reproductive System, and Soil Microbial Community. *Small* **2013**, *9* (1), 115–123. https://doi.org/10.1002/smll.201201225.
(9) Irin, F.; Shrestha, B.; Cañas, J. E.; Saed, M. A.; Green, M. J. Detection of Carbon Nanotubes in Biological Samples through Microwave-Induced Heating. *Carbon* **2012**, *50* (12), 4441–4449. https://doi.org/10.1016/j.carbon.2012.05.022.
(10) Chae, Y.; An, Y.-J. Nanoplastic Ingestion Induces Behavioral Disorders in Terrestrial Snails: Trophic Transfer Effects via Vascular Plants. *Environ. Sci.: Nano* **2020**, *7* (3), 975–983. https://doi.org/10.1039/C9EN01335K.
(11) Baroudi, F.; Al Alam, J.; Fajloun, Z.; Millet, M. Snail as Sentinel Organism for Monitoring the Environmental Pollution; a Review. *Ecological Indicators* **2020**, *113*, 106240. https://doi.org/10.1016/j.ecolind.2020.106240.

Trophic transfer and soil exposure to a cocktail of contaminants (carbon nanotubes and trace metal) in a terrestrial food chain

Leroy Mathieu[1,2], Frédéric Gimbert[3], Silvestre Jérôme[1], Stéphanie Sorieul[4], Flahaut Emmanuel[2], Larue Camille[1*]

[1]Laboratoire Ecologie Fonctionnelle et Environnement, Université de Toulouse, CNRS, Toulouse, France,

[2]CIRIMAT, Université de Toulouse, CNRS, INPT, UPS, UMR CNRS-UPS-INP N°5085, Université Toulouse 3 Paul Sabatier, Bât. CIRIMAT, 118, route de Narbonne, 31062 Toulouse cedex 9, France

[3]UMR 6249 Chrono-environnement CNRS - Université de Franche-Comté Usc INRAe, 16 route de Gray, 25030, Besançon, cedex, France

[4]Université Bordeaux 1, CNRS/IN2P3, Centre d'Etudes Nucléaires de Bordeaux Gradignan, CENBG, Chemin du Solarium, BP120, 33175 Gradignan, France

1. Intoduction

The properties of carbon nanomaterials (CNM) have made it possible to initiate a great deal of research on these materials and their applications in various sectors are striking. As the use of CNM in everyday consumer products begin to become widespread and on the light of past experience with poor preliminary risk assessment, notably with asbestos fibers, (eco)toxicological studies have been set up in parallel with CNM development to estimate potential risks to the environment.

With 20 years of research, the scientific corpus on the ecotoxicity of CNM is increasing and several reviews report the effects of CNM on terrestrial organisms[1–9]. Among the terrestrial ecosystems most likely to accumulate CNM are agrosystems. Indeed, some studies suggest that CNM would offer agricultural opportunities since they could increase crop yields[5,10]. In addition, sewage sludge, which is spread on agrosystems as fertilizer, is known to accumulate CNM and could be a major source of entry

into agrosystems[11,12]. Modelling predicts that concentration of CNM in biosolids could reach up to 10 $mg.kg^{-1}$ while in natural soil it could be up to 0.01 $mg.kg^{-1}$ [12].

However, the overwhelming majority of studies focus on the toxicity of CNM on a single organism; this approach misses the complexity of natural environment and could thus be of little relevance from an environmental point of view. In particular, very little data is available so far to characterize trophic transfer from soil to primary producer to primary consumers. Also, there are very few studies focusing on the ecotoxicity of CNM on primary consumers in general, and on crop pests in particular which are ubiquitous and can colonize other terrestrial ecosystems. Among these, snails have proven to cause significant crop and economic yield losses[13]. In addition, snails are recognized as sentinels for assessing the contamination of the terrestrial environment for other pollutants such as the trace metallic elements (TME). For example, after topical application of 1/10 and 1/50 of the lethal dose (LD_{50} = 79.6 $\mu g.snail^{-1}$), Abdel-Halim *et al.*[14] showed that CNT induced toxic effects by interaction with cell membranes or penetration in the digestive gland cells through generation of reactive oxygen species (ROS). CNT could also induced DNA damage in digestive gland cells in *Lymnea luteola*[15]. Furthermore, snails are also very interesting for ecological risk assessment as they present several routes of exposure: an active route via ingestion of plants and soil, and a second passive route *via* dermal transfer.

In addition to toxicity, a specific issue regarding CNM, is their quantification in biological matrices. Indeed, essentially composed of carbon, quantitatively determining the transfer of CNM in biological matrices themselves composed of carbon remains a technical challenge. A solution used by Petersen *et al.*[16,17], Ferguson *et al.*[18] and Larue *et al.*[19] is the use of radioactive isotope labelling. In a study exposing biofilm and *Lymnaea stagnalis* which consumed biofilm in aquatic systems exposed to CNT doped with ^{14}C, the authors demonstrated that CNT could penetrate in all parts of the digestive tract included digestive gland. The enrichment of biofilm and *L. stagnalis* in ^{14}C-CNT was calculated and amounted 529.0 and 79.6 $\mu g.g^{-1}$ dry weight, respectively. After depuration, no CNT were found

extracellularly in the digestive system, which evidenced the elimination capabilities of *L. stagnalis*[20]. Others studies tried to quantify CNT transfer using different tools such as microscopic observations[19,21,22], Raman spectroscopy[23] or microwave-induced heating[24] but with a low sensitivity and/or specificity.

Finally, CNM also raise questions due to their interactions with other contaminants. In particular, they are able to adsorb compounds such as pesticides[25] and TME[26] on their surface, compounds whose monitoring is already implemented in agrosystems in order to guarantee food safety. Many examples in the scientific literature report a modification of TME transfer from the exposure matrix to the organisms due to their interactions with CNM[9,26–38], which can ultimately modify their toxiciy[26]. For instance, in a previous study we demonstrated that when earthworms were exposed to TME contaminated soils (Zn, Pb and Cd), the addition of CNT led to an increase of 34% and 25% respectively for Pb and Zn concentrations in earthworms [9].

Thus, the objectives of this study were three fold: (1) implement a new method to characterize CNT uptake in organisms (plants and snails) relying on ^{13}C-CNT synthesis and detection through spectroscopic based techniques (py-IRMS and µNRA) (ii) quantify the trophic transfer of CNT to snails via two exposure routes (soil or plant consumption) and (iii) assess the impact of a co-contamination CNT/TME on the toxicity and the transfer of the mixture in a reconstituted trophic chain (soil / primary producer: *Lactuca sativa* / primary consumer: *Helix aspersa*)

2. Material and methods

2.1. CNT synthesis and characterization

CNTs were synthesized at the Interuniversity Center of Materials Research and Engineering (CIRIMAT, Toulouse University). In brief, a catalytic powder was prepared by impregnation of MgO powder (Honeywell, ref. 372493) by Co (cobalt nitrate hexahydrate) and Mo (ammonium heptamolybdate) salts to reach an elemental composition of $Mg_{0.99}(Co_{0.0075}Mo_{0.0025})O$. After incubation 1h at 50°C, the

suspension was frozen in liquid nitrogen to limit sedimentation, before freeze drying. The obtained powder was calcined in air at 450°C for 1h in air flow. 1g of catalytic powder was introduced in an alumina boat, placed at the center of a quartz reactor. A N_2 flow (3 $L.h^{-1}$) was used to carry EtOH vapors by flowing in a flask containing 2 g of 100% ^{13}C ethanol (Sigma-Aldrich, CAS 14742-23-5, ref Sigma 427039). The flask was immerged in an oil bath thermostatically controlled at 25°C to avoid interferences from room temperature variations. A heating wire (60°C) was rolled around the hose connecting the EtOH reservoir to the reactor to avoid the condensation of EtOH vapors. The catalytic powder was heated at 850°C (5°C/min) in N_2 atmosphere (3 $L.h^{-1}$). During a 30 min dwell time at this temperature, a valve was operated to force the flow of N_2 through the washing bottle containing the ^{13}C EtOH. Then, the temperature was decreased to room temperature (5°C/min) in N_2 atmosphere (3 $L.h^{-1}$). At the end of the synthesis, a black composite powder was obtained. CNTs were first extracted from the nanocomposite powder by processing in an aqueous solution of HCl, then washed to neutrality using deionised water. Then, the wet CNTs were oxidised in 3M HNO_3 by refluxing them at 130°C for 24h. Finally, the oxidized CNTs were washed to neutrality using deionised water and used wet. They were oxidized multiwalled CNT (MWCNT) with length varying from 1 to 20 µm, an average diameter of 22.5 ± 5.0 nm (Figure 37) and a specific surface area of 60 $m^2.g^{-1}$.

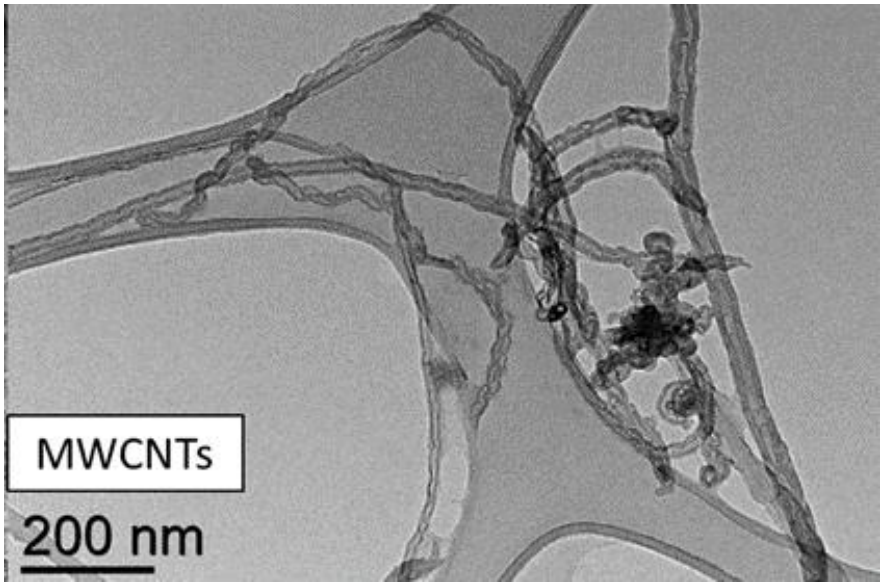

Figure 37: Transmission Electronic Microscopy observations of o-MWCNT used in this study

CNT were suspended in deionised water at 3 $g.L^{-1}$ and homogenized for 15 min in an ultrasonic bath before use.

2.2. Soil characterization and contamination

A loamy sand standard soil was used (LUFA-Speyer 2.1) for this experiment with 80.20% of sand, 18.80% of loam and 1.0% of clay. It contained 1.82% of organic carbon, 0.1% of nitrogen with a pH of 7.00 ± 0.21 and a cation exchange capacity of 2.9 ± 0.2 $meq.100g^{-1}$.

Soils were contaminated by the addition of the required volume of CNT suspension to reach a final concentration of 0.1 or 10 $mg.kg^{-1}$ dry soil; the first concentration being close to environmentally predicted concentrations[12] and the second one representing a worst case scenario (use of nanofertiliser for instance). Additionally, part of the soils was contaminated with Cd, Cu, Pb and Zn at 0.2, 7, 20 and 40 $mg.kg^{-1}$ with solutions of $CdN_2O_6{\cdot}4H_2O$, $CuN_2O_6{\cdot}2.5H_2O$, $Pb(NO_3)_2$, and $Zn(NO_3)_2{\cdot}6H_2O$ (98%, Sigma) corresponding of the average concentrations in French soils[39]. They were then mixed manually for 10 min every day for a week to ensure that CNT and TME were homogeneously distributed in the soil. Effective concentrations of Cd, Cu, Pb and Zn in soils are presented in Table 8.

Table 8: Average total concentrations and standard deviation of Cd, Cu, Pb and Zn in the soil in the two levels of contamination (CTRL: control soils and TME: soils with trace metal addition, unit: $mg.kg^{-1}$). Same lowercase letters indicate treatments that do not differ significantly (p-value > 0.05) following a t-test (n = 15).

	Cd	Cu	Pb	Zn
CTRL	0.20 ± 0.05 **a**	1.93 ± 0.36 **a**	10.82 ± 2.84 **a**	9.34 ± 1.68 **a**
TME	0.40 ± 0.06 **b**	9.13 ± 1.03 **b**	31.76 ± 3.82 **b**	52.42 ± 7.91 **b**

2.3. Experimental set-up

Two connected experiments were set-up to investigate the transfer and toxicity of the two exposure routes: one trophic exposure with snails feeding on contaminated lettuce leaves and the second with snails feeding on contaminated soil (and fresh non contaminated lettuce leaves). Two TME modalities were tested in experiments as one control soil without TME and a second one with TME added in soil

(Table 1). Three CNT concentrations were tested for each TME modalities: one control without CNT (0 and TME 0), a second one with the addition of 0.1 $mg.kg^{-1}$ CNT (0.1 and TME 0.1) and finally one with 10 $mg.kg^{-1}$ CNT (10 and TME 10). For the six exposure modalities, experimental units were replicated 5 times (n = 30).

320 g of soil were distributed in each experimental unit for the growth of the lettuce model used (*Lactuva sativa* var. Laitue romaine). Lettuces were previously grown during 4 weeks on hydroponic system in an environmental chamber (14 h/10 h day/night cycle, 24°/18°C and a hygrometry rate of 85%) to obtain sufficient biomass to feed snails properly. Then, lettuces were exposed to control or contaminated soil during 2 weeks in the same environmental chamber. Two days before snail exposure, juvenile snails were awaken and selected in a restricted body mass range (1.41 ± 0.26 g). Two snails were placed in each experimental unit (L = 12 cm, l = 11 cm, H = 5.2 cm) with 60 g of non-contaminated soil moistened at 40% of its water holding capacity. Then, 2 g of fresh lettuce leaves were added every 2 days corresponding to an adequate amount of food provision for snails of that developmental stage. The snail exposure lasted for 2 weeks in an environmental chamber with controlled parameters (18 h/6 h day/night cycle, 20 ± 1°C and a hygrometry rate of 80%). After plant exposure, 200 g of control or contaminated soils were oven-dried at 50°C during 3 days to reuse it for snail soil exposure.

For snail soil exposure, 150 g of control or contaminated dried soil used for plant growth were placed in each experimental unit. Soil was moistened at 40% of its water holding capacity. Two juvenile snails selected in a restricted body mass range (1.43 ± 0.32 g) were placed in each experimental unit and fed with 2 g of uncontaminated lettuce leaves. The exposure was conducted over 10 days.

During both exposure experiments, snail faeces were removed of the experimental units every 2 days. Faeces which were not in contact with soils were dried for ICP-AES analyses.

At the end of exposure, snails were weighted using a balance then dissected to collect the digestive gland. One digestive gland per condition as well as the corresponding lettuce leaf (for trophic exposure

pathway) were included in an OCT TissueTeck resin and kept in the freezer for further spectroscopic analyzes (see section 2.6.). One gram of lettuce leaf and the digestive gland of the second snail for each condition were dried at 80°C during 4 days and used for ICP-AES and py-IRMS measurements.

2.4. Sample preparation and chemical analysis by ICP-AES

Soil and plant samples (500 mg) were added to 3 ml HNO_3 overnight. Then, 1 ml of a mix of HNO_3 and HCl (3:1 v/v) (only for soil samples) and 1 ml of H_2O_2 were added before being introduced in a microwave system (MARS 2, CEM corporation, Matthews, NC, USA) to perform digestion (ramp time: 20-25 min; holding time: 10 min; temperature: 190 °C). For soil, a filtration step (0.45 µm, polypropylene membrane) was added. Digested samples were then diluted to reach 5% HNO_3 in samples before analysis on an ICP-AES (ARCOS FHX22, AMETEK Spectral) along with control samples (blanks with only chemicals).

2.5. Sample preparation and isotopic ^{13}C analysis by py-IRMS

Soil, lettuce leaves and digestive glands of snails were analyzed by pyrolysis Isotopic Ratio Mass spectrometry (py-IRMS) to detect the ^{13}C signal constitutive of the CNT used. Soil and lettuce leaves were dried for 2 days at 80°C while digestive glands were freeze-dried during 24 h. Then, samples were ground using a FastPrep-24™ (MpBio) at 6 $m.s^{-1}$ during 40 sec and py-IRMS analyses were performed at the GISMO platform (Université de Bourgogne).

2.6. Sample preparation and microbeam analysis

Upon harvest, samples of leaves and digestive glands were cut in small pieces of few millimeters long and placed in Tissue-Teck OCT (Optimal Cutting Temperature) resin in an Eppendorf tube and frozen at -80°C. 30 µm thick cross sections were done using a cryo-microtome with a chamber set at -20°C (Thermo Fisher Scientific). Cross sections were then freeze-dried (Christ Alpha 1,4 LSCbasic).

For analyses, cross-sections were placed between two ultralene foils and taped on a PEEK support. Energy of the beam was 1300 keV and with a current of an intensity of 1 nA on sample. Beam size was 1 µm. More information about technique on Barberet *et al.*[40].

2.7. Statistical analyses and calculations

For statistical analyses, 2-way ANOVAs were performed. Preliminary tests were carried out to check the normality, independence and homoscedasticity of the residues using Shapiro, Durbin-Watson and Breusch-Pagan tests, respectively. If one of the three conditions of validity was not met, data were transformed to log or square root and a Kruskal-Wallis test was performed in the case of failed transformations. Principal component analyses (PCA) were performed on the elemental concentrations in plants, digestive glands and faeces. Statistical analyses were performed on RStudio software (version 3.4.1).

Transfer factors for trophic and soil exposure were calculated as following equations (1) and (2), respectively:

(1) $$TF = \frac{\text{TME concentration in digestive glands}}{\text{TME concentration in lettuce leaves}}$$

(2) $$TF = \frac{\text{TME concentration in digestive glands}}{\text{TME concentration in soil}}$$

3. Results

3.1. Trophic transfer from soils to lettuce to snails

3.1.1. Quantification of CNT and TME transfer in lettuce and snails

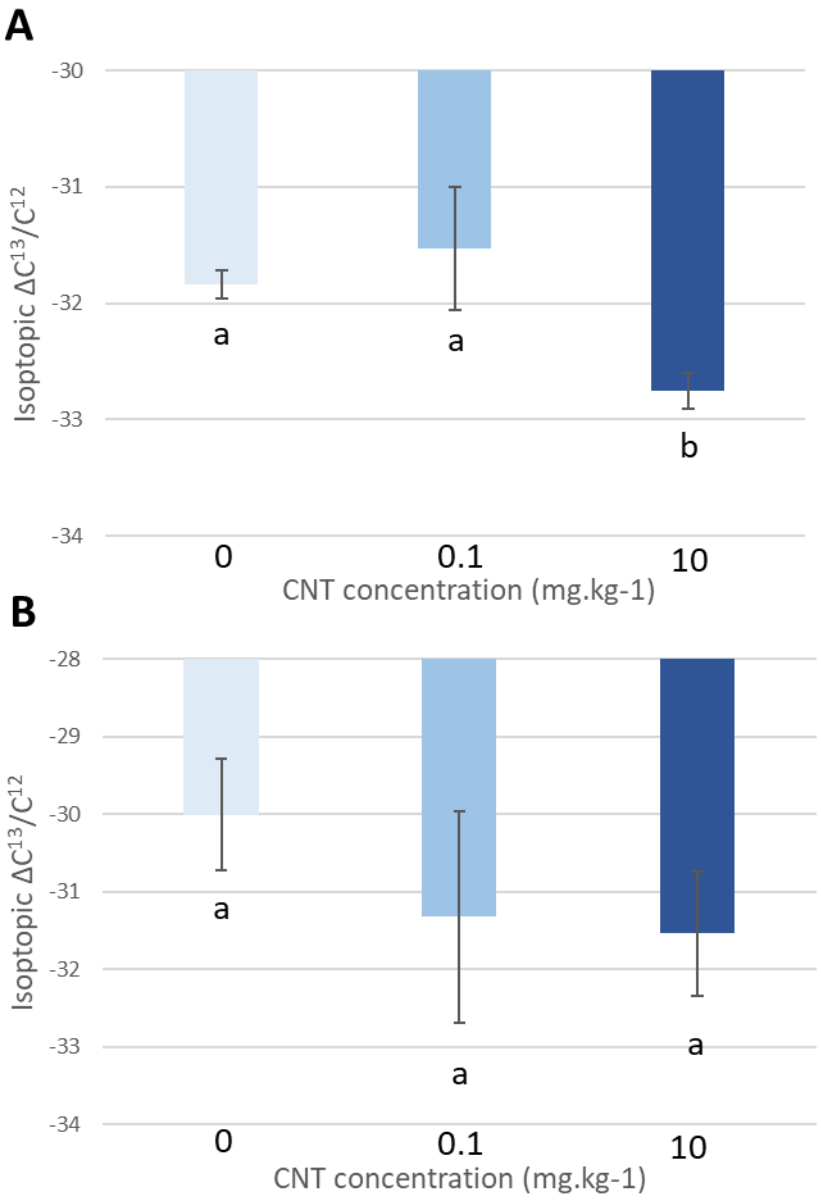

Figure 38: Average isotopic $\Delta C^{13}/C^{12}$ of (A) lettuce leaves grown in soil contaminated with CNT (CTRL: control soils, 0.1: CNT exposure at 0.1 mg.kg^{-1}, 10: CNT exposure at 10 mg.kg^{-1}) and (B) in the digestive gland of snails feeding on the lettuce grown on contaminated soils. Same lowercase letters indicate treatments that do not differ significantly (p-value > 0.05) following a 1 way ANOVA test (n = 5).

Isotopic Δ C^{13}/C^{12} in lettuce leaves was significantly higher up to 3% for lettuce exposed to 10 mg.kg^{-1} than control lettuce (without CNT, $p < 0.01$, Figure 38A). It was not the case for lettuce exposed to 0.1 mg.kg^{-1} with on average -30.7.

Isotopic Δ C^{13}/C^{12} in digestive glands of snails feeding on lettuce grown on contaminated soil was not significantly different among CNT modalities (p = 0.21, Figure 38B) with on average -30.6. However, a trend is noticeable with an increase of 4.8% (same extent as in lettuce leaves) for snails feeding on contaminated lettuce leaves.

Table 9: Average concentrations and standard deviation of Cd, Cu, Pb and Zn after trophic transfer experiment in (A) lettuce leaves grown on contaminated soils, (B) digestive glands and (C) snail faeces feeding on lettuce grown in contaminated soil (mg.kg^{-1}) for the six exposure modalities used in experiment (0: control soils without CNT, 0.1: CNT exposure at 0.1 mg.kg^{-1}, 10: CNT exposure at 10 mg.kg^{-1}, TME: soils with added trace metals (final concentration:s Cd: 0.40, Cu: 9.13, Pb: 31.76, Zn: 52.42 mg.kg^{-1}), *TME 0.1: soils with added trace metals and CNT exposure at 0.1 mg.kg^{-1} and TME 10: soils with added trace metals and CNT exposure at 10 mg.kg^{-1}). Same lowercase letters indicate treatments that do not differ significantly (p-value > 0.05) following a Kruskal Wallis test for Cd, Cu and Zn and 2 way ANOVA test for Pb for lettuce, a 2 way ANOVA test for Cd, Cu and Pb and Kruskal Wallis test for Zn for digestive glands and a 2 way ANOVA for each metals for snail faeces. Time exposure for lettuces and snails: 2 weeks. (n = 5)*

A	**Cd**	**Cu**	**Pb**	**Zn**
0	0.06 ± 0.03 **a**	1.21 ± 0.12 **a**	0.60 ± 0.23 **a**	4.86 ± 0.70 **a**
0.1	0.08 ± 0.03 **a**	1.14 ± 0.38 **a**	0.71 ± 0.14 **bc**	5.41 ± 1.21 **a**
10	0.07 ± 0.03 **a**	0.86 ± 0.19 **a**	0.67 ± 0.22 **abc**	5.36 ± 4.93 **a**
TME	0.12 ± 0.01 **ab**	0.72 ± 0.03 **a**	1.28 ± 0.25 **c**	7.75 ± 6.68 **a**
TME 0.1	0.12 ± 0.03 **ab**	0.73 ± 0.33 **a**	1.18 ± 0.36 **c**	8.46 ± 5.51 **a**
TME 10	0.16 ± 0.05 **b**	0.77 ± 0.12 **a**	0.93 ± 0.05 **bc**	20.30 ± 5.41 **b**

B	**Cd**	**Cu**	**Pb**	**Zn**
0	0.70 ± 0.22 **ab**	7.59 ± 2.00 **a**	3.43 ± 1.47 **bc**	61.40 ± 10.81 **a**
0.1	0.54 ± 0.18 **a**	8.80 ± 1.92 **a**	4.04 ± 1.44 **c**	127.57 ± 30.48 **ab**
10	0.54 ± 0.18 **a**	6.10 ± 1.51 **a**	2.67 ± 0.90 **abc**	63.53 ± 9.42 **a**
TME 0	0.74 ± 0.25 **ab**	5.10 ± 2.54 **a**	1.67 ± 0.32 **ab**	109.53 ± 40.30 **ab**
TME 0.1	0.48 ± 0.25 **a**	4.85 ± 1.44 **a**	0.66 ± 0.49 **a**	96.06 ± 2.11 **ab**
TME 10	1.13 ± 0.28 **b**	6.11 ± 2.18 **a**	1.85 ± 0.87 **abc**	150.56 ± 24.70 **b**

C	**Cd**	**Cu**	**Pb**	**Zn**
0	0.0030 **a**	0.24 ± 0.11 **a**	0.44 ± 0.23 **a**	2.54 ± 0.90 **a**
0.1	0.0027 ± 0.0021 **a**	0.22 ± 0.06 **a**	0.46 ± 0.13 **a**	2.33 ± 1.01 **a**
10	0.0038 ± 0.0027 **a**	0.18 ± 0.05 **a**	0.42 ± 0.21 **a**	2.16 ± 0.51 **a**
TME 0.1	0.0023 ± 0.0011 **a**	0.18 ± 0.03 **a**	0.41 ± 0.08 **a**	2.51 ± 1.18 **a**
TME 0.1	0.0018 ± 0.0016 **a**	0.17 ± 0.06 **a**	0.41 ± 0.08 **a**	3.66 ± 1.53 **a**
TME 10	0.005 ± 0.0026 **a**	0.19 ± 0.05 **a**	0.45 ± 0.12 **a**	3.70 ± 1.58 **a**

Concentrations of Cd, Pb and Zn in lettuce leaves were 87%, 70% and 121% higher, respectively, for lettuce exposed to TME than unexposed while it was not the case for Cu (p_{Cd} < 0.01, p_{Cu} = 0.06 p_{Pb} < 0.01, p_{Zn} < 0.01, Table 9A).

There was no significant effect of CNT addition on Cd, Cu, Pb and Zn concentration in lettuce leaves (p_{Cd} = 0.31, p_{Cu} = 0.45, p_{Pb} = 0.61, p_{Zn} = 0.08, Table 9A).

Only for Zn concentration in lettuce leaves, an interaction between CNT and TME was found (p_{Zn} = 0.02, Table 9A). Lettuces exposed to 10 mg.kg^{-1} of CNT in soils with TME contained 162% more Zn in their leaves than lettuces exposed to TME without CNT, while it was not the case for lettuces without addition of TME. No CNT/TME interactions were detected for Cd, Cu and Pb concentration in lettuces leaves (p_{Cd} = 0.24, p_{Cu} = 0.27, p_{Pb} = 0.25, Table 9A).

TME effect was significant for both Cd and Zn concentrations in the digestive gland of snails feeding on exposed plants with an increase up to 32% and 49% upon addition of TME, respectively (p_{Cd} = 0.04, p_{Zn} < 0.01, Table 9B). On the opposite, for Pb it was significantly lower for snails exposed to soils with TME (TME, TME 0.1 an TME 10) than those exposed to soils without TME (0, 0.1 and 10) with an decrease of 56% (p_{Pb} < 0.01, Table 9B). Cu concentration in the digestive gland of snails was not different between exposure modalities with on average 6.47 mg.kg^{-1} whatever the conditions (p_{Cu} = 0.06).

There was a significant CNT/TME interaction on Cd concentration in the digestive gland of snails so that snails exposed to 10 mg.kg^{-1} of CNT in soils with TME contained 52% more Cd in their digestive gland than with other CNT concentrations (0 and 0.1 mg kg^{-1}) which was not the case for snails exposed to soils without addition of TME (p_{Cd} = 0.02). This interaction was not detected for Cu, Pb and Zn (p_{Cu} = 0.77, p_{Pb} = 0.85, p_{Zn} = 0.06).

Concerning Cd, Cu, Pb and Zn concentrations in snail faeces, no significant differences were detected with on average 0.003, 0.20, 0.43 and 2.88 mg.kg^{-1}, respectively (Table 9C).

3.1.2. Trophic transfer impact on plants and snails

The PCA on nutrient concentration in lettuce leaves and snail digestive gland did not individualized any group and indicated that nutrient concentrations in these organs were similar among exposure modalities (Figure 39).

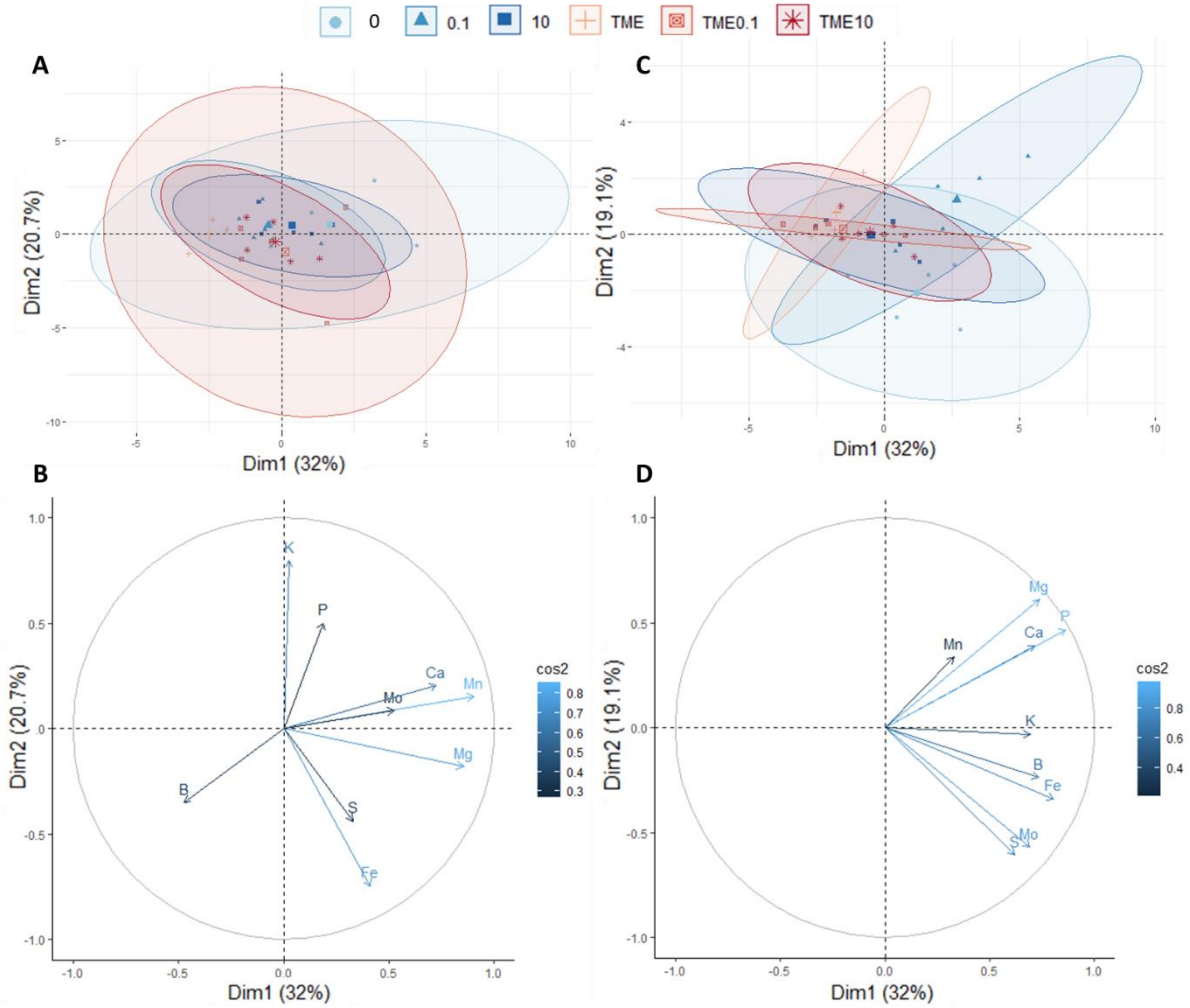

Figure 39: PCA on the concentrations of nutrients (B, Ca, Fe, K, Mg, Mn, Mo, P and S) in lettuce leaves (A, B) and snail digestive glands (C, D) for the six exposure modalities (0: control soils without CNT, 0.1: CNT exposure at 0.1 mg.kg^{-1}, 10: CNT exposure at 10 mg.kg^{-1}, TME: soils with added trace metals (final concentrations: Cd: 0.40, Cu: 9.13, Pb: 31.76, Zn: 52.42 mg.kg^{-1}), TME 0.1: soils with added trace metals and CNT exposure at 0.1 mg.kg^{-1} and TME 10: soils with added trace metals and CNT exposure at 10 mg.kg^{-1}) at the end of exposure (2 weeks). PCA represent individuals and correlation circle graphs and Cos2 corresponds to the level of variable contributions (elements) to dimensions 1 and 2.

No significant effect of TME, CNT and their interactions were found on snail biomass (p_{TME} = 0.40, p_{CNT} = 0.73, $p_{CNT/TME}$ = 0.97, Figure 40), with on average 1.82 g.snails^{-1} whatever the condition.

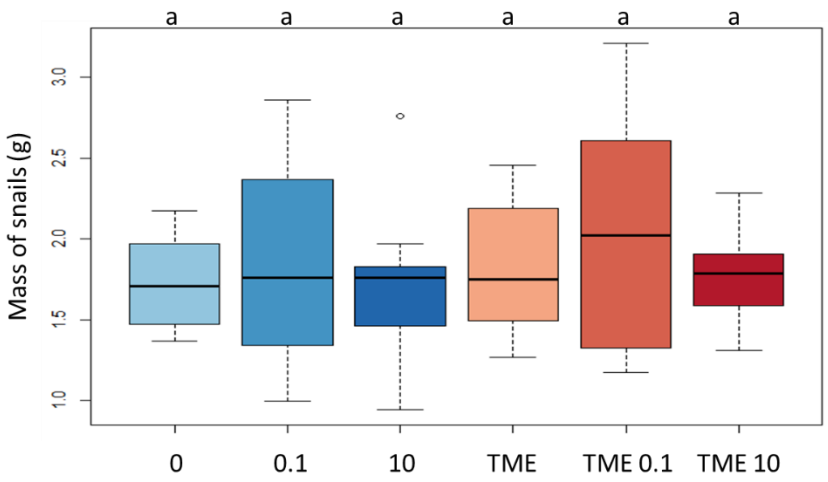

Figure 40: Average biomass of snails fed with control or contaminated lettuce leaves for 14 days for the six exposure modalities (CTRL: control soils, 0.1: fed with plants exposed to CNT at 0.1 mg.kg^{-1}, 10: fed with plants exposed to CNT at 10 mg.kg^{-1}, TME: fed with plants exposed to soils with trace metals (final concentrations: Cd: 0.40, Cu: 9.13, Pb: 31.76, Zn: 52.42 mg.kg^{-1}), TME 0.1: fed with plants exposed to soils with trace metals and CNT at 0.1 mg.kg^{-1} and TME 10: fed with plants exposed to soils with trace metals and CNT at 10 mg.kg^{-1}). Same lowercase letters indicate treatments that do not differ significantly (p-value > 0.05) following a 2 way ANOVA (n = 5).

3.2. Soil to snail transfer experiment

3.2.1. Quantification of CNT and TME transfer in snails

^{13}C quantification py-IRMS on the digestive gland of snails are currently being analyzed on the GISMO platform (Université de Bourgogne) and will be provided soon.

Cd, Cu, Pb and Zn concentrations in the digestive gland of snails were significantly higher for snails exposed to soils with TME than those exposed to soils without addition of TME with an increase up to 18%, 7%, 265% and 33%, respectively ($p_{Cd} < 0.01$, $p_{Cu} < 0.01$, $p_{Pb} < 0.01$, $p_{Zn} = 0.02$, Table 10A).

There was no significant effect of CNT on the transfer of all TME into the snail digestive gland ($p_{Cd} = 0.54$, $p_{Cu} = 0.11$, $p_{Pb} = 0.08$, $p_{Zn} = 0.74$).

However, for Cu transfer to the digestive gland, a CNT/TME interaction was found so that snails exposed to 10 mg.kg^{-1} of CNT in soils with added TME contained 61% more Cu in their digestive gland than when exposed to other CNT concentrations (0 and 0.1 mg.kg^{-1}) which was not the case for snails exposed to soils without TME ($p_{Cd} = 0.01$). The same CNT/TME interaction effect was observed for Cd and Zn but not significant while it was not the case for Pb ($p_{Cd} = 0.07$, $p_{Pb} = 0.38$, $p_{Zn} = 0.04$).

For all TME studied (Cd, Cu, Pb and Zn), their concentrations in snail faeces were significantly higher for snails exposed to soils with added TME with an increase up to 136%, 258%, 259% and 183%, respectively ($p_{Cd} < 0.01$, $p_{Cu} < 0.01$, $p_{Pb} < 0.01$, $p_{Zn} < 0.01$, Table 10B).

No effects of CNT addition was detected ($p_{Cd} = 0.14$, $p_{Cu} = 0.09$, $p_{Pb} = 0.63$, $p_{Zn} = 0.10$). Also, there was no CNT/TME interaction in snail faeces ($p_{Cd} = 0.72$, $p_{Cu} = 0.37$, $p_{Pb} = 0.51$, $p_{Zn} = 0.78$). However, trends could be noticed so that Cd, Cu and Pb concentrations in snail dejections were lower with 10 $mg.kg^{-1}$ CNT than without CNT when snails were exposed to TME soils while it was not the case for Pb.

Table 10: Average total concentrations and standard deviation (n = 5) of Cd, Cu, Pb and Zn contained in (A) the digestive gland and (B) faeces ($mg.kg^{-1}$ dry weight) of snails after a 10-day exposure for the six exposure modalities (CTRL: control soils, 0.1: soil contaminated with 0.1 $mg.kg^{-1}$ CNT, 10: soil contaminated with 10 $mg.kg^{-1}$ CNT, TME: soils with added trace metals (final concentrations: Cd: 0.40, Cu: 9.13, Pb: 31.76, Zn: 52.42 $mg.kg^{-1}$), TME 0.1: soil contaminated with trace metals and 0.1 $mg.kg^{-1}$ CNT and TME 10: soil contaminated with trace metals and 10 $mg.kg^{-1}$ CNT. Same lowercase letters indicate treatments that do not differ significantly (p-value > 0.05) following a 2 way ANOVA for Cd, Pb and Zn and Kruskal Wallis test for Cu for digestive gland transfer results (A) and a 2 way ANOVA test for faeces results (B).

A

	Cd	Cu	Pb	Zn
0	0.67 ± 0.09 **ab**	5.72 ± 2.03 **ab**	2.26 ± 0.40 **a**	90.57 ± 9.58 **a**
0.1	0.64 ± 0.13 **ab**	4.70 ± 0.28 **a**	2.56 ± 0.71 **a**	90.43 ± 14.22 **a**
10	0.51 ± 0.09 **a**	4.93 ± 0.68 **a**	2.28 ± 0.18 **a**	71.21 ± 14.42 **a**
TME 0	0.89 ± 0.14 **bc**	7.21 ± 2.40 **ab**	13.41 ± 2.15 **b**	169.46 ± 20.22 **b**
TME 0.1	1.02 ± 0.12 **c**	8.63 ± 1.29 bc	16.07 ± 2.31 **b**	176.15 ± 22.54 **b**
TME 10	1.12 ± 0.28 c	11.65 ± 2.24 **c**	13.76 ± 3.01 **b**	206.83 ± 38.95 **b**

B

	Cd	Cu	Pb	Zn
0	0.009 ± 0.003 **ab**	0.26 ± 0.04 **a**	0.99 ± 0.20 **a**	2.61 ± 0.62 **a**
0.1	0.007 ± 0.003 **a**	0.27 ± 0.03 **a**	1.05 ± 0.22 **a**	2.44 ± 0.71 **a**
10	0.006 ± 0.004 **a**	0.24 ± 0.03 **a**	0.81 ± 0.15 **a**	1.96 ± 0.08 **a**
TME 0	0.021 ± 0.011 **b**	1.03 ± 0.40 **b**	3.45 ± 0.65 **b**	8.00 ± 3.11 **b**
TME 0.1	0.019 ± 0.004 **b**	0.85 ± 0.11 **b**	3.38 ± 0.73 **b**	7.03 ± 2.11 **b**
TME 10	0.014 ± 0.004 **ab**	0.88 ± 0.24 **b**	3.46 ± 1.04 **b**	5.21 ± 2.18 **b**

3.2.2. Impacts of soil exposure to snails

The PCA on nutrient concentration snail digestive gland did not individualized any group and indicated that nutrient concentrations in these organs were similar among exposure modalities (Figure 41).

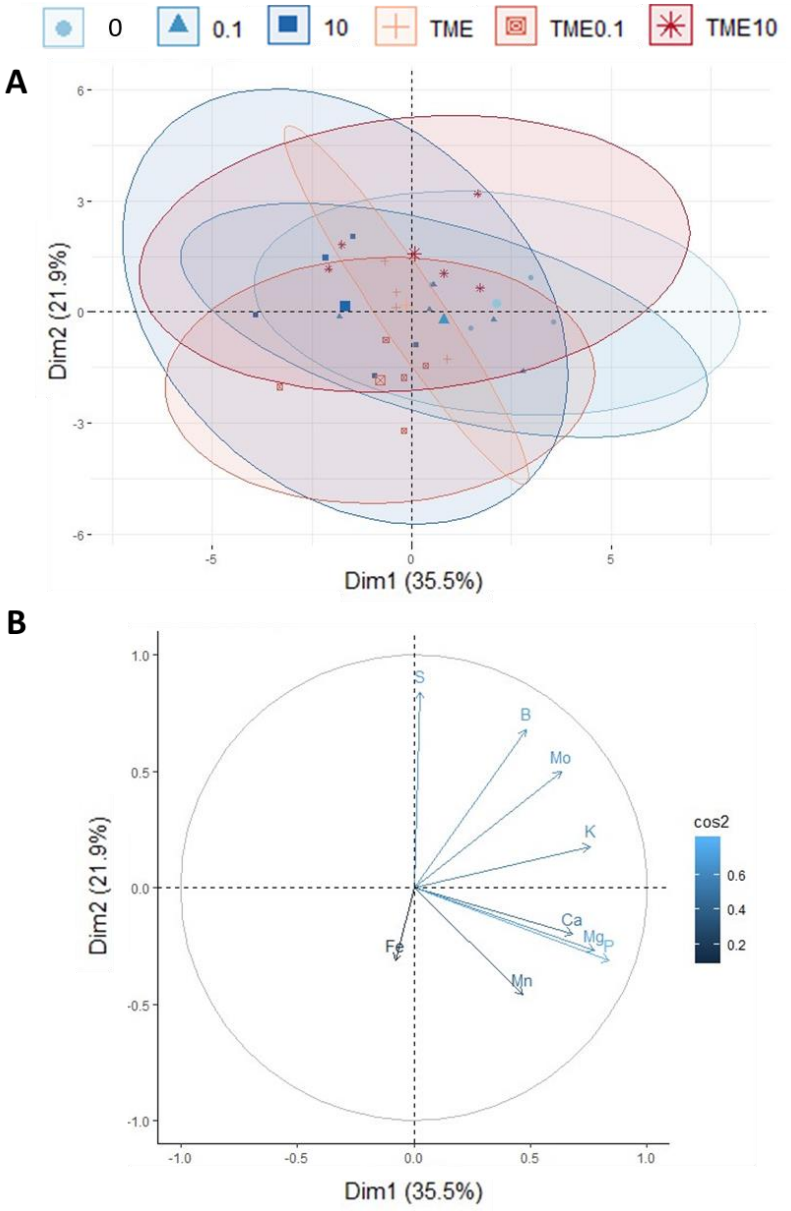

Figure 41: PCA on the concentrations of nutrients (B, Ca, Fe, K, Mg, Mn, Mo, P and S) in snail digestive glands for the six exposure modalities (0: control soils without CNT, 0.1: CNT exposure at 0.1 mg.kg^{-1}, 10: CNT exposure at 10 mg.kg^{-1}, TME: soils with added trace metals (final concentrations: Cd: 0.40, Cu: 9.13, Pb: 31.76, Zn: 52.42 mg.kg^{-1}), TME 0.1: soils with added trace metals and CNT exposure at 0.1 mg.kg^{-1} and TME 10: soils with added trace metals and CNT exposure at 10 mg.kg^{-1}) at the end of exposure (2 weeks). PCA represent individuals (A) and correlation circle (B) graphs and Cos2 corresponds to the level of variable contributions (elements) to dimensions 1 and 2.

No significant effect of TME, CNT and their interactions were found on snail biomass (p_{TME} = 0.17, p_{CNT} = 0.55, $p_{CNT/TME}$ = 0.79, Figure 42) with on average 1.69 g.snails^{-1} whatever condition after 10 days of soil exposure.

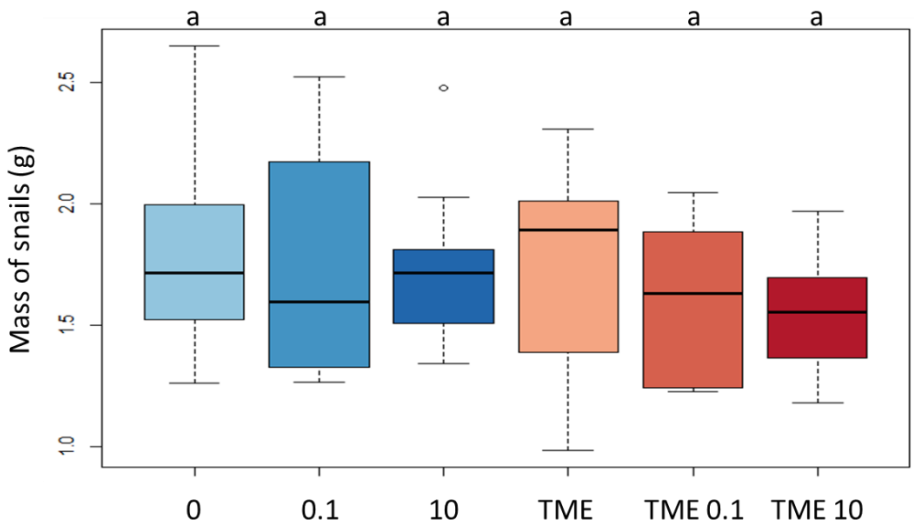

Figure 42: Average snail biomass after a 10-day soil exposure for the six exposure modalities (0: control soils without CNT, 0.1: CNT exposure at 0.1 mg.kg^{-1}, 10: CNT exposure at 10 mg.kg^{-1}, TME: soils with added trace metals (final concentrations: Cd: 0.40, Cu: 9.13, Pb: 31.76, Zn: 52.42 mg.kg^{-1}), TME 0.1: soils with trace metals and CNT exposure at 0.1 mg.kg^{-1} and TME 10: soils with trace metals and CNT exposure at 10 mg.kg^{-1}). Same lowercase letters indicate treatments that do not differ significantly (p-value > 0.05) following a 2 way ANOVA (n = 5).

4. Discussion

4.1. CNT isotopic labeling for detection in environmental matrices

After 2 weeks of exposure at 10 mg.kg^{-1} CNT, the isotopic Δ C^{13}/C^{12} signal results indicated that ^{13}CNT (L = 1 to 20 µm, diameter = 22.5 ± 5.0 nm) were transferred from soils to plant leaves. This results confirm some data of the literature suggesting CNT internalization in plants using other techniques as optical observation techniques[19,21,22], radioactive labelling[16–19], microwave-induced heating[24] or Raman observation[23] (among references, only one them was made on soil, one in aquatic exposure and the rest were made in hydroponic). However, our results indicate that the CNT concentration must be sufficiently high for their transfer and translocation in lettuce leaves to be detected, since CNT could not be detected with the addition of 0.1 mg.kg^{-1}.

Labeling CNM with a radioactive isotope implies substantial funding, both for synthesis and for isotopic analysis. Furthermore, this technique requires dedicated facilities that are not often equipped for experiments involving living organisms. This technique is thus not an option in many cases. So the labelling with a stable isotope seems to be an ideal compromise. However, CNM need to be highly enriched to enable their detection in biological matrices. Preliminary tests in Liné's PhD thesis[41] using

17% ^{13}C enrichment failed to detect a distinct signal between plants exposed and unexposed to CNM. However, this technique offers the possibility of further microbeam analysis, enabling both quantification of CNM transfer and qualitative analysis by 2D mapping.

4.2. Trophic transfer and toxicity along the soil-plant-snail system

Despite the translocation of CNT detected at 10 mg.kg^{-1}, the transfer of CNT from the lettuce leaves to the snail digestive gland indicates either that CNT do not accumulate in the snail digestive gland or that trophic transfer of CNT to the digestive gland is not sufficiently high to be detected by ^{13}C quantification by py-IRMS. However, a trend can be observed as snails displayed a higher isotopic ^{13}C signal when they ate lettuces exposed to 10 mg.kg^{-1} but the high variability of the results did not permit to conclude statistically. In their study, Weis et *al.*[20] detected CNT transfer from the biofilm to an aquatic snail (*L. stagnalis*) but the exposure set-up maximized the contact with the contaminant allowing both trophic and tegumentary exposure routes.

As expected, TME transfer results from soil to lettuce leaves showed that TME transfer was higher in lettuces exposed to added TME, except for Cu. Surprisingly, although not statistically significant, a trend of decreased Cu concentration in the leaves of lettuces exposed to TME could be seen. Several elements may explain this different behavior; the first being that Cu may be less translocated to the leaves than the other TME used in this study. Indeed, it has been shown that Cu can be strongly bound to root cells and of relatively low mobility compared with Cd and Zn[42]. In addition, Cu and Zn are micronutrients, and plants have specific transporters to control the concentrations of these two elements precisely[43]. As a result, plants can implement TME detoxification strategies by compartmentalizing TME in specific parts of the plant[44]. For example, after *Lactuca sativa* exposure to 39.6, 53.7, and 74.5 mg.kg^{-1} of Cu in three agricultural soils during 28 days, Cu concentrations in roots were 14.0, 53.6, and 96.3 mg.kg^{-1}, while they were 3.5, 3.0, and 1.6 and mg.kg^{-1} in lettuce leaves, respectively[45].

For lettuce exposure, a synergistic impact of the cocktail of contaminant could be detected on Zn transfer which was enhanced in presence of CNT, the same trend was also seen for Cd. Similarly, in a previous study with *Lactuca sativa*, the addition of CNT (10 $mg.kg^{-1}$) in soil with low contamination of TME (Cd:13, Pb: 524, Zn: 689 $mg.kg^{-1}$) and with low OM content (2.4%) led to the same increase of Cd and Zn transfer (+39% and +26% for Cd and Zn, respectively) but not for Pb[9]. This synergistic behavior in the previous study was attributed to the low OM content in the soil which is also the case in this one (previous study: 2.3%, present study: 1.82%). Additionally, when studying the adsorption behavior in another study in simplified liquid media, we demonstrated that the addition of OM to the medium led to a decrease in Cu and Pb adsorption onto CNT (chapter 3); which is in agreement with the fact that in this study these two TME experienced no transfer modifications after CNT addition in soil.

Overall, TME content of snails followed that of the plants they consumed. Indeed, the increase in Cd and Zn in lettuce leaves led to an increase in Cd and Zn in snail digestive glands while the addition of Cu and Pb in soil had no impact on both plant and snail concentrations; this could reflect the lack of control of Cd and Zn in snails. Moreover, based on a toxicokinetic approach it has been demonstrated that in the snail *Helix aspersa* Cd and Zn elimination tend to be null and low, respectively, while it is high for Pb[46]. This approach also corroborates the results of Cd and Zn accumulation in the snail digestive gland and the lack of increase of these two TME in the faeces observed in our study. These results are also in agreement with the study by Notten *et al.*[47] in which the concentrations of Cd and Zn in *Urtica dioica* leaves and in the snail *Cepaea nemoralis* followed a positively more pronounced relationships than Cu and Pb (and to a lesser extent for Cu).

Surprisingly, an effect of the addition of CNT and a CNT/TME interaction were detected for Cd concentrations in the digestive gland of snails such that snails feeding on leaves contaminated with TME and 10 $mg.kg^{-1}$ of CNT accumulated more Cd in their digestive glands than those exposed to leaves contaminated with TME without CNT.

4.3. Contaminant transfer to snails after soil exposure

As expected, snails exposed to TME had more Cd, Cu, Pb and Zn in their digestive glands. Furthermore, for Cu transfer to the digestive gland, a CNT/TME interaction was found leading to a significant increase of Cu accumulation (+61%) with the addition of CNT (only at the highest concentration used). This results is an agreement with results of a previous study which studied transfer of Cd, Pb and Zn transfer to earthworms in a soil with a similar OM content[9] (see transfer results only for LC soil with 2.4 % of organic carbon, chapter 5). However, if this Cu increase is consistent in between studies for animals feeding on soil, it was not detected on snail feeding on contaminated lettuce. Additionally, although not statistically validated, the addition of CNT to the soil also increased the transfer of Cd and Zn from 27% and 22% to the snail digestive gland.

One explanation for these results is that the presence of CNT in ingested soil may damage the snail digestive tract membrane, leading to a facilitated absorption of TME and hence greater accumulation in the digestive gland. Results on nutrient concentrations in snails digestive gland did not confirm this hypothesis because there was no modifications on nutrient transfer with the addition of CNT.

4.4. Exposure pathway comparison

Although transfer factors are higher for trophic exposure than for soil exposure (SI, Table S1), TME concentrations in snail digestive glands are slightly higher with soil exposure. However, transfer factors for soil exposure were <1 while those for trophic exposure were >1, indicating dilution and accumulation respectively. According to transfer factors results, the process of bioconcentration of TME via soil exposure is less important than the biomagnification process that occurs in trophic transfer and support previous hypothesis that the uptake of TME were more important than their elimination.

A hypothesis concerning the fact that the accumulation is higher in the trophic pathway than in the soil pathway is related to contaminant bioaccessibility that might be different in the two different matrices (plant and soil, respectively).

5. Conclusion

These results provide further evidence that interactions among contaminants should be included in ecological risk assessment and in particular for nanomaterials and TME as CNT can modify the transfer of TME in a trophic chain up to the primary producers, which to date have not been very fully considered in contaminant risk assessments. This would then guarantee a safe and sustainable development of nanotechnology. Additionally, considering different exposure routes is also of tremendous importance for a proper risk assessment and trophic transfer experiments should be further initiated. Indeed, in this study the bioaccumulation was much higher after trophic exposure than after soil exposure.

Bibliography (article: Assessing the impact of a mixture of carbon nanotube and metals and their aging on agrosystems):

(1) He, K.; Chen, G.; Zeng, G.; Peng, M.; Huang, Z.; Shi, J.; Huang, T. Stability, Transport and Ecosystem Effects of Graphene in Water and Soil Environments. *Nanoscale* **2017**, *9* (17), 5370–5388. https://doi.org/10.1039/C6NR09931A.

(2) Helland Aasgeir; Wick Peter; Koehler Andreas; Schmid Kaspar; Som Claudia. Reviewing the Environmental and Human Health Knowledge Base of Carbon Nanotubes. *Environmental Health Perspectives* **2007**, *115* (8), 1125–1131. https://doi.org/10.1289/ehp.9652.

(3) Jackson, P.; Jacobsen, N. R.; Baun, A.; Birkedal, R.; Kühnel, D.; Jensen, K. A.; Vogel, U.; Wallin, H. Bioaccumulation and Ecotoxicity of Carbon Nanotubes. *Chem Cent J* **2013**, *7*, 154. https://doi.org/10.1186/1752-153X-7-154.

(4) Nowack, B.; Bucheli, T. D. Occurrence, Behavior and Effects of Nanoparticles in the Environment. *Environmental Pollution* **2007**, *150* (1), 5–22. https://doi.org/10.1016/j.envpol.2007.06.006.

(5) Paramo, L. A.; Feregrino-Pérez, A. A.; Guevara, R.; Mendoza, S.; Esquivel, K. Nanoparticles in Agroindustry: Applications, Toxicity, Challenges, and Trends. *Nanomaterials* **2020**, *10* (9), 1654. https://doi.org/10.3390/nano10091654.

(6) Petersen, E. J.; Zhang, L.; Mattison, N. T.; O'Carroll, D. M.; Whelton, A. J.; Uddin, N.; Nguyen, T.; Huang, Q.; Henry, T. B.; Holbrook, R. D.; Chen, K. L. Potential Release Pathways, Environmental Fate, And Ecological Risks of Carbon Nanotubes. *Environ. Sci. Technol.* **2011**, *45* (23), 9837–9856. https://doi.org/10.1021/es201579y.

(7) Tejral, G.; Panyala, N. R.; Havel, J. Carbon Nanotubes: Toxicological Impact on Human Health and Environment. *J Appl Biomed* **2009**, *7* (1), 1–13. https://doi.org/10.32725/jab.2009.001.

(8) Liné, C.; Larue, C.; Flahaut, E. Carbon Nanotubes: Impacts and Behaviour in the Terrestrial Ecosystem - A Review. *Carbon* **2017**, *123*, 767–785. https://doi.org/10.1016/j.carbon.2017.07.089.

(9) Leroy, M.; Pey, B.; Jassey, V. E. J.; Liné, C.; Elger, A.; Probst, A.; Flahaut, E.; Silvestre, J.; Larue, C. Interactive Effects of Metals and Carbon Nanotubes in a Microcosm Agrosystem. *Journal of Hazardous Materials* **2022**, *431*, 128613. https://doi.org/10.1016/j.jhazmat.2022.128613.

(10) Chen, Z.; Zhao, J.; Cao, J.; Zhao, Y.; Huang, J.; Zheng, Z.; Li, W.; Jiang, S.; Qiao, J.; Xing, B.; Zhang, J. Opportunities for Graphene, Single-Walled and Multi-Walled Carbon Nanotube Applications in Agriculture: A Review. *Crop Design* **2022**, *1* (1), 100006. https://doi.org/10.1016/j.cropd.2022.100006.

(11) Gottschalk, F.; Sun, T.; Nowack, B. Environmental Concentrations of Engineered Nanomaterials: Review of Modeling and Analytical Studies. *Environmental Pollution* **2013**, *181*, 287–300. https://doi.org/10.1016/j.envpol.2013.06.003.

(12) Holden, P. A.; Klaessig, F.; Turco, R. F.; Priester, J. H.; Rico, C. M.; Avila-Arias, H.; Mortimer, M.; Pacpaco, K.; Gardea-Torresdey, J. L. Evaluation of Exposure Concentrations Used in Assessing Manufactured Nanomaterial Environmental Hazards: Are They Relevant? *Environ. Sci. Technol.* **2014**, *48* (18), 10541–10551. https://doi.org/10.1021/es502440s.

(13) Kumar, P. A Review—On Molluscs as an Agricultural Pest and Their Control. *IJFSA* **2020**, *4* (4), 383–389. https://doi.org/10.26855/ijfsa.2020.12.004.
(14) Abdel-Halim, K. Y.; Osman, S. R.; El-Danasoury, H. T. M.; Ziada, R. M. Potential Toxic Effects of Titanium Dioxide Nanoparticles and Carbon Nanotubes on Land Snail Helix Aspersa: Use of Oxidative Stress as a Reliable Biomarker for Ecotoxicology Assessment. *Invertebrate Survival Journal* **2021**, 119–129. https://doi.org/10.25431/1824-307X/isj.v18i1.119-129.
(15) Ali, D.; Ahmed, M.; Alarifi, S.; Ali, H. Ecotoxicity of Single-Wall Carbon Nanotubes to Freshwater Snail Lymnaea Luteola L.: Impacts on Oxidative Stress and Genotoxicity. *Environmental Toxicology* **2015**, *30* (6), 674–682. https://doi.org/10.1002/tox.21945.
(16) Petersen, E. J.; Huang, Q.; Weber, Jr., Walter J. Bioaccumulation of Radio-Labeled Carbon Nanotubes by Eisenia Foetida. *Environ. Sci. Technol.* **2008**, *42* (8), 3090–3095. https://doi.org/10.1021/es071366f.
(17) Petersen, E. J.; Huang, Q.; Weber, W. J. Ecological Uptake and Depuration of Carbon Nanotubes by Lumbriculus Variegatus. *Environ Health Perspect* **2008**, *116* (4), 496–500. https://doi.org/10.1289/ehp.10883.
(18) Ferguson, P. L.; Chandler, G. T.; Templeton, R. C.; DeMarco, A.; Scrivens, W. A.; Englehart, B. A. Influence of Sediment−Amendment with Single-Walled Carbon Nanotubes and Diesel Soot on Bioaccumulation of Hydrophobic Organic Contaminants by Benthic Invertebrates. *Environ. Sci. Technol.* **2008**, *42* (10), 3879–3885. https://doi.org/10.1021/es702830b.
(19) Larue, C.; Pinault, M.; Czarny, B.; Georgin, D.; Jaillard, D.; Bendiab, N.; Mayne-L'Hermite, M.; Taran, F.; Dive, V.; Carrière, M. Quantitative Evaluation of Multi-Walled Carbon Nanotube Uptake in Wheat and Rapeseed. *Journal of Hazardous Materials* **2012**, *227–228*, 155–163. https://doi.org/10.1016/j.jhazmat.2012.05.033.
(20) Weise, K.; Kurth, T.; Politowski, I.; Winkelmann, C.; Schäffer, A.; Kretschmar, S.; Berendonk, T. U.; Jungmann, D. A Workflow to Investigate the Impacts of Weathered Multi-Walled Carbon Nanotubes to the Mud Snail Lymnaea Stagnalis. *Environ Sci Pollut Res* **2022**, *29* (18), 26706–26725. https://doi.org/10.1007/s11356-021-17691-0.
(21) Chen, G.; Qiu, J.; Liu, Y.; Jiang, R.; Cai, S.; Liu, Y.; Zhu, F.; Zeng, F.; Luan, T.; Ouyang, G. Carbon Nanotubes Act as Contaminant Carriers and Translocate within Plants. *Scientific Reports* **2015**, *5*, 15682. https://doi.org/10.1038/srep15682.
(22) Martínez-Ballesta, M. C.; Zapata, L.; Chalbi, N.; Carvajal, M. Multiwalled Carbon Nanotubes Enter Broccoli Cells Enhancing Growth and Water Uptake of Plants Exposed to Salinity. *Journal of Nanobiotechnology* **2016**, *14* (1), 42. https://doi.org/10.1186/s12951-016-0199-4.
(23) Khodakovskaya, M. V.; Kim, B.-S.; Kim, J. N.; Alimohammadi, M.; Dervishi, E.; Mustafa, T.; Cernigla, C. E. Carbon Nanotubes as Plant Growth Regulators: Effects on Tomato Growth, Reproductive System, and Soil Microbial Community. *Small* **2013**, *9* (1), 115–123. https://doi.org/10.1002/smll.201201225.
(24) Irin, F.; Shrestha, B.; Cañas, J. E.; Saed, M. A.; Green, M. J. Detection of Carbon Nanotubes in Biological Samples through Microwave-Induced Heating. *Carbon* **2012**, *50* (12), 4441–4449. https://doi.org/10.1016/j.carbon.2012.05.022.
(25) Jakubus, A.; Paszkiewicz, M.; Stepnowski, P. Carbon Nanotubes Application in the Extraction Techniques of Pesticides: A Review. *Critical Reviews in Analytical Chemistry* **2017**, *47* (1), 76–91. https://doi.org/10.1080/10408347.2016.1209105.

(26) Leroy, M.; Flahaut, E.; Larue, C. Carbon Based Nanomaterial Interactions with Metals and Metalloids in Terrestrial Environment: A Review. *Carbon* **2023**, *206*, 325–339. https://doi.org/10.1016/j.carbon.2023.02.047.
(27) Hu, X.; Kang, J.; Lu, K.; Zhou, R.; Mu, L.; Zhou, Q. Graphene Oxide Amplifies the Phytotoxicity of Arsenic in Wheat. *Scientific Reports* **2014**, *4* (1), 6122. https://doi.org/10.1038/srep06122.
(28) Li, J.; Wu, F.; Fang, Q.; Wu, Z.; Duan, Q.; Li, X.; Ye, W. The Mutual Effects of Graphene Oxide Nanosheets and Cadmium on the Growth, Cadmium Uptake and Accumulation in Rice. *Plant Physiology and Biochemistry* **2020**, *147*, 289–294. https://doi.org/10.1016/j.plaphy.2019.12.034.
(29) Gao, M.; Yang, Y.; Song, Z. Effects of Graphene Oxide on Cadmium Uptake and Photosynthesis Performance in Wheat Seedlings. *Ecotoxicology and Environmental Safety* **2019**, *173*, 165–173. https://doi.org/10.1016/j.ecoenv.2019.01.093.
(30) Zhao, L.; Guan, X.; Yu, B.; Ding, N.; Liu, X.; Ma, Q.; Yang, S.; Yilihamu, A.; Yang, S.-T. Carboxylated Graphene Oxide-Chitosan Spheres Immobilize Cu2+ in Soil and Reduce Its Bioaccumulation in Wheat Plants. *Environment International* **2019**, *133*, 105208. https://doi.org/10.1016/j.envint.2019.105208.
(31) He, Y.; Qian, L.; Zhou, K.; Hu, R.; Huang, M.; Wang, M.; Zhao, G.; Liu, Y.; Xu, Z.; Zhu, H. Graphene Oxide Promoted Cadmium Uptake by Rice in Soil. *ACS Sustainable Chem. Eng.* **2019**, *7* (12), 10283–10292. https://doi.org/10.1021/acssuschemeng.8b06823.
(32) Gong, X.; Huang, D.; Liu, Y.; Zeng, G.; Wang, R.; Xu, P.; Zhang, C.; Cheng, M.; Xue, W.; Chen, S. Roles of Multiwall Carbon Nanotubes in Phytoremediation: Cadmium Uptake and Oxidative Burst in Boehmeria Nivea (L.) Gaudich. *Environ. Sci.: Nano* **2019**, *6* (3), 851–862. https://doi.org/10.1039/C8EN00723C.
(33) Manjate, E.; Ramos, S.; Almeida, C. M. R. Potential Interferences of Microplastics in the Phytoremediation of Cd and Cu by the Salt Marsh Plant Phragmites Australis. *Journal of Environmental Chemical Engineering* **2020**, *8* (2), 103658. https://doi.org/10.1016/j.jece.2020.103658.
(34) Li, M.; Liu, Y.; Xu, G.; Wang, Y.; Yu, Y. Impacts of Polyethylene Microplastics on Bioavailability and Toxicity of Metals in Soil. *Science of The Total Environment* **2021**, *760*, 144037. https://doi.org/10.1016/j.scitotenv.2020.144037.
(35) Gao, M.; Xu, Y.; Chang, X.; Dong, Y.; Song, Z. Effects of Foliar Application of Graphene Oxide on Cadmium Uptake by Lettuce. *Journal of Hazardous Materials* **2020**, *398*, 122859. https://doi.org/10.1016/j.jhazmat.2020.122859.
(36) Dong, Y.; Gao, M.; Song, Z.; Qiu, W. Microplastic Particles Increase Arsenic Toxicity to Rice Seedlings. *Environmental Pollution* **2020**, *259*, 113892. https://doi.org/10.1016/j.envpol.2019.113892.
(37) Yang, X.; Gong, J.; Zhang, X.; Huang, Y.; Zhang, W.; Yang, J.; Lin, J.; Chai, Y.; Liu, J. Evaluation of the Combined Toxicity of Multi-Walled Carbon Nanotubes and Cadmium on Earthworms in Soil Using Multi-Level Biomarkers. *Ecotoxicology and Environmental Safety* **2021**, *221*, 112441. https://doi.org/10.1016/j.ecoenv.2021.112441.
(38) Xu, K.; Liu, Y.-X.; Wang, X.-F.; Li, S.-W.; Cheng, J.-M. Combined Toxicity of Functionalized Nano-Carbon Black and Cadmium on Eisenia Fetida Coelomocytes: The Role of Adsorption. *Journal of Hazardous Materials* **2020**, *398*, 122815. https://doi.org/10.1016/j.jhazmat.2020.122815.
(39) Baize, D. Teneurs Totales En « métaux Lourds » Dans Les Sols Français : Résultats Généraux Du Programme ASPITET. *Courrier de l'Environnement de l'Inra* **2000**, *39*.

(40) Barberet, P.; Jouve, J.; Sorieul, S.; Alfaurt, P.; Mathieu, L. AIFIRA: A Light Ion Beam Facility for Ion Beam Analysis and Irradiation. *Eur. Phys. J. Plus* **2021**, *136* (1), 67. https://doi.org/10.1140/epjp/s13360-020-01045-9.
(41) Liné, C. Evaluation of Parameters Influencing Plant Response to Carbon Nanotube Contamination. These de doctorat, Toulouse, INPT, 2019. http://www.theses.fr/2019INPT0082 (accessed 2021-07-06).
(42) Kabata-Pendias, A. *Trace Elements in Soils and Plants*, 4th ed.; CRC Press: Boca Raton, 2010. https://doi.org/10.1201/b10158.
(43) Ma, J. F.; Tsay, Y.-F. Transport Systems of Mineral Elements in Plants: Transporters, Regulation and Utilization. *Plant and Cell Physiology* **2021**, *62* (4), 539–540. https://doi.org/10.1093/pcp/pcab026.
(44) Mishra, S.; Dubey, R. S. Heavy Metal Uptake and Detoxification Mechanisms in Plants. *International Journal of Agricultural Research* **2010**, *5* (7), 482–501.
(45) Sacristán, D.; Recatalá, L.; Rossel, R. A. V. Toxicity and Bioaccumulation of Cu in an Accumulator Crop (Lactuca Sativa L.) in Different Australian Agricultural Soils. *Scientia Horticulturae* **2015**, *193*, 346–352. https://doi.org/10.1016/j.scienta.2015.06.051.
(46) Gimbert, F.; Vijver, M. G.; Coeurdassier, M.; Scheifler, R.; Peijnenburg, W. J. G. M.; Badot, P.-M.; de Vaufleury, A. How Subcellular Partitioning Can Help to Understand Heavy Metal Accumulation and Elimination Kinetics in Snails. *Environmental Toxicology and Chemistry* **2008**, *27* (6), 1284–1292. https://doi.org/10.1897/07-503.1.
(47) Notten, M. J. M.; Oosthoek, A. J. P.; Rozema, J.; Aerts, R. Heavy Metal Concentrations in a Soil–Plant–Snail Food Chain along a Terrestrial Soil Pollution Gradient. *Environmental Pollution* **2005**, *138* (1), 178–190. https://doi.org/10.1016/j.envpol.2005.01.011.

6. Supporting Information

Trophic transfer and soil exposure to a cocktail of contaminants (carbon nanotubes and trace metal) in a terrestrial food chain

Leroy Mathieu[1,2], Frédéric Gimbert[3], Silvestre Jérôme[1], Stéphanie Sorieul[4], Flahaut Emmanuel[2], Larue Camille[1*]

[1]Laboratoire Ecologie Fonctionnelle et Environnement, Université de Toulouse, CNRS, Toulouse, France,

[2]CIRIMAT, Université de Toulouse, CNRS, INPT, UPS, UMR CNRS-UPS-INP N°5085, Université Toulouse 3 Paul Sabatier, Bât. CIRIMAT, 118, route de Narbonne, 31062 Toulouse cedex 9, France

[3]UMR 6249 Chrono-environnement CNRS - Université de Franche-Comté Usc INRAe, 16 route de Gray, 25030, Besançon, cedex, France

[4]Université Bordeaux 1, CNRS/IN2P3, Centre d'Etudes Nucléaires de Bordeaux Gradignan, CENBG, Chemin du Solarium, BP120, 33175 Gradignan, France

4. Discussion

4.4. Transfer factors

Table S1: Average transfer factor and standard deviation (SD) of Cd, Cu, Pb and Zn in digestive glands of snails for trophic and soil transfer exposed to soil with TME. Same lowercase letters indicate treatments that do not differ significantly (p-value > 0.05) following a Kruskal Wallis test for Cd, Cu, Pb and Zn (n = 14).

	Cd	Cu	Pb	Zn
Trophic exposure	6.7 ± 3.2 **b**	3.8 ± 2.1 **b**	21.8 ± 15.4 **b**	8.3 ± 3.8 **b**
Soil exposure	2.5 ± 0.5 **a**	1.02 ± 0.3 **a**	0.46 ± 0.08 **a**	3.6 ± 0.6 **a**

Transfer factor of Cd, Cu, Pb and Zn to digestive glands of snails were 60%, 73%, 98% and 57% higher in the trophic exposure than soil exposure, respectively ($p_{Cd} < 0.01$, $p_{Cu} < 0.01$, $p_{Pb} < 0.01$, $p_{Zn} < 0.01$, Table SI1).

Conclusion générale

A l'issue de l'étude du corpus scientifique et des travaux expérimentaux réalisés au cours de cette thèse, des voies de réponses aux questions de recherches initiales ont pu émerger.

La première interrogation soulevée visait à déterminer quels étaient les paramètres physico-chimiques qui régissent les interactions entre NMC et ETM dans un contexte faisant intervenir des conditions représentatives de l'environnement. L'analyse bibliographique, essentiellement par l'intermédiaire d'expériences d'adsorption monospécifique en ETM, a permis de mettre en évidence que des facteurs tels que 1) les propriétés intrinsèques des NMC (SSA, degré d'oxydation et nombre de parois) et 2) les conditions expérimentales (concentrations en NMC et en ETM, nature de l'ETM, pH du milieu et durée de contact) influencent l'adsorption des ETM à la surface des NMC[1]. Aussi, d'autres études davantage orientées sur l'influence de paramètres associés aux conditions intrinsèques des écosystèmes naturels comme la présence de MO ont mis en évidence à la fois une diminution[2] ou une augmentation[3,4] de l'adsorption des ETM en surface des NMC, pour lesquelles les mécanismes ne sont pas encore très bien compris. Enfin, les études d'adsorption des ETM dans des milieux aux niveaux de complexité qui se rapprochent des écosystèmes naturels (solutions de sol et sol) restent très rares à ce jour[1], principalement en raison de la complexité du système.

Dans le chapitre 3, les études d'adsorption multispécifique en ETM qui ont été menées ont tout d'abord permis de confirmer que les modélisations largement utilisées (modèles de Langmuir et de pseudo-second ordre, par exemple) pour décrire l'adsorption d'un ETM en surface des NMC, tant sur un rapport de concentrations que sur la vitesse d'adsorption se sont aussi avérées adaptées pour caractériser l'adsorption de plusieurs ETM lorsqu'ils sont en mélange dans le milieu. Il a aussi été confirmé que les quantités d'adsorption des ETM en surface des NMC dépendent du pH du milieu en tout premier lieu et varient selon la nature des ETM étudiés (Cd, Cu, Pb et Zn). Une hypothèse envisageable est que la nature des liaisons (chimisorption ou physisorption) varie en fonction du pH du milieu. De la même manière, l'expérience visant à mettre en évidence l'influence du degré

d'oxydation du NMC révèle des comportements d'adsorption différents selon l'ETM considéré, de sorte que le Cu et Pb s'adsorbent davantage sur des NMC oxydés que le Cd et Zn. Il a été montré que la présence de MO diminue l'adsorption des ETM qui possèdent le plus d'affinité pour les sites d'adsorption (Cu et Pb), et des interactions complexes entre ETM, NMC et MO sont certainement en jeu. Les composés contenus dans la solution de sol ne semblent pas modifier l'adsorption des ETM en surface des NMC et une grande variabilité dans les résultats est à l'œuvre lorsque le milieu se complexifie. En tentant de généraliser à un milieu sol complexe les résultats obtenus dans le chapitre 3 en milieu simplifié, les quantités d'ETM adsorbés en surface des NMC oxydés seraient différentes selon le type de sol. Dans un sol à faible pH acide (pH = 4-6), il y aurait de faibles quantités d'ETM adsorbés en surface des NMC et l'adsorption serait homogène entre les différents ETM présents (à pH = 5 : $Cd_{adsoprtion}$ = 0.15 $mM.g^{-1}$, $Cu_{adsoprtion}$ = 0.17 $mM.g^{-1}$, $Pb_{adsoprtion}$ = 0.92 $mM.g^{-1}$ et $Zn_{adsoprtion}$ = 0.73 $mM.g^{-1}$). En revanche, des adsorptions plus prononcées seraient attendues à pH neutre à faiblement basique (pH= 7-8) et les quantités adsorbées dépendraient de l'ETM considéré puisqu'ils ne présentent pas tous les mêmes affinités pour les sites d'adsorption dans cette gamme de pH. Par exemple, le Cu et le Pb s'adsorberaient davantage que le Cd et le Zn (à pH = 7 : $Cd_{adsoprtion}$ = 0.71 $mM.g^{-1}$, $Cu_{adsoprtion}$ = 5.77 $mM.g^{-1}$, $Pb_{adsoprtion}$ = 4.22 $mM.g^{-1}$ et $Zn_{adsoprtion}$ = 1.58 $mM.g^{-1}$). Dans un sol pauvre en MO, l'adsorption des ETM ne serait pas modifiée tandis que l'adsorption du Cu et Pb serait diminuée dans un sol riche en MO (avec 0 $mg.L^{-1}$ de MO : $Cd_{adsoprtion}$ = 0.53 $mM.g^{-1}$, $Cu_{adsoprtion}$ = 1.27 $mM.g^{-1}$, $Pb_{adsoprtion}$ = 5.51 $mM.g^{-1}$, $Zn_{adsoprtion}$ = 1.12 $mM.g^{-1}$ *vs* 20 $mg.L^{-1}$ de MO : $Cd_{adsoprtion}$ = 1.41 $mM.g^{-1}$, $Cu_{adsoprtion}$ = -2.87 $mM.g^{-1}$, $Pb_{adsoprtion}$ = 0.35 $mM.g^{-1}$, $Zn_{adsoprtion}$ = 0.91 $mM.g^{-1}$). La solution de sol (contenant des argiles et les ions « libres ») ne semble pas agir sur l'adsorption des ETM en surface des NMC. En revanche, la littérature suggère que selon la granulométrie du sol, les NMC sont plus mobiles dans un sol sableux que dans un sol argileux[5–8] ce qui pourrait également entrainer différents comportement d'adsorption. Aussi, la chimie de surface des silicates et de la silice est différente et est plus favorable pour les interactions avec les ETM dans le cas des silicates. Il serait donc attendu que les argiles interagissent

davantage avec les ETM du milieu et par conséquent modifierait le comportement d'adsorption des ETM en surface des NMC s'ils sont présents.

Malgré le travail mené dans le cadre de cette thèse, davantage de recherches doivent être entreprises afin d'établir plus clairement le rôle et l'influence des composés contenus dans la solution de sol sur les interactions NMC/ETM.

La deuxième question de recherche visait à déterminer quels étaient les impacts des NTC en tant que tels sur les cycles biogéochimiques du carbone et de l'azote et de l'eau dans un agrosystème, aspect encore peu étudié dans la littérature. La bibliographie fait état d'effets contrastés des NTC seuls sur les plantes d'intérêt agronomique tant sur leur développement que sur leur fonctionnement[9], une toxicité chez les bactéries[10–12] pouvant aboutir à une baisse de l'activité microbienne[12–15], une modification de la structure des communautés bactériennes[12,15–17] et donc une possible perturbation des processus tels que la minéralisation et le cycle de l'azote[18–21]. Pour mieux comprendre les effets d'un contaminant à l'échelle d'un écosystème, il est important de prendre en compte à la fois les composantes abiotiques et biotiques et les différentes interactions qu'elles entretiennent ce qui est rarement fait dans la littérature à ce jour.

Dans le chapitre 4, pour répondre à cette question, une expérience a été mise en place visant à déterminer la toxicité des NTC sur les fonctions d'un agrosystème en combinant des biomarqueurs à l'échelle individuelle et des écomarqueurs intégratifs et émergents en écologie à la fois sur les bactéries du sol et sur des végétaux. Cette expérience a permis de mettre en évidence des effets contrastés des NTC sur l'agrosystème en fonction de la concentration dans le sol. Sur le cycle du carbone, l'ajout de quantités de NTC de l'ordre du $mg.kg^{-1}$ a augmenté la décomposition de la litière, le nombre de copies du gène universel rARN 16S - indiquant une augmentation des décomposeurs bactériens - et a conduit à une diminution de la concentration en chlorophylle dans les feuilles de maïs. Avec l'ajout de 0,1 $mg.kg^{-1}$ de NTC, l'abondance bactérienne du sol a été diminuée sans modification

de la décomposition de la litière. La concentration en chlorophylle dans les feuilles de maïs a aussi été diminuée. Toutefois, ces diminutions semblent avoir été compensées à l'échelle de l'écosystème puisqu'aucune modification dans l'émission de CO_2 et CH_4 n'a été révélée. En ce qui concerne le cycle de l'azote, les copies de gène des archées impliquées dans le processus de nitrification (*amoA*-AOA) ont augmenté avec l'ajout de 10 $mg.kg^{-1}$ de NTC dans le sol. Aucun effet n'a été observé sur les gènes liés à la dénitrification (nosZ et nirK), suggérant un effet toxique des NTC plus prononcé sur acteurs de la nitrification que sur ceux de la dénitrification. En ce qui concerne le cycle de l'eau, le contenu en matière sèche des plantes exposées à 10 $mg.kg^{-1}$ de NTC était 17% plus important que celui des plantes témoins. Cette augmentation dans le contenu de matière sèche n'était pas visible à 0,1 $mg.kg^{-1}$ de NTC. Toutefois, une diminution de l'émission de l'H_2O a été observée aux deux concentrations en NTC, suggérant un impact de ces derniers sur le cycle de l'eau aux deux concentrations testées. Une obstruction du transport d'eau depuis le sol jusqu'aux racines en raison de NTC accolés sur les racines pourrait expliquer les effets observés sur le cycle de l'eau. Enfin, malgré les modifications énumérées précédemment sur les biomarqueurs à l'échelle individuelle, l'approche intégrative par l'intermédiaire d'écomarqueurs tels que l'index de multifonctionnalité de l'agrosystème n'a pas permis de mettre en évidence d'effet significatif de l'ajout de NTC, quelle que soit la concentration. Ainsi, les effets des NTC seuls sur les cycles biogéochimiques du carbone, de l'azote et de l'eau dans un agrosystème s'avèrent contrastés et dépendants de la concentration en NTC, mais vraisemblablement compensés sur le plan fonctionnel à l'échelle de l'écosystème.

La troisième question s'intéressait aux effets d'une contamination conjointe en NTC et ETM sur un agrosystème en prenant en compte la notion de vieillissement des contaminants dans l'environnement. Les résultats répertoriés dans la bibliographie, en raison des interactions NMC/ETM, témoignent d'une modification de transfert des ETM suite à l'ajout de NTC dans le milieu pour les vers de terre et les plantes, responsable d'une modification de toxicité des contaminants par rapport à s'ils

étaient appliqués de manière individuelle dans le milieu[1]. A ce jour, trop peu d'études de la bibliographie se sont intéressées aux effets conjoints des NTC et ETM dans des systèmes intégratifs, systèmes dans lesquels les interactions entre espèces représentatives d'un même écosystème sont prononcées. Bien que les approches intégratives soient plus complexes dans leurs interprétations, les interactions entre espèces tout comme le vieillissement des contaminants peuvent moduler le transfert et la toxicité des contaminants présents pour l'écosystème, et être témoin d'effets toxiques plus ou moins prononcés lorsque les effets des contaminants sont considérés simultanément (synergie *vs* antagonisme) que s'ils avaient été considérés individuellement.

En ce sens, la première expérience du chapitre 5 réalisée sur un sol standard de référence dans lequel les contaminations ont été apportées a permis d'indiquer résultats qu'après une exposition de 8 semaines, l'abondance des communautés fongiques et la décomposition de la matière organique ont été diminué avec l'ajout de 0.025 $mg.kg^{-1}$ de NTC tandis que l'activité enzymatique lié au cycle du carbone (pyranosidase) a été augmenté à la même concentration. L'exposition aux ETM n'a eu que peu d'effets sur les marqueurs des processus du sol (communautés fongiques, activités enzymatiques liés au carbone, azote et phosphore et decomposition de la litière). Chez le maïs, l'ajout de NTC dans le milieu n'a pas modifié le transfert des ETM. L'ajout de 0.025 $mg.kg^{-1}$ de NTC a diminué la transpiration du maïs (16%) et bien que pas statistiquement mis en évidence, la teneur en matière sèche du maïs a été augmenté à la même concentration (22%) ce qui témoigne d'un stress hydrique. D'ailleurs, les composés phénoliques, connus pour être impliqué dans la réponse au stress hydrique à été augmenté (30%). L'ajout des ETM dans le sol à uniquement diminué la biomasse du maïs. A l'échelle de l'écosystèmes, la respiration ainsi que la productivité primaire ont été diminué en raison de l'exposition des ETM. En revanche, aucune modification n'a été observé sur l'émission de CO_2 avec l'ajout de NTC. Le vieillissement du sol tend à atténuer les effets toxiques imposés par les NTC. De nombreuses interactions ont été mises en évidence sur l'activité enzymatique lié au carbone (pyranosidase), la décomposition de la litière, la transpiration et la concentration en composés phénoliques. Pour tous ces marqueurs, des effets antagonistes sont à l'oeuvre c'est à dire que l'ajout

des ETM dans le milieu diminue la toxicité des NTC. La seconde expérience, réalisée avec un sol à la contamination métallique historique suite à des rejets industriels a permis d'établir qu'aucun effet de l'ajout de NTC dans ces sols n'a été détecté sur la concentration bactérienne ou la croissance des vers de terre. En revanche, des **effets interactifs** entre les NTC et les ETM ont été observés de sorte que dans le sol contenant des concentrations élevées en ETM, l'ajout de 0,1 mg kg^{-1} de NTC a entraîné une diminution de 29% et 30% du transfert de Cd et de Zn depuis le sol jusqu'aux feuilles de laitues (pas d'effet à 10 $mg.kg^{-1}$) et une perte de biomasse (-22%). Parallèlement, l'ajout de NTC a eu des effets différents selon les caractéristiques physico-chimiques du sol sur l'absorption des éléments dans les feuilles de laitue, probablement en rapport avec la teneur en MO du sol puisque qu'avec l'ajout de 10 $mg.kg^{-1}$ de NTC dans les sols plus pauvres en MO, il y a eu augmentation de transfert de Cd et Pb de 37% et 21% comparativement aux témoins. Pour les vers de terre, l'ajout de 10 mg kg^{-1} de NTC a entraîné une augmentation du transfert élémentaire dans les tissus après exposition dans le sol à la plus forte teneur en MO (Pb : +34% et Zn : +25%) sans répercussion sur les marqueurs de toxicité étudiés. Les résultats obtenus à l'issue de ces deux expériences permettent d'apporter des éléments de réponse à la question de recherche posée dans ce chapitre ; en effet il semble que les effets conjoints des NTC/ETM dans un agrosystème dépendent fortement du type de sols (teneur en MO en particulier) qui a des répercussions à la fois sur l'adsorption entre ETM/NTC (cf chapitre 3) mais également sur le comportement des organismes considérés. Parmi les deux expériences de ce chapitre, seule la première (sur le maïs) permet de mettre en évidence de possibles effets synergiques/antagonistes associés à la toxicité des contaminants. Globalement, peu d'effets synergiques/antagonistes ont été mis en évidence. Toutefois, il semble que le vieillissement des contaminants soient responsables d'une façon générale de l'atténuation de la toxicité associé des NTC.

Enfin, la dernière question abordée dans cette thèse visait à identifier le transfert des NTC au sein d'une chaîne trophique reconstituée et de déterminer si les NTC modifiaient le transfert et la toxicité

des ETM. Dans la littérature, des études ont mis en évidence l'internalisation de NTC chez certains végétaux[9,22] notamment en conditions hydroponiques[23–27]. Toutefois, la caractérisation du transfert des NTC dans des conditions « environnementalement » pertinentes (sur sol) au sein d'une chaîne trophique sont à ce jour peu représentée dans la bibliographie. De plus, dans le cas des agrosystèmes, l'enjeu est double puisque la compréhension quantitative du transfert des NTC depuis le sol jusqu'aux plantes d'intérêts agronomiques permettrait d'évaluer l'exposition et le risque associé des NTC pour l'environnement et l'Homme.

Suite à l'expérience qui compose le sixième chapitre, l'internalisation et l'accumulation de NTC chez la plante exposée à 10 mg kg^{-1} de NTC ont pu être mis en évidence grâce au dopage en ^{13}C des NTC, modifiant uniquement le transfert du Zn. En revanche, le transfert des NTC depuis la laitue ou le sol jusqu'aux escargots n'a pas pu être démontré de façon significative. Le transfert des ETM chez l'escargot n'a pas été modifié en raison de l'ajout de NTC par exposition trophique, en revanche la concentration du Cu a été augmentée de 61% dans le cas de l'exposition par le sol suite l'ajout à 10 mg kg^{-1} de NTC. Le transfert de nutriment de la laitue et de l'escargot n'a pas été modifié par l'ajout de NTC dans le milieu. La biomasse des escargots n'a pas été modifié par l'exposition simultanée en NTC et ETM, quel que soit l'exposition. Les résultats de ce chapitre ne sont pas complets et d'autres résultats sur le transfert des NTC par voie sédimentaire chez l'escargot ainsi que des inducteurs de stress oxydatif chez la plante complèterons ultérieurement ce chapitre.

Discussion générale

L'évaluation des risques écologiques pour les mélanges reste à ce jour basée sur l'additivité des risques liés à chacun des composés considérés indépendamment et alors que de nombreux éléments dans la littérature suggèrent que des interactions entre contaminants entrent en jeu invalidant ce modèle. De plus, il s'avère que le comportement écotoxique des NMC diffère sur de nombreux points par rapport aux contaminants « historiques » comme les ETM, tel que le mettent en avant les documents produits par différentes agences gouvernementales. Ces différents éléments génèrent donc des interrogations

quant à la robustesse de notre modèle d'évaluation des risques écologiques pour garantir non seulement la pérennité de la bonne santé des agrosystèmes mais également la sécurité sanitaire.

Par exemple, la toxicité associée aux ETM suit un schéma classiquement retrouvé pour de nombreux contaminants à savoir des courbes **d'effets doses dépendantes** où la toxicité augmente avec la concentration du contaminant, pour lesquelles des EC_{50} sont calculées permettant de fixer des seuils quantitatifs liés à la toxicité. Pour les NMC, les EC_{50} qui ont été calculées atteignent des valeurs extrêmement élevées par rapport aux autres contaminants[1] (1480.3 $mg.kg^{-1}$ pour les vers de terre et 389 $mg.L^{-1}$ pour $LOEC_{NTC}$ des plantes) et ne reflètent pas la toxicité des NMC. En effet, de nombreux effets (diminution ou induction) ont été observés à de faibles concentrations mais n'étaient pas visibles ou inversés aux plus fortes concentrations. Par exemple, une diminution de l'abondance bactérienne et des communautés nitrifiantes a été observée avec l'exposition à 0,1 $mg.kg^{-1}$ de NTC tandis qu'une induction de ces 2 mêmes communautés a été observée avec l'exposition à 10 $mg.kg^{-1}$ de NTC (cf. chapitre 4). De même, dans l'expérience n°2 du chapitre 5, la biomasse fraiche des salades a été diminuée de 22% à 0,1 $mg.kg^{-1}$ de NTC tandis qu'aucune modification n'a été observée avec une exposition à 10 $mg.kg^{-1}$ de NTC dans le sol. Ces résultats pourraient être mis en lien avec le comportement d'homo-agglomération des NTC lorsqu'ils sont présents à fortes concentrations (diminuant leur SSA et leurs possibilités d'interactions avec d'autres composants)[28].

De plus, nos résultats rejoignent ceux de la bibliographie sur le fait que l'**adsorption** des ETM en surface des NMC peut dans certains cas modifier leur transfert, provoquant alors une toxicité différente par rapport à une situation où les ETM et les NTC seraient appliqués seuls séparément. Il est également important de noter que les modifications de transfert des ETM en raison des interactions avec les NMC se réalisent dès de faibles concentrations. Par exemple dans l'étude n°2 du chapitre 5, une diminution de 29% et 30% du transfert de Cd et de Zn depuis le sol jusqu'aux feuilles de laitues a été observée avec l'ajout de 0.1 $mg.kg^{-1}$ de NTC (concentration pertinente d'un point de vue environnemental dans les agrosystèmes) et bien que non significatif, le transfert du Pb a lui aussi été diminué de 32%. Dans

la littérature également, Zhao et *al.*[29] ont observé une diminution à hauteur de 60% et 67% de la concentration de Cu dans les racines et les tiges de *Triticum aestivum* avec l'ajout dans le sol de 5 $mg.L^{-1}$ de sphères de GO pendant 14 jours. De la même façon que pour la toxicité, la modification du transfert n'apparait pas nécessairement dose dépendante, ce qui peut être lié au comportement d'agglomération des NMC aux fortes concentrations en milieu liquide[28] comme spécifié précédemment. Parmi les études réalisées dans ce manuscrit, la modification de transfert des ETM par les NMC chez la plante n'a été détecté que pour la laitue contrairement au maïs, laissant penser que les caractéristiques physiologiques/morphologiques de la plantes peuvent être responsables du comportement du transfert des NMC et des interactions entre NMC/ETM. Différents schémas de modifications du transfert des ETM par l'ajout des NMC dans le milieu ont été observé chez la plante, le vers de terre et l'escargot, soit par augmentation ou diminution du transfert des ETM vraisemblablement lié aux **conditions édaphiques**.

Les modifications de transfert des ETM (et des autres éléments présents) sont en partie liées aux **propriétés des NMC**. Les expériences d'adsorption ont révélé que l'adsorption était plus importante pour des NMC oxydés que pour des NMC bruts. Par exemple, l'adsorption cumulée de Cd, Cu, Pb et Zn était de 17,52 $mM.g^{-1}$ pour les NMC oxydés (GO, o-DWCNTs et o-MWCNTs) tandis qu'elle n'était que de 7,85 $mM.g^{-1}$ pour des NTC bruts de synthèse (DWCNTs, 8CNTs et AC). Ainsi, les matériaux oxydés sont plus enclins à modifier le transfert des ETM que les matériaux bruts en raison de leurs plus fortes interactions, qui pourraient être liées à la nature des interactions NMC/ETM qui diffèrent selon l'oxydation du matériau (chimisorption pour matériaux oxydés *vs* physisorption pour des matériaux bruts). Il semble aussi que d'autres propriétés des NMC régissent les interactions NMC et ETM mais davantage de recherches sont nécessaires pour répondre pleinement à la question.

Une autre conclusion de ce travail est la véritable importance de la prise en compte des **conditions édaphiques** dans l'évaluation des risques tant elles influencent le comportement des NTC et la biodisponibilité et spéciation des ETM ainsi que le comportement des organismes inféodés. Tout

d'abord, il est reconnu que le transport des NMC dépend de la **texture du sol** de telle sorte que les NMC ont tendance à avoir une plus grande rétention (faible transport) dans les sols argileux que dans les sols sableux[5–8]. De plus, on peut poser l'hypothèse que les NMC s'agglomèrent de manière plus prononcée (réduisant leurs possibilités d'interactions) dans les sols sableux où leur transport est facilité en comparaison avec les sols argileux où le transport est limité. Ces deux derniers points pourraient être une explication sur les différences observées dans l'impact des NTC sur le transfert d'ETM entre les sols argileux (modification du transfert des ETM, argiles: 11,8%, limons : 82,2%, sables : 5,9%) et le sol standard Lufa Speyer 2.1 (pas d'effet de l'ajout des NTC sur le transfert des ETM, argiles : 1,1%, limons : 16,8%, sables : 82,1%). A l'inverse, dans les sols argileux, il y aurait davantage d'hétéro-agglomération avec le complexe argilo-humique et les ions de la solution de sol.

Outre la texture du sol, les études d'adsorption ont démontré une forte influence du **pH** sur l'adsorption des ETM en surface des NMC. La gamme de pH à laquelle la plus forte adsorption est observée se situe entre 7-8, or le pH du sol Lufa Speyer 2.1 pour lequel il y a eu peu ou pas de modification de transfert d'ETM se situe autour de pH = 5, alors que le pH des sols historiquement contaminés de MetalEurop, quant à eux, étaient de 7,0 et 7,2. De plus, au-delà des phénomènes d'adsorption des ETM en surface des NTC, la spéciation des ETM s'avère également étroitement liée au pH du sol[30]. Ainsi, selon le pH du sol, les formes ioniques des ETM peuvent être plus ou moins biodisponibles et toxiques pour les organismes exposés.

Pour essayer de d'avancer un peu plus sur l'influence du pH sur l'adsorption élémentaire, une expérience complémentaire confiée à des étudiants de master a mis en évidence que la réhausse de 1 ou 2 points de pH du sol Lufa Speyer 2.1 (de pH = 4.7 à pH = 5.7 et pH = 6.7, cf annexe 1-2-3 p268-269-270) n'a pas modifié le transfert de Cd, Pb et Zn chez le maïs. Une nouvelle hypothèse découlant de ces résultats est donc le rôle de **l'espèce végétale** dans les réponses aux contaminants puisque les modifications de transfert ont été constatés sur la laitue (sur sol historiquement contaminé à pH = 7-7,2). Ce rôle avait d'ailleurs déjà été mis en avant dans une précédente étude au laboratoire[31] et fait actuellement l'objet d'une expérience dédiée.

Aussi, les études d'adsorption ont permis de révéler que la **MO** diminue l'adsorption des ETM qui possèdent le plus d'affinité pour les sites d'adsorption à savoir le Cu et Pb et il serait donc attendu que le transfert de Cu et Pb soit moins important que celui du Cd et du Zn dans des sols riche en MO. Dans l'expérience du dernier chapitre (6), les résultats de modifications de transfert des ETM suite à l'ajout de NTC dans un sol composé à 1,8% de carbone organique suivent la logique observée dans les études d'adsorption en milieu simplifié. En effet, bien que non significatif statistiquement, le transfert du Pb suite à l'ajout de 10 $mg.kg^{-1}$ a été diminué de 27%, tandis qu'aucune modification du transfert du Cu n'a été détectée et que le transfert du Zn a augmenté de 162%.

Enfin, le **vieillissement** des contaminants dans le sol peut modifier les interactions NMC/ETM dans la mesure où premièrement, les propriétés intrinsèques des NMC peuvent être modifiées (notamment degré d'oxydation) et deuxièmement la toxicité des ETM s'avère différente selon leur origine/vieillissement (ajout sels métalliques *vs* émissions atmosphériques industrielles). En effet, Il a été démontré que le vieillissement naturel (simulé par un réacteur plasma à décharge à barrière diélectrique) pouvait modifier la structure des NTC : diminution de la surface spécifique, augmentation des défauts, structure déformée et ajout de groupes fonctionnels contenant de l'oxygène à la surface[32], autant de propriétés qui régissent les interactions NMC/ETM. Aussi, aucune modification du transfert d'ETM n'a été observée dans l'expérience dans laquelle les contaminations ont été apportées dans les sols et été vieillis durant deux ans, mais l'espèce végétale utilisé dans cet expérience (le maïs) n'est peut-être pas encline à ce que ces modifications puissent se produire.

Troisièmement, les résultats indiquent que les **traits d'histoires de vie** sont également une caractéristique majeure à prendre en compte afin d'évaluer convenablement les risques associés aux contaminants. En effet, selon l'organisme considéré, la modification du transfert et de la toxicité des ETM par l'ajout de NMC s'est avérée différente en raison de ses traits d'histoire de vie. Par exemple, les organismes étudiés dans les expériences de ce document ne présentent pas le même mode vie ; les plantes d'intérêt agronomique vivent de manière fixée, tandis que les vers de terre et les escargots

sont mobiles. Ainsi, les plantes fixées sont contraintes par l'environnement dans lequel elles croissent et dépendent totalement des conditions édaphiques et des contaminations dans le sol tandis que les vers de terre et escargots, de par leur mode de vie mobile, peuvent adopter des comportements afin de limiter leur exposition. Par exemple, au cours de l'expérience menée avec les vers de terre, davantage d'observations visuelles de vers de terre hors du sol ont été faites en fin d'expérience dans les unités aux plus fortes contaminations ce qui n'était pas le cas pour les unités expérimentales aux plus faibles contaminations. D'ailleurs, quelques exemples d'évitement plus prononcés des vers de terre pour des environnements contaminés par plusieurs substances que par une seule substance sont disponibles dans la bibliographie[33,34].

De plus, les plantes et les escargots/ ne présentent pas les mêmes voies d'exposition, qui peuvent aussi moduler les effets des NMC sur le transfert des ETM. En effet, les producteurs primaires sont exposés de manière directe par la voie racinaire, tandis que les escargots peuvent être également exposés via le sol (exposition dermique et ingestion de sol) et par voie trophique. Par exemple, dans l'expérience du chapitre 6, l'augmentation du transfert de Zn et dans une moindre mesure du Cd chez la laitue en raison de l'ajout de 10 mg kg^{-1} de NTC est accompagné par une augmentation de la concentration de Cd et Zn dans la glande digestive de l'escargot par l'exposition trophique. A la même concentration de NTC, l'exposition par le sol de l'escargot à démontré une augmentation de 61% de la concentration de Cu dans la glande digestive de l'escargot. Les résultats de cette expérience démontrent des modifications de transfert des ETM en raison de l'ajout de NTC dépendante de la voie d'exposition de l'escargot, voies qui peuvent être activent simultanément dans l'environnement.

De même, il est avancée par Petersen et *al.*[35] que même si un **transfert trophique** de NMC peut se produire, il est peu probable qu'une absorption significative à travers le tractus intestinal se produise chez les organismes de niveau trophique supérieur. Dans notre cas, malgré la mise en évidence de transfert de NTC chez la plante, aucun NTC n'a pu être détecté dans la glande digestive de l'escargot, confirmant en partie l'hypothèse de Petersen *et al.*[35]. Toutefois, l'organe ciblé (la glande digestive)

peut ne pas être le plus enclin à l'accumulation de NMC et/ou la bioaccumulation être trop faible pour être détectée par quantification isotopique ^{13}C. Les résultats des observations réalisées sous micro-faisceau apporteront un supplément d'information afin de répondre à cette hypothèse. Parallèlement, les animaux peuvent davantage excréter les contaminants qu'ils absorbent que les plantes. La capacité de dépuration des contaminants chez les vers de terre[36–39] et les escargots[40,41] est prononcée, ce qui leur permet de limiter non seulement l'accumulation des contaminants mais aussi la toxicité qui est associée. En outre, certains organismes possèdent des mécanismes de détoxification des ETM[42–45] qui, par divers processus, permettent de les rendre moins toxiques. Toutefois, tous les organismes ne possèdent pas les mêmes capacités de détoxification des ETM et la modification du transfert des ETM par les NMC peut s'avérer plus ou moins toxiques selon les mécanismes qu'ils possèdent. Enfin, l'avenir des ETM adsorbés en surface des NMC dans les organismes reste pour le moment incertain. En effet, au regard du comportement d'adsorption des ETM en fonction du pH du milieu, il est difficile de savoir si les ETM restent adsorbés en surface des NMC ou s'ils se désorbent suite à un changement de milieu au pH différent. D'après les résultats des expériences d'adsorption, les interactions NMC/ETM sont plus prononcées à pH = 7-8 qu'à pH = 5-6. Ainsi, il est donc par exemple possible que des désorptions métalliques puissent se produire une fois les NMC internalisés notamment dans les vacuoles chez les végétaux (pH vacuole : 5,50[46]), et que d'autres ETM et éléments présents dans le tractus digestif des vers de terre/escargots s'adsorbent en surface des NMC (pH tractus digestif : 6.9[47]) laissant ainsi incertaines les interactions NMC/ETM une fois absorbés et intégrés chez l'Homme (pH estomac : 1 à 3, pH intestin autour de 8). Aussi, des indices dans les expériences d'adsorption nous suggèrent que des ETM peuvent s'adsorber rapidement en surface des NMC puis se désorber pour laisser la place à d'autres ETM présentant une affinité plus élevée. En effet, l'expérience de cinétique d'adsorption du chapitre 3 a révélé que le Zn s'adsorbait plus rapidement que le Pb (constante de vitesse de pseudo-second ordre (K_2) du Zn: 0,26 g.mM.min^{-1} *vs* K_{2Pb} : 0,18 g.mM.min^{-1}) mais à l'issue des 6h d'interaction entre NTC et ETM, les quantités de Pb adsorbées étaient plus importante que le Zn en raison de sa plus

grande force d'interaction avec les NTC (quantité de Pb adsorbé à l'équilibre (q_e) : 2.50 mM.g^{-1} *vs* q_{eZn} : 1.64 mM.g^{-1} et constante d'équilibre de Langmuir (K_L) du Pb: 9.24 *vs* K_{LZn}: 0.23).

Quatrièmement, différents schémas de transfert des ETM en raison de l'ajout de NMC ont été observés aussi bien dans la bibliographie que dans les expériences menées dans nos travaux et pourraient être liés à **l'espèce végétale**. En effet, Gong *et al.*[48] ont observé une augmentation du transfert de Cd de 15%, 12% ou 9% dans les feuilles de *Boehmeria nivea* (dicotylédone, Rosidée) avec l'ajout de 100, 500 ou 1000 mg.L^{-1} de NTC dans le sol tandis que Chen et *al.*[49] n'ont pas observé de modifications de transfert de Cd chez *Solanum nigrum L.* (dicotylédone archaïque, Magnolidée), avec l'ajout de 100, 500, 1000 mg.kg^{-1} dans le sol. Dans le présent travail, l'ajout de NTC a modifié à deux reprises le transfert des ETM chez la salade (dicotylédone, Astéridée) tandis qu'aucune modification n'a été observée chez le maïs (monocotylédone, Commélinidée). En effet, l'ajout de 0,1 mg.kg^{-1} a diminué la concentration de Cd, Zn et dans une moindre mesure de Pb chez *Lactuca sativa* de 29%, 32% et 30% dans l'une des expériences du chapitre 5, et le transfert du Zn a augmenté de 162% avec l'ajout de 10 mg.kg^{-1} de NTC. Ces différences peuvent être liées aux groupes de plantes à laquelle elles appartiennent, le maïs est une plante monocotylédone, au réseau racinaire plus développé et possède plus de surface de contact avec le sol que les plantes dicotylédones (comme la laitue) au réseau racinaire moins ramifié[50]. Dès lors, un système racinaire plus développé, comme pour les monocotylédones, pourrait impliquer des interactions accrues entre les racines des plantes et les NTC présents dans le sol. Ainsi, les NTC pourraient davantage 1) obstruer l'entrée d'eau chez le maïs en s'accumulant autour des racines, et être ainsi responsables du stress hydrique visible chez cette espèce (chapitre 4 et 5) et/ou 2) pénétrer et s'accumuler dans les racines menant également à une obstruction du transport d'eau chez les monocotylédones. Il est intéressant de noter qu'en plus des indices qui démontrent d'un stress hydrique chez le maïs monocotylédone dans ce manuscrit, une précédente étude de Liné *et al.*[31] avait mis en évidence que parmi les 4 espèces végétales étudiés, seul le maïs monocotylédone présentait un retard de développement (taille) et de teneur en eau contrairement

aux autres plantes dicotylédones (tomate, colza et concombre). A l'inverse, les plantes dicotylédones comme la laitue, auraient un système racinaire moins développé, impliquant des interactions entre racines et NTC moins prononcées, conduisant à moins ou pas 1) d'obstruction d'eau chez la laitue et/ou 2) d'entrée et d'accumulation de NTC dans les racines chez les dicotylédones pour lesquels aucun stress hydrique n'a été observé dans ce manuscrit comme chez les 3 espèces de cotylédones[31] (tomate, colza et concombre). Un point qui reste à éclairer concerne les différences observées dans la modification de transfert des ETM par les NTC entre les deux clades de plantes. Suivant les hypothèses énoncées précédemment, les NTC avec des ETM adsorbés chez les monocotylédones pourraient stagner et s'accumuler dans les racines, tandis que leur transport jusqu'au partie aérienne des dicotylédones pourrait se réaliser sans encombre, chez qui ont observe des modifications de transfert. Enfin, même si aucune modification de transfert des ETM n'a été observés dans les parties aériennes du maïs, il se peut que des modifications aient eu lieu dans d'autres parties de la plante comme dans les racines, de lesquelles les NTC s'accumulent. D'ailleurs, le maïs est connu pour accumuler davantage de Cd, Cu, Pb et Zn dans les racines que dans les parties aériennes[51].

De la même manière, ces deux groupes possèdent des caractéristiques foliaires différentes qui peuvent aussi expliquer les différences de comportement de transfert des ETM suite à l'ajout de NTC. En effet, la grande surface foliaire des monocotylédones témoigne d'une demande aérienne en eau *via* la transpiration importante (pour assurer la thermorégulation des feuilles[52,53]) à laquelle la plantes répond par une absorption en eau importante. A l'inverse, les dicotylédones avec des feuilles plus petites sont plutôt associées aux environnements à faibles disponibilités en eau selon diverses études[54–57] et donc potentiellement plus résistantes au stress hydrique.

Les interactions démontrant des effets toxiques synergiques et/ou antagonistes ont peu été mis en évidence dans le cadre des études du manuscrit. Seule l'expérience sur le maïs du chapitre 5 et celle du chapitre 6 possède un design expérimental permettant de caractériser ce type d'interactions. Or, l'expérience sur le maïs semble peut encline à ces interactions en raison de l'absence de modification

du transfert des ETM par les NTC chez cette espèce et que très peu de marqueurs de toxicité sont disponible à ce jour sur l'expérience du chapitre 6.

Enfin, les **conditions d'exposition** sont un facteur à l'origine des nombreuses disparités dans les résultats observés dans la bibliographie. Par exemple, la **durée d'exposition** est un facteur qui doit être pris en compte dans l'interprétation des résultats et dans leur comparaison avec ceux de la bibliographie en raison du temps nécessaire dans la mise en place des défenses chez les organismes et d'excrétions des contaminants mais aussi en raison des phénomènes de dilution des contaminants (vis-à-vis de la concentration d'un contaminant pour la taille de l'organisme). Par exemple, Xu *et al.*[58] ont observé une augmentation de Cd, Cu, Pb et Zn de 775%, 1166%, 1750% et 33% chez *Lactuca sativa* suite à l'ajout de 100 $mg.kg^{-1}$ de microplastiques à l'issue de 20 jours d'exposition tandis que l'augmentation n'était que de 33% pour le Cd, qu'aucune augmentation significative de Cu et Pb n'a été observé et qu'une baisse de 33% de Zn a été observée après 60 jours d'exposition[58]. La durée de l'expérience régit aussi la durée de la mise en place de l'**équilibre d'adsorption**, comme il a été démontré dans les expériences d'adsorption du chapitre n°3. Dans ce chapitre, l'équilibre d'adsorption s'est produit à partir de 3H d'interactions NTC/ETM en conditions simplifiés (milieu aqueux), équilibre qui pourrait prendre plus temps à se mettre en place dans des conditions plus complexes (cad sur sol) en raison des autres composés du sol qui peuvent modifier les interactions NTC/ETM. En outre, la durée de l'exposition détermine l'excrétion des contaminants par les organismes, réponses physiologiques qui peut mettre plus ou moins de temps à se mettre en place selon 1) le degré de contamination du milieu et 2) les capacités intrinsèques de l'organisme à excréter les contaminants. Par exemple, dans l'expérience avec le modèle escargot du chapitre 6, malgré une augmentation de Zn et de Cd dans une moindre mesure suite à l'ajout de 10 $mg.kg^{-1}$ de NTC, aucune modification de l'excrétion de ces ETM n'a été détecté certainement parce-que les degrés contaminations en ETM (Cd :0,40 et Zn :52,42 $mg.kg^{-1}$) étaient trop faibles, tout comme la durée de l'exposition (14 jours).

Malgré la complexité déjà existante dans l'approche des études de stress multiples, la nécessité de complexification des unités d'exposition afin qu'elles relèvent d'une cohérence et d'une

représentativité environnementale s'avère essentielle car les interactions entre espèces inhérentes des écosystèmes peuvent être à l'origine de rétroactions tant sur le transfert des contaminants que sur leur toxicité. En effet, **l'approche intégrative** de l'expérience ayant fait intervenir les vers de terre et la laitue a démontré des comportements de rétroactions en raison des conditions édaphiques à savoir que la bioturbation des vers de terre était plus élevée dans les sols à forte concentration en MO, ce qui a sans doute participé à la dispersion des NMC dans le sol et qui pourrait ainsi avoir mené aux différences de transfert des ETM chez la laitue observées avec celles exposées aux sols moins contaminés en ETM avec moins de MO. Les liens et interactions entre espèces inféodés à un même écosystème sont étroits or la plupart des études réalisées à ce jour ne permettent pas que ces interactions entre espèces puissent se réaliser. En effet, la majorité des designs expérimentaux des études de la bibliographie sont construits de façon à caractériser l'écotoxicité des contaminants sur une seule espèce. Aussi, grâce à l'évolution des outils en écologie de nouveaux indicateurs s'offrent aux écotoxicologues afin d'avoir une vision plus globale du fonctionnement de l'écosystème comme les approches à l'aide d'index multifonctionnel, afin d'accompagner les interprétations des marqueurs à l'échelle individuelle. Ainsi, il a été observé dans l'expérience du chapitre 3 que des effets toxiques sur les biomarqueurs à l'échelle individuelle pouvaient être prononcés mais ne pas être mis en évidence par les écomarqueurs (index multifonctionnel) puisque compensés à l'échelle globale du système.

Perspectives

Les interactions entre NMC et ETM qui ont été mises en évidence dans la littérature scientifique et dans le présent manuscrit s'avèrent fortes et remettent en cause l'évaluation actuelle des risques écologiques associée aux contaminants en mélange. Des modifications du transfert des ETM s'opèrent suite à l'ajout de NMC dans le milieu ; modifications qui ont été aussi observées à plusieurs reprises avec les micro-nano-plastiques[59–61]. Il semble aussi nécessaire de vérifier l'accumulation des ETM dans toutes les parties consommables des plantes. En effet, certaines plantes ont la capacité de compartimenter préférentiellement les ETM dans des parties spécifiques comme les racines, les tiges et les feuilles[62], il semble donc intéressant d'analyser la concentration en ETM dans les différentes parties de la plante afin de mieux comprendre les différences de résultats observées dans la littérature sur transfert des ETM suite à l'ajout de NMC dans le milieu et mieux évaluer les risques sanitaires liés à la consommation des parties comestibles. Par exemple, Gong *et al.*[48] ont observé une augmentation du transfert de Cd de 15%, 12% et 9% dans les feuilles mais aussi une diminution de 22%, 21% et 29% dans les racines de *Boehmeria nivea* avec l'ajout de 100, 500 ou 1000 $mg.L^{-1}$ de NTC dans le sol. Outre les ETM, toutes les espèces ioniques peuvent interagir avec les NMC, comme les nutriments essentiels pour la vie des organismes tels qu'il a pu être observé dans la seconde expérience du chapitre 5, où l'ajout de 0,1 $mg.kg^{-1}$ NTC dans le sol le plus contaminé en ETM a diminué l'ensemble des éléments nutritifs dans les feuilles de laitues. La modification de la nutrition des organismes peut s'avérer délétère à long terme pour le bon fonctionnement de la plante et donc pour les rendements agricoles et davantage d'études sont nécessaires afin de comprendre l'entièreté des mécanismes sous-jacents. De plus, les NMC sont aussi connus pour interagir avec des pesticides[63] et herbicides[64] et ceci soulève des questions quant aux devenir de ces contaminants dans les agrosystèmes et dans les écosystèmes connexes. Une fois intégrés dans les écosystèmes, les NMC agiront ils comme vecteurs d'entrée des pesticides comme il a pu être observé avec les ETM ? Aussi, qu'en est-il du devenir des NMC s'ils sont appliqués directement sur les plantes d'intérêt agronomique ? Par exemple, une étude intéressante de Gao *et al.*[65] a mis en évidence une diminution du transfert de Cd de 19% et 33% dans les racines et

feuilles respectivement suite à une pulvérisation foliaire de GO, qui a provoqué des effets antagonistes sur la qualité nutritive (vitamine C) en diminuant la toxicité du Cd du sol chez *Lactuca sativa*. Cette voie d'exposition semble donc aussi encline aux interactions NMC/ETM et bien que spéculatif, les résultats peuvent laisser penser à ce que les NMC pulvérisé soient transporté hors de la plante dans la rhizosphère, comme ce qui a été démontré avec des nanoparticule d'or[66]. Enfin, la plupart des designs expérimentaux utilisés dans la littérature ne permettent pas de mettre en évidence les possibles interactions entre contaminants notamment les phénomènes de synergie et d'antagonisme puisqu'ils ne testent pas l'effet individuel à la fois des NMC et des ETM et les effets conjoints de ces deux contaminants. Afin d'établir un diagnostic complet et des réponses quant aux effets des interactions des contaminants en mélange, il est plus que nécessaire de réaliser des études aux designs expérimentaux qui permettent de caractériser les interactions. Le document "Mélanges de polluants, toxicité, écotoxicité et évaluation des risques" paru en 2011[67] fournit de multiples possibilités dans les outils statistiques et méthodes qui permettent de caractériser les interactions des contaminants en mélange tel que les iso-bologrammes, polygonogrammes et des méthodes où les effets des mélanges sont comparés à deux modèles de références (addition des effets et modèle d'indépendance d'action). Toutefois, les compétences et connaissances requises pour utiliser de tels outils ne sont, à ce jour, pas assez maîtrisées par les chercheurs/institutions gouvernementales et la communication et leur formation à ces outils semble plus que nécessaire dans le cadre où des interactions entre contaminants sont évidentes. Les effets synergiques et/ou antagonistes en raison de l'exposition conjointe NMC/ETM qui ont été répertoriés dans la littérature et observés dans le présent manuscrit ne permettent pas d'établir des généralisations tant les facteurs qui régissent les interactions entre contaminants sont importants et tant les réponses biologiques diffèrent.

Biblioagraphie (conclusion et discussion générale):

(1) Leroy, M.; Flahaut, E.; Larue, C. Carbon Based Nanomaterial Interactions with Metals and Metalloids in Terrestrial Environment: A Review. *Carbon* **2023**, *206*, 325–339. https://doi.org/10.1016/j.carbon.2023.02.047.

(2) Sheng, G.; Li, J.; Shao, D.; Hu, J.; Chen, C.; Chen, Y.; Wang, X. Adsorption of Copper(II) on Multiwalled Carbon Nanotubes in the Absence and Presence of Humic or Fulvic Acids. *Journal of Hazardous Materials* **2010**, *178* (1–3), 333–340. https://doi.org/10.1016/j.jhazmat.2010.01.084.

(3) Lin, D.; Tian, X.; Li, T.; Zhang, Z.; He, X.; Xing, B. Surface-Bound Humic Acid Increased Pb2+ Sorption on Carbon Nanotubes. *Environmental Pollution* **2012**, *167*, 138–147. https://doi.org/10.1016/j.envpol.2012.03.044.

(4) Tian, X.; Li, T.; Yang, K.; Xu, Y.; Lu, H.; Lin, D. Effect of Humic Acids on Physicochemical Property and Cd(II) Sorption of Multiwalled Carbon Nanotubes. *Chemosphere* **2012**, *89* (11), 1316–1322. https://doi.org/10.1016/j.chemosphere.2012.05.082.

(5) Zhang, W.; Zhang, F.; Han, Z.; Lü, X.; Lin, D.; Werner, D. Effect of Clay Minerals on Transport of Surfactants Dispersed Multi-walled Carbon Nanotubes in Porous Media. *Acta Geologica Sinica - English Edition* **2017**, *1* (91), 135–144. https://doi.org/10.1111/1755-6724.13067.

(6) Han, B.; Liu, W.; Zhao, X.; Cai, Z.; Zhao, D. Transport of Multi-Walled Carbon Nanotubes Stabilized by Carboxymethyl Cellulose and Starch in Saturated Porous Media: Influences of Electrolyte, Clay and Humic Acid. *Science of The Total Environment* **2017**, *599–600*, 188–197. https://doi.org/10.1016/j.scitotenv.2017.04.222.

(7) Lu, T.; Xia, T.; Qi, Y.; Zhang, C.; Chen, W. Effects of Clay Minerals on Transport of Graphene Oxide in Saturated Porous Media. *Environ Toxicol Chem* **2017**, *36* (3), 655–660. https://doi.org/10.1002/etc.3605.

(8) Kasel, D.; Bradford, S. A.; Šimůnek, J.; Heggen, M.; Vereecken, H.; Klumpp, E. Transport and Retention of Multi-Walled Carbon Nanotubes in Saturated Porous Media: Effects of Input Concentration and Grain Size. *Water Research* **2013**, *47* (2), 933–944. https://doi.org/10.1016/j.watres.2012.11.019.

(9) Liné, C.; Larue, C.; Flahaut, E. Carbon Nanotubes: Impacts and Behaviour in the Terrestrial Ecosystem - A Review. *Carbon* **2017**, *123*, 767–785. https://doi.org/10.1016/j.carbon.2017.07.089.

(10) Giraud, L.; Tourrette, A.; Flahaut, E. Carbon Nanomaterials-Based Polymer-Matrix Nanocomposites for Antimicrobial Applications: A Review. *Carbon* **2021**. https://doi.org/10.1016/j.carbon.2021.06.002.

(11) Chung, H.; Son, Y.; Yoon, T. K.; Kim, S.; Kim, W. The Effect of Multi-Walled Carbon Nanotubes on Soil Microbial Activity. *Ecotoxicology and Environmental Safety* **2011**, *74* (4), 569–575. https://doi.org/10.1016/j.ecoenv.2011.01.004.

(12) Jin, L.; Son, Y.; DeForest, J. L.; Kang, Y. J.; Kim, W.; Chung, H. Single-Walled Carbon Nanotubes Alter Soil Microbial Community Composition. *Sci. Total Environ.* **2014**, *466–467*, 533–538. https://doi.org/10.1016/j.scitotenv.2013.07.035.

(13) Chung, H.; Son, Y.; Yoon, T. K.; Kim, S.; Kim, W. The Effect of Multi-Walled Carbon Nanotubes on Soil Microbial Activity. *Ecotoxicology and Environmental Safety* **2011**, *74* (4), 569–575. https://doi.org/10.1016/j.ecoenv.2011.01.004.

(14) Jin, L.; Son, Y.; Yoon, T. K.; Kang, Y. J.; Kim, W.; Chung, H. High Concentrations of Single-Walled Carbon Nanotubes Lower Soil Enzyme Activity and Microbial Biomass. *Ecotoxicology and Environmental Safety* **2013**, *88*, 9–15. https://doi.org/10.1016/j.ecoenv.2012.10.031.

(15) Ge, Y.; Priester, J. H.; Mortimer, M.; Chang, C. H.; Ji, Z.; Schimel, J. P.; Holden, P. A. Long-Term Effects of Multiwalled Carbon Nanotubes and Graphene on Microbial Communities in Dry Soil. *Environ. Sci. Technol.* **2016**, *50* (7), 3965–3974. https://doi.org/10.1021/acs.est.5b05620.

(16) Kerfahi, D.; Tripathi, B. M.; Singh, D.; Kim, H.; Lee, S.; Lee, J.; Adams, J. M. Effects of Functionalized and Raw Multi-Walled Carbon Nanotubes on Soil Bacterial Community Composition. *PLOS ONE* **2015**, *10* (3), e0123042. https://doi.org/10.1371/journal.pone.0123042.
(17) Evariste, L.; Braylé, P.; Mouchet, F.; Silvestre, J.; Gauthier, L.; Flahaut, E.; Pinelli, E.; Barret, M. Graphene-Based Nanomaterials Modulate Internal Biofilm Interactions and Microbial Diversity. *Front. Microbiol.* **2021**, *12*. https://doi.org/10.3389/fmicb.2021.623853.
(18) Wu, F.; You, Y.; Werner, D.; Jiao, S.; Hu, J.; Zhang, X.; Wan, Y.; Liu, J.; Wang, B.; Wang, X. Carbon Nanomaterials Affect Carbon Cycle-Related Functions of the Soil Microbial Community and the Coupling of Nutrient Cycles. *Journal of Hazardous Materials* **2020**, *390*, 122144. https://doi.org/10.1016/j.jhazmat.2020.122144.
(19) Yang, X.; He, Q.; Guo, F.; Sun, X.; Zhang, J.; Chen, Y. Impacts of Carbon-Based Nanomaterials on Nutrient Removal in Constructed Wetlands: Microbial Community Structure, Enzyme Activities, and Metabolism Process. *Journal of Hazardous Materials* **2021**, *401*, 123270. https://doi.org/10.1016/j.jhazmat.2020.123270.
(20) Yan, C.; Huang, J.; Wang, Y.; Lin, X.; Cao, C.; Qian, X. Assessment on the Treatment of Nitrogen Contaminant by Constructed Wetland Exposed to Different Concentrations of Graphene Oxide. *Journal of Cleaner Production* **2022**, *338*, 130567. https://doi.org/10.1016/j.jclepro.2022.130567.
(21) Das, P.; Davis, K.; Penton, C. R.; Westerhoff, P.; Bi, Y. Impacts of Graphitic Nanofertilizers on Nitrogen Cycling in a Sandy, Agricultural Soil. *J Nanopart Res* **2022**, *24* (6), 120. https://doi.org/10.1007/s11051-022-05500-9.
(22) Rezaei Cherati, S.; Anas, M.; Liu, S.; Shanmugam, S.; Pandey, K.; Angtuaco, S.; Shelton, R.; Khalfaoui, A. N.; Alena, S. V.; Porter, E.; Fite, T.; Cao, H.; Green, M. J.; Basnakian, A. G.; Khodakovskaya, M. V. Comprehensive Risk Assessment of Carbon Nanotubes Used for Agricultural Applications. *ACS Nano* **2022**, *16* (8), 12061–12072. https://doi.org/10.1021/acsnano.2c02201.
(23) Tiwari, D. K.; Dasgupta-Schubert, N.; Villaseñor Cendejas, L. M.; Villegas, J.; Carreto Montoya, L.; Borjas García, S. E. Interfacing Carbon Nanotubes (CNT) with Plants: Enhancement of Growth, Water and Ionic Nutrient Uptake in Maize (Zea Mays) and Implications for Nanoagriculture. *Appl Nanosci* **2014**, *4* (5), 577–591. https://doi.org/10.1007/s13204-013-0236-7.
(24) Lahiani, M. H.; Dervishi, E.; Chen, J.; Nima, Z.; Gaume, A.; Biris, A. S.; Khodakovskaya, M. V. Impact of Carbon Nanotube Exposure to Seeds of Valuable Crops. *ACS Appl. Mater. Interfaces* **2013**, *5* (16), 7965–7973. https://doi.org/10.1021/am402052x.
(25) Lahiani, M. H.; Dervishi, E.; Ivanov, I.; Chen, J.; Khodakovskaya, M. Comparative Study of Plant Responses to Carbon-Based Nanomaterials with Different Morphologies. *Nanotechnology* **2016**, *27* (26), 265102. https://doi.org/10.1088/0957-4484/27/26/265102.
(26) Hao, Y.; Yu, F.; Lv, R.; Ma, C.; Zhang, Z.; Rui, Y.; Liu, L.; Cao, W.; Xing, B. Carbon Nanotubes Filled with Different Ferromagnetic Alloys Affect the Growth and Development of Rice Seedlings by Changing the C:N Ratio and Plant Hormones Concentrations. *PLOS ONE* **2016**, *11* (6), e0157264. https://doi.org/10.1371/journal.pone.0157264.
(27) Martínez-Ballesta, M. C.; Zapata, L.; Chalbi, N.; Carvajal, M. Multiwalled Carbon Nanotubes Enter Broccoli Cells Enhancing Growth and Water Uptake of Plants Exposed to Salinity. *Journal of Nanobiotechnology* **2016**, *14* (1), 42. https://doi.org/10.1186/s12951-016-0199-4.
(28) Kharissova, O. V.; Kharisov, B. I.; Ortiz, E. G. de C. Dispersion of Carbon Nanotubes in Water and Non-Aqueous Solvents. *RSC Adv.* **2013**, *3* (47), 24812–24852. https://doi.org/10.1039/C3RA43852J.
(29) Zhao, L.; Guan, X.; Yu, B.; Ding, N.; Liu, X.; Ma, Q.; Yang, S.; Yilihamu, A.; Yang, S.-T. Carboxylated Graphene Oxide-Chitosan Spheres Immobilize Cu2+ in Soil and Reduce Its Bioaccumulation in Wheat Plants. *Environment International* **2019**, *133*, 105208. https://doi.org/10.1016/j.envint.2019.105208.

(30) Kabata-Pendias, A. *Trace Elements in Soils and Plants*, 4th ed.; CRC Press: Boca Raton, 2010. https://doi.org/10.1201/b10158.
(31) Liné, C.; Manent, F.; Wolinski, A.; Flahaut, E.; Larue, C. Comparative Study of Response of Four Crop Species Exposed to Carbon Nanotube Contamination in Soil. *Chemosphere* **2021**, *274*, 129854. https://doi.org/10.1016/j.chemosphere.2021.129854.
(32) Zhao, X.; Liu, H.; Yan, Z.; Song, C. Aging of Carbon Nanotubes Increases Their Adsorption towards Tetracycline. *Water* **2022**, *14* (17), 2731. https://doi.org/10.3390/w14172731.
(33) Hu, C. W.; Zhang, L. J.; Wang, W. L.; Cui, Y. B.; Li, M. Evaluation of the Combined Toxicity of Multi-Walled Carbon Nanotubes and Sodium Pentachlorophenate on the Earthworm Eisenia Fetida Using Avoidance Bioassay and Comet Assay. *Soil Biology and Biochemistry* **2014**, *70*, 123–130. https://doi.org/10.1016/j.soilbio.2013.12.018.
(34) Lukkari, T.; Haimi, J. Avoidance of Cu- and Zn-Contaminated Soil by Three Ecologically Different Earthworm Species. *Ecotoxicology and Environmental Safety* **2005**, *62* (1), 35–41. https://doi.org/10.1016/j.ecoenv.2004.11.012.
(35) Petersen, E.; Barrios, A. C.; Bjorkland, R.; Goodwin, D. G.; Li, J.; Waissi, G.; Henry, T. Evaluation of Bioaccumulation of Nanoplastics, Carbon Nanotubes, Fullerenes, and Graphene Family Materials. *Environment International* **2023**, *173*, 107650. https://doi.org/10.1016/j.envint.2022.107650.
(36) Petersen, E. J.; Pinto, R. A.; Zhang, L.; Huang, Q.; Landrum, P. F.; Weber, W. J. Effects of Polyethyleneimine-Mediated Functionalization of Multi-Walled Carbon Nanotubes on Earthworm Bioaccumulation and Sorption by Soils. *Environ. Sci. Technol.* **2011**, *45* (8), 3718–3724. https://doi.org/10.1021/es103004r.
(37) Li, S.; Irin, F.; Atore, F. O.; Green, M. J.; Cañas-Carrell, J. E. Determination of Multi-Walled Carbon Nanotube Bioaccumulation in Earthworms Measured by a Microwave-Based Detection Technique. *Science of The Total Environment* **2013**, *445–446*, 9–13. https://doi.org/10.1016/j.scitotenv.2012.12.037.
(38) Eom, H.-J.; Roca, C. P.; Roh, J.-Y.; Chatterjee, N.; Jeong, J.-S.; Shim, I.; Kim, H.-M.; Kim, P.-J.; Choi, K.; Giralt, F.; Choi, J. A Systems Toxicology Approach on the Mechanism of Uptake and Toxicity of MWCNT in Caenorhabditis Elegans. *Chemico-Biological Interactions* **2015**, *239*, 153–163. https://doi.org/10.1016/j.cbi.2015.06.031.
(39) Nahmani, J.; Hodson, M. E.; Black, S. A Review of Studies Performed to Assess Metal Uptake by Earthworms. *Environmental Pollution* **2007**, *145* (2), 402–424. https://doi.org/10.1016/j.envpol.2006.04.009.
(40) Gimbert, F.; Vijver, M. G.; Coeurdassier, M.; Scheifler, R.; Peijnenburg, W. J. G. M.; Badot, P.-M.; de Vaufleury, A. How Subcellular Partitioning Can Help to Understand Heavy Metal Accumulation and Elimination Kinetics in Snails. *Environmental Toxicology and Chemistry* **2008**, *27* (6), 1284–1292. https://doi.org/10.1897/07-503.1.
(41) Weise, K.; Kurth, T.; Politowski, I.; Winkelmann, C.; Schäffer, A.; Kretschmar, S.; Berendonk, T. U.; Jungmann, D. A Workflow to Investigate the Impacts of Weathered Multi-Walled Carbon Nanotubes to the Mud Snail Lymnaea Stagnalis. *Environ Sci Pollut Res* **2022**, *29* (18), 26706–26725. https://doi.org/10.1007/s11356-021-17691-0.
(42) Cobbett, C. S. Phytochelatins and Their Roles in Heavy Metal Detoxification. *Plant Physiology* **2000**, *123* (3), 825–832. https://doi.org/10.1104/pp.123.3.825.
(43) Mishra, S.; Dubey, R. S. Heavy Metal Uptake and Detoxification Mechanisms in Plants. *International Journal of Agricultural Research* **2010**, *5* (7), 482–501.
(44) Bhat, S. A.; Singh, S.; Singh, J.; Kumar, S.; Bhawana; Vig, A. P. Bioremediation and Detoxification of Industrial Wastes by Earthworms: Vermicompost as Powerful Crop Nutrient in Sustainable Agriculture. *Bioresource Technology* **2018**, *252*, 172–179. https://doi.org/10.1016/j.biortech.2018.01.003.
(45) Swaileh, K. M.; Ezzughayyar, A. Dose-Dependent Effects of Dietary Pb and Zn on Feeding and Growth Rates of the Landsnail Helix Engaddensis. *Ecotoxicology and Environmental Safety* **2001**, *50* (1), 9–14. https://doi.org/10.1006/eesa.2001.2051.

(46) Mathieu, Y.; Guern, J.; Kurkdjian, A.; Manigault, P.; Manigault, J.; Zielinska, T.; Gillet, B.; Beloeil, J.-C.; Lallemand, J.-Y. Regulation of Vacuolar PH of Plant Cells. *Plant Physiol* **1989**, *89* (1), 19–26.
(47) Horn, M. A.; Schramm, A.; Drake, H. L. The Earthworm Gut: An Ideal Habitat for Ingested N2O-Producing Microorganisms. *Appl Environ Microbiol* **2003**, *69* (3), 1662–1669. https://doi.org/10.1128/AEM.69.3.1662-1669.2003.
(48) Gong, X.; Huang, D.; Liu, Y.; Zeng, G.; Wang, R.; Xu, P.; Zhang, C.; Cheng, M.; Xue, W.; Chen, S. Roles of Multiwall Carbon Nanotubes in Phytoremediation: Cadmium Uptake and Oxidative Burst in Boehmeria Nivea (L.) Gaudich. *Environ. Sci.: Nano* **2019**, *6* (3), 851–862. https://doi.org/10.1039/C8EN00723C.
(49) Chen, X.; Wang, J.; Hayat, K.; Zhang, D.; Zhou, P. Small Structures with Big Impact: Multi-Walled Carbon Nanotubes Enhanced Remediation Efficiency in Hyperaccumulator Solanum Nigrum L. under Cadmium and Arsenic Stress. *Chemosphere* **2021**, *276*, 130130. https://doi.org/10.1016/j.chemosphere.2021.130130.
(50) Bouguerra, S.; Gavina, A.; Ksibi, M.; da Graça Rasteiro, M.; Rocha-Santos, T.; Pereira, R. Ecotoxicity of Titanium Silicon Oxide (TiSiO4) Nanomaterial for Terrestrial Plants and Soil Invertebrate Species. *Ecotoxicology and Environmental Safety* **2016**, *129*, 291–301. https://doi.org/10.1016/j.ecoenv.2016.03.038.
(51) Wang, F. Y.; Lin, X. G.; Yin, R. Effect of Arbuscular Mycorrhizal Fungal Inoculation on Heavy Metal Accumulation of Maize Grown in a Naturally Contaminated Soil. *International Journal of Phytoremediation* **2007**, *9* (4), 345–353. https://doi.org/10.1080/15226510701476214.
(52) Okajima, Y.; Taneda, H.; Noguchi, K.; Terashima, I. Optimum Leaf Size Predicted by a Novel Leaf Energy Balance Model Incorporating Dependencies of Photosynthesis on Light and Temperature. *Ecol Res* **2012**, *27* (2), 333–346. https://doi.org/10.1007/s11284-011-0905-5.
(53) Leigh, A.; Sevanto, S.; Close, J. d.; Nicotra, A. b. The Influence of Leaf Size and Shape on Leaf Thermal Dynamics: Does Theory Hold up under Natural Conditions? *Plant, Cell & Environment* **2017**, *40* (2), 237–248. https://doi.org/10.1111/pce.12857.
(54) Halloy, S. R. P.; Mark, A. F. Comparative Leaf Morphology Spectra of Plant Communities in New Zealand, the Andes and the European Alps. *Journal of the Royal Society of New Zealand* **1996**, *26* (1), 41–78. https://doi.org/10.1080/03014223.1996.9517504.
(55) Ackerly, D.; Knight, C.; Weiss, S.; Barton, K.; Starmer, K. Leaf Size, Specific Leaf Area and Microhabitat Distribution of Chaparral Woody Plants: Contrasting Patterns in Species Level and Community Level Analyses. *Oecologia* **2002**, *130* (3), 449–457. https://doi.org/10.1007/s004420100805.
(56) Peppe, D. J.; Royer, D. L.; Cariglino, B.; Oliver, S. Y.; Newman, S.; Leight, E.; Enikolopov, G.; Fernandez-Burgos, M.; Herrera, F.; Adams, J. M.; Correa, E.; Currano, E. D.; Erickson, J. M.; Hinojosa, L. F.; Hoganson, J. W.; Iglesias, A.; Jaramillo, C. A.; Johnson, K. R.; Jordan, G. J.; Kraft, N. J. B.; Lovelock, E. C.; Lusk, C. H.; Niinemets, Ü.; Peñuelas, J.; Rapson, G.; Wing, S. L.; Wright, I. J. Sensitivity of Leaf Size and Shape to Climate: Global Patterns and Paleoclimatic Applications. *New Phytologist* **2011**, *190* (3), 724–739. https://doi.org/10.1111/j.1469-8137.2010.03615.x.
(57) Moles, A. T.; Perkins, S. E.; Laffan, S. W.; Flores-Moreno, H.; Awasthy, M.; Tindall, M. L.; Sack, L.; Pitman, A.; Kattge, J.; Aarssen, L. W.; Anand, M.; Bahn, M.; Blonder, B.; Cavender-Bares, J.; Cornelissen, J. H. C.; Cornwell, W. K.; Díaz, S.; Dickie, J. B.; Freschet, G. T.; Griffiths, J. G.; Gutierrez, A. G.; Hemmings, F. A.; Hickler, T.; Hitchcock, T. D.; Keighery, M.; Kleyer, M.; Kurokawa, H.; Leishman, M. R.; Liu, K.; Niinemets, Ü.; Onipchenko, V.; Onoda, Y.; Penuelas, J.; Pillar, V. D.; Reich, P. B.; Shiodera, S.; Siefert, A.; Sosinski Jr, E. E.; Soudzilovskaia, N. A.; Swaine, E. K.; Swenson, N. G.; van Bodegom, P. M.; Warman, L.; Weiher, E.; Wright, I. J.; Zhang, H.; Zobel, M.; Bonser, S. P. Which Is a Better Predictor of Plant Traits: Temperature or Precipitation? *Journal of Vegetation Science* **2014**, *25* (5), 1167–1180. https://doi.org/10.1111/jvs.12190.
(58) Xu, G.; Lin, X.; Yu, Y. Different Effects and Mechanisms of Polystyrene Micro- and Nano-Plastics on the Uptake of Heavy Metals (Cu, Zn, Pb and Cd) by Lettuce (Lactuca Sativa L.). *Environmental Pollution* **2023**, *316*, 120656. https://doi.org/10.1016/j.envpol.2022.120656.

(59) Dong, Y.; Gao, M.; Song, Z.; Qiu, W. Microplastic Particles Increase Arsenic Toxicity to Rice Seedlings. *Environmental Pollution* **2020**, *259*, 113892. https://doi.org/10.1016/j.envpol.2019.113892.
(60) Manjate, E.; Ramos, S.; Almeida, C. M. R. Potential Interferences of Microplastics in the Phytoremediation of Cd and Cu by the Salt Marsh Plant Phragmites Australis. *Journal of Environmental Chemical Engineering* **2020**, *8* (2), 103658. https://doi.org/10.1016/j.jece.2020.103658.
(61) Li, M.; Liu, Y.; Xu, G.; Wang, Y.; Yu, Y. Impacts of Polyethylene Microplastics on Bioavailability and Toxicity of Metals in Soil. *Science of The Total Environment* **2021**, *760*, 144037. https://doi.org/10.1016/j.scitotenv.2020.144037.
(62) Yaashikaa, P. R.; Kumar, P. S.; Jeevanantham, S.; Saravanan, R. A Review on Bioremediation Approach for Heavy Metal Detoxification and Accumulation in Plants. *Environmental Pollution* **2022**, *301*, 119035. https://doi.org/10.1016/j.envpol.2022.119035.
(63) Pyrzynska, K. Carbon Nanotubes as Sorbents in the Analysis of Pesticides. *Chemosphere* **2011**, *83* (11), 1407–1413. https://doi.org/10.1016/j.chemosphere.2011.01.057.
(64) Pyrzynska, K.; Stafiej, A.; Biesaga, M. Sorption Behavior of Acidic Herbicides on Carbon Nanotubes. *Microchim Acta* **2007**, *159* (3), 293–298. https://doi.org/10.1007/s00604-007-0739-6.
(65) Gao, M.; Xu, Y.; Chang, X.; Dong, Y.; Song, Z. Effects of Foliar Application of Graphene Oxide on Cadmium Uptake by Lettuce. *Journal of Hazardous Materials* **2020**, *398*, 122859. https://doi.org/10.1016/j.jhazmat.2020.122859.
(66) Avellan, A.; Yun, J.; Zhang, Y.; Spielman-Sun, E.; Unrine, J. M.; Thieme, J.; Li, J.; Lombi, E.; Bland, G.; Lowry, G. V. Nanoparticle Size and Coating Chemistry Control Foliar Uptake Pathways, Translocation, and Leaf-to-Rhizosphere Transport in Wheat. *ACS Nano* **2019**, *13* (5), 5291–5305. https://doi.org/10.1021/acsnano.8b09781.
(67) Ribera, D.; Taberly, J. Mélanges de polluants, toxicité, écotoxicité et évaluation des risques.

Annexe :

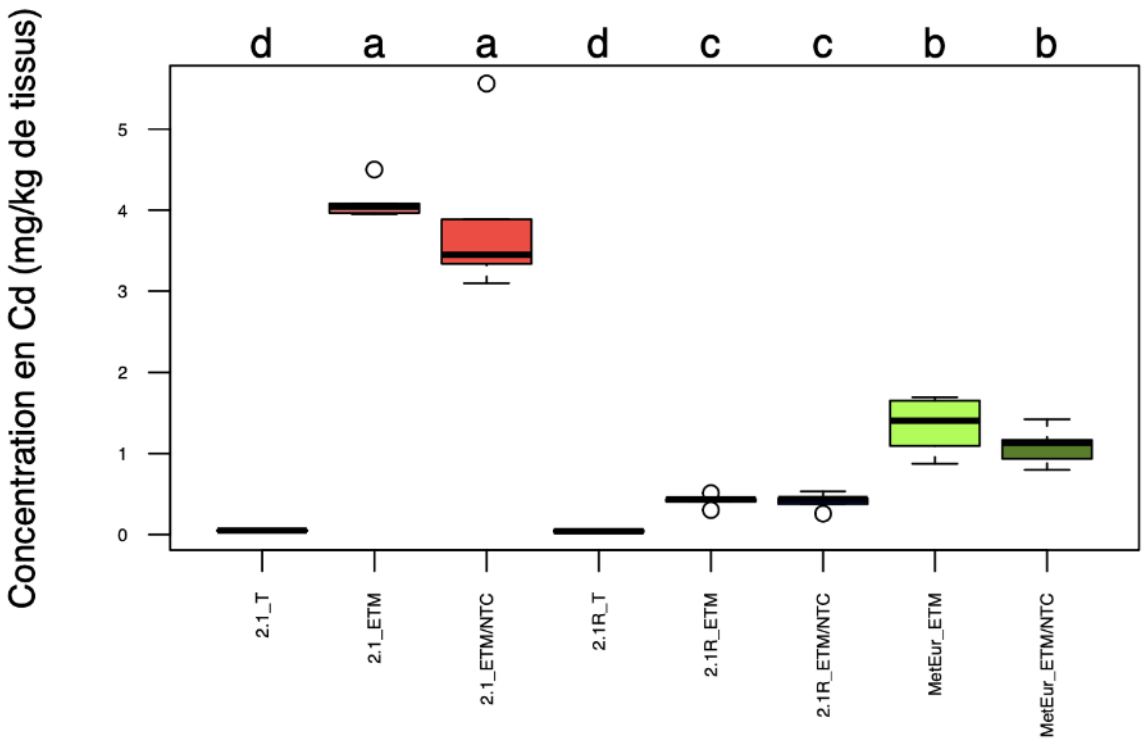

Annexe 1: Concentration en Cd contenu dans les feuilles de maïs exposés à différentes modalités (2.1_T : sol Lufa speyer 2.1 témoin sans réhausse de pH (pH = 5.0), 2.1_RT : sol Lufa speyer 2.1 au pH réhaussé (pH = 8.0), MetalEur : sol de MétalEurope (pH = 7.2), $[Cd]_{soi}$= 13 mg.kg^{-1}) après 2 semaines d'exposition

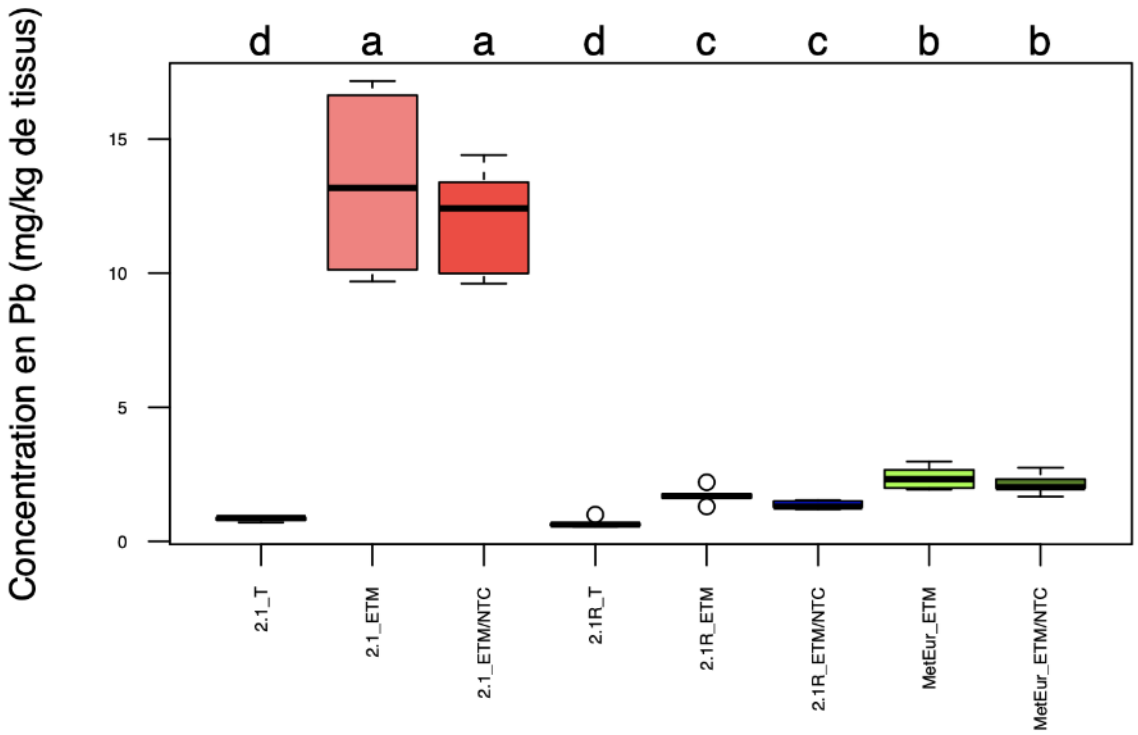

Annexe 2: Concentration en Pb contenu dans les feuilles de maïs exposés à différentes modalités (2.1_T : sol Lufa speyer 2.1 témoin sans réhausse de pH (pH = 5.0), 2.1_RT : sol Lufa speyer 2.1 au pH réhaussé (pH = 8.0), MetalEur : sol de MétalEurope (pH = 7.2), $[Pb]_{sol}$= 524 mg.kg^{-1}) après 2 semaines d'exposition

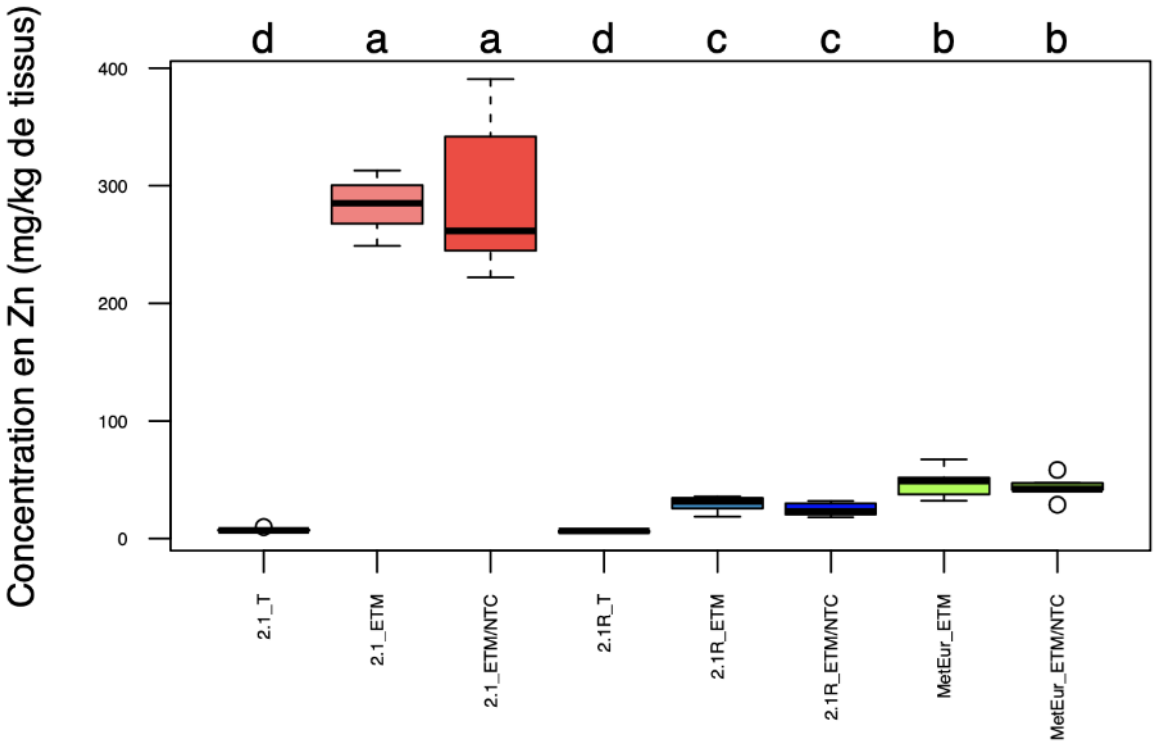

Annexe 3: Concentration en Zn contenu dans les feuilles de maïs exposés à différentes modalités (2.1_T : sol Lufa speyer 2.1 témoin sans réhausse de pH (pH = 5.0), 2.1_RT : sol Lufa speyer 2.1 au pH réhaussé (pH = 8.0), MetalEur : sol de MétalEurope (pH = 7.2), $[Zn]_{sol}$= 689 mg.kg^{-1}) après 2 semaines d'exposition

1. Formations suivies

Catégorie : Qualité de vie au travail

☛ Organisation de la journée des doctorants (03 janvier 2022 - 12 mai 2022) Laboratoire d'écologie fonctionnelle et environnement
5 heures enregistrées par : SDU2E - Sciences de l'Univers, de l'Environnement et de l'Espace.

Total du nombre d'heures pour la catégorie Qualité de vie au travail : *5 h*

Catégorie : Éthique et intégrité scientifique

☛ Ethique et intégrité scientifique (04 mai 2021 - 4 mai 2021) Université Fédérale de Toulouse Midi Pyrénées - Maison de la Recherche et de la Valorisation (MRV), 75 Cours des Sciences, 118 route de Narbonne
6 heures

Total du nombre d'heures pour la catégorie Éthique et intégrité scientifique : *6 h*

Catégorie : International, Langues

☛ Cours d'anglais/English Le lieu et la salle ne pourront être communiqués qu'au moment de l'organisation du cours
15 heures Note : 13

Total du nombre d'heures pour la catégorie International, Langues : *15 h*

Catégorie : Interdisciplinarité / Scientifique

☛ Formation autoclave (09 mars 2021 - 9 mars 2021) INP-ENSAT
3 heures enregistrées par : SDU2E - Sciences de l'Univers, de l'Environnement et de l'Espace.

☛ Ma Terre en 180 min (18 mai 2021) Université Grenoble-Alpes
6 heures enregistrées par : SDU2E - Sciences de l'Univers, de l'Environnement et de l'Espace.
La formation participe à l'objectif suivant : conforter la culture scientifique des doctorants dans leur champ disciplinaire ou en interdisciplinaire

☛ Séminaire d'Écologie Politique (SÉMÉCOL) - Ecologie et travail : Réinventer le travail pour des sociétés soutenables (07 mars 2022)
3 heures

Total du nombre d'heures pour la catégorie Interdisciplinarité / Scientifique : *12 h*

Catégorie : Méthodologie de la thèse recherche documentaire et publication

☛ MOOC : Rédiger et publier un article scientifique (28 juin 2021 - 27 juin 2022) Formation à distance
16 heures

Total du nombre d'heures pour la catégorie Méthodologie de la thèse recherche documentaire et publication : *16 h*

Catégorie : Pratiques pédagogiques pour l'Université

☛ Améliorer les situations d'enseignement/apprentissage pour rendre les étudiants acteurs de leur apprentissage (07 juin 2021 - 7 juin 2021) Université Fédérale de Toulouse Midi Pyrénées- Maison de la Recherche et de la Valorisation (MRV) 75 Cours des Sciences 118 route de Narbonne
6 heures

☛ MOOC : Se former pour enseigner dans le supérieur (08 septembre 2021) Formation à distance
24 heures

☛ Pratiques théatrales pour la didactique (04 juin 2021) Université Fédérale de Toulouse Midi Pyrénées - Maison de la Recherche et de la Valorisation (MRV) 75 Cours des Sciences, 118 route de Narbonne
6 heures

Total du nombre d'heures pour la catégorie *: 36 h*

Total participation : 90 heures / 10 modules

2. Enseignements

Au cours de ma première année de thèse, j'ai pu enseigner à l'université Paul Sabatier (64H) aux côtés de Sergine Ponsard et Fabien Mounet dans les unités écologie et biologie quantitative et de physiologie végétale. J'ai pu donner à la fois des TD, TP, cours magistraux et des examens de fin d'année.

Lors de ma deuxième et troisième année de thèse, j'ai enseigné à l'École Nationale Supérieur Agronomique de Toulouse (2x32H) aux cotés Annie Ouin et Séverine Jean sur des aspects de caractérisation de la biodiversité et son implication sur le terrain à travers des TP à Lacroix Falgarde.

3. Publications

(1) Leroy, M.; Flahaut, E.; Larue, C. Carbon Based Nanomaterial Interactions with Metals and Metalloids in Terrestrial Environment: A Review. *Carbon* **2023**, *206*, 325–339. https://doi.org/10.1016/j.carbon.2023.02.047.

(2) Leroy, M.; Pey, B.; Jassey, V. E. J.; Liné, C.; Elger, A.; Probst, A.; Flahaut, E.; Silvestre, J.; Larue, C. Interactive Effects of Metals and Carbon Nanotubes in a Microcosm Agrosystem. *Journal of Hazardous Materials* **2022**, *431*, 128613. https://doi.org/10.1016/j.jhazmat.2022.128613.

4. Conférences internationales

J'ai eu l'honore de participer à la SETAC europe 2022 en qualité de présentateur oral mes travaux issus de mon stage de M2.

5. Investissement dans la vie du laboratoire

Au cours de ma thèse, je me suis engagé dans la vie du laboratoire d'écologie fonctionnelle et environnement à travers mon mandat de représentant des doctorants au comité du laboratoire. J'ai également été le représentant des doctorants à l'Observatoire Midi-Pyrénées.

J'ai mis en place une journée scientifique dédié aux doctorants du laboratoire dans laquelle les doctorants étaient conviés à partager leurs travaux sous forme de présentation et/ou de posters. Aussi, un journal club a été créé afin de discuter sur des articles scientifiques.

Résumé :

Les récentes avancées dans le domaine de la nanotechnologie offrent d'innombrables possibilités dans beaucoup de domaine si bien que le rejet de nanomatériaux dans l'environnement est inéluctable. Les nanomatériaux carbonés (NMC), notamment, sont réputés pour s'accumuler dans les boues de stations d'épuration qui sont largement épandues dans les agrosystèmes. Or, de nouvelles découvertes ont permis de révéler que les NMC étaient capable d'interagir avec d'autres contaminants et plus particulièrement avec les éléments traces métalliques (ETM) qui sont déjà sous surveillance accrue dans les agrosystèmes. Ces interactions soulèvent donc des questions en ce qui concerne le transfert et les impacts écotoxiques de ces contaminants en mélange sur les agrosystèmes.

Cette étude avait donc pour but d'évaluer le transfert et les impacts écotoxiques d'un NMC, les nanotubes de carbone (NTC), et d'ETM en mélange avec un accent particulier sur la caractérisation des interactions NMC et ETM dans des conditions simplifiées mais pertinentes d'un point de vue environnemental. Il a été mis en évidence que les propriétés intrinsèques des NMC (surface spécifique, degré d'oxydation, nombre de parois, etc.) et que les conditions d'exposition (ratio de concentration NMC/ETM, temps de contact, pH, concentration de MO) régissent les interactions NMC/ETM. Des expériences en microcosmes ont démontré que l'ajout de NTC dans un sol contaminé modifiait le transfert des ETM chez la laitue romaine et les vers de terre, tandis que le transfert des ETM chez le maïs et l'escargot n'a pas été significativement modifié. Les cycles biogéochimiques du carbone et de l'azote ont été modifiés par l'exposition au NTC avec notamment une induction de la décomposition de la matière organique et du nombre de copie de gène impliqué dans la nitrification. Les disparités observées dans les résultats de transfert des ETM en raison de l'ajout de NTC dans le sol sont probablement dû aux concentrations des NTC, conditions édaphiques, aux traits d'histoires de vie et à l'espèce végétale elle-même. Aussi, les réponses toxicologiques des marqueurs à l'échelle de l'organisme qui résultent d'une contamination simultanée en NTC et ETM se sont avérés différents que s'ils avaient été appliqués individuellement. En revanche, aucune modification fonctionnelle à l'échelle de l'écosystème n'a été observé à l'issue de l'exposition simultanée en NTC et ETM. L'effet du vieillissement des contaminants sur le transfert la toxicité des NTC et ETM a également été abordé dans les travaux de ce document. Grâce à l'enrichissement isotopique ^{13}C des NTC et à des techniques de détection de pointe, il a été possible d'identifier une accumulation de NTC dans les feuilles de laitues romaines suite à une exposition à 10 $mg.kg^{-1}$ de NTC dans le sol ; la bioaccumulation vers un consommateur primaire est cependant limitée puisqu'aucune trace de NTC n'a été relevée dans la glande digestive de l'escargot. A l'issue des résultats présentés dans ce document, la nécessité de la prise en considération des interactions entre contaminants dans le cadre de l'évaluation des risques est soulevée et des pistes de réflexions afin de les caractériser sont données.

Recent advances in nanotechnology open up countless possibilities in many areas, making the release of nanomaterials into the environment inevitable. In particular, carbonaceous nanomaterials (CNMs) are known to accumulate in sewage sludge, which is widely spread in agrosystems as fertilizer. However, new findings have revealed that CNMs are capable of interacting with other contaminants, particularly trace metal elements (TMEs), which are already monitored in agrosystems. These interactions raise concerns about the transfer and ecotoxic impact of these mixed contaminants on agrosystems.

The aim of this study was to assess the transfer and ecotoxic impacts of a CNM, namely carbon nanotubes (CNTs), and a mix of TMEs (Pb, Cd, Zn, Cu) on an agrosystem. A particular emphasis was placed on characterizing CNM and TME interactions under simplified but environmentally relevant conditions. It was shown that intrinsic CNM properties (specific surface area, degree of oxidation, number of walls, etc.) and exposure conditions (CNM/TME concentration ratio, contact time, pH, organic matter concentration) govern CNM/TME interactions. Microcosm experiments demonstrated that biogeochemical cycles of carbon and nitrogen were altered by CNT exposure alone, with induction of organic matter decomposition and nitrification gene copy number. Furthermore, the addition of CNT to previously contaminated soil altered the transfer of TMEs in lettuce and earthworms, while the transfer of TMEs in maize and snails was not significantly altered. The disparities observed in TME transfer results are probably due to different CNT concentrations, edaphic conditions, life-history traits and the plant species itself. As a result, the toxicological responses of organism-level markers resulting from simultaneous contamination with CNT and TMEs were different from those when applied individually. On the other hand, no functional changes at ecosystem level were observed following simultaneous exposure to CNT and ETM. The effect of contaminant aging on the transfer of CNT and ETM toxicity has also been addressed in the work in this document. ^{13}C isotopic enrichment of CNTs coupled with the use of cutting edge spectroscopic techniques permitted to demonstrate that CNTs accumulated in lettuce leaves following exposure to 10 $mg.kg^{-1}$ of CNT in soil, but that bioaccumulation towards a primary consumer was limited since no trace of CNTs was found in the snail's digestive gland. Altogether these results highlight the need to take interactions among contaminants into consideration in ecological risk assessment, and avenues of reflection to characterize them are given.